arXiv:1606.02266v2 [hep-ex] 15 Sep 2016

Measurements of the Higgs boson production and decay rates and constraints on its couplings from a combined ATLAS and CMS analysis of the LHC pp collision data at $\sqrt{s} = 7$ and 8 TeV

The ATLAS and CMS Collaborations

Abstract

Combined ATLAS and CMS measurements of the Higgs boson production and decay rates, as well as constraints on its couplings to vector bosons and fermions, are presented. The combination is based on the analysis of five production processes, namely gluon fusion, vector boson fusion, and associated production with a W or a Z boson or a pair of top quarks, and of the six decay modes $H \rightarrow ZZ, WW, \gamma\gamma, \tau\tau, bb$, and $\mu\mu$. All results are reported assuming a value of 125.09 GeV for the Higgs boson mass, the result of the combined measurement by the ATLAS and CMS experiments. The analysis uses the CERN LHC proton–proton collision data recorded by the ATLAS and CMS experiments in 2011 and 2012, corresponding to integrated luminosities per experiment of approximately 5 fb^{-1} at $\sqrt{s} = 7$ TeV and 20 fb^{-1} at $\sqrt{s} = 8$ TeV. The Higgs boson production and decay rates measured by the two experiments are combined within the context of three generic parameterisations: two based on cross sections and branching fractions, and one on ratios of coupling modifiers. Several interpretations of the measurements with more model-dependent parameterisations are also given. The combined signal yield relative to the Standard Model prediction is measured to be 1.09 ± 0.11. The combined measurements lead to observed significances for the vector boson fusion production process and for the $H \rightarrow \tau\tau$ decay of 5.4 and 5.5 standard deviations, respectively. The data are consistent with the Standard Model predictions for all parameterisations considered.

1. Introduction

The elucidation of the mechanism of electroweak (EW) symmetry breaking has been one of the main goals driving the design of the ATLAS [1] and CMS [2] experiments at the CERN LHC. In the Standard Model (SM) of particle physics [3–6], the breaking of the symmetry is achieved through the introduction of a complex doublet scalar field, leading to the prediction of the existence of one physical neutral scalar particle, commonly known as the Higgs boson [7–12]. Through Yukawa interactions, the Higgs scalar field can also account for fermion masses [4, 13]. While the SM does not predict the value of the Higgs boson mass, m_H, the production cross sections and decay branching fractions (B) of the Higgs boson can be precisely calculated once its mass is known.

In 2012, the ATLAS and CMS Collaborations reported the observation of a new particle with a mass of approximately 125 GeV and Higgs-boson-like properties [14–16]. Subsequent results from both experiments, summarised in Refs. [17–21], established that all measurements of the properties of the new particle, including its spin, CP properties, and coupling strengths to SM particles, are consistent within the uncertainties with those expected for the SM Higgs boson. ATLAS and CMS have published a combined measurement of the Higgs boson mass [22], using LHC Run 1 data for the $H \to \gamma\gamma$ and $H \to ZZ$ channels, where Run 1 indicates the LHC proton–proton (pp) data taking period in 2011 and 2012 at centre-of-mass energies $\sqrt{s} = 7$ and 8 TeV. The combined mass measurement is

$$m_H = 125.09 \pm 0.21(\text{stat.}) \pm 0.11(\text{syst.}) \text{ GeV}, \tag{1}$$

where the total uncertainty is dominated by the statistical component. The Higgs boson mass is assumed to be $m_H = 125.09$ GeV for all analyses presented in this paper.

This paper reports the first ATLAS and CMS combined measurements of the Higgs boson production and decay rates as well as constraints on its couplings to SM particles. These measurements yield the most precise and comprehensive experimental results on these quantities to date. The main production processes studied are gluon fusion (ggF), vector boson fusion (VBF), and associated production with vector bosons (WH and ZH, denoted together as VH) or a pair of top quarks (ttH). The decay channels considered are those to bosons, $H \to ZZ$, $H \to WW$, and $H \to \gamma\gamma$; and to fermions, $H \to \tau\tau$, $H \to bb$, and $H \to \mu\mu$. Throughout this paper, Z and W indicate both real and virtual vector bosons, and no distinction is made between particles and antiparticles.

All analyses used in the combination are based on the complete Run 1 collision data collected by the ATLAS and CMS experiments. These data correspond to integrated luminosities per experiment of approximately 5 fb^{-1} at $\sqrt{s} = 7$ TeV (recorded in 2011) and 20 fb^{-1} at $\sqrt{s} = 8$ TeV (recorded in 2012). The results of the ATLAS and CMS individual combinations based on the Run 1 data are reported in Refs. [17, 18].

Unless otherwise stated, in this paper it is assumed, as in Refs. [17, 18], that the particle under study is a single SM-like Higgs boson state, i.e. a CP-even scalar particle with the tensor coupling structure of the SM for its interactions. The Higgs boson width, predicted to be approximately 4 MeV in the SM, is assumed to be small enough that the narrow-width approximation is valid and that the Higgs boson production and decay mechanisms can be factorised. These assumptions are corroborated by tests of the spin and CP properties of the Higgs boson [20, 21] and by studies of its width [18, 23–25]. The Higgs boson signal modelling is based on the hypothesis of a SM Higgs boson in terms of its production and decay kinematics. Measurements of differential production cross sections [26–29] support these assumptions within the current statistical uncertainties. The inherent model dependence related to these hypotheses

applies to all results presented here; the reliance on this model has a negligible impact for small deviations from the SM, but could be important for significant deviations from the SM predictions.

The results presented here for each experiment separately are slightly different from those reported in Refs. [17, 18]. Some small variations with respect to the earlier results are related to a different choice for the value of the Higgs boson mass. Other differences arise from minor modifications to the signal parameterisation and to the treatment of systematic uncertainties. These modifications are introduced in the present analysis to allow a fully consistent and correlated treatment of the dominant theoretical uncertainties in the signal modelling between the two experiments.

This paper is organised as described below. Section 2 briefly reviews the theoretical calculations of Higgs boson production and decay, and the modelling of the Higgs boson signal in Monte Carlo (MC) simulation; it also introduces the formalisms of signal strengths and coupling modifiers used for the interpretation of the data. Section 3 gives an overview of the analyses included in this combination, describes the statistical procedure used, together with the treatment of systematic uncertainties, and summarises modifications to the individual analyses for the combination. Section 4 describes the parameterisation of the measured signal yields in generic terms and reports the results using three distinct parameterisations. Section 5 compares the measured Higgs boson yields to the SM predictions for different production processes and decay modes, and reports the results of a test for the possible presence of multiple mass-degenerate states. Section 6 studies the couplings of the Higgs boson to probe for possible deviations from the SM predictions, using various assumptions motivated in many cases by beyond the SM (BSM) physics scenarios. Finally, Section 7 presents a summary of the results.

2. Higgs boson phenomenology and interpretation framework

This section briefly reviews Higgs boson phenomenology and introduces the most important aspects of the interpretation framework used to combine the measurements and to assess their compatibility with the SM predictions. The dominant production processes and major decay modes of the SM Higgs boson, along with the theoretical predictions for the cross sections and branching fractions, are presented. The main features of the MC generators used to simulate Higgs boson production and decay in each experiment are described. Finally, the formalisms of two widely used frameworks, based on signal strengths and coupling modifiers, for the interpretation of the Higgs boson measurements at the LHC, are introduced.

2.1. Higgs boson production and decay

In the SM, Higgs boson production at the LHC mainly occurs through the following processes, listed in order of decreasing cross section at the Run 1 centre-of-mass energies:

- gluon fusion production $gg \to H$ (Fig. 1a);

- vector boson fusion production $qq \to qqH$ (Fig. 1b);

- associated production with a W boson, $qq \to WH$ (Fig. 2a), or with a Z boson, $pp \to ZH$, including a small ($\sim 8\%$) but less precisely known contribution from $gg \to ZH$ ($ggZH$) (Figs. 2a, 2b, and 2c);

- associated production with a pair of top quarks, $qq, gg \to ttH$ (Fig. 3).
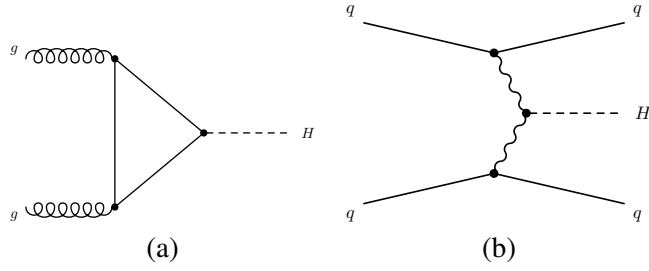
Figure 1: Examples of leading-order Feynman diagrams for Higgs boson production via the (a) ggF and (b) VBF production processes.
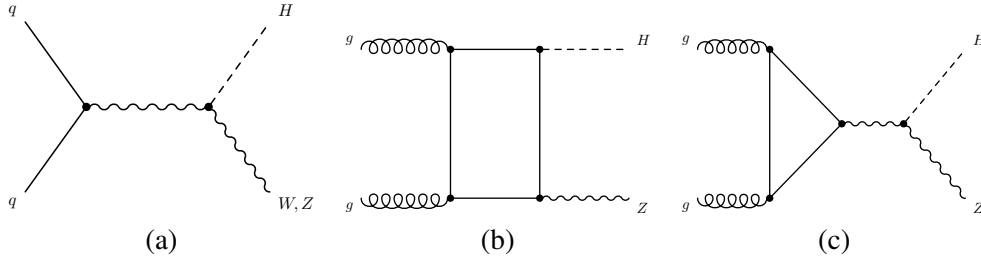

Figure 2: Examples of leading-order Feynman diagrams for Higgs boson production via the (a) $qq \rightarrow VH$ and (b, c) $gg \rightarrow ZH$ production processes.
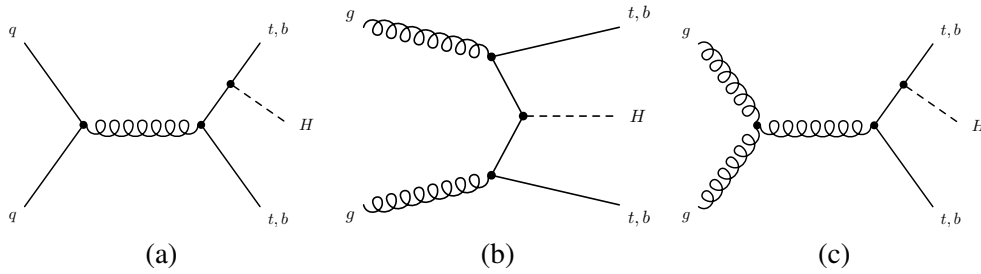

Figure 3: Examples of leading-order Feynman diagrams for Higgs boson production via the $qq/gg \rightarrow ttH$ and $qq/gg \rightarrow bbH$ processes.

Other less important production processes in the SM, which are not the target of a direct search but are included in the combination, are $qq, gg \rightarrow bbH$ (bbH), also shown in Fig. 3, and production in association with a single top quark (tH), shown in Fig. 4. The latter process proceeds through either $qq/qb \rightarrow tHb/tHq'$ (tHq) (Figs. 4a and 4b) or $gb \rightarrow tHW$ (tHW) (Figs. 4c and 4d) production.

Examples of leading-order (LO) Feynman diagrams for the Higgs boson decays considered in the combination are shown in Figs. 5 and 6. The decays to W and Z bosons (Fig. 5a) and to fermions (Fig. 5b) proceed through tree-level processes whereas the $H \rightarrow \gamma\gamma$ decay is mediated by W boson or heavy quark loops (Fig. 6).

The SM Higgs boson production cross sections and decay branching fractions are taken from Refs. [30–32] and are based on the extensive theoretical work documented in Refs. [33–77]. The inclusive cross sections and branching fractions for the most important production and decay modes are summarised with their overall uncertainties in Tables 1 and 2 for a Higgs boson mass m_H = 125.09 GeV. The SM predictions of the branching fractions for $H \rightarrow gg, cc$, and $Z\gamma$ are included for completeness. Although
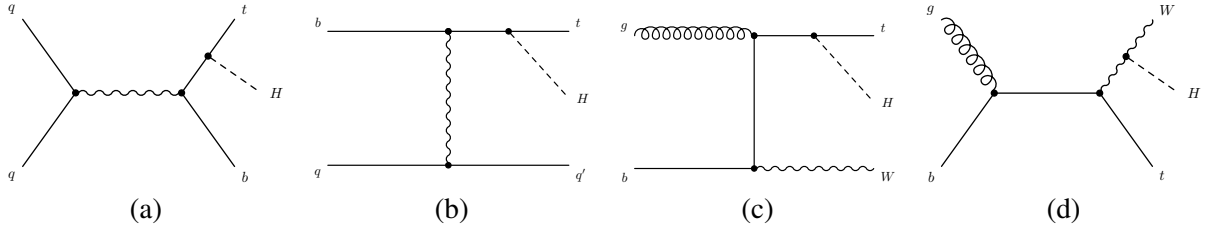
Figure 4: Examples of leading-order Feynman diagrams for Higgs boson production in association with a single top quark via the (a, b) *tHq* and (c, d) *tHW* production processes.
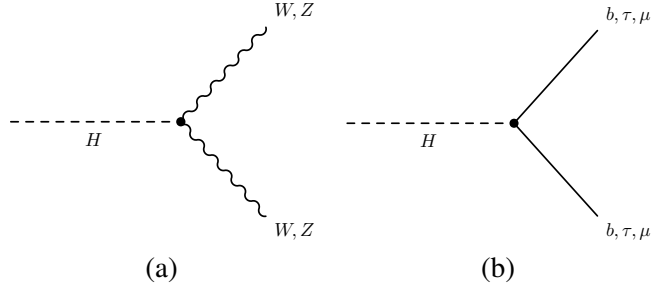
Figure 5: Examples of leading-order Feynman diagrams for Higgs boson decays (a) to W and Z bosons and (b) to fermions.
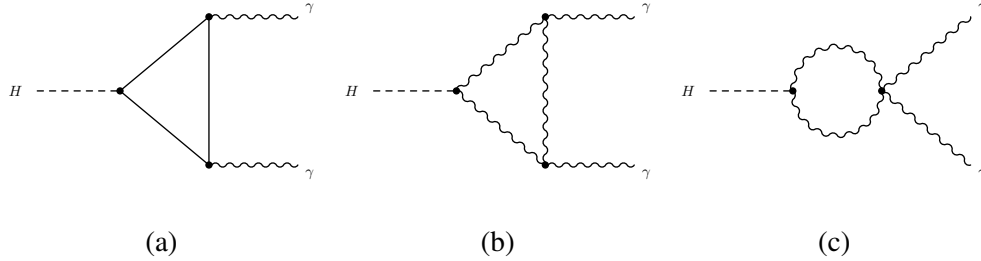
Figure 6: Examples of leading-order Feynman diagrams for Higgs boson decays to a pair of photons.

not an explicit part of the searches, they impact the combination through their contributions to the Higgs boson width and, at a small level, through their expected yields in some of the individual analyses.

2.2. Signal Monte Carlo simulation

All analyses use MC samples to model the Higgs boson production and decay kinematics, to estimate the acceptance and selection efficiency, and to describe the distributions of variables used to discriminate between signal and background events. The main features of the signal simulation are summarised here; for more details, the reader is referred to the individual publications:

- for ggF and VBF production, both experiments use Powheg [80–84] for the event generation, interfaced either to Pythia8 [85] (ATLAS) or Pythia6.4 [86] (CMS) for the simulation of the parton shower, the hadronisation, and the underlying event, collectively referred to in the following as UEPS.

Table 1: Standard Model predictions for the Higgs boson production cross sections together with their theoretical uncertainties. The value of the Higgs boson mass is assumed to be m_H = 125.09 GeV and the predictions are obtained by linear interpolation between those at 125.0 and 125.1 GeV from Ref. [32] except for the tH cross section, which is taken from Ref. [78]. The $pp \to ZH$ cross section, calculated at NNLO in QCD, includes both the quark-initiated, i.e. $qq \to ZH$ or $qg \to ZH$, and the $gg \to ZH$ contributions. The contribution from the $gg \to ZH$ production process, calculated only at NLO in QCD and indicated separately in brackets, is given with a theoretical uncertainty assumed to be 30%. The uncertainties in the cross sections are evaluated as the sum in quadrature of the uncertainties resulting from variations of the QCD scales, parton distribution functions, and α_s. The uncertainty in the tH cross section is calculated following the procedure of Ref. [79]. The order of the theoretical calculations for the different production processes is also indicated. In the case of bbH production, the values are given for the mixture of five-flavour (5FS) and four-flavour (4FS) schemes recommended in Ref. [74].

Production process	Cross section [pb]		Order of calculation
	$\sqrt{s}$ = 7 TeV	$\sqrt{s}$ = 8 TeV	
ggF	15.0 ± 1.6	19.2 ± 2.0	NNLO(QCD) + NLO(EW)
VBF	1.22 ± 0.03	1.58 ± 0.04	NLO(QCD+EW) + APPROX. NNLO(QCD)
WH	0.577 ± 0.016	0.703 ± 0.018	NNLO(QCD) + NLO(EW)
ZH	0.334 ± 0.013	0.414 ± 0.016	NNLO(QCD) + NLO(EW)
[$ggZH$]	0.023 ± 0.007	0.032 ± 0.010	NLO(QCD)
ttH	0.086 ± 0.009	0.129 ± 0.014	NLO(QCD)
tH	0.012 ± 0.001	0.018 ± 0.001	NLO(QCD)
bbH	0.156 ± 0.021	0.203 ± 0.028	5FS NNLO(QCD) + 4FS NLO(QCD)
Total	17.4 ± 1.6	22.3 ± 2.0	

Table 2: Standard Model predictions for the decay branching fractions of a Higgs boson with a mass of 125.09 GeV, together with their uncertainties [32]. Included are decay modes that are either directly studied or important for the combination because of their contributions to the Higgs boson width.

Decay mode	Branching fraction [%]
$H \to bb$	57.5 ± 1.9
$H \to WW$	21.6 ± 0.9
$H \to gg$	8.56 ± 0.86
$H \to \tau\tau$	6.30 ± 0.36
$H \to cc$	2.90 ± 0.35
$H \to ZZ$	2.67 ± 0.11
$H \to \gamma\gamma$	0.228 ± 0.011
$H \to Z\gamma$	0.155 ± 0.014
$H \to \mu\mu$	0.022 ± 0.001

- for *WH* and *ZH* production, both experiments use LO event generators for all quark-initiated processes, namely Pythia8 in ATLAS and Pythia6.4 in CMS. A prominent exception is the $H \rightarrow bb$ decay channel, for which ATLAS uses Powheg interfaced to Pythia8, while CMS uses Powheg interfaced to Herwig++ [87]. The *ggZH* production process is also considered, even though it contributes only approximately 8% of the total *ZH* production cross section in the SM, because it is expected to yield a relatively hard Higgs boson transverse momentum (p_T) spectrum, enhancing the contribution to the most sensitive categories in the $H \rightarrow bb$ decay channel. Both experiments therefore include *ggZH* production as a separate process in the *VH* analysis for the $H \rightarrow bb$ channel. ATLAS uses Powheg interfaced to Pythia8 while CMS uses a reweighted $qq \rightarrow ZH$ sample to model the *ggZH* contribution, including next-to-leading order (NLO) effects [66,67]. For the other channels, the contribution from this process is only accounted for as a correction to the overall signal cross section.

- for *ttH* production, ATLAS uses the NLO calculation of the HELAC-Oneloop package [88] interfaced to Powheg, often referred to as Powhel [89], while CMS simulates this process with the LO Pythia6.4 program.

- within the SM, the contribution from *tH* production to analyses searching for *ttH* production is small, but in certain BSM scenarios it may become large through interference effects (see Section 2.4). The *tH* production processes are simulated in both experiments using MadGraph5_aMC@NLO [79] interfaced to Herwig++ in the case of *tHW* production, while the *tHq* production process is simulated using MadGraph [90] interfaced to Pythia8 in ATLAS and MadGraph5_aMC@NLO interfaced to Pythia6.4 in CMS.

- finally, *bbH* production contributes approximately 1% to the total Higgs boson cross section in the SM. It is studied using Pythia8 in ATLAS and Pythia6.4 and MadGraph5_aMC@NLO in CMS, for the categories most sensitive to this production process in the various channels. Given that the selection efficiencies of *bbH* production are similar to those of the *gg*F process, the latter process is used to model the *bbH* signal for all decay channels, with an approximate correction to account for the difference in overall efficiency.

Table 3 summarises the event generators used by ATLAS and CMS for the $\sqrt{s} = 8$ TeV data analyses. For each production process and decay mode, the cross section and branching fraction used correspond to the higher-order state-of-the-art theoretical calculations, namely the values given in Tables 1 and 2.

Furthermore, the p_T distribution of the Higgs boson in the *gg*F process, which in many cases affects categorisation and selection efficiencies, is reweighted to match the HRes2.1 prediction [45–47], which accounts for next-to-next-to-leading-order (NNLO) and next-to-next-to-leading-logarithmic (NNLL) QCD corrections. In addition, the Higgs boson p_T spectrum in $gg \rightarrow H$ events with two or more jets is reweighted to match the prediction of the Powheg MiNLO H+2-jet generator [91]. This consistent treatment by the two experiments of the most prominent theoretical aspects of Higgs boson production and decay is quite important since all theoretical uncertainties in the various signal processes described in Table 3 are treated as correlated for the combination (see Section 3). The impact of using different generators for the less sensitive channels is negligible compared to their dominant sources of uncertainty.

Table 3: Summary of the event generators used by ATLAS and CMS to model the Higgs boson production processes and decay channels at $\sqrt{s} = 8$ TeV.

Production process	Event generator	
	ATLAS	CMS
ggF	Powheg [80–84]	Powheg
VBF	Powheg	Powheg
WH	Pythia8 [85]	Pythia6.4 [86]
ZH ($qq \rightarrow ZH$ or $qg \rightarrow ZH$)	Pythia8	Pythia6.4
$ggZH$ ($gg \rightarrow ZH$)	Powheg	See text
ttH	Powhel [88]	Pythia6.4
tHq ($qb \rightarrow tHq$)	MadGraph [90]	aMC@NLO [79]
tHW ($gb \rightarrow tHW$)	aMC@NLO	aMC@NLO
bbH	Pythia8	Pythia6.4, aMC@NLO

2.3. Signal strengths

The signal strength μ, defined as the ratio of the measured Higgs boson rate to its SM prediction, is used to characterise the Higgs boson yields. For a specific production process and decay mode $i \rightarrow H \rightarrow f$, the signal strengths for the production, μ_i, and for the decay, μ^f, are defined as

$$\mu_i = \frac{\sigma_i}{(\sigma_i)_{\text{SM}}} \quad \text{and} \quad \mu^f = \frac{\text{B}^f}{(\text{B}^f)_{\text{SM}}}. \tag{2}$$

Here σ_i ($i = gg$F, VBF, WH, ZH, ttH) and B^f ($f = ZZ, WW, \gamma\gamma, \tau\tau, bb, \mu\mu$) are respectively the production cross section for $i \rightarrow H$ and the decay branching fraction for $H \rightarrow f$. The subscript "SM" refers to their respective SM predictions, so by definition, $\mu_i = 1$ and $\mu^f = 1$ in the SM. Since σ_i and B^f cannot be separated without additional assumptions, only the product of μ_i and μ^f can be measured experimentally, leading to a signal strength μ_i^f for the combined production and decay:

$$\mu_i^f = \frac{\sigma_i \cdot \text{B}^f}{(\sigma_i)_{\text{SM}} \cdot (\text{B}^f)_{\text{SM}}} = \mu_i \cdot \mu^f. \tag{3}$$

The ATLAS and CMS data are combined and analysed using this signal strength formalism and the results are presented in Section 5. For all these signal strength fits, as well as for the generic parameterisations presented in Section 4.1, the parameterisations of the expected yields in each analysis category are performed with a set of assumptions, which are needed because some production processes or decay modes, which are not specifically searched for, contribute to other channels. These assumptions are the following: for the production processes, the bbH signal strength is assumed to be the same as for ggF, the tH signal strength is assumed to be the same as for ttH, and the $ggZH$ signal strength is assumed to be the same as for quark-initiated ZH production; for the Higgs boson decays, the $H \rightarrow gg$ and $H \rightarrow cc$ signal strengths are assumed to be the same as for $H \rightarrow bb$ decays, and the $H \rightarrow Z\gamma$ signal strength is assumed to be the same as for $H \rightarrow \gamma\gamma$ decays.

2.4. Coupling modifiers

Based on a LO-motivated framework [32] (κ-framework), coupling modifiers have been proposed to interpret the LHC data by introducing specific modifications of the Higgs boson couplings related to BSM physics. Within the assumptions already mentioned in Section 1, the production and decay of the Higgs boson can be factorised, such that the cross section times branching fraction of an individual channel $\sigma(i \to H \to f)$ contributing to a measured signal yield can be parameterised as:

$$\sigma_i \cdot B^f = \frac{\sigma_i(\vec{\kappa}) \cdot \Gamma^f(\vec{\kappa})}{\Gamma_H}, \tag{4}$$

where Γ_H is the total width of the Higgs boson and Γ^f is the partial width for Higgs boson decay to the final state f. A set of coupling modifiers, $\vec{\kappa}$, is introduced to parameterise possible deviations from the SM predictions of the Higgs boson couplings to SM bosons and fermions. For a given production process or decay mode, denoted "j", a coupling modifier κ_j is defined such that:

$$\kappa_j^2 = \sigma_j/\sigma_j^{\text{SM}} \quad \text{or} \quad \kappa_j^2 = \Gamma^j/\Gamma_{\text{SM}}^j, \tag{5}$$

where all κ_j values equal unity in the SM; here, by construction, the SM cross sections and branching fractions include the best available higher-order QCD and EW corrections. This higher-order accuracy is not necessarily preserved for κ_j values different from unity, but the dominant higher-order QCD corrections factorise to a large extent from any rescaling of the coupling strengths and are therefore assumed to remain valid over the entire range of κ_j values considered in this paper. Different production processes and decay modes probe different coupling modifiers, as can be visualised from the Feynman diagrams shown in Figs. 1–6. Individual coupling modifiers, corresponding to tree-level Higgs boson couplings to the different particles, are introduced, as well as two effective coupling modifiers, κ_g and κ_γ, which describe the loop processes for ggF production and $H \to \gamma\gamma$ decay. This is possible because BSM particles that might be present in these loops are not expected to appreciably change the kinematics of the corresponding process. The $gg \to H$ and $H \to \gamma\gamma$ loop processes can thus be studied, either through these effective coupling modifiers, thereby providing sensitivity to potential BSM particles in the loops, or through the coupling modifiers corresponding to the SM particles. In contrast, the $gg \to ZH$ process, which occurs at LO through box and triangular loop diagrams (Figs. 2b and 2c), is always taken into account, within the limitations of the framework, by resolving the loop in terms of the corresponding coupling modifiers, κ_Z and κ_t.

Contributions from interference effects between the different diagrams provide some sensitivity to the relative signs of the Higgs boson couplings to different particles. As discussed in Section 6.4, such effects are potentially largest for the $H \to \gamma\gamma$ decays, but may also be significant in the case of $ggZH$ and tH production. The ggF production process, when resolved in terms of its SM structure, provides sensitivity, although limited, to the relative signs of κ_t and κ_b through the t–b interference. The relative signs of the coupling modifiers κ_τ and κ_μ with respect to other coupling modifiers are not considered in this paper, since the current sensitivity to possible interference terms is negligible.

As an example of the possible size of such interference effects, the tH cross section is small in the SM, approximately 14% of the ttH cross section, because of destructive interference between diagrams involving the couplings to the W boson and the top quark, as shown in Table 4. However, the interference becomes constructive for negative values of the product $\kappa_W \cdot \kappa_t$. In the specific case where $\kappa_W \cdot \kappa_t = -1$, the tHW and tHq cross sections increase by factors of 6 and 13, respectively, so that the tH process displays some

Table 4: Higgs boson production cross sections σ_i, partial decay widths Γ^f, and total decay width (in the absence of BSM decays) parameterised as a function of the κ coupling modifiers as discussed in the text, including higher-order QCD and EW corrections to the inclusive cross sections and decay partial widths. The coefficients in the expression for Γ_H do not sum exactly to unity because some contributions that are negligible or not relevant to the analyses presented in this paper are not shown.

Production	Loops	Interference	Effective scaling factor	Resolved scaling factor
$\sigma(gg\mathrm{F})$	✓	t–b	κ_g^2	$1.06 \cdot \kappa_t^2 + 0.01 \cdot \kappa_b^2 - 0.07 \cdot \kappa_t\kappa_b$
$\sigma(\mathrm{VBF})$	–	–		$0.74 \cdot \kappa_W^2 + 0.26 \cdot \kappa_Z^2$
$\sigma(WH)$	–	–		κ_W^2
$\sigma(qq/qg \to ZH)$	–	–		κ_Z^2
$\sigma(gg \to ZH)$	✓	t–Z		$2.27 \cdot \kappa_Z^2 + 0.37 \cdot \kappa_t^2 - 1.64 \cdot \kappa_Z\kappa_t$
$\sigma(ttH)$	–	–		κ_t^2
$\sigma(gb \to tHW)$	–	t–W		$1.84 \cdot \kappa_t^2 + 1.57 \cdot \kappa_W^2 - 2.41 \cdot \kappa_t\kappa_W$
$\sigma(qq/qb \to tHq)$	–	t–W		$3.40 \cdot \kappa_t^2 + 3.56 \cdot \kappa_W^2 - 5.96 \cdot \kappa_t\kappa_W$
$\sigma(bbH)$	–	–		κ_b^2
Partial decay width				
Γ^{ZZ}	–	–		κ_Z^2
Γ^{WW}	–	–		κ_W^2
$\Gamma^{\gamma\gamma}$	✓	t–W	κ_γ^2	$1.59 \cdot \kappa_W^2 + 0.07 \cdot \kappa_t^2 - 0.66 \cdot \kappa_W\kappa_t$
$\Gamma^{\tau\tau}$	–	–		κ_τ^2
Γ^{bb}	–	–		κ_b^2
$\Gamma^{\mu\mu}$	–	–		κ_μ^2
Total width ($B_{\mathrm{BSM}} = 0$)				
Γ_H	✓	–	κ_H^2	$0.57 \cdot \kappa_b^2 + 0.22 \cdot \kappa_W^2 + 0.09 \cdot \kappa_g^2 +$ $0.06 \cdot \kappa_\tau^2 + 0.03 \cdot \kappa_Z^2 + 0.03 \cdot \kappa_c^2 +$ $0.0023 \cdot \kappa_\gamma^2 + 0.0016 \cdot \kappa_{(Z\gamma)}^2 +$ $0.0001 \cdot \kappa_s^2 + 0.00022 \cdot \kappa_\mu^2$

sensitivity to the relative sign between the W boson and top quark couplings, despite its small SM cross section.

The relations among the coupling modifiers, the production cross sections σ_i, and partial decay widths Γ^f are derived within this context, as shown in Table 4, and are used as a parameterisation to extract the coupling modifiers from the measurements. The coefficients are derived from Higgs production cross sections and decay rates evaluated including the best available higher-order QCD and EW corrections (up to NNLO QCD and NLO EW precision), as indicated in Tables 1 and 2. The numerical values are obtained from Ref. [32] and are given for $\sqrt{s} = 8$ TeV and $m_H = 125.09$ GeV (they are similar for $\sqrt{s} = 7$ TeV).

The current LHC data are insensitive to the coupling modifiers κ_c and κ_s, and have limited sensitivity to κ_μ. Thus, in the following, it is assumed that κ_c varies as κ_t, κ_s as κ_b, and κ_μ as κ_τ. Other coupling modifiers (κ_u, κ_d, and κ_e) are irrelevant for the combination provided they are of order unity. When probing the total width, the partial decay width Γ^{gg} is assumed to vary as κ_g^2. These assumptions are not the same as those described for the signal strength framework in Section 2.3, so the two parameterisations are only approximately equivalent. The two sets of assumptions have a negligible impact on the measurements reported here provided that the unmeasured parameters do not deviate strongly from unity.

Changes in the values of the couplings will result in a variation of the Higgs boson width. A new modifier, κ_H, defined as $\kappa_H^2 = \sum_j B_{SM}^j \kappa_j^2$ and assumed to be positive without loss of generality, is introduced to characterise this variation. In the case where the SM decays of the Higgs boson are the only ones allowed, the relation $\kappa_H^2 = \Gamma_H / \Gamma_H^{SM}$ holds. If instead deviations from the SM are introduced in the decays, the width Γ_H can be expressed as:

$$\Gamma_H = \frac{\kappa_H^2 \cdot \Gamma_H^{SM}}{1 - B_{BSM}}, \tag{6}$$

where B_{BSM} indicates the total branching fraction into BSM decays. Such BSM decays can be of three types: decays into BSM particles that are invisible to the detector because they do not appreciably interact with ordinary matter, decays into BSM particles that are not detected because they produce event topologies that are not searched for, or modifications of the decay branching fractions into SM particles in the case of channels that are not directly measured, such as $H \to cc$. Although direct and indirect experimental constraints on the Higgs boson width exist, they are either model dependent or are not stringent enough to constrain the present fits, and are therefore not included in the combinations. Since Γ_H is not experimentally constrained in a model-independent manner with sufficient precision, only ratios of coupling strengths can be measured in the most generic parameterisation considered in the κ-framework.

3. Combination procedure and experimental inputs

The individual ATLAS and CMS analyses of the Higgs boson production and decay rates are combined using the profile likelihood method described in Section 3.2. The combination is based on simultaneous fits to the data from both experiments taking into account the correlations between systematic uncertainties within each experiment and between the two experiments. The analyses included in the combination, the statistical procedure used, the treatment of systematic uncertainties, and the changes made to the analyses for the combination are summarised in this section.

3.1. Overview of input analyses

The individual analyses included in the combination were published separately by each experiment. Most of these analyses examine a specific Higgs boson decay mode, with categories related to the various production processes. They are $H \to \gamma\gamma$ [92, 93], $H \to ZZ$ [94, 95], $H \to WW$ [96–98], $H \to \tau\tau$ [99, 100], $H \to bb$ [101, 102], and $H \to \mu\mu$ [103, 104]. The ttH production process was also studied separately [78, 105–108] and the results are included in the combination. The $H \to \mu\mu$ analysis is included in the combination fit only for the measurement of the corresponding decay signal strength reported in Section 5.2 and for the specific parameterisation of the coupling analysis described in Section 6.2. It provides constraints on the coupling of the Higgs boson to second-generation fermions, but offers no relevant constraints for other parameterisations. The ATLAS [17] and CMS [18] individual combined publications

take into account other results, such as upper limits on the $H \to Z\gamma$ decay [109,110], results on VBF production in the $H \to bb$ decay channel [111], constraints on off-shell Higgs boson production [23,24], and upper limits on invisible Higgs boson decays [112–114]. These results are not considered further here since they were not included in both combined publications of the individual experiments. In the case of the $H \to bb$ decay mode, the ggF production process is not considered by either experiment because of the overwhelming QCD multijet background.

Almost all input analyses are based on the concept of event categorisation. For each decay mode, events are classified in different categories, based on their kinematic characteristics and their detailed properties. This categorisation increases the sensitivity of the analysis and also allows separation of the different production processes on the basis of exclusive selections that identify the decay products of the particles produced in association with the Higgs boson: W or Z boson decays, VBF jets, and so on. A total of approximately 600 exclusive categories addressing the five production processes explicitly considered are defined for the five main decay channels. The exception is $H \to bb$, for which only the VH and ttH production processes are used in the combination for the reasons stated above.

The signal yield in a category k, $n_{\text{signal}}(k)$, can be expressed as a sum over all possible Higgs boson production processes i, with cross section σ_i, and decay modes f, with branching fraction B^f:

$$
\begin{aligned}
n_{\text{signal}}(k) &= \mathcal{L}(k) \cdot \sum_i \sum_f \left\{ \sigma_i \cdot A_i^{f,SM}(k) \cdot \varepsilon_i^f(k) \cdot \mathrm{B}^f \right\} \\
&= \mathcal{L}(k) \cdot \sum_i \sum_f \mu_i \mu^f \left\{ \sigma_i^{\text{SM}} \cdot A_i^{f,SM}(k) \cdot \varepsilon_i^f(k) \cdot \mathrm{B}_{\text{SM}}^f \right\},
\end{aligned}
\tag{7}
$$

where $\mathcal{L}(k)$ represents the integrated luminosity, $A_i^{f,SM}(k)$ the detector acceptance assuming SM Higgs boson production and decay, and $\varepsilon_i^f(k)$ the overall selection efficiency for the signal category k. The symbols μ_i and μ^f are the production and decay signal strengths, respectively, defined in Section 2.3. As Eq. (7) shows, the measurements considered in this paper are only sensitive to the products of the cross sections and branching fractions, $\sigma_i \cdot \mathrm{B}^f$.

In the ideal case, each category would only contain signal events from a given production process and decay mode. Most decay modes approach this ideal case, but, in the case of the production processes, the categories are much less pure and there is significant cross-contamination in most channels.

3.2. Statistical treatment

The overall statistical methodology used in the combination to extract the parameters of interest in various parameterisations is the same as that used for the individual ATLAS and CMS combinations, as published in Refs. [17,18]. It was developed by the ATLAS and CMS Collaborations and is described in Ref. [115]. Some details of this procedure are important for this combination and are briefly reviewed here.

The statistical treatment of the data is based on the standard LHC data modelling and handling toolkits: RooFit [116], RooStats [117], and HistFactory [118]. The parameters of interest, $\vec{\alpha}$, e.g. signal strengths (μ), coupling modifiers (κ), production cross sections, branching fractions, or ratios of the above quantities, are estimated, together with their corresponding confidence intervals, via the profile likelihood ratio

test statistic $\Lambda(\vec{\alpha})$ [119]. The latter depends on one or more parameters of interest, as well as on the nuisance parameters, $\vec{\theta}$, which reflect various experimental or theoretical uncertainties:

$$\Lambda(\vec{\alpha}) = \frac{L(\vec{\alpha}, \hat{\hat{\vec{\theta}}}(\vec{\alpha}))}{L(\hat{\vec{\alpha}}, \hat{\vec{\theta}})}. \tag{8}$$

The likelihood functions in the numerator and denominator of this equation are constructed using products of signal and background probability density functions (pdfs) of the discriminating variables. The pdfs are obtained from simulation for the signal and from both data and simulation for the background, as described in Refs. [17, 18]. The vectors $\hat{\vec{\alpha}}$ and $\hat{\vec{\theta}}$ represent the unconditional maximum likelihood estimates of the parameter values, while $\hat{\hat{\vec{\theta}}}$ denotes the conditional maximum likelihood estimate for given values of the parameters of interest $\vec{\alpha}$. Systematic uncertainties and their correlations are a subset of the nuisance parameters $\vec{\theta}$, described by likelihood functions associated with the estimate of the corresponding parameter.

As an example of a specific choice of parameters of interest, the parameterisation considered in Section 6.4 assumes that all fermion couplings are scaled by κ_F and all weak vector boson couplings by κ_V. The likelihood ratio is therefore a function of the two parameters of interest, κ_F and κ_V, and the profile likelihood ratio is expressed as:

$$\Lambda(\kappa_F, \kappa_V) = \frac{L(\kappa_F, \kappa_V, \hat{\hat{\vec{\theta}}}(\kappa_F, \kappa_V))}{L(\hat{\kappa}_F, \hat{\kappa}_V, \hat{\vec{\theta}})}. \tag{9}$$

Likelihood fits are performed to determine the parameters of interest and their uncertainties, using the data to obtain the observed values and Asimov data sets to determine the predicted values in the SM. An Asimov data set [119] is a pseudo-data distribution that is equal to the signal plus background prediction for given values of the parameters of interest and of all nuisance parameters, and does not include statistical fluctuations. It is a representative data set of a given parameterisation that yields a result corresponding to the median of an ensemble of pseudo-experiments generated from the same parameterisation. A pre-fit Asimov data set is meant to represent the predictions of the theory, and all parameters are fixed to their estimates prior to the fit to the data.

These fits are rather challenging, involving many parameters of interest and a very large number of nuisance parameters. All the fit results were independently cross-checked to a very high level of precision by ATLAS and CMS, both for the combination and for the individual results. In particular, fine likelihood scans of all the parameters of interest were inspected to verify the convergence and stability of the fits.

For all results presented in this paper, unless otherwise stated, the negative log-likelihood estimator $q(\vec{\alpha}) = -2 \ln \Lambda(\vec{\alpha})$ is assumed to follow a χ^2 distribution (asymptotic approximation). The 1σ and 2σ confidence level (CL) intervals for one-dimensional measurements are defined by requiring $q(\alpha_i) = 1$ and $q(\alpha_i) = 4$, respectively. In the case of disjoint intervals, the uncertainties corresponding only to the interval around the best fit value with $q(\alpha_i) < 1$ are also given for some parameterisations. The 68% (95%) confidence level regions for two-dimensional scans are defined at $q(\alpha_i) = 2.30$ (5.99). For the derivation of the upper limit on B_{BSM} in Section 6.1, the test statistic $\tilde{t}(\alpha)$ of Ref. [119] is used to account for the constraint $\alpha = B_{BSM} \geq 0$. This is equivalent to the confidence interval estimation method of Ref. [120]. The upper limit at 95% CL corresponds to $\tilde{t}(\alpha) = 3.84$. The p-values, characterising the compatibility of a fit result with a given hypothesis, are likewise computed in the asymptotic approximation.

3.3. Treatment of systematic uncertainties

The treatment of the systematic uncertainties and of their correlations is a crucial aspect of the combination of Higgs boson coupling measurements. The details of the chosen methodology for treating systematic uncertainties, characterised by nuisance parameters, are given in Ref. [115]. The combined analysis presented here incorporates approximately 4200 nuisance parameters. A large fraction of these are statistical in nature, i.e. related to the finite size of the simulated samples used to model the expected signals and backgrounds, but are classified as part of the systematic uncertainties, as described below.

Nuisance parameters can be associated with a single analysis category or can be correlated between categories, channels, and/or experiments. A very important and delicate part of this combination is the estimation of the correlations between the various sources of systematic uncertainty, both between the various channels and between the two experiments. The correlations within each experiment are modelled following the procedure adopted for their individual combinations. The systematic uncertainties that are correlated between the two experiments are theoretical systematic uncertainties affecting the signal yield, certain theoretical systematic uncertainties in the background predictions, and a part of the experimental uncertainty related to the measurement of the integrated luminosity.

The main sources of theoretical uncertainties affecting the signal yield are the following: missing higher-order QCD corrections (estimated through variation of the QCD scales, i.e. renormalisation and factorisation scale) and uncertainties in parton distribution functions (PDF), in the treatment of UEPS, and in Higgs boson branching fractions. These uncertainties apply both to the inclusive cross sections and to the acceptances and selection efficiencies in the various categories. The PDF uncertainties in the inclusive rates are correlated between the two experiments for a given production process, but are treated as uncorrelated between different processes, except for the WH, ZH, and VBF production processes, where they are assumed to be fully correlated. A cross-check with the full PDF correlation matrix, as given in Ref. [32], yields differences no larger than 1% for the generic parameterisations discussed in Section 4. Similarly, QCD scale and UEPS uncertainties are assumed to be correlated between the two experiments in the same production processes and to be uncorrelated between different processes. The effects of correlations between Higgs boson branching fractions were determined to be negligible in general, and are ignored in the fits, except for the uncertainties in the branching fractions to WW and ZZ, which are assumed to be fully correlated. When measuring ratios, however, there are cases, e.g. the measurements of ratios of coupling modifiers described in Section 4.2, where such uncertainties become the dominant theoretical uncertainties, and in these cases the full branching fraction correlation model specified in Ref. [32] was applied. Other theoretical uncertainties in the signal acceptance and selection efficiencies are also usually small. They are estimated and treated in very different manners by the two experiments and therefore are assumed to be uncorrelated between ATLAS and CMS. It was verified that treating them as correlated would have a negligible impact on the results.

Whereas the signal selection criteria are quite inclusive in most channels, this is not the case for the backgrounds, which are often restricted to very limited regions of phase space and which are often treated differently by the two experiments. For these reasons, the ATLAS and CMS background modelling uncertainties cannot be easily correlated, even though such correlations should be considered for channels where they represent significant contributions to the overall systematic uncertainty. Obvious examples are those where the background estimates are obtained from simulation, as is the case for the ZZ continuum background in the $H \rightarrow ZZ$ channel, and for the ttW and ttZ backgrounds in the ttH multi-lepton channel. For these two cases, the background cross section uncertainties are treated as fully correlated between the two experiments. Other more complex examples are the WW continuum background in the $H \rightarrow WW$

channel, the *ttbb* background in the *ttH*, $H \rightarrow bb$ channel, and the *Wbb* background in the *WH*, $H \rightarrow bb$ channel. In these cases, it was verified that the choice of not implementing correlations in the background modelling uncertainties between the two experiments has only a small impact on the measurements. The most significant impact was found for the *ttbb* background in the *ttH*, $H \rightarrow bb$ channel, for which the choice of different correlation models between the two experiments yields an impact below 10% of the total uncertainty in the signal strength measurement in this specific channel.

Finally, all experimental systematic uncertainties are treated independently by the two experiments, reflecting independent assessments of these uncertainties, except for the integrated luminosity uncertainties, which are treated as partially correlated through the contribution arising from the imperfect knowledge of the beam currents in the LHC accelerator.

The various sources of uncertainties can be broadly classified in four groups:

1. uncertainties (labelled as "stat" in the following) that are statistical in nature. In addition to the data, these include the statistical uncertainties in certain background control regions and certain fit parameters used to describe backgrounds measured from data, but they exclude the finite size of MC simulation samples;

2. theoretical uncertainties affecting the Higgs boson signal (labelled as "thsig" in the following);

3. theoretical uncertainties affecting background processes only (these are not correlated with any of the signal theoretical uncertainties and are labelled as "thbgd" in the following);

4. all other uncertainties (labelled as "expt" in the following), which include the experimental uncertainties and those related to the finite size of the MC simulation samples.

Some of the results are provided with a full breakdown of the uncertainties into these four categories, but, in most cases, the uncertainties are divided only into their statistical and systematic (syst) components. In some cases, as in Section 4, when considering ratios of cross sections or coupling strengths, the theoretical systematic uncertainties are very small, because the signal normalisation uncertainties, which are in general dominant, do not affect the measurements. The precision with which the uncertainties and their components are quoted is typically of order 1% relative to the SM prediction.

As mentioned above, the Higgs boson mass is fixed, for all results reported in this paper, at the measured value of 125.09 GeV. The impact of the Higgs boson mass uncertainty (±0.24 GeV) on the measurements has two main sources. One is the dependence of the $\sigma \cdot B$ product on the mass. This dependence has an impact only on the measurements of the signal strengths and of the coupling modifiers, in which the SM signal yield predictions enter directly. The associated uncertainties are up to 4% for the signal strengths and 2% for the coupling modifiers. The other source of uncertainty is the dependence of the measured yields on the mass, arising from the fit to the mass spectra in the high-resolution $H \rightarrow \gamma\gamma$ and $H \rightarrow ZZ$ decay channels. In principle, this uncertainty affects all the measurements, including those related to the generic parameterisations, and is expected to be of the same order as the first one, namely 1% to 2%. In practice, since the measured masses in the $H \rightarrow \gamma\gamma$ and $H \rightarrow ZZ$ decay channels, resulting from the combination of ATLAS and CMS data, agree within 100 MeV, this uncertainty is less than 1% for all combined ATLAS and CMS measurements reported in this paper. Additional uncertainties of approximately 1% in the measurements of the Higgs boson signal strengths and coupling modifiers arise from the uncertainty in the LHC beam energy, which is estimated to be 0.66% at 8 TeV [121]. The uncertainties in the Higgs boson mass and the LHC beam energy are much smaller than the statistical uncertainties in the measurements and are neglected in the following.

3.4. Analysis modifications for the combination

There are some differences in the treatment of signal and background in the combined analysis compared to the published analyses from each experiment. The differences are larger for CMS than for ATLAS, mainly because the CMS analyses were published earlier, before some refinements for the SM Higgs boson predictions were made available. The main differences are the following:

- ATLAS now uses the Stewart-Tackmann prescription [48] for the jet bin uncertainties in the $H \to WW$ channel instead of the jet-veto-efficiency procedure [49];

- CMS now includes the bbH, tH, and $ggZH$ production processes in the signal model for all the channels in which they are relevant;

- CMS now uses the signal cross section calculations from Ref. [32] for all channels;

- CMS now adopts a unified prescription for the treatment of the Higgs boson p_T in the ggF production process, as described in Section 2.2;

- The cross sections for the dominant backgrounds were adjusted to the most recent theoretical calculations in the cases where they are estimated from simulation (ZZ background in the $H \to ZZ$ channel and ttZ and ttW backgrounds in the ttH channels);

- Both experiments have adopted the same correlation scheme for some of the signal theoretical uncertainties: for example, the treatment of the PDF uncertainties in the signal production cross sections now follows a common scheme for all decay channels, as described in Section 3.3.

The total effect of these modifications is small, both for the expected and observed results. All measurements differ from the individual combined results by less than approximately 10% of the total uncertainty for CMS and by even less for ATLAS.

Table 5 gives an overview of the Higgs boson decay and production processes that are combined in the following. To provide a snapshot of the relative importance of the various channels, the results from the analysis presented in this paper (Tables 12 and 13 in Section 5.2) are shown separately for each experiment, as measurements of the overall signal strengths μ, for each of the six decay channels and for the ttH production process. The total observed and expected statistical significances for $m_H = 125.09$ GeV are also shown, except for the $H \to \mu\mu$ channel, which has very low sensitivity. These results are quite close to those published for the individual analyses by each experiment, which are cited in Table 5. For several decay channels, these refer only to the most sensitive analyses, e.g. the VH analysis for the $H \to bb$ decay channel. Even though they are less sensitive, the ttH analyses have a contribution from all the decay channels, and this is one of the reasons for quoting this production process specifically in this table. As stated above, the differences between the analysis in this paper and the published ones are also in part due to the different values assumed for the Higgs boson mass, and to adjustments in the various analyses for the purposes of this combination, mostly in terms of the signal modelling and of the treatment of the correlations of the signal theoretical uncertainties between different channels.

4. Generic parameterisations of experimental results

This section describes three generic parameterisations and presents their results. The first two are based on cross sections and branching fractions, either expressed as independent products $\sigma_i \cdot B^f$ for each

Table 5: Overview of the decay channels analysed in this paper. The *ttH* production process, which has contributions from all decay channels, is also shown. To show the relative importance of the various channels, the results from the combined analysis presented in this paper for m_H = 125.09 GeV (Tables 12 and 13 in Section 5.2) are reported as observed signal strengths μ with their measured uncertainties. The expected uncertainties are shown in parentheses. Also shown are the observed statistical significances, together with the expected significances in parentheses, except for the $H \rightarrow \mu\mu$ channel, which has very low sensitivity. For most decay channels, only the most sensitive analyses are quoted as references, e.g. the *gg*F and VBF analyses for the $H \rightarrow WW$ decay channel or the *VH* analysis for the $H \rightarrow bb$ decay channel. Although not exactly the same, the results are close to those from the individual publications, in which slightly different values for the Higgs boson mass were assumed and in which the signal modelling and signal uncertainties were slightly different, as discussed in the text.

Channel	References for individual publications		Signal strength [μ] from results in this paper (Section 5.2)		Signal significance [σ]	
	ATLAS	CMS	ATLAS	CMS	ATLAS	CMS
$H \rightarrow \gamma\gamma$	[92]	[93]	$1.14^{+0.27}_{-0.25}$ $\left(^{+0.26}_{-0.24}\right)$	$1.11^{+0.25}_{-0.23}$ $\left(^{+0.23}_{-0.21}\right)$	5.0 (4.6)	5.6 (5.1)
$H \rightarrow ZZ$	[94]	[95]	$1.52^{+0.40}_{-0.34}$ $\left(^{+0.32}_{-0.27}\right)$	$1.04^{+0.32}_{-0.26}$ $\left(^{+0.30}_{-0.25}\right)$	7.6 (5.6)	7.0 (6.8)
$H \rightarrow WW$	[96, 97]	[98]	$1.22^{+0.23}_{-0.21}$ $\left(^{+0.21}_{-0.20}\right)$	$0.90^{+0.23}_{-0.21}$ $\left(^{+0.23}_{-0.20}\right)$	6.8 (5.8)	4.8 (5.6)
$H \rightarrow \tau\tau$	[99]	[100]	$1.41^{+0.40}_{-0.36}$ $\left(^{+0.37}_{-0.33}\right)$	$0.88^{+0.30}_{-0.28}$ $\left(^{+0.31}_{-0.29}\right)$	4.4 (3.3)	3.4 (3.7)
$H \rightarrow bb$	[101]	[102]	$0.62^{+0.37}_{-0.37}$ $\left(^{+0.39}_{-0.37}\right)$	$0.81^{+0.45}_{-0.43}$ $\left(^{+0.45}_{-0.43}\right)$	1.7 (2.7)	2.0 (2.5)
$H \rightarrow \mu\mu$	[103]	[104]	$-0.6^{+3.6}_{-3.6}$ $\left(^{+3.6}_{-3.6}\right)$	$0.9^{+3.6}_{-3.5}$ $\left(^{+3.3}_{-3.2}\right)$		
ttH production	[78, 105, 106]	[108]	$1.9^{+0.8}_{-0.7}$ $\left(^{+0.7}_{-0.7}\right)$	$2.9^{+1.0}_{-0.9}$ $\left(^{+0.9}_{-0.8}\right)$	2.7 (1.6)	3.6 (1.3)

channel $i \rightarrow H \rightarrow f$, or as ratios of cross sections and branching fractions plus one reference $\sigma_i \cdot$ B^f product. In these parameterisations, the theoretical uncertainties in the signal inclusive cross sections for the various production processes do not affect the measured observables, in contrast to measurements of signal strengths, such as those described in Section 2.3. These analyses lead to the most model-independent results presented in this paper and test, with minimal assumptions, the compatibility of the measurements with the SM. The third generic parameterisation is derived from the one described in Section 2.4 and is based on ratios of coupling modifiers. None of these parameterisations incorporate any assumption about the Higgs boson total width other than the narrow-width approximation. Some theoretical and experimental systematic uncertainties largely cancel in the parameterisations involving ratios but at the current level of sensitivity the impact is small.

Table 6 gives an overview of the parameters of interest for the two generic parameterisations involving ratios which are described in more detail in Sections 4.1.2 and 4.2. The first row makes explicit that the $gg \rightarrow H \rightarrow ZZ$ channel is chosen as a reference. The $\lambda_{Zg} = \kappa_Z/\kappa_g$ term in the fourth row is related to the ratio of the *ZH* and *gg*F production cross sections. Once $\lambda_{WZ} = \kappa_W/\kappa_Z$ is also specified, the VBF, *WH*,

Table 6: Parameters of interest in the two generic parameterisations described in Sections 4.1.2 and 4.2. For both parameterisations, the $gg \rightarrow H \rightarrow ZZ$ channel is chosen as a reference, expressed through the first row in the table. All other measurements are expressed as ratios of cross sections or branching fractions in the first column and of coupling modifiers in the second column. There are fewer parameters of interest in the case of the coupling parameterisation, in which the ratios of cross sections for the WH, ZH, and VBF processes can all be expressed as functions of the two parameters, λ_{Zg} and λ_{WZ}. The slightly different additional assumptions in each parameterisation are discussed in the text.

σ and B ratio parameterisation	Coupling modifier ratio parameterisation
$\sigma(gg \rightarrow H \rightarrow ZZ)$	$\kappa_{gZ} = \kappa_g \cdot \kappa_Z / \kappa_H$
$\sigma_{\mathrm{VBF}} / \sigma_{ggF}$	
$\sigma_{WH} / \sigma_{ggF}$	
$\sigma_{ZH} / \sigma_{ggF}$	$\lambda_{Zg} = \kappa_Z / \kappa_g$
$\sigma_{ttH} / \sigma_{ggF}$	$\lambda_{tg} = \kappa_t / \kappa_g$
$\mathrm{B}^{WW} / \mathrm{B}^{ZZ}$	$\lambda_{WZ} = \kappa_W / \kappa_Z$
$\mathrm{B}^{\gamma\gamma} / \mathrm{B}^{ZZ}$	$\lambda_{\gamma Z} = \kappa_\gamma / \kappa_Z$
$\mathrm{B}^{\tau\tau} / \mathrm{B}^{ZZ}$	$\lambda_{\tau Z} = \kappa_\tau / \kappa_Z$
$\mathrm{B}^{bb} / \mathrm{B}^{ZZ}$	$\lambda_{bZ} = \kappa_b / \kappa_Z$

and ZH production cross sections are fully defined. This explains the smaller number of independent parameters of interest in the coupling modifier ratio parameterisation compared to the parameterisation based mostly on ratios of cross sections and branching fractions. In addition, these two parameterisations rely on slightly different assumptions and approximations, which are summarised in Sections 2.3 and 2.4. These approximations are due to the fact that one cannot experimentally constrain all possible Higgs boson production processes and decay modes, in particular those that are expected to be small in the SM, but might be enhanced, should specific BSM physics scenarios be realised in nature.

4.1. Parameterisations using cross sections and branching fractions

4.1.1. Parameterisation using independent products of cross sections and branching fractions

In a very generic approach, one can extract for each specific channel $i \rightarrow H \rightarrow f$ a measurement of the product $\sigma_i \cdot \mathrm{B}^f$ and then compare it to the theoretical prediction. Based on all the categories considered in the various analyses and on the five production processes (ggF, VBF, WH, ZH, and ttH) and five main decay channels ($H \rightarrow ZZ$, $H \rightarrow WW$, $H \rightarrow \gamma\gamma$, $H \rightarrow \tau\tau$, and $H \rightarrow bb$) considered in this paper, there are in principle 25 such independent products to be measured. In practice, as already mentioned, the ggF and VBF production processes are not probed in the case of the $H \rightarrow bb$ decay mode and are assumed to have the values predicted by the SM, so the fit is performed with 23 parameters of interest, which are specified in Table 7. The individual experiments cannot provide constraints on all the parameters of interest because of the low overall expected and observed yields in the current data. Even when combining the ATLAS and CMS data, the ZH, WH, and ttH production processes cannot be measured with meaningful precision

Table 7: The signal parameterisation used to express the $\sigma_i \cdot \mathrm{B}^f$ values for each specific channel $i \to H \to f$. The values labelled with a "−" are not measured and are therefore fixed to the SM predictions.

Production process	Decay channel				
	$H \to \gamma\gamma$	$H \to ZZ$	$H \to WW$	$H \to \tau\tau$	$H \to bb$
ggF	$(\sigma \cdot \mathrm{B})_{gg\mathrm{F}}^{\gamma\gamma}$	$(\sigma \cdot \mathrm{B})_{gg\mathrm{F}}^{ZZ}$	$(\sigma \cdot \mathrm{B})_{gg\mathrm{F}}^{WW}$	$(\sigma \cdot \mathrm{B})_{gg\mathrm{F}}^{\tau\tau}$	−
VBF	$(\sigma \cdot \mathrm{B})_{\mathrm{VBF}}^{\gamma\gamma}$	$(\sigma \cdot \mathrm{B})_{\mathrm{VBF}}^{ZZ}$	$(\sigma \cdot \mathrm{B})_{\mathrm{VBF}}^{WW}$	$(\sigma \cdot \mathrm{B})_{\mathrm{VBF}}^{\tau\tau}$	−
WH	$(\sigma \cdot \mathrm{B})_{WH}^{\gamma\gamma}$	$(\sigma \cdot \mathrm{B})_{WH}^{ZZ}$	$(\sigma \cdot \mathrm{B})_{WH}^{WW}$	$(\sigma \cdot \mathrm{B})_{WH}^{\tau\tau}$	$(\sigma \cdot \mathrm{B})_{WH}^{bb}$
ZH	$(\sigma \cdot \mathrm{B})_{ZH}^{\gamma\gamma}$	$(\sigma \cdot \mathrm{B})_{ZH}^{ZZ}$	$(\sigma \cdot \mathrm{B})_{ZH}^{WW}$	$(\sigma \cdot \mathrm{B})_{ZH}^{\tau\tau}$	$(\sigma \cdot \mathrm{B})_{ZH}^{bb}$
ttH	$(\sigma \cdot \mathrm{B})_{ttH}^{\gamma\gamma}$	$(\sigma \cdot \mathrm{B})_{ttH}^{ZZ}$	$(\sigma \cdot \mathrm{B})_{ttH}^{WW}$	$(\sigma \cdot \mathrm{B})_{ttH}^{\tau\tau}$	$(\sigma \cdot \mathrm{B})_{ttH}^{bb}$

in the $H \to ZZ$ decay channel. The fit results are therefore quoted only for the remaining 20 parameters and for the combined ATLAS and CMS data.

Table 8 presents, for the combination of ATLAS and CMS, the fit results for each $\sigma_i \cdot \mathrm{B}^f$ product along with its statistical and systematic uncertainties. The corresponding SM predictions are also given. The ratios of the fit results to SM predictions are included in Table 8 and displayed in Fig. 7. Figure 7 additionally shows the theoretical uncertainties in the SM predictions for the fitted parameters. In almost all cases, the dominant uncertainty is statistical. The results presented in Table 8 and Fig. 7 clearly exhibit which decay modes are probed best for each production process, and conversely which production processes are probed best for each decay mode. With the current sensitivity of the combination, six of the $\sigma_i \cdot \mathrm{B}^f$ products can be measured with a precision better than 40%, namely the $H \to \gamma\gamma$, $H \to ZZ$, and $H \to WW$ decay modes for the ggF production process, and the $H \to \gamma\gamma$, $H \to WW$, and $H \to \tau\tau$ decay modes for the VBF production process. Because of the sizeable cross-contamination between the ggF and VBF categories, the corresponding results are significantly anticorrelated, as illustrated by the measured correlation matrix in Fig. 27 of Appendix A.

4.1.2. Parameterisation using ratios of cross sections and branching fractions

If there is only one Higgs boson, each row or column in Table 7 can be derived from the others by identical ratios of cross sections for the rows and of branching fractions for the columns. Therefore, in a second generic approach, ratios of cross sections and of branching fractions can be extracted from a combined fit to the data by normalising the yield of any specific channel $i \to H \to f$ to a reference process. In this paper, the $gg \to H \to ZZ$ channel is chosen as the reference because it has very little background and is one of the channels with the smallest overall and systematic uncertainties. The $gg \to H \to WW$ channel, which has the smallest overall uncertainty but larger systematic uncertainties, is used as an alternate reference for comparison, and the corresponding results are reported in Appendix B.

The product of the cross section and the branching fraction of $i \to H \to f$ can then be expressed using the ratios as:

$$\sigma_i \cdot \mathrm{B}^f = \sigma(gg \to H \to ZZ) \cdot \left(\frac{\sigma_i}{\sigma_{gg\mathrm{F}}}\right) \cdot \left(\frac{\mathrm{B}^f}{\mathrm{B}^{ZZ}}\right), \qquad (10)$$

where $\sigma(gg \to H \to ZZ) = \sigma_{gg\mathrm{F}} \cdot \mathrm{B}^{ZZ}$ in the narrow-width approximation. With $\sigma(gg \to H \to ZZ)$ constraining the overall normalisation, the ratios in Eq. (10) can be determined separately, based on the

Table 8: Best fit values of $\sigma_i \cdot B^f$ for each specific channel $i \to H \to f$, as obtained from the generic parameterisation with 23 parameters for the combination of the ATLAS and CMS measurements, using the $\sqrt{s}$ = 7 and 8 TeV data. The cross sections are given for $\sqrt{s}$ = 8 TeV, assuming the SM values for $\sigma_i(7\,\text{TeV})/\sigma_i(8\,\text{TeV})$. The results are shown together with their total uncertainties and their breakdown into statistical and systematic components. The expected uncertainties in the measurements are displayed in parentheses. The SM predictions [32] and the ratios of the results to these SM predictions are also shown. The values labelled with a "−" are either not measured with a meaningful precision and therefore not quoted, in the case of the $H \to ZZ$ decay channel for the WH, ZH, and ttH production processes, or not measured at all and therefore fixed to their corresponding SM predictions, in the case of the $H \to bb$ decay mode for the ggF and VBF production processes.

Production process		H → γγ [fb] Best fit value	Unc. Stat	Unc. Syst	H → ZZ [fb] Best fit value	Unc. Stat	Unc. Syst	H → WW [pb] Best fit value	Unc. Stat	Unc. Syst	H → ττ [fb] Best fit value	Unc. Stat	Unc. Syst	H → bb [pb] Best fit value	Unc. Stat	Unc. Syst
ggF	Measured	$48.0^{+10.0}_{-9.7}$	$^{+9.4}_{-9.4}$	$^{+3.2}_{-2.3}$	580^{+170}_{-160}	$^{+170}_{-160}$	$^{+40}_{-40}$	$3.5^{+0.7}_{-0.7}$	$^{+0.5}_{-0.5}$	$^{+0.5}_{-0.5}$	1300^{+700}_{-700}	$^{+400}_{-400}$	$^{+500}_{-500}$	–		
	(expected)	$\left(^{+9.7}_{-9.5}\right)$	$\left(^{+9.4}_{-9.4}\right)$	$\left(^{+2.5}_{-1.6}\right)$	$\left(^{+150}_{-130}\right)$	$\left(^{+140}_{-130}\right)$	$\left(^{+30}_{-20}\right)$	$\left(^{+0.7}_{-0.7}\right)$	$\left(^{+0.5}_{-0.5}\right)$	$\left(^{+0.5}_{-0.5}\right)$	$\left(^{+700}_{-700}\right)$	$\left(^{+400}_{-400}\right)$	$\left(^{+500}_{-500}\right)$	–		
	Predicted	44 ± 5			510 ± 60			4.1 ± 0.5			1210 ± 140			11.0 ± 1.2		
	Ratio	$1.10^{+0.23}_{-0.22}$	$^{+0.22}_{-0.21}$	$^{+0.07}_{-0.05}$	$1.13^{+0.34}_{-0.31}$	$^{+0.33}_{-0.30}$	$^{+0.09}_{-0.07}$	$0.84^{+0.17}_{-0.17}$	$^{+0.12}_{-0.12}$	$^{+0.12}_{-0.11}$	$1.0^{+0.6}_{-0.6}$	$^{+0.4}_{-0.4}$	$^{+0.4}_{-0.4}$	–		
VBF	Measured	$4.6^{+1.9}_{-1.8}$	$^{+1.8}_{-1.7}$	$^{+0.6}_{-0.5}$	3^{+46}_{-26}	$^{+46}_{-25}$	$^{+7}_{-7}$	$0.39^{+0.14}_{-0.13}$	$^{+0.13}_{-0.12}$	$^{+0.07}_{-0.05}$	125^{+39}_{-37}	$^{+34}_{-32}$	$^{+19}_{-18}$	–		
	(expected)	$\left(^{+1.8}_{-1.6}\right)$	$\left(^{+1.7}_{-1.6}\right)$	$\left(^{+0.5}_{-0.4}\right)$	$\left(^{+60}_{-39}\right)$	$\left(^{+60}_{-39}\right)$	$\left(^{+8}_{-5}\right)$	$\left(^{+0.15}_{-0.13}\right)$	$\left(^{+0.13}_{-0.12}\right)$	$\left(^{+0.07}_{-0.06}\right)$	$\left(^{+39}_{-37}\right)$	$\left(^{+34}_{-32}\right)$	$\left(^{+19}_{-18}\right)$	–		
	Predicted	3.60 ± 0.20			42.2 ± 2.0			0.341 ± 0.017			100 ± 6			0.91 ± 0.04		
	Ratio	$1.3^{+0.5}_{-0.5}$	$^{+0.5}_{-0.5}$	$^{+0.2}_{-0.1}$	$0.1^{+1.1}_{-0.6}$	$^{+1.1}_{-0.6}$	$^{+0.2}_{-0.2}$	$1.2^{+0.4}_{-0.4}$	$^{+0.4}_{-0.3}$	$^{+0.2}_{-0.2}$	$1.3^{+0.4}_{-0.4}$	$^{+0.3}_{-0.3}$	$^{+0.2}_{-0.2}$	–		
WH	Measured	$0.7^{+2.1}_{-1.9}$	$^{+2.1}_{-1.8}$	$^{+0.3}_{-0.3}$	–			$0.24^{+0.18}_{-0.16}$	$^{+0.15}_{-0.14}$	$^{+0.10}_{-0.08}$	-64^{+64}_{-61}	$^{+55}_{-50}$	$^{+32}_{-34}$	$0.42^{+0.21}_{-0.20}$	$^{+0.17}_{-0.16}$	$^{+0.12}_{-0.11}$
	(expected)	$\left(^{+1.9}_{-1.8}\right)$	$\left(^{+1.9}_{-1.8}\right)$	$\left(^{+0.1}_{-0.1}\right)$	–			$\left(^{+0.16}_{-0.14}\right)$	$\left(^{+0.14}_{-0.13}\right)$	$\left(^{+0.08}_{-0.07}\right)$	$\left(^{+67}_{-64}\right)$	$\left(^{+60}_{-54}\right)$	$\left(^{+30}_{-32}\right)$	$\left(^{+0.22}_{-0.21}\right)$	$\left(^{+0.18}_{-0.17}\right)$	$\left(^{+0.12}_{-0.11}\right)$
	Predicted	1.60 ± 0.09			18.8 ± 0.9			0.152 ± 0.007			44.3 ± 2.8			0.404 ± 0.017		
	Ratio	$0.5^{+1.3}_{-1.2}$	$^{+1.3}_{-1.1}$	$^{+0.2}_{-0.2}$	–			$1.6^{+1.2}_{-1.0}$	$^{+1.0}_{-0.9}$	$^{+0.6}_{-0.5}$	$-1.4^{+1.4}_{-1.4}$	$^{+1.2}_{-1.1}$	$^{+0.7}_{-0.8}$	$1.0^{+0.5}_{-0.5}$	$^{+0.4}_{-0.4}$	$^{+0.3}_{-0.3}$
ZH	Measured	$0.5^{+2.9}_{-2.4}$	$^{+2.8}_{-2.3}$	$^{+0.5}_{-0.2}$	–			$0.53^{+0.23}_{-0.20}$	$^{+0.21}_{-0.19}$	$^{+0.10}_{-0.07}$	58^{+56}_{-47}	$^{+52}_{-44}$	$^{+20}_{-16}$	$0.08^{+0.09}_{-0.09}$	$^{+0.08}_{-0.08}$	$^{+0.04}_{-0.04}$
	(expected)	$\left(^{+2.3}_{-1.9}\right)$	$\left(^{+2.3}_{-1.9}\right)$	$\left(^{+0.1}_{-0.1}\right)$	–			$\left(^{+0.17}_{-0.14}\right)$	$\left(^{+0.16}_{-0.14}\right)$	$\left(^{+0.05}_{-0.04}\right)$	$\left(^{+49}_{-40}\right)$	$\left(^{+46}_{-38}\right)$	$\left(^{+16}_{-12}\right)$	$\left(^{+0.10}_{-0.09}\right)$	$\left(^{+0.09}_{-0.08}\right)$	$\left(^{+0.05}_{-0.04}\right)$
	Predicted	0.94 ± 0.06			11.1 ± 0.6			0.089 ± 0.005			26.1 ± 1.8			0.238 ± 0.012		
	Ratio	$0.5^{+3.0}_{-2.5}$	$^{+3.0}_{-2.5}$	$^{+0.5}_{-0.2}$	–			$5.9^{+2.6}_{-2.2}$	$^{+2.3}_{-2.1}$	$^{+1.1}_{-0.8}$	$2.2^{+2.2}_{-1.8}$	$^{+2.0}_{-1.7}$	$^{+0.8}_{-0.6}$	$0.4^{+0.4}_{-0.4}$	$^{+0.3}_{-0.3}$	$^{+0.2}_{-0.2}$
ttH	Measured	$0.64^{+0.48}_{-0.38}$	$^{+0.48}_{-0.38}$	$^{+0.07}_{-0.04}$	–			$0.14^{+0.05}_{-0.05}$	$^{+0.04}_{-0.04}$	$^{+0.03}_{-0.03}$	-15^{+30}_{-26}	$^{+26}_{-22}$	$^{+15}_{-15}$	$0.08^{+0.07}_{-0.07}$	$^{+0.04}_{-0.04}$	$^{+0.06}_{-0.06}$
	(expected)	$\left(^{+0.45}_{-0.34}\right)$	$\left(^{+0.44}_{-0.33}\right)$	$\left(^{+0.10}_{-0.05}\right)$	–			$\left(^{+0.04}_{-0.04}\right)$	$\left(^{+0.04}_{-0.04}\right)$	$\left(^{+0.02}_{-0.02}\right)$	$\left(^{+31}_{-26}\right)$	$\left(^{+26}_{-22}\right)$	$\left(^{+16}_{-13}\right)$	$\left(^{+0.07}_{-0.06}\right)$	$\left(^{+0.04}_{-0.04}\right)$	$\left(^{+0.06}_{-0.05}\right)$
	Predicted	0.294 ± 0.035			3.4 ± 0.4			0.0279 ± 0.0032			8.1 ± 1.0			0.074 ± 0.008		
	Ratio	$2.2^{+1.6}_{-1.3}$	$^{+1.6}_{-1.3}$	$^{+0.2}_{-0.1}$	–			$5.0^{+1.8}_{-1.7}$	$^{+1.5}_{-1.5}$	$^{+1.0}_{-0.9}$	$-1.9^{+3.7}_{-3.3}$	$^{+3.2}_{-2.7}$	$^{+1.9}_{-1.8}$	$1.1^{+1.0}_{-1.0}$	$^{+0.5}_{-0.5}$	$^{+0.8}_{-0.8}$

five production processes (ggF, VBF, WH, ZH, and ttH) and five decay modes ($H \to ZZ$, $H \to WW$, $H \to \gamma\gamma$, $H \to \tau\tau$, and $H \to bb$). The combined fit results can be presented as a function of nine parameters of interest: one reference cross section times branching fraction, $\sigma(gg \to H \to ZZ)$, four ratios of production cross sections, σ_i/σ_{ggF}, and four ratios of branching fractions, B^f/B^{ZZ}, as reported in the left column of Table 6.
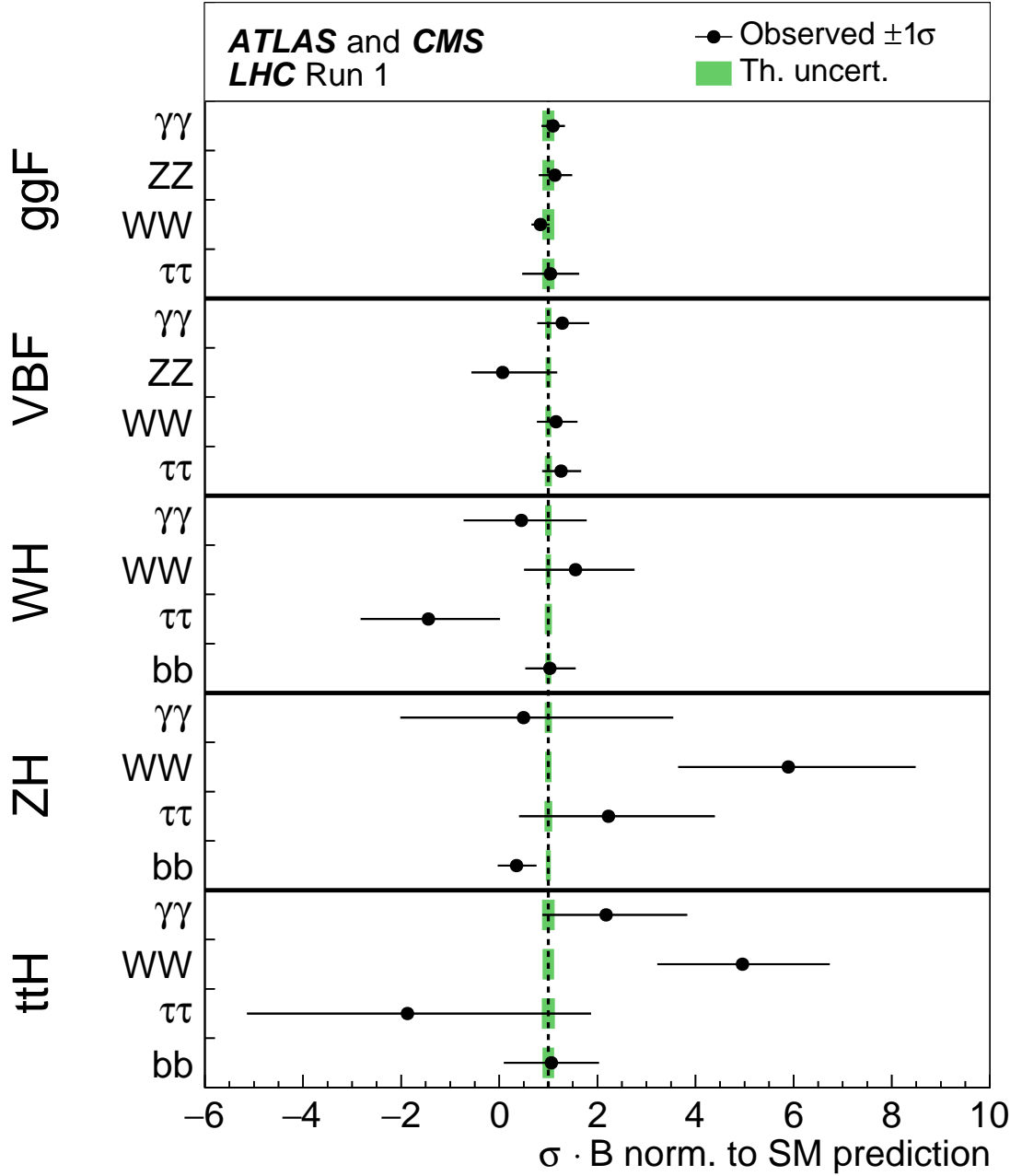
Figure 7: Best fit values of $\sigma_i \cdot B^f$ for each specific channel $i \to H \to f$, as obtained from the generic parameterisation with 23 parameters for the combination of the ATLAS and CMS measurements. The error bars indicate the 1σ intervals. The fit results are normalised to the SM predictions for the various parameters and the shaded bands indicate the theoretical uncertainties in these predictions. Only 20 parameters are shown because some are either not measured with a meaningful precision, in the case of the $H \to ZZ$ decay channel for the WH, ZH, and ttH production processes, or not measured at all and therefore fixed to their corresponding SM predictions, in the case of the $H \to bb$ decay mode for the ggF and VBF production processes.

Expressing the measurements through ratios of cross sections and branching fractions has the advantage that the ratios are independent of the theoretical predictions for the inclusive production cross sections and decay branching fractions of the Higgs boson. In particular, they are not subject to the dominant signal theoretical uncertainties in the inclusive cross sections for the various production processes. These measurements will therefore remain valid when, for example, improved theoretical calculations of Higgs boson production cross sections become available. The remaining theoretical uncertainties are those related to the acceptances and selection efficiencies in the various categories, for which SM Higgs boson production and decay kinematics are assumed in the simulation, based on the MC generators discussed in Section 2.2.

Table 9 shows the results of the fit to the data with a breakdown of the uncertainties into their statistical and systematic components. The full breakdown of the uncertainties into the four components is shown in Table 20 of Appendix B, while the measured correlation matrix can be found in Fig. 28 of Appendix A. The results are shown for the combination of ATLAS and CMS and also separately for each experiment. They are illustrated in Fig. 8, where the fit result for each parameter is normalised to the corresponding SM prediction. Also shown in Fig. 8 are the theoretical uncertainties in the SM predictions for the fitted parameters. For the ratios of branching fractions, the theoretical uncertainties in the predictions are barely visible since they are below 5%. Compared to the results of the fit of Table 8, where the ggF parameters are independent for each decay mode, the uncertainties in $\sigma(gg \to H \to ZZ)$ are reduced by almost a factor of two in Table 9, owing to the contributions from the other decay channels (mainly $H \to \gamma\gamma$ and $H \to WW$). The total uncertainty in $\sigma(gg \to H \to ZZ)$ is approximately 18%, with its main contribution coming from the statistical uncertainty. The total relative systematic uncertainty is only ~4%. Appendix B shows the results obtained when choosing the $H \to WW$ decay mode as an alternative reference process. This yields a smaller total uncertainty of approximately 15% in $\sigma(gg \to H \to WW)$, but with a much larger contribution of ~11% from the systematic uncertainties. The ratios $\sigma_{VBF}/\sigma_{ggF}$, B^{WW}/B^{ZZ}, $B^{\gamma\gamma}/B^{ZZ}$, and $B^{\tau\tau}/B^{ZZ}$ are measured with relative uncertainties of 30–40%.

The p-value of the compatibility between the data and the SM predictions is 16%. Most measurements are consistent with the SM predictions within less than 2σ; however, the production cross section ratio $\sigma_{ttH}/\sigma_{ggF}$ relative to the SM ratio is measured to be $3.3^{+1.0}_{-0.9}$, corresponding to an excess of approximately 3.0σ relative to the SM prediction. This excess is mainly due to the multi-lepton categories. The ratio σ_{ZH}/σ_{ggF} relative to the SM ratio is measured to be $3.2^{+1.8}_{-1.4}$, with the observed excess mainly due to the ZH, $H \to WW$ measurements. The ratio of branching fractions B^{bb}/B^{ZZ} is measured to be $0.19^{+0.21}_{-0.12}$ relative to the SM prediction. In this parameterisation, the high values found for the production cross section ratios for the ZH and ttH processes induce a low value for the $H \to bb$ decay branching fraction because the $H \to bb$ decay mode does not contribute to the observed excesses. The likelihood scan of the B^{bb}/B^{ZZ} parameter is very asymmetric, as shown in Fig. 9, resulting in an overall deficit of approximately 2.5σ relative to the SM prediction. This deviation is anticorrelated with the ones quoted above for the $\sigma_{ttH}/\sigma_{ggF}$ and σ_{ZH}/σ_{ggF} production cross section ratios, as shown in Fig. 28 of Appendix A.

In the various fits, the combination of the 7 and 8 TeV data is performed assuming that the ratios of the production cross sections at 7 and 8 TeV are the same as in the SM. One can introduce as free parameters in the fit the ratios of the production cross sections at 7 and 8 TeV of the five main production processes: $\sigma_i(7\text{TeV})/\sigma_i(8\text{TeV})$. Given the limited size of the data samples at 7 TeV, only the ggF and VBF ratios can be extracted with a meaningful precision. The results are: $\sigma_{ggF}(7 \text{ TeV})/\sigma_{ggF}(8 \text{ TeV}) = 1.12^{+0.33}_{-0.29}$ and $\sigma_{VBF}(7 \text{ TeV})/\sigma_{VBF}(8 \text{ TeV}) = 0.37^{+0.49}_{-0.43}$. Both values are consistent with the SM predictions of $\sigma_{ggF}(7 \text{ TeV})/\sigma_{ggF}(8 \text{ TeV}) = 0.78$ and $\sigma_{VBF}(7 \text{ TeV})/\sigma_{VBF}(8 \text{ TeV}) = 0.77$.

Table 9: Best fit values of $\sigma(gg \to H \to ZZ)$, σ_i/σ_{ggF}, and B^f/B^{ZZ}, as obtained from the generic parameterisation with nine parameters for the combined analysis of the $\sqrt{s}$ = 7 and 8 TeV data. The values involving cross sections are given for $\sqrt{s}$ = 8 TeV, assuming the SM values for $\sigma_i(7\,\text{TeV})/\sigma_i(8\,\text{TeV})$. The results are reported for the combination of ATLAS and CMS and also separately for each experiment, together with their total uncertainties and their breakdown into statistical and systematic components. The expected uncertainties in the measurements are displayed in parentheses. The SM predictions [32] are also shown with their total uncertainties.

Parameter	SM prediction	Best fit value	Uncertainty Stat	Syst	Best fit value	Uncertainty Stat	Syst	Best fit value	Uncertainty Stat	Syst
		ATLAS+CMS			ATLAS			CMS		
$\sigma(gg \to$ $H \to ZZ)$ [pb]	0.51 ±0.06	$0.59\,^{+0.11}_{-0.10}$ $\left(^{+0.11}_{-0.10}\right)$	$^{+0.11}_{-0.10}$ $\left(^{+0.11}_{-0.09}\right)$	$^{+0.02}_{-0.02}$ $\left(^{+0.03}_{-0.02}\right)$	$0.77\,^{+0.19}_{-0.17}$ $\left(^{+0.16}_{-0.14}\right)$	$^{+0.19}_{-0.16}$ $\left(^{+0.16}_{-0.13}\right)$	$^{+0.05}_{-0.03}$ $\left(^{+0.03}_{-0.02}\right)$	$0.44\,^{+0.14}_{-0.12}$ $\left(^{+0.15}_{-0.13}\right)$	$^{+0.13}_{-0.11}$ $\left(^{+0.15}_{-0.13}\right)$	$^{+0.05}_{-0.03}$ $\left(^{+0.04}_{-0.03}\right)$
$\sigma_{\text{VBF}}/\sigma_{ggF}$	0.082 ±0.009	$0.109\,^{+0.034}_{-0.027}$ $\left(^{+0.029}_{-0.024}\right)$	$^{+0.029}_{-0.024}$ $\left(^{+0.024}_{-0.020}\right)$	$^{+0.018}_{-0.013}$ $\left(^{+0.016}_{-0.014}\right)$	$0.079\,^{+0.035}_{-0.026}$ $\left(^{+0.042}_{-0.031}\right)$	$^{+0.030}_{-0.023}$ $\left(^{+0.036}_{-0.028}\right)$	$^{+0.019}_{-0.012}$ $\left(^{+0.022}_{-0.014}\right)$	$0.138\,^{+0.073}_{-0.051}$ $\left(^{+0.043}_{-0.033}\right)$	$^{+0.061}_{-0.046}$ $\left(^{+0.037}_{-0.029}\right)$	$^{+0.039}_{-0.023}$ $\left(^{+0.023}_{-0.015}\right)$
σ_{WH}/σ_{ggF}	0.037 ±0.004	$0.031\,^{+0.028}_{-0.026}$ $\left(^{+0.021}_{-0.017}\right)$	$^{+0.024}_{-0.022}$ $\left(^{+0.019}_{-0.015}\right)$	$^{+0.015}_{-0.014}$ $\left(^{+0.011}_{-0.007}\right)$	$0.054\,^{+0.036}_{-0.026}$ $\left(^{+0.033}_{-0.022}\right)$	$^{+0.031}_{-0.023}$ $\left(^{+0.029}_{-0.020}\right)$	$^{+0.020}_{-0.013}$ $\left(^{+0.015}_{-0.009}\right)$	$0.005\,^{+0.044}_{-0.037}$ $\left(^{+0.032}_{-0.022}\right)$	$^{+0.037}_{-0.028}$ $\left(^{+0.027}_{-0.020}\right)$	$^{+0.023}_{-0.024}$ $\left(^{+0.017}_{-0.010}\right)$
σ_{ZH}/σ_{ggF}	0.0216 ±0.0024	$0.066\,^{+0.039}_{-0.031}$ $\left(^{+0.016}_{-0.011}\right)$	$^{+0.032}_{-0.025}$ $\left(^{+0.014}_{-0.010}\right)$	$^{+0.023}_{-0.018}$ $\left(^{+0.009}_{-0.004}\right)$	$0.013\,^{+0.028}_{-0.014}$ $\left(^{+0.027}_{-0.014}\right)$	$^{+0.021}_{-0.012}$ $\left(^{+0.023}_{-0.013}\right)$	$^{+0.018}_{-0.007}$ $\left(^{+0.014}_{-0.005}\right)$	$0.123\,^{+0.076}_{-0.053}$ $\left(^{+0.024}_{-0.013}\right)$	$^{+0.063}_{-0.046}$ $\left(^{+0.020}_{-0.012}\right)$	$^{+0.044}_{-0.026}$ $\left(^{+0.014}_{-0.006}\right)$
$\sigma_{ttH}/\sigma_{ggF}$	0.0067 ±0.0010	$0.022\,^{+0.007}_{-0.006}$ $\left(^{+0.004}_{-0.004}\right)$	$^{+0.005}_{-0.005}$ $\left(^{+0.003}_{-0.003}\right)$	$^{+0.004}_{-0.003}$ $\left(^{+0.003}_{-0.002}\right)$	$0.013\,^{+0.007}_{-0.005}$ $\left(^{+0.006}_{-0.004}\right)$	$^{+0.005}_{-0.004}$ $\left(^{+0.005}_{-0.004}\right)$	$^{+0.004}_{-0.003}$ $\left(^{+0.004}_{-0.003}\right)$	$0.034\,^{+0.016}_{-0.012}$ $\left(^{+0.007}_{-0.005}\right)$	$^{+0.012}_{-0.010}$ $\left(^{+0.005}_{-0.004}\right)$	$^{+0.010}_{-0.006}$ $\left(^{+0.004}_{-0.004}\right)$
B^{WW}/B^{ZZ}	8.09 ± < 0.01	$6.7\,^{+1.6}_{-1.3}$ $\left(^{+2.2}_{-1.7}\right)$	$^{+1.5}_{-1.2}$ $\left(^{+2.0}_{-1.6}\right)$	$^{+0.6}_{-0.5}$ $\left(^{+0.9}_{-0.7}\right)$	$6.5\,^{+2.1}_{-1.6}$ $\left(^{+3.5}_{-2.4}\right)$	$^{+2.0}_{-1.4}$ $\left(^{+3.3}_{-2.2}\right)$	$^{+0.8}_{-0.6}$ $\left(^{+1.2}_{-0.9}\right)$	$7.1\,^{+2.9}_{-2.1}$ $\left(^{+3.2}_{-2.2}\right)$	$^{+2.6}_{-1.8}$ $\left(^{+2.9}_{-2.0}\right)$	$^{+1.3}_{-0.9}$ $\left(^{+1.4}_{-1.0}\right)$
$B^{\gamma\gamma}/B^{ZZ}$	0.0854 ±0.0010	$0.069\,^{+0.018}_{-0.014}$ $\left(^{+0.025}_{-0.019}\right)$	$^{+0.018}_{-0.014}$ $\left(^{+0.024}_{-0.019}\right)$	$^{+0.004}_{-0.003}$ $\left(^{+0.006}_{-0.004}\right)$	$0.062\,^{+0.024}_{-0.018}$ $\left(^{+0.040}_{-0.027}\right)$	$^{+0.023}_{-0.017}$ $\left(^{+0.039}_{-0.027}\right)$	$^{+0.007}_{-0.005}$ $\left(^{+0.010}_{-0.006}\right)$	$0.079\,^{+0.034}_{-0.023}$ $\left(^{+0.035}_{-0.025}\right)$	$^{+0.032}_{-0.023}$ $\left(^{+0.034}_{-0.024}\right)$	$^{+0.010}_{-0.006}$ $\left(^{+0.008}_{-0.005}\right)$
$B^{\tau\tau}/B^{ZZ}$	2.36 ±0.05	$1.8\,^{+0.6}_{-0.5}$ $\left(^{+0.9}_{-0.6}\right)$	$^{+0.5}_{-0.4}$ $\left(^{+0.8}_{-0.6}\right)$	$^{+0.3}_{-0.2}$ $\left(^{+0.5}_{-0.3}\right)$	$2.2\,^{+1.1}_{-0.7}$ $\left(^{+1.5}_{-1.0}\right)$	$^{+0.9}_{-0.6}$ $\left(^{+1.3}_{-0.9}\right)$	$^{+0.6}_{-0.4}$ $\left(^{+0.8}_{-0.5}\right)$	$1.6\,^{+0.9}_{-0.6}$ $\left(^{+1.2}_{-0.9}\right)$	$^{+0.8}_{-0.5}$ $\left(^{+1.0}_{-0.7}\right)$	$^{+0.5}_{-0.3}$ $\left(^{+0.7}_{-0.4}\right)$
B^{bb}/B^{ZZ}	21.5 ±1.0	$4.2\,^{+4.4}_{-2.6}$ $\left(^{+16.8}_{-9.0}\right)$	$^{+2.8}_{-2.0}$ $\left(^{+13.9}_{-7.9}\right)$	$^{+3.4}_{-1.6}$ $\left(^{+9.5}_{-4.4}\right)$	$9.6\,^{+10.1}_{-5.7}$ $\left(^{+29.3}_{-11.8}\right)$	$^{+7.4}_{-4.4}$ $\left(^{+24.2}_{-10.5}\right)$	$^{+6.9}_{-3.6}$ $\left(^{+16.6}_{-5.3}\right)$	$3.7\,^{+4.1}_{-2.4}$ $\left(^{+29.4}_{-11.9}\right)$	$^{+3.1}_{-2.0}$ $\left(^{+23.4}_{-10.4}\right)$	$^{+2.7}_{-1.4}$ $\left(^{+17.8}_{-5.9}\right)$

4.2. Parameterisation using ratios of coupling modifiers

The parameterisation using the Higgs boson coupling modifiers is based on the κ-framework described in Section 2.4 and the parameters of interest are listed in the right column of Table 6. The cross section times branching fraction for the $gg \to H \to ZZ$ channel is parameterised as a function of $\kappa_{gZ} = \kappa_g \cdot \kappa_Z/\kappa_H$, where κ_g is the effective coupling modifier of the Higgs boson to the gluon in ggF production, which in the SM occurs mainly through loops involving top and bottom quarks. The $\lambda_{Zg} = \kappa_Z/\kappa_g$ parameter is probed by the measurements of VBF and ZH production, while the measurements of the ttH production process are sensitive to $\lambda_{tg} = \kappa_t/\kappa_g$. Three of the decay modes, namely $H \to WW$, $H \to \tau\tau$, and $H \to bb$, probe the three ratios $\lambda_{WZ} = \kappa_W/\kappa_Z$, $\lambda_{\tau Z} = \kappa_\tau/\kappa_Z$, and $\lambda_{bZ} = \kappa_b/\kappa_Z$, through their respective ratios to the $H \to ZZ$ branching fraction. The remaining decay mode, $H \to \gamma\gamma$, which in the SM occurs through loops involving predominantly the top quark and the W boson, is sensitive to the ratio $\lambda_{\gamma Z} = \kappa_\gamma/\kappa_Z$. In this parameterisation, $\lambda_{WZ} = \kappa_W/\kappa_Z$ is also probed by the VBF, WH, and ZH production processes. Without any loss of generality, the signs of κ_Z and κ_g can be assumed to be the same, constraining λ_{Zg} and κ_{gZ} to be positive.
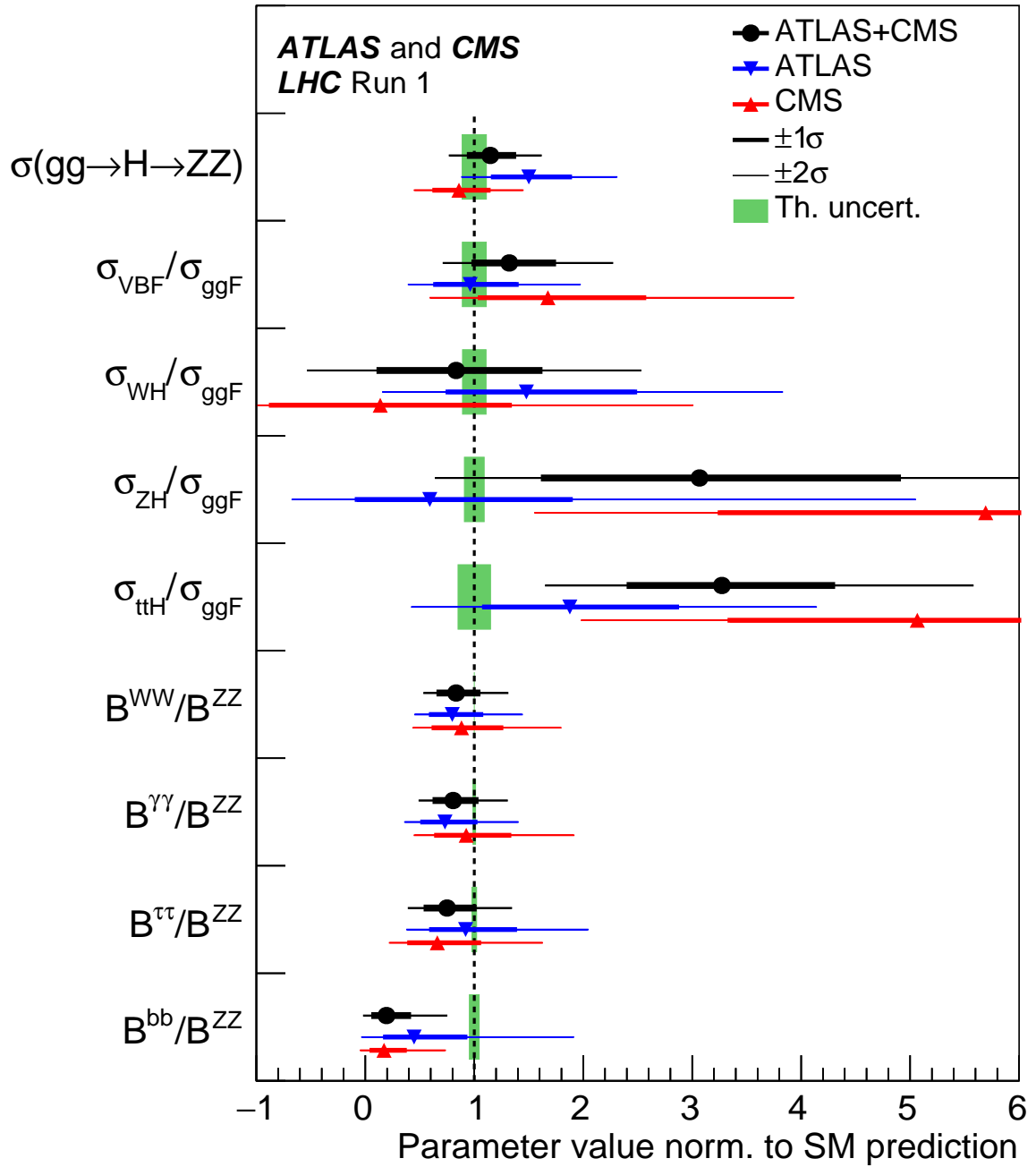
Figure 8: Best fit values of the $\sigma(gg \to H \to ZZ)$ cross section and of ratios of cross sections and branching fractions, as obtained from the generic parameterisation with nine parameters and tabulated in Table 9 for the combination of the ATLAS and CMS measurements. Also shown are the results from each experiment. The values involving cross sections are given for $\sqrt{s} = 8$ TeV, assuming the SM values for $\sigma_i(7 \text{ TeV})/\sigma_i(8 \text{ TeV})$. The error bars indicate the 1σ (thick lines) and 2σ (thin lines) intervals. The fit results are normalised to the SM predictions for the various parameters and the shaded bands indicate the theoretical uncertainties in these predictions.
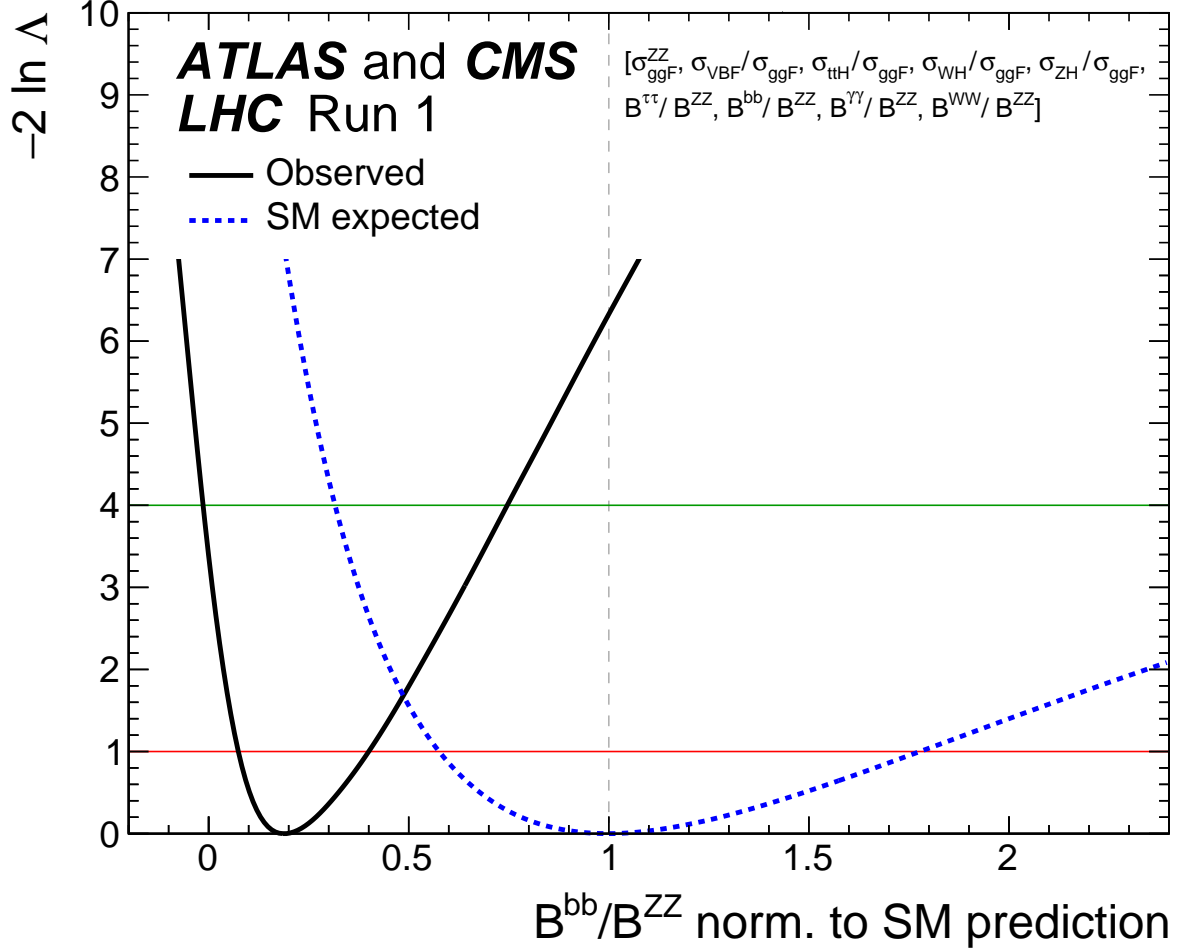
Figure 9: Observed (solid line) and expected (dashed line) negative log-likelihood scan of the B^{bb}/B^{ZZ} parameter normalised to the corresponding SM prediction. All the other parameters of interest are also varied in the minimisation procedure. The red (green) horizontal line at the $-2\Delta\ln\Lambda$ value of 1 (4) indicates the value of the profile likelihood ratio corresponding to a 1σ (2σ) CL interval for the parameter of interest, assuming the asymptotic χ^2 distribution of the test statistic. The vertical dashed line indicates the SM prediction.

Table 10 shows the results of the fit to the data with a breakdown of uncertainties into their statistical and systematic components, while the complete breakdown of the uncertainties into the four components is shown in Table 22 of Appendix B. The measured correlation matrix can be found in Fig. 29 of Appendix A. The coupling modifiers are assumed to be the same at the two centre-of-mass energies, as in the parameterisation based on the ratios of cross sections and branching fractions. Figure 10 illustrates the complete ranges of allowed values with their total uncertainties, including the negative ranges allowed for λ_{WZ} and λ_{tg}, the two parameters chosen to illustrate possible interference effects due to $ggZH$ or tH production. Figure 11 shows the likelihood scan results for these two parameters for the combination of ATLAS and CMS, both for the observed and expected results. As described in Section 2.4, the interference terms are responsible for the small asymmetry between the likelihood curves for the positive and negative values of the parameters of interest. In both cases, the best fit values correspond to the positive sign, but the sensitivity to the interference terms remains small. Appendix C, with the specific example of λ_{bZ} (shown in Fig. 31), describes how the four possible sign combinations between λ_{WZ} and λ_{tg} may

25

Table 10: Best fit values of $\kappa_{gZ} = \kappa_g \cdot \kappa_Z / \kappa_H$ and of the ratios of coupling modifiers, as defined in the parameterisation studied in the context of the κ-framework, from the combined analysis of the $\sqrt{s} = 7$ and 8 TeV data. The results are shown for the combination of ATLAS and CMS and also separately for each experiment, together with their total uncertainties and their breakdown into statistical and systematic components. The uncertainties in λ_{tg} and λ_{WZ}, for which a negative solution is allowed, are calculated around the overall best fit value. The combined 1σ CL intervals are $\lambda_{tg} = [-2.00, -1.59] \cup [1.50, 2.07]$ and $\lambda_{WZ} = [-0.96, -0.82] \cup [0.80, 0.98]$. The expected uncertainties in the measurements are displayed in parentheses. For those parameters with no sensitivity to the sign, only the absolute values are shown.

Parameter	Best fit value	Uncertainty Stat	Uncertainty Syst	Best fit value	Uncertainty Stat	Uncertainty Syst	Best fit value	Uncertainty Stat	Uncertainty Syst
	ATLAS+CMS			ATLAS			CMS		
κ_{gZ}	$1.09^{+0.11}_{-0.11}$ $\left(^{+0.11}_{-0.11}\right)$	$^{+0.09}_{-0.09}$ $\left(^{+0.09}_{-0.09}\right)$	$^{+0.06}_{-0.06}$ $\left(^{+0.06}_{-0.05}\right)$	$1.20^{+0.16}_{-0.15}$ $\left(^{+0.15}_{-0.15}\right)$	$^{+0.14}_{-0.14}$ $\left(^{+0.14}_{-0.13}\right)$	$^{+0.08}_{-0.07}$ $\left(^{+0.07}_{-0.06}\right)$	$0.99^{+0.14}_{-0.13}$ $\left(^{+0.14}_{-0.14}\right)$	$^{+0.12}_{-0.12}$ $\left(^{+0.13}_{-0.12}\right)$	$^{+0.07}_{-0.06}$ $\left(^{+0.07}_{-0.06}\right)$
λ_{Zg}	$1.27^{+0.23}_{-0.20}$ $\left(^{+0.20}_{-0.17}\right)$	$^{+0.18}_{-0.16}$ $\left(^{+0.15}_{-0.14}\right)$	$^{+0.15}_{-0.12}$ $\left(^{+0.12}_{-0.10}\right)$	$1.07^{+0.26}_{-0.22}$ $\left(^{+0.28}_{-0.23}\right)$	$^{+0.21}_{-0.18}$ $\left(^{+0.23}_{-0.20}\right)$	$^{+0.15}_{-0.11}$ $\left(^{+0.16}_{-0.11}\right)$	$1.47^{+0.45}_{-0.34}$ $\left(^{+0.27}_{-0.23}\right)$	$^{+0.35}_{-0.28}$ $\left(^{+0.21}_{-0.19}\right)$	$^{+0.28}_{-0.20}$ $\left(^{+0.16}_{-0.13}\right)$
λ_{tg}	$1.78^{+0.30}_{-0.27}$ $\left(^{+0.28}_{-0.38}\right)$	$^{+0.21}_{-0.20}$ $\left(^{+0.20}_{-0.30}\right)$	$^{+0.21}_{-0.18}$ $\left(^{+0.20}_{-0.24}\right)$	$1.40^{+0.34}_{-0.33}$ $\left(^{+0.38}_{-0.54}\right)$	$^{+0.25}_{-0.24}$ $\left(^{+0.28}_{-0.39}\right)$	$^{+0.23}_{-0.23}$ $\left(^{+0.25}_{-0.37}\right)$	$-2.26^{+0.50}_{-0.53}$ $\left(^{+0.42}_{-0.64}\right)$	$^{+0.43}_{-0.39}$ $\left(^{+0.31}_{-0.42}\right)$	$^{+0.26}_{-0.36}$ $\left(^{+0.28}_{-0.49}\right)$
λ_{WZ}	$0.88^{+0.10}_{-0.09}$ $\left(^{+0.12}_{-0.10}\right)$	$^{+0.09}_{-0.08}$ $\left(^{+0.11}_{-0.09}\right)$	$^{+0.04}_{-0.04}$ $\left(^{+0.05}_{-0.04}\right)$	$0.92^{+0.14}_{-0.12}$ $\left(^{+0.18}_{-0.15}\right)$	$^{+0.13}_{-0.11}$ $\left(^{+0.17}_{-0.13}\right)$	$^{+0.05}_{-0.05}$ $\left(^{+0.06}_{-0.06}\right)$	$-0.85^{+0.13}_{-0.15}$ $\left(^{+0.17}_{-0.14}\right)$	$^{+0.11}_{-0.13}$ $\left(^{+0.15}_{-0.13}\right)$	$^{+0.06}_{-0.07}$ $\left(^{+0.07}_{-0.06}\right)$
$|\lambda_{\gamma Z}|$	$0.89^{+0.11}_{-0.10}$ $\left(^{+0.13}_{-0.12}\right)$	$^{+0.10}_{-0.09}$ $\left(^{+0.13}_{-0.11}\right)$	$^{+0.04}_{-0.03}$ $\left(^{+0.04}_{-0.03}\right)$	$0.87^{+0.15}_{-0.13}$ $\left(^{+0.20}_{-0.17}\right)$	$^{+0.15}_{-0.13}$ $\left(^{+0.20}_{-0.17}\right)$	$^{+0.05}_{-0.04}$ $\left(^{+0.06}_{-0.04}\right)$	$0.91^{+0.17}_{-0.14}$ $\left(^{+0.18}_{-0.16}\right)$	$^{+0.16}_{-0.14}$ $\left(^{+0.18}_{-0.15}\right)$	$^{+0.05}_{-0.04}$ $\left(^{+0.05}_{-0.04}\right)$
$|\lambda_{\tau Z}|$	$0.85^{+0.13}_{-0.12}$ $\left(^{+0.17}_{-0.15}\right)$	$^{+0.12}_{-0.10}$ $\left(^{+0.14}_{-0.13}\right)$	$^{+0.07}_{-0.06}$ $\left(^{+0.09}_{-0.08}\right)$	$0.96^{+0.21}_{-0.18}$ $\left(^{+0.27}_{-0.23}\right)$	$^{+0.18}_{-0.15}$ $\left(^{+0.23}_{-0.19}\right)$	$^{+0.11}_{-0.09}$ $\left(^{+0.14}_{-0.12}\right)$	$0.78^{+0.20}_{-0.17}$ $\left(^{+0.23}_{-0.20}\right)$	$^{+0.17}_{-0.15}$ $\left(^{+0.19}_{-0.17}\right)$	$^{+0.10}_{-0.09}$ $\left(^{+0.12}_{-0.11}\right)$
$|\lambda_{bZ}|$	$0.58^{+0.16}_{-0.20}$ $\left(^{+0.25}_{-0.22}\right)$	$^{+0.12}_{-0.17}$ $\left(^{+0.21}_{-0.20}\right)$	$^{+0.10}_{-0.10}$ $\left(^{+0.13}_{-0.10}\right)$	$0.61^{+0.24}_{-0.24}$ $\left(^{+0.36}_{-0.29}\right)$	$^{+0.20}_{-0.19}$ $\left(^{+0.31}_{-0.26}\right)$	$^{+0.14}_{-0.16}$ $\left(^{+0.18}_{-0.13}\right)$	$0.47^{+0.26}_{-0.17}$ $\left(^{+0.38}_{-0.37}\right)$	$^{+0.23}_{-0.13}$ $\left(^{+0.32}_{-0.34}\right)$	$^{+0.13}_{-0.12}$ $\left(^{+0.20}_{-0.16}\right)$

impact the best fit value and the uncertainty in the other parameters of interest. The p-value of the compatibility between the data and the SM predictions is 13%. All results are consistent with the SM predictions within less than 2σ, except those for λ_{tg} and λ_{bZ}, which exhibit deviations from the SM similar to those reported and explained in Section 4.1.2 for the measurement of the ratios of the ttH and ggF production cross sections, and of the ratios of the bb and ZZ decay branching fractions.
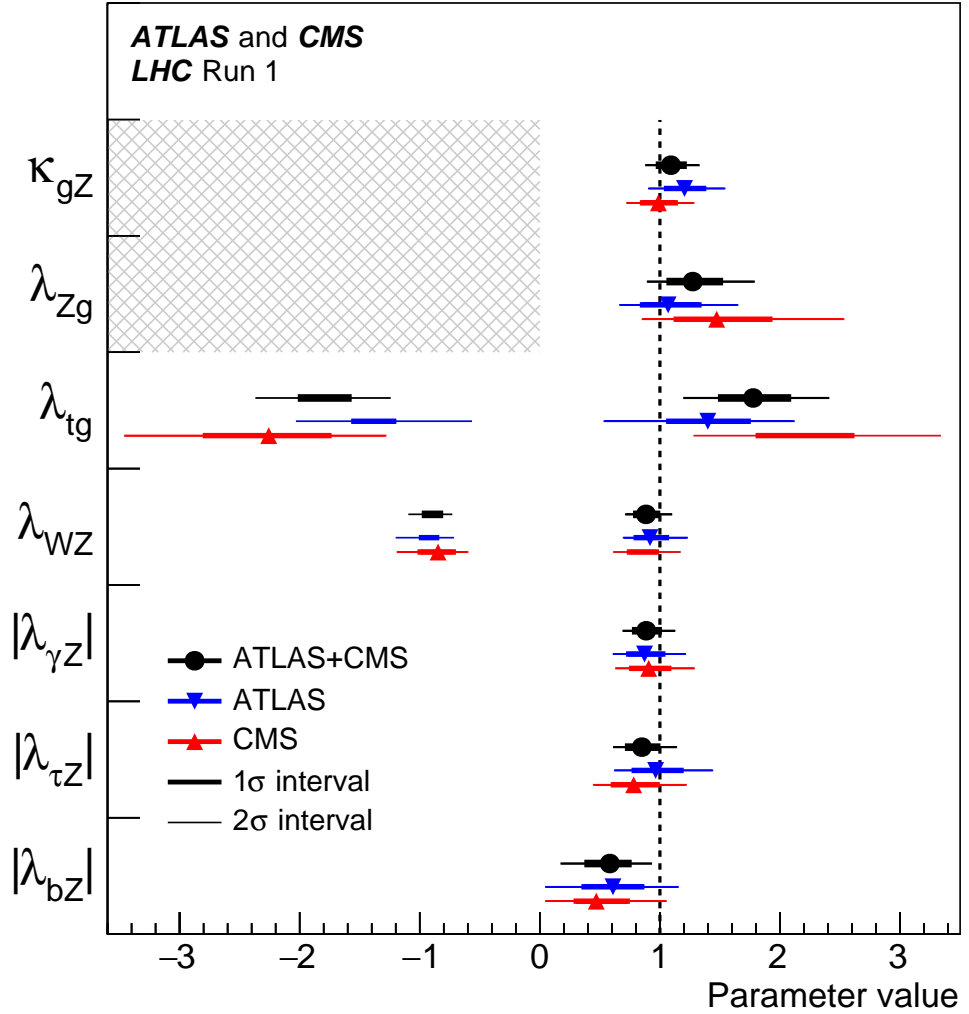
Figure 10: Best fit values of ratios of Higgs boson coupling modifiers, as obtained from the generic parameterisation described in the text and as tabulated in Table 10 for the combination of the ATLAS and CMS measurements. Also shown are the results from each experiment. The error bars indicate the 1σ (thick lines) and 2σ (thin lines) intervals. The hatched areas indicate the non-allowed regions for the parameters that are assumed to be positive without loss of generality. For those parameters with no sensitivity to the sign, only the absolute values are shown.
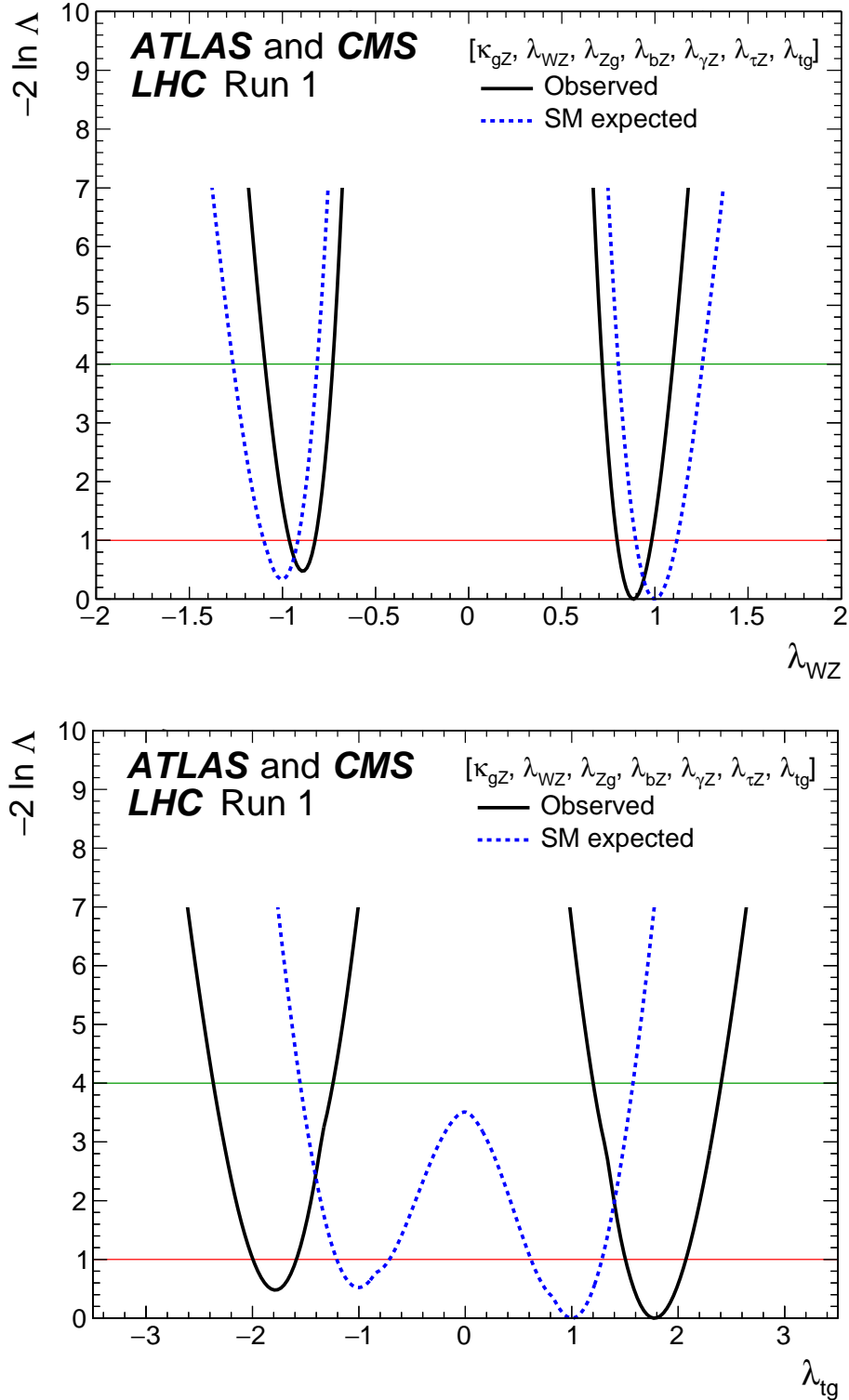
Figure 11: Observed (solid line) and expected (dashed line) negative log-likelihood scans for λ_{WZ} (top) and λ_{tg} (bottom), the two parameters of Fig. 10 that are of interest in the negative range in the generic parameterisation of ratios of Higgs boson coupling modifiers described in the text. All the other parameters of interest from the list in the legend are also varied in the minimisation procedure. The red (green) horizontal lines at the $-2\Delta \ln \Lambda$ value of 1 (4) indicate the value of the profile likelihood ratio corresponding to a 1σ (2σ) CL interval for the parameter of interest, assuming the asymptotic χ^2 distribution of the test statistic.

Table 11: Measured global signal strength μ and its total uncertainty, together with the breakdown of the uncertainty into its four components as defined in Section 3.3. The results are shown for the combination of ATLAS and CMS, and separately for each experiment. The expected uncertainty, with its breakdown, is also shown.

	Best fit μ	Uncertainty				
		Total	Stat	Expt	Thbgd	Thsig
ATLAS + CMS (measured)	1.09	$+0.11$ -0.10	$+0.07$ -0.07	$+0.04$ -0.04	$+0.03$ -0.03	$+0.07$ -0.06
ATLAS + CMS (expected)		$+0.11$ -0.10	$+0.07$ -0.07	$+0.04$ -0.04	$+0.03$ -0.03	$+0.07$ -0.06
ATLAS (measured)	1.20	$+0.15$ -0.14	$+0.10$ -0.10	$+0.06$ -0.06	$+0.04$ -0.04	$+0.08$ -0.07
ATLAS (expected)		$+0.14$ -0.13	$+0.10$ -0.10	$+0.06$ -0.05	$+0.04$ -0.04	$+0.07$ -0.06
CMS (measured)	0.97	$+0.14$ -0.13	$+0.09$ -0.09	$+0.05$ -0.05	$+0.04$ -0.03	$+0.07$ -0.06
CMS (expected)		$+0.14$ -0.13	$+0.09$ -0.09	$+0.05$ -0.05	$+0.04$ -0.03	$+0.08$ -0.06

5. Measurements of signal strengths

Section 4.1 presents the results from generic parameterisations, expressed in terms of cross sections and branching fractions. This section probes more specific parameterisations, with additional assumptions. Results for these parameterisations are presented, starting with the most restrictive one using a single parameter of interest, which was used to assess the sensitivity of the experimental analyses to the presence of a Higgs boson at the time of its discovery. Section 5.4 describes the test of a hypothesis that two or more neutral Higgs bosons might be present with similar masses.

5.1. Global signal strength

The simplest and most restrictive signal strength parameterisation is to assume that the values of the signal strengths μ_i^f, as defined in Eq. (3), are the same for all production processes i and decay channels f. In this case, the SM predictions of signal yields in all categories are scaled by a global signal strength μ. Such a parameterisation provides the simplest test of the compatibility of the experimental data with the SM predictions. A fit to the ATLAS and CMS data at $\sqrt{s} = 7$ and 8 TeV with μ as the parameter of interest results in the best fit value:

$$\mu = 1.09^{+0.11}_{-0.10} = 1.09^{+0.07}_{-0.07} \text{ (stat) } ^{+0.04}_{-0.04} \text{ (expt) } ^{+0.03}_{-0.03} \text{ (thbgd)}^{+0.07}_{-0.06} \text{ (thsig),}$$

where the breakdown of the uncertainties into their four components is performed as described in Section 3.3. The overall systematic uncertainty of $^{+0.09}_{-0.08}$ is larger than the statistical uncertainty and its largest component is the theoretical uncertainty in the ggF cross section. This result is consistent with the SM prediction of $\mu = 1$ within less than 1σ and the p-value of the compatibility between the data and the SM predictions is 40%. This result is shown in Table 11, together with that from each experiment, including the breakdown of the uncertainties into their four components. The expected uncertainties and their breakdown are also given.

Table 12: Measured signal strengths μ and their total uncertainties for different Higgs boson production processes. The results are shown for the combination of ATLAS and CMS, and separately for each experiment, for the combined $\sqrt{s}$ = 7 and 8 TeV data. The expected uncertainties in the measurements are displayed in parentheses. These results are obtained assuming that the Higgs boson branching fractions are the same as in the SM.

Production process	ATLAS+CMS	ATLAS	CMS
μ_{ggF}	$1.03^{+0.16}_{-0.14}$ $\binom{+0.16}{-0.14}$	$1.26^{+0.23}_{-0.20}$ $\binom{+0.21}{-0.18}$	$0.84^{+0.18}_{-0.16}$ $\binom{+0.20}{-0.17}$
μ_{VBF}	$1.18^{+0.25}_{-0.23}$ $\binom{+0.24}{-0.23}$	$1.21^{+0.33}_{-0.30}$ $\binom{+0.32}{-0.29}$	$1.14^{+0.37}_{-0.34}$ $\binom{+0.36}{-0.34}$
μ_{WH}	$0.89^{+0.40}_{-0.38}$ $\binom{+0.41}{-0.39}$	$1.25^{+0.56}_{-0.52}$ $\binom{+0.56}{-0.53}$	$0.46^{+0.57}_{-0.53}$ $\binom{+0.60}{-0.57}$
μ_{ZH}	$0.79^{+0.38}_{-0.36}$ $\binom{+0.39}{-0.36}$	$0.30^{+0.51}_{-0.45}$ $\binom{+0.55}{-0.51}$	$1.35^{+0.58}_{-0.54}$ $\binom{+0.55}{-0.51}$
μ_{ttH}	$2.3^{+0.7}_{-0.6}$ $\binom{+0.5}{-0.5}$	$1.9^{+0.8}_{-0.7}$ $\binom{+0.7}{-0.7}$	$2.9^{+1.0}_{-0.9}$ $\binom{+0.9}{-0.8}$

5.2. Signal strengths of individual production processes and decay channels

The global signal strength is the most precisely measured Higgs boson coupling-related observable, but this simple parameterisation is very model dependent, since all Higgs boson production and decay measurements are combined assuming that all their ratios are the same as in the SM. The compatibility of the measurements with the SM can be tested in a less model-dependent way by relaxing these assumptions separately for the production cross sections and the decay branching fractions.

Assuming the SM values for the Higgs boson branching fractions, namely μ^f = 1 in Eq. (7), the five main Higgs boson production processes are explored with independent signal strengths: μ_{ggF}, μ_{VBF}, μ_{WH}, μ_{ZH}, and μ_{ttH}. A combined analysis of the ATLAS and CMS data is performed with these five signal strengths as parameters of interest. The results are shown in Table 12 for the combined $\sqrt{s}$ = 7 and 8 TeV data sets. The signal strengths at the two energies are assumed to be the same for each production process. Figure 12 illustrates these results with their total uncertainties. The p-value of the compatibility between the data and the SM predictions is 24%.
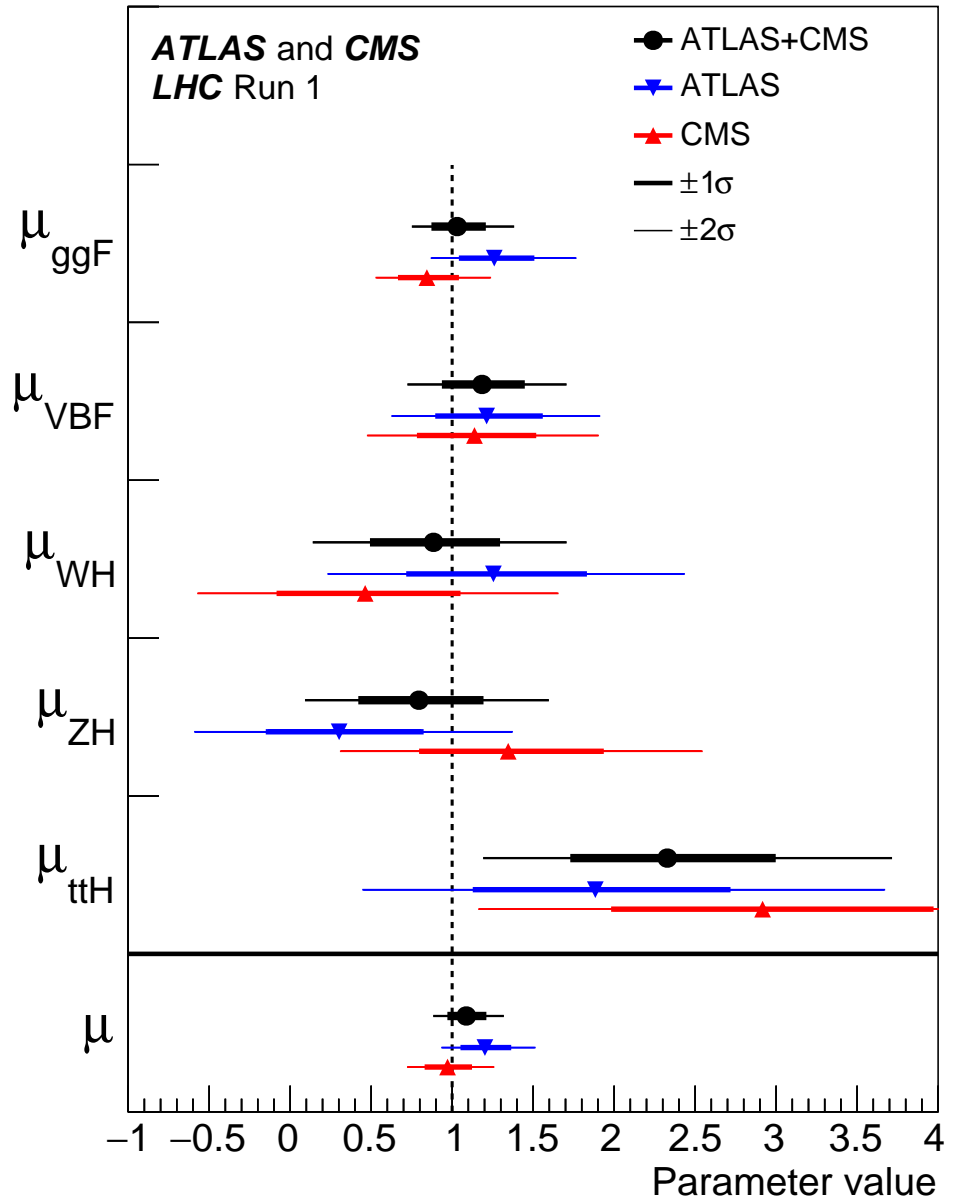
Figure 12: Best fit results for the production signal strengths for the combination of ATLAS and CMS data. Also shown are the results from each experiment. The error bars indicate the 1σ (thick lines) and 2σ (thin lines) intervals. The measurements of the global signal strength μ are also shown.

Table 13: Measured signal strengths μ and their total uncertainties for different Higgs boson decay channels. The results are shown for the combination of ATLAS and CMS, and separately for each experiment, for the combined $\sqrt{s}$ = 7 and 8 TeV data. The expected uncertainties in the measurements are displayed in parentheses. These results are obtained assuming that the Higgs boson production process cross sections at $\sqrt{s}$ = 7 and 8 TeV are the same as in the SM.

Decay channel	ATLAS+CMS	ATLAS	CMS
$\mu^{\gamma\gamma}$	$1.14\,^{+0.19}_{-0.18}$ $\left(^{+0.18}_{-0.17}\right)$	$1.14\,^{+0.27}_{-0.25}$ $\left(^{+0.26}_{-0.24}\right)$	$1.11\,^{+0.25}_{-0.23}$ $\left(^{+0.23}_{-0.21}\right)$
μ^{ZZ}	$1.29\,^{+0.26}_{-0.23}$ $\left(^{+0.23}_{-0.20}\right)$	$1.52\,^{+0.40}_{-0.34}$ $\left(^{+0.32}_{-0.27}\right)$	$1.04\,^{+0.32}_{-0.26}$ $\left(^{+0.30}_{-0.25}\right)$
μ^{WW}	$1.09\,^{+0.18}_{-0.16}$ $\left(^{+0.16}_{-0.15}\right)$	$1.22\,^{+0.23}_{-0.21}$ $\left(^{+0.21}_{-0.20}\right)$	$0.90\,^{+0.23}_{-0.21}$ $\left(^{+0.23}_{-0.20}\right)$
$\mu^{\tau\tau}$	$1.11\,^{+0.24}_{-0.22}$ $\left(^{+0.24}_{-0.22}\right)$	$1.41\,^{+0.40}_{-0.36}$ $\left(^{+0.37}_{-0.33}\right)$	$0.88\,^{+0.30}_{-0.28}$ $\left(^{+0.31}_{-0.29}\right)$
μ^{bb}	$0.70\,^{+0.29}_{-0.27}$ $\left(^{+0.29}_{-0.28}\right)$	$0.62\,^{+0.37}_{-0.37}$ $\left(^{+0.39}_{-0.37}\right)$	$0.81\,^{+0.45}_{-0.43}$ $\left(^{+0.45}_{-0.43}\right)$
$\mu^{\mu\mu}$	$0.1\,^{+2.5}_{-2.5}$ $\left(^{+2.4}_{-2.3}\right)$	$-0.6\,^{+3.6}_{-3.6}$ $\left(^{+3.6}_{-3.6}\right)$	$0.9\,^{+3.6}_{-3.5}$ $\left(^{+3.3}_{-3.2}\right)$

Higgs boson decays are also studied with six independent signal strengths, one for each decay channel included in the combination, assuming that the Higgs boson production cross sections are the same as in the SM. Unlike the production signal strengths, these decay-based signal strengths are independent of the collision centre-of-mass energy and therefore the $\sqrt{s}$ = 7 and 8 TeV data sets can be combined without additional assumptions. Table 13 and Fig. 13 present the best fit results for the combination of ATLAS and CMS, and separately for each experiment (the results for $\mu^{\mu\mu}$ are only reported in Table 13). The p-value of the compatibility between the data and the SM predictions is 75%.

From the combined likelihood scans it is possible to evaluate the significances for the observation of the different production processes and decay channels. The combination of the data from the two experiments corresponds to summing their recorded integrated luminosities and consequently increases the sensitivity by approximately a factor of $\sqrt{2}$, since the theoretical uncertainties in the Higgs boson signal are only weakly relevant for this evaluation and all the other significant uncertainties are uncorrelated between the two experiments. The results are reported in Table 14 for all production processes and decay channels, except for those that have already been clearly observed, namely the ggF production process and the $H \to ZZ$, $H \to WW$, and $H \to \gamma\gamma$ decay channels. The combined significances for the observation of the VBF production process and of the $H \to \tau\tau$ decay are each above 5σ, and the combined significance for the VH production process is above 3σ. The combined significance for the ttH process is 4.4σ, whereas only 2.0σ is expected, corresponding to a measured excess of 2.3σ with respect to the SM prediction.
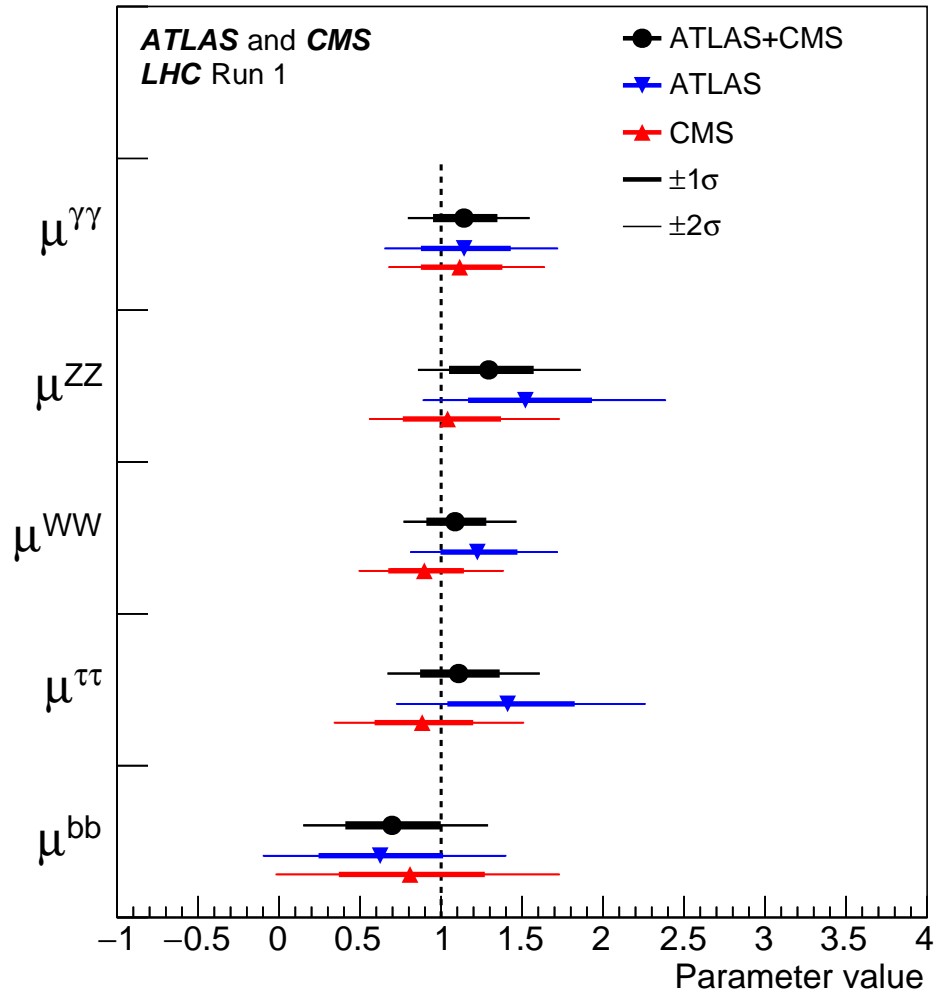
Figure 13: Best fit results for the decay signal strengths for the combination of ATLAS and CMS data (the results for $\mu^{\mu\mu}$ are reported in Table 13). Also shown are the results from each experiment. The error bars indicate the 1σ (thick lines) and 2σ (thin lines) intervals.

Table 14: Measured and expected significances for the observation of Higgs boson production processes and decay channels for the combination of ATLAS and CMS. Not included are the ggF production process and the $H \to ZZ$, $H \to WW$, and $H \to \gamma\gamma$ decay channels, which have already been clearly observed. All results are obtained constraining the decay branching fractions to their SM values when considering the production processes, and constraining the production cross sections to their SM values when studying the decays.

Production process	Measured significance (σ)	Expected significance (σ)
VBF	5.4	4.6
WH	2.4	2.7
ZH	2.3	2.9
VH	3.5	4.2
ttH	4.4	2.0
Decay channel		
$H \to \tau\tau$	5.5	5.0
$H \to bb$	2.6	3.7

5.3. Boson- and fermion-mediated production processes

The Higgs boson production processes can be associated with Higgs boson couplings to either fermions (ggF and ttH) or vector bosons (VBF, WH, and ZH). Potential deviations of these couplings from the SM predictions can be tested by using a parameterisation with two signal strengths for each decay channel f: $\mu_F^f = \mu_{ggF+ttH}^f$ for the fermion-mediated production processes and $\mu_V^f = \mu_{VBF+VH}^f$ for the vector-boson-mediated production processes. The branching fraction cancels in the ratio μ_V^f/μ_F^f that can be formed for each Higgs boson decay channel. Two fits are performed for the combination of ATLAS and CMS, and also separately for each experiment. The first is a ten-parameter fit of μ_F^f and μ_V^f for each of the five decay channels, while the second is a six-parameter fit of μ_V/μ_F and μ_F^f for each of the five decay channels.

Figure 14 shows the 68% CL region for the ten-parameter fit of the five decay channels included in the combination of the ATLAS and CMS measurements. These results are obtained by combining the $\sqrt{s} = 7$ and 8 TeV data, assuming that μ_F^f and μ_V^f are the same at the two energies. The SM predictions of $\mu_F^f = 1$ and $\mu_V^f = 1$ lie within the 68% CL regions of all these measurements. Combinations of these regions would require assumptions about the branching fractions and are therefore not performed. Table 15 reports the best fit values and the total uncertainties for all the parameters of the fits, together with the expected uncertainties for the combination of ATLAS and CMS. The p-values of the compatibility between the data and the SM predictions are 90% and 75% for the ten-parameter and six-parameter fits, respectively. The six-parameter fit, without any additional assumptions about the Higgs boson branching fractions, yields: $\mu_V/\mu_F = 1.09^{+0.36}_{-0.28}$, in agreement with the SM.

5.4. Search for mass-degenerate states with different coupling structures

One important assumption underlying all the results reported elsewhere in this paper is that the observations are due to the presence of a single particle with well defined mass that has been precisely measured [22]. This section addresses the case in which the observed signal could be due to the presence of two or more particles with similar masses, such that they cannot be resolved within the current precision of the
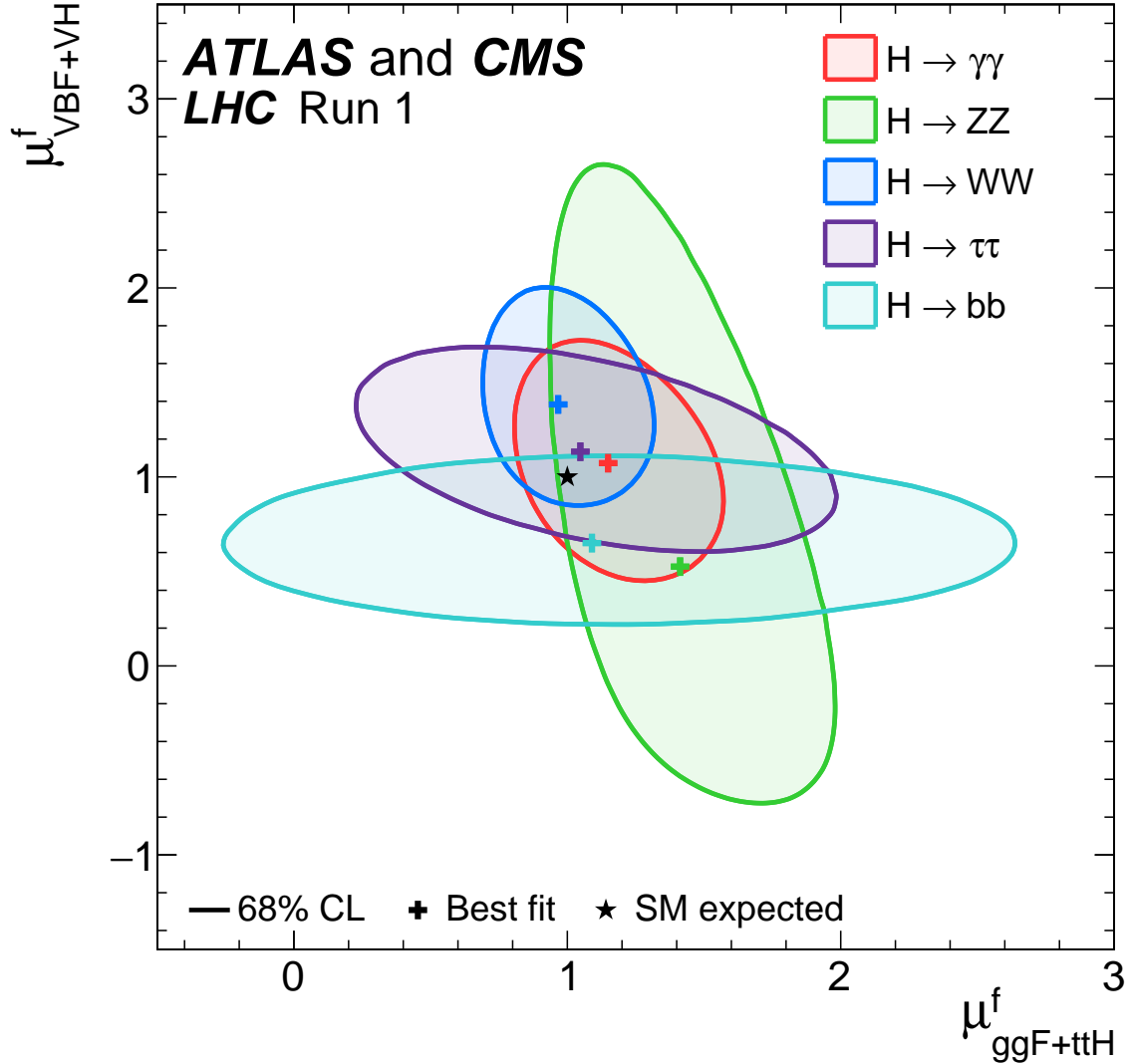
Figure 14: Negative log-likelihood contours at 68% CL in the $(\mu^f_{ggF+ttH}, \mu^f_{VBF+VH})$ plane for the combination of ATLAS and CMS, as obtained from the ten-parameter fit described in the text for each of the five decay channels $H \to ZZ$, $H \to WW$, $H \to \gamma\gamma$, $H \to \tau\tau$, and $H \to bb$. The best fit values obtained for each of the five decay channels are also shown, together with the SM expectation.

mass measurements in the different channels. Several BSM models predict, for example, a superposition of states with indistinguishable mass values [122–125], possibly with different coupling structures to the SM particles. With such an assumption, it may be possible to distinguish between single and multiple states by measuring the cross sections of individual production processes independently for each decay mode, as described in Section 4.1.1. Several methods have been proposed to assess the compatibility of the data with a single state [126, 127]. A test for the possible presence of overlapping Higgs boson states is performed, based on a profile likelihood ratio suggested in Ref. [128]. This test accounts both for missing measurements, such as the $H \to bb$ decay mode in the ggF and VBF production processes, and for uncertainties in the measurements, including their correlations.

Table 15: Results of the ten-parameter fit of $\mu_F^f = \mu_{ggF+ttH}^f$ and $\mu_V^f = \mu_{VBF+VH}^f$ for each of the five decay channels, and of the six-parameter fit of the global ratio $\mu_V/\mu_F = \mu_{VBF+VH}/\mu_{ggF+ttH}$ together with μ_F^f for each of the five decay channels. The results are shown for the combination of ATLAS and CMS, together with their measured and expected uncertainties. The measured results are also shown separately for each experiment.

Parameter	ATLAS+CMS Measured	ATLAS+CMS Expected uncertainty	ATLAS Measured	CMS Measured
Ten-parameter fit of μ_F^f and μ_V^f				
$\mu_V^{\gamma\gamma}$	$1.05^{+0.44}_{-0.41}$	$^{+0.41}_{-0.38}$	$0.69^{+0.63}_{-0.58}$	$1.37^{+0.62}_{-0.56}$
μ_V^{ZZ}	$0.47^{+1.37}_{-0.92}$	$^{+1.16}_{-0.84}$	$0.24^{+1.60}_{-0.93}$	$1.45^{+2.32}_{-2.29}$
μ_V^{WW}	$1.38^{+0.41}_{-0.37}$	$^{+0.38}_{-0.35}$	$1.56^{+0.52}_{-0.46}$	$1.08^{+0.65}_{-0.58}$
$\mu_V^{\tau\tau}$	$1.12^{+0.37}_{-0.35}$	$^{+0.38}_{-0.35}$	$1.29^{+0.58}_{-0.53}$	$0.88^{+0.49}_{-0.45}$
μ_V^{bb}	$0.65^{+0.31}_{-0.29}$	$^{+0.32}_{-0.30}$	$0.50^{+0.39}_{-0.37}$	$0.85^{+0.47}_{-0.44}$
$\mu_F^{\gamma\gamma}$	$1.16^{+0.27}_{-0.24}$	$^{+0.25}_{-0.23}$	$1.30^{+0.37}_{-0.33}$	$1.00^{+0.33}_{-0.30}$
μ_F^{ZZ}	$1.42^{+0.37}_{-0.33}$	$^{+0.29}_{-0.25}$	$1.74^{+0.51}_{-0.44}$	$0.96^{+0.53}_{-0.41}$
μ_F^{WW}	$0.98^{+0.22}_{-0.20}$	$^{+0.21}_{-0.19}$	$1.10^{+0.29}_{-0.26}$	$0.84^{+0.27}_{-0.24}$
$\mu_F^{\tau\tau}$	$1.06^{+0.60}_{-0.56}$	$^{+0.56}_{-0.53}$	$1.72^{+1.24}_{-1.12}$	$0.89^{+0.67}_{-0.63}$
μ_F^{bb}	$1.15^{+0.99}_{-0.94}$	$^{+0.90}_{-0.86}$	$1.52^{+1.16}_{-1.09}$	$0.11^{+1.85}_{-1.90}$
Six-parameter fit of global μ_V/μ_F and of μ_F^f				
μ_V/μ_F	$1.09^{+0.36}_{-0.28}$	$^{+0.34}_{-0.27}$	$0.92^{+0.40}_{-0.30}$	$1.31^{+0.68}_{-0.47}$
$\mu_F^{\gamma\gamma}$	$1.10^{+0.23}_{-0.21}$	$^{+0.21}_{-0.19}$	$1.17^{+0.32}_{-0.28}$	$1.01^{+0.29}_{-0.25}$
μ_F^{ZZ}	$1.27^{+0.28}_{-0.24}$	$^{+0.24}_{-0.20}$	$1.55^{+0.43}_{-0.35}$	$0.98^{+0.32}_{-0.26}$
μ_F^{WW}	$1.06^{+0.21}_{-0.18}$	$^{+0.19}_{-0.17}$	$1.25^{+0.28}_{-0.24}$	$0.84^{+0.25}_{-0.21}$
$\mu_F^{\tau\tau}$	$1.05^{+0.33}_{-0.27}$	$^{+0.33}_{-0.27}$	$1.50^{+0.64}_{-0.48}$	$0.74^{+0.38}_{-0.29}$
μ_F^{bb}	$0.64^{+0.37}_{-0.28}$	$^{+0.45}_{-0.34}$	$0.67^{+0.58}_{-0.41}$	$0.63^{+0.53}_{-0.35}$

The 25 possible combinations resulting from five production processes times five decay modes can be parameterised using a 5×5 matrix $\mathcal{M}$ in two ways:

- allowing full freedom for all yields except the two mentioned above, which are not addressed in the combined analyses, leading to 23 free parameters, similarly to the fit performed for all products of cross sections times branching fractions and presented in Section 4.1.1;

- assuming that all yields originate from five production processes and five decay modes, leading to nine free parameters, as shown in Table 6, similarly to the fit performed for one reference cross section times branching fraction and eight ratios of cross sections and branching fractions, described in Section 4.1.2.

There is a direct relation between the rank of the 5×5 matrix $\mathcal{M}$ and the number of degenerate states. More specifically, if the observations are due to a single state, the matrix can be obtained from one of its

Table 16: The two signal parameterisations used to scale the expected yields of the 5×5 combinations of production processes and decay modes. The first parameterisation corresponds to the most general case with 25 independent parameters, while the second parameterisation corresponds to that expected for a single Higgs boson state. As explained in the text for the case of the general matrix parameterisation, the two parameters μ_{ggF}^{bb} and λ_{VBF}^{bb} are set to unity in the fits, since the current analyses are not able to constrain them.

General matrix parameterisation: rank($\mathcal{M}$) = 5					
	$H \to \gamma\gamma$	$H \to ZZ$	$H \to WW$	$H \to \tau\tau$	$H \to bb$
ggF	$\mu_{ggF}^{\gamma\gamma}$	μ_{ggF}^{ZZ}	μ_{ggF}^{WW}	$\mu_{ggF}^{\tau\tau}$	μ_{ggF}^{bb}
VBF	$\lambda_{VBF}^{\gamma\gamma}\,\mu_{ggF}^{\gamma\gamma}$	$\lambda_{VBF}^{ZZ}\,\mu_{ggF}^{ZZ}$	$\lambda_{VBF}^{WW}\,\mu_{ggF}^{WW}$	$\lambda_{VBF}^{\tau\tau}\,\mu_{ggF}^{\tau\tau}$	$\lambda_{VBF}^{bb}\,\mu_{ggF}^{bb}$
WH	$\lambda_{WH}^{\gamma\gamma}\,\mu_{ggF}^{\gamma\gamma}$	$\lambda_{WH}^{ZZ}\,\mu_{ggF}^{ZZ}$	$\lambda_{WH}^{WW}\,\mu_{ggF}^{WW}$	$\lambda_{WH}^{\tau\tau}\,\mu_{ggF}^{\tau\tau}$	$\lambda_{WH}^{bb}\,\mu_{ggF}^{bb}$
ZH	$\lambda_{ZH}^{\gamma\gamma}\,\mu_{ggF}^{\gamma\gamma}$	$\lambda_{ZH}^{ZZ}\,\mu_{ggF}^{ZZ}$	$\lambda_{ZH}^{WW}\,\mu_{ggF}^{WW}$	$\lambda_{ZH}^{\tau\tau}\,\mu_{ggF}^{\tau\tau}$	$\lambda_{ZH}^{bb}\,\mu_{ggF}^{bb}$
ttH	$\lambda_{ttH}^{\gamma\gamma}\,\mu_{ggF}^{\gamma\gamma}$	$\lambda_{ttH}^{ZZ}\,\mu_{ggF}^{ZZ}$	$\lambda_{ttH}^{WW}\,\mu_{ggF}^{WW}$	$\lambda_{ttH}^{\tau\tau}\,\mu_{ggF}^{\tau\tau}$	$\lambda_{ttH}^{bb}\,\mu_{ggF}^{bb}$

Single-state matrix parameterisation: rank($\mathcal{M}$) = 1					
	$H \to \gamma\gamma$	$H \to ZZ$	$H \to WW$	$H \to \tau\tau$	$H \to bb$
ggF	$\mu_{ggF}^{\gamma\gamma}$	μ_{ggF}^{ZZ}	μ_{ggF}^{WW}	$\mu_{ggF}^{\tau\tau}$	μ_{ggF}^{bb}
VBF	$\lambda_{VBF}\,\mu_{ggF}^{\gamma\gamma}$	$\lambda_{VBF}\,\mu_{ggF}^{ZZ}$	$\lambda_{VBF}\,\mu_{ggF}^{WW}$	$\lambda_{VBF}\,\mu_{ggF}^{\tau\tau}$	$\lambda_{VBF}\,\mu_{ggF}^{bb}$
WH	$\lambda_{WH}\,\mu_{ggF}^{\gamma\gamma}$	$\lambda_{WH}\,\mu_{ggF}^{ZZ}$	$\lambda_{WH}\,\mu_{ggF}^{WW}$	$\lambda_{WH}\,\mu_{ggF}^{\tau\tau}$	$\lambda_{WH}\,\mu_{ggF}^{bb}$
ZH	$\lambda_{ZH}\,\mu_{ggF}^{\gamma\gamma}$	$\lambda_{ZH}\,\mu_{ggF}^{ZZ}$	$\lambda_{ZH}\,\mu_{ggF}^{WW}$	$\lambda_{ZH}\,\mu_{ggF}^{\tau\tau}$	$\lambda_{ZH}\,\mu_{ggF}^{bb}$
ttH	$\lambda_{ttH}\,\mu_{ggF}^{\gamma\gamma}$	$\lambda_{ttH}\,\mu_{ggF}^{ZZ}$	$\lambda_{ttH}\,\mu_{ggF}^{WW}$	$\lambda_{ttH}\,\mu_{ggF}^{\tau\tau}$	$\lambda_{ttH}\,\mu_{ggF}^{bb}$

rows by using one common multiplier per row and therefore rank($\mathcal{M}$) = 1, in contrast to rank($\mathcal{M}$) = 5 in the most general case. The two parameterisations of $\mathcal{M}$ used in this test are shown in Table 16. They are both expressed in terms of μ_{ggF}^{j}, defined as in Eq. (3). Then, for the general case, the other parameters are $\lambda_i^j = \mu_i^j / \mu_{ggF}^j$, whereas for the rank($\mathcal{M}$) = 1 case the other parameters are $\lambda_i = \mu_i / \mu_{ggF}$. In this section, the index i runs over the VBF, WH, ZH, and ttH production processes and the index j runs over the five decay modes. The two statistical parameterisations are nested since the second one can be obtained from the first by imposing $\lambda_i^j = \lambda_i$. The SM prediction corresponds to the rank($\mathcal{M}$) =1 case, where $\mu_{ggF}^j = \lambda_i = \lambda_i^j = 1$.

In contrast to the fits described previously, all the parameters of interest are constrained to be positive for the fits performed in this section. This choice to restrict the parameter space to the physically meaningful region improves the convergence of the fits. The results of the fits to the data are consistent with those presented in Section 4.1 for the two similar parameterisations and are not reported here.

In order to quantify the compatibility of the data with the single-state hypothesis, a profile likelihood ratio test statistic, q_λ, is built that compares the hypothesis of a single-state matrix with rank($\mathcal{M}$) = 1 to the general hypothesis with rank($\mathcal{M}$) = 5:

$$q_\lambda = -2\ln \frac{L(\text{data}|\lambda_i^j = \hat{\lambda}_i, \hat{\mu}_{ggF}^j)}{L(\text{data}|\hat{\lambda}_i^j, \hat{\mu}_{ggF}'^j)}, \tag{11}$$

where $\hat{\mu}_{ggF}^j$ and $\hat{\mu}_{ggF}'^j$ represent the best fit values of the parameters of interest, respectively for the single-state and general hypotheses. The observed value of q_λ in data is compared with the expected distribution,

as obtained from pseudo-data samples randomly generated from the best fit values of the rank($\mathcal{M}$) =1 hypothesis. The p-value of the data with the single-state hypothesis is $(29\pm2)\%$, where the uncertainty reflects the finite number of pseudo-data samples generated, and does not show any significant departure from the single-state hypothesis. The p-values obtained for the individual experiments are 58% and 33% for ATLAS and CMS, respectively. These p-values can only be considered as the results of compatibility tests with the single-state hypothesis, represented by the rank($\mathcal{M}$) = 1 parameterisation described above.

6. Constraints on Higgs boson couplings

Section 4.2 discusses the fit results from the most generic parameterisation in the context of the κ-framework. This section probes more specific parameterisations with additional assumptions. In the following, results from a few selected parameterisations, with increasingly restrictive assumptions, are presented. The results are obtained from the combined fits to the $\sqrt{s}$ = 7 and 8 TeV data assuming that the coupling modifiers are the same at the two energies.

6.1. Parameterisations allowing contributions from BSM particles in loops and in decays

As discussed in Sections 2 and 3, the rates of Higgs boson production in the various decay modes are inversely proportional to the Higgs boson width, which is sensitive to potential invisible or undetected decay modes predicted by BSM theories. To directly measure the individual coupling modifiers, an assumption about the Higgs boson width is necessary. Two possible scenarios are considered in this section: the first leaves B_{BSM} free, provided that $B_{BSM} \geq 0$, but assumes that $|\kappa_W| \leq 1$ and $|\kappa_Z| \leq 1$ and that the signs of κ_W and κ_Z are the same, assumptions denoted $|\kappa_V| \leq 1$ in the following; the second assumes $B_{BSM} = 0$. The constraints assumed in the first scenario are compatible with a wide range of BSM physics, which may become manifest in the loop-induced processes of $gg \rightarrow H$ production and $H \rightarrow \gamma\gamma$ decay. These processes are particularly sensitive to loop contributions from new heavy particles, carrying electric or colour charge, or both, and such new physics can be probed using the effective coupling modifiers κ_g and κ_γ. Furthermore, potential deviations from the SM of the tree-level couplings to ordinary particles are parameterised with their respective coupling modifiers. The parameters of interest in the fits to data are thus the seven independent coupling modifiers, κ_Z, κ_W, κ_t, κ_τ, κ_b, κ_g, and κ_γ, one for each SM particle involved in the production processes and decay modes studied, plus B_{BSM} in the case of the first fit. Here and in Section 6.2, the coupling modifier κ_t is assumed to be positive, without any loss of generality.

Figure 15 and Table 17 show the results of the two fits, assuming either $|\kappa_V| \leq 1$ and $B_{BSM} \geq 0$ or $B_{BSM} = 0$. In the former case, an upper limit of $B_{BSM} = 0.34$ at 95% CL is obtained, compared to an expected upper limit of 0.39. The corresponding negative log-likelihood scan is shown in Fig. 16. Appendix C describes how the two possible sign combinations between κ_W and κ_Z impact the likelihood scan of B_{BSM} for the observed and expected results, as illustrated in Fig. 32. The p-value of the compatibility between the data and the SM predictions is 11% with the assumption that $B_{BSM} = 0$.

Another fit, motivated, for example, by BSM scenarios with new heavy particles that may contribute to loop processes in Higgs boson production or decay, assumes that all the couplings to SM particles are the same as in the SM, that there are no BSM decays ($B_{BSM} = 0$), and that only the gluon–gluon production
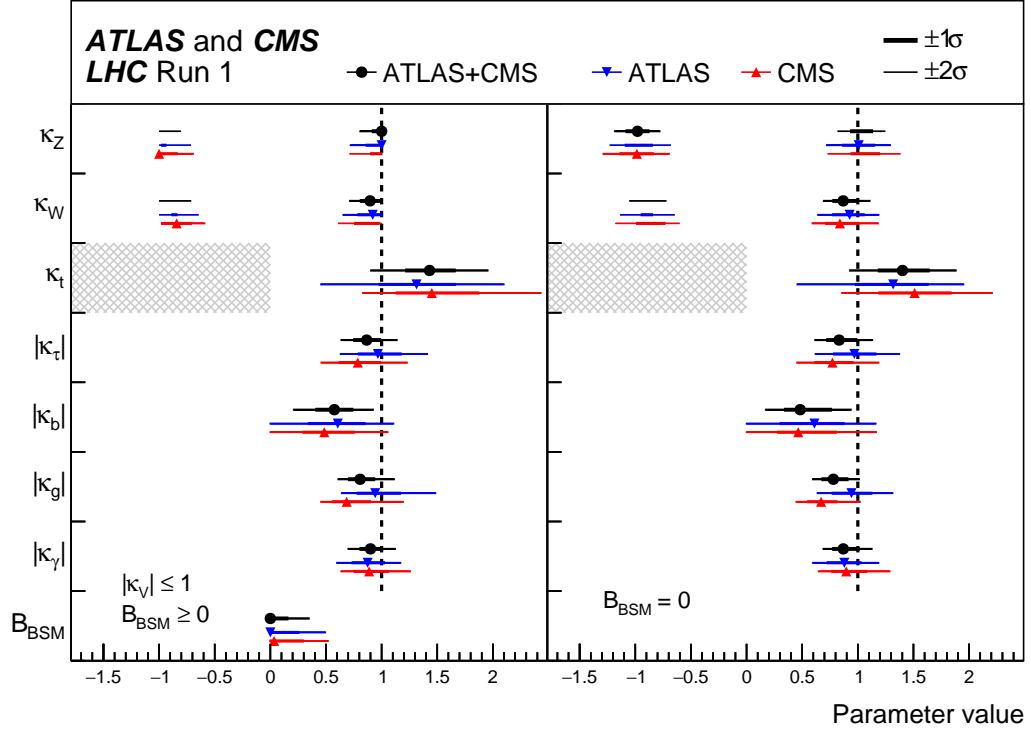
Figure 15: Fit results for two parameterisations allowing BSM loop couplings discussed in the text: the first one assumes that $B_{BSM} \geq 0$ and that $|\kappa_V| \leq 1$, where κ_V denotes κ_Z or κ_W, and the second one assumes that there are no additional BSM contributions to the Higgs boson width, i.e. $B_{BSM} = 0$. The measured results for the combination of ATLAS and CMS are reported together with their uncertainties, as well as the individual results from each experiment. The hatched areas show the non-allowed regions for the κ_t parameter, which is assumed to be positive without loss of generality. The error bars indicate the 1σ (thick lines) and 2σ (thin lines) intervals. When a parameter is constrained and reaches a boundary, namely $|\kappa_V| = 1$ or $B_{BSM} = 0$, the uncertainty is not defined beyond this boundary. For those parameters with no sensitivity to the sign, only the absolute values are shown.

and $\gamma\gamma$ decay loops may be affected by the presence of additional particles. The results of this fit, which has only the effective coupling modifiers κ_γ and κ_g as free parameters, with all other coupling modifiers fixed to their SM values of unity, are shown in Fig. 17. The point $\kappa_\gamma = 1$ and $\kappa_g = 1$ lies within the 68% CL region and the p-value of the compatibility between the data and the SM predictions is 82%.

Table 17: Fit results for two parameterisations allowing BSM loop couplings discussed in the text: the first one assumes that $|\kappa_V| \leq 1$, where κ_V denotes κ_Z or κ_W, and that $B_{BSM} \geq 0$, while the second one assumes that there are no additional BSM contributions to the Higgs boson width, i.e. $B_{BSM} = 0$. The results for the combination of ATLAS and CMS are reported with their measured and expected uncertainties. Also shown are the results from each experiment. For the parameters with both signs allowed, the 1σ intervals are shown on a second line. When a parameter is constrained and reaches a boundary, namely $B_{BSM} = 0$, the uncertainty is not indicated. For those parameters with no sensitivity to the sign, only the absolute values are shown.

| Parameter	ATLAS+CMS Measured	ATLAS+CMS Expected uncertainty	ATLAS Measured	CMS Measured
Parameterisation assuming $	\kappa_V	\leq 1$ and $B_{BSM} \geq 0$
κ_Z	1.00		1.00	-1.00
	$[0.92, 1.00]$	$[-1.00, -0.89] \cup$	$[-0.97, -0.94] \cup$	$[-1.00, -0.84] \cup$
		$[0.89, 1.00]$	$[0.86, 1.00]$	$[0.90, 1.00]$
κ_W	0.90		0.92	-0.84
	$[0.81, 0.99]$	$[-1.00, -0.90] \cup$	$[-0.88, -0.84] \cup$	$[-1.00, -0.71] \cup$
		$[0.89, 1.00]$	$[0.79, 1.00]$	$[0.76, 0.98]$
κ_t	$1.43^{+0.23}_{-0.22}$	$^{+0.27}_{-0.32}$	$1.31^{+0.35}_{-0.33}$	$1.45^{+0.42}_{-0.32}$
$|\kappa_\tau|$	$0.87^{+0.12}_{-0.11}$	$^{+0.14}_{-0.15}$	$0.97^{+0.21}_{-0.17}$	$0.79^{+0.20}_{-0.16}$
$|\kappa_b|$	$0.57^{+0.16}_{-0.16}$	$^{+0.19}_{-0.23}$	$0.61^{+0.24}_{-0.26}$	$0.49^{+0.26}_{-0.19}$
$|\kappa_g|$	$0.81^{+0.13}_{-0.10}$	$^{+0.17}_{-0.14}$	$0.94^{+0.23}_{-0.16}$	$0.69^{+0.21}_{-0.13}$
$|\kappa_\gamma|$	$0.90^{+0.10}_{-0.09}$	$^{+0.10}_{-0.12}$	$0.87^{+0.15}_{-0.14}$	$0.89^{+0.17}_{-0.13}$
B_{BSM}	$0.00^{+0.16}$	$^{+0.19}$	$0.00^{+0.25}$	$0.03^{+0.26}$
Parameterisation assuming $B_{BSM} = 0$
κ_Z	-0.98		1.01	-0.99
	$[-1.08, -0.88] \cup$	$[-1.01, -0.87] \cup$	$[-1.09, -0.85] \cup$	$[-1.14, -0.84] \cup$
	$[0.94, 1.13]$	$[0.89, 1.11]$	$[0.87, 1.15]$	$[0.94, 1.19]$
κ_W	0.87		0.92	0.84
	$[0.78, 1.00]$	$[-1.08, -0.90] \cup$	$[-0.94, -0.85] \cup$	$[-0.99, -0.74] \cup$
		$[0.88, 1.11]$	$[0.78, 1.05]$	$[0.71, 1.01]$
κ_t	$1.40^{+0.24}_{-0.21}$	$^{+0.26}_{-0.39}$	$1.32^{+0.31}_{-0.33}$	$1.51^{+0.33}_{-0.32}$
$|\kappa_\tau|$	$0.84^{+0.15}_{-0.11}$	$^{+0.16}_{-0.15}$	$0.97^{+0.19}_{-0.19}$	$0.77^{+0.18}_{-0.15}$
$|\kappa_b|$	$0.49^{+0.27}_{-0.15}$	$^{+0.25}_{-0.28}$	$0.61^{+0.26}_{-0.31}$	$0.47^{+0.34}_{-0.19}$
$|\kappa_g|$	$0.78^{+0.13}_{-0.10}$	$^{+0.17}_{-0.14}$	$0.94^{+0.18}_{-0.17}$	$0.67^{+0.14}_{-0.12}$
$|\kappa_\gamma|$	$0.87^{+0.14}_{-0.09}$	$^{+0.12}_{-0.13}$	$0.88^{+0.15}_{-0.15}$	$0.89^{+0.19}_{-0.13}$
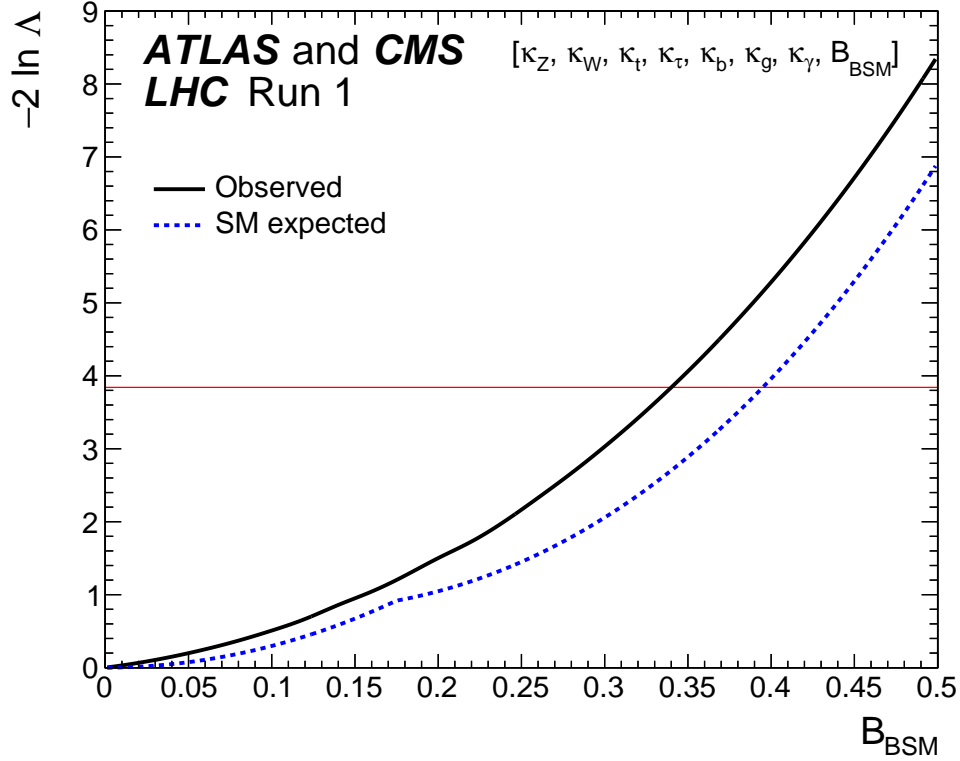
Figure 16: Observed (solid line) and expected (dashed line) negative log-likelihood scan of B_{BSM}, shown for the combination of ATLAS and CMS when allowing additional BSM contributions to the Higgs boson width. The results are shown for the parameterisation with the assumptions that $|\kappa_V| \leq 1$ and $B_{BSM} \geq 0$ in Fig. 15. All the other parameters of interest from the list in the legend are also varied in the minimisation procedure. The red horizontal line at 3.84 indicates the log-likelihood variation corresponding to the 95% CL upper limit, as discussed in Section 3.2.

6.2. Parameterisation assuming SM structure of the loops and no BSM decays

In this section it is assumed that there are no new particles in the loops entering ggF production and $H \rightarrow \gamma\gamma$ decay. This assumption is supported by the measurements of the effective coupling modifiers κ_g and κ_γ, which are consistent with the SM predictions. The cross section for ggF production and the branching fraction for the $H \rightarrow \gamma\gamma$ decay are expressed in terms of the coupling modifiers of the SM particles in the loops, as indicated in Table 4. This leads to a parameterisation with six free coupling modifiers: κ_W, κ_Z, κ_t, κ_τ, κ_b, and κ_μ; the results of the $H \rightarrow \mu\mu$ analysis are included for this specific case. In this more constrained fit, it is also assumed that $B_{BSM} = 0$.

Figure 18 and Table 18 show the results of the fit for the combination of ATLAS and CMS, and separately for each experiment. Compared to the results from the fitted decay signal strengths (Table 13) or the global signal strength $\mu = 1.09 \pm 0.11$ (Section 5.1), this fit yields values of the coupling modifiers lower than those predicted by the SM. This is a consequence of the low value of κ_b, as measured by the combination of ATLAS and CMS and by each experiment. A low value of κ_b decreases the total Higgs boson width through the dominant Γ^{bb} partial decay width, and, as a consequence, the measured values of all the
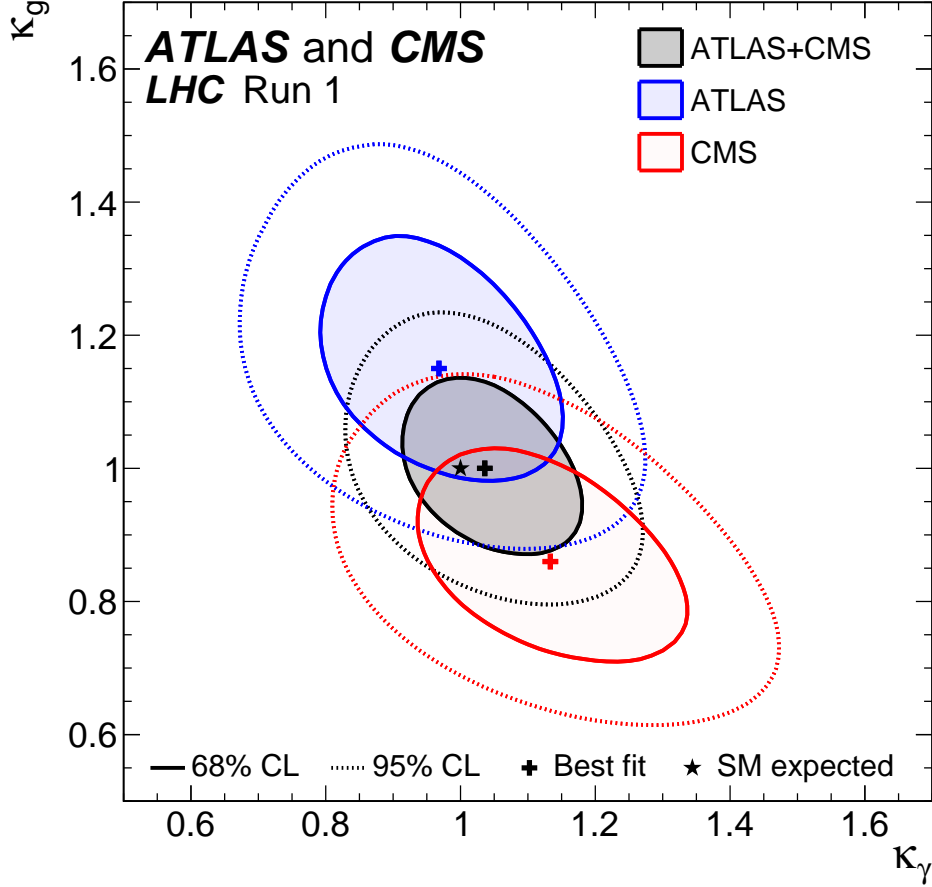
Figure 17: Negative log-likelihood contours at 68% and 95% CL in the $(\kappa_\gamma, \kappa_g)$ plane for the combination of ATLAS and CMS and for each experiment separately, as obtained from the fit to the parameterisation constraining all the other coupling modifiers to their SM values and assuming $B_{BSM} = 0$.

coupling modifiers decrease, such that the values of $\sigma_i(\vec{\kappa}) \cdot B^f$ remain consistent with the observed signal yields. The p-value of the compatibility between the data and the SM predictions is 74%.

A different view of the relation between the fitted coupling modifiers and the SM predictions is presented in Fig. 19. New parameters are derived from the coupling modifiers, to make explicit the dependence on the particle masses: linear for the Yukawa couplings to the fermions and quadratic for the gauge couplings of the Higgs boson to the weak vector bosons. These new parameters are all assumed in this case to be positive. For fermions with mass $m_{F,i}$, the parameters are $\kappa_{F,i} \cdot y_{F,i}/\sqrt{2} = \kappa_{F,i} \cdot m_{F,i}/v$, where $y_{F,i}$ is the Yukawa coupling strength, assuming a SM Higgs boson with a mass of 125.09 GeV, and $v = 246$ GeV is the vacuum expectation value of the Higgs field. For the weak vector bosons with mass $m_{V,i}$, the new parameters are $\sqrt{\kappa_{V,i} \cdot g_{V,i}/2v} = \sqrt{\kappa_{V,i}} \cdot m_{V,i}/v$, where $g_{V,i}$ is the absolute Higgs boson gauge coupling strength. The linear scaling of these new parameters as a function of the particle masses observed in Fig. 19 indicates qualitatively the compatibility of the measurements with the SM. For the b quark, the running mass evaluated at a scale equal to m_H, $m_b(m_H) = 2.76$ GeV, is used.

Following the phenomenological model suggested in Ref. [129], the coupling modifiers can also be ex-
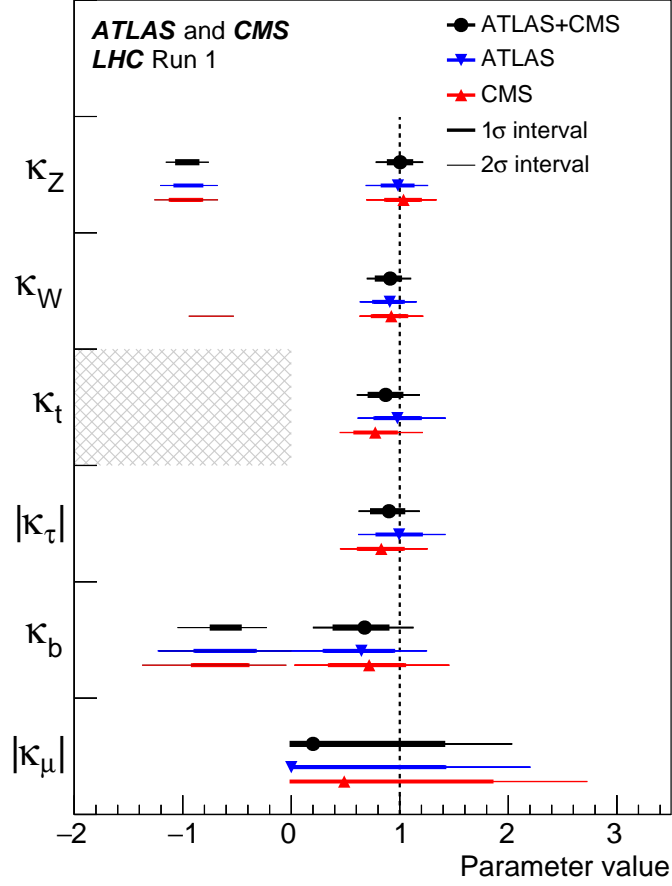
Figure 18: Best fit values of parameters for the combination of ATLAS and CMS data, and separately for each experiment, for the parameterisation assuming the absence of BSM particles in the loops, $B_{BSM} = 0$. The hatched area indicates the non-allowed region for the parameter that is assumed to be positive without loss of generality. The error bars indicate the 1σ (thick lines) and 2σ (thin lines) intervals. When a parameter is constrained and reaches a boundary, namely $|\kappa_\mu| = 0$, the uncertainty is not defined beyond this boundary. For those parameters with no sensitivity to the sign, only the absolute values are shown.

pressed as a function of a mass scaling parameter ϵ, with a value $\epsilon = 0$ in the SM, and a free parameter M, equal to v in the SM: $\kappa_{F,i} = v \cdot m_{F,i}^\epsilon / M^{1+\epsilon}$ and $\kappa_{V,i} = v \cdot m_{V,i}^{2\epsilon} / M^{1+2\epsilon}$. A fit is then performed with the same assumptions as those of Table 18 with ϵ and M as parameters of interest. The results for the combination of ATLAS and CMS are $\epsilon = 0.023^{+0.029}_{-0.027}$ and $M = 233^{+13}_{-12}$ GeV, and are compatible with the SM predictions. Figure 19 shows the results of this fit with its corresponding 68% and 95% CL bands.

6.3. Parameterisations related to the fermion sector

Common coupling modifications for up-type fermions versus down-type fermions or for leptons versus quarks are predicted by many extensions of the SM. One such class of theoretically well motivated models is the 2HDM [130].

The ratios of the coupling modifiers are tested in the most generic parameterisation proposed in Ref. [32],

Table 18: Fit results for the parameterisation assuming the absence of BSM particles in the loops ($B_{BSM} = 0$). The results with their measured and expected uncertainties are reported for the combination of ATLAS and CMS, together with the individual results from each experiment. For the parameters with both signs allowed, the 1σ CL intervals are shown on a second line. When a parameter is constrained and reaches a boundary, namely $|\kappa_\mu| = 0$, the uncertainty is not indicated. For those parameters with no sensitivity to the sign, only the absolute values are shown.

Parameter	ATLAS+CMS Measured	ATLAS+CMS Expected uncertainty	ATLAS Measured	CMS Measured
κ_Z	1.00		0.98	1.03
	$[-1.05, -0.86]\cup$	$[-1.00, -0.88]\cup$	$[-1.07, -0.83]\cup$	$[-1.11, -0.83]\cup$
	$[0.90, 1.11]$	$[0.90, 1.10]$	$[0.84, 1.12]$	$[0.87, 1.19]$
κ_W	$0.91^{+0.10}_{-0.12}$	$^{+0.10}_{-0.11}$	$0.91^{+0.12}_{-0.15}$	$0.92^{+0.14}_{-0.17}$
κ_t	$0.87^{+0.15}_{-0.15}$	$^{+0.15}_{-0.18}$	$0.98^{+0.21}_{-0.20}$	$0.77^{+0.20}_{-0.18}$
$|\kappa_\tau|$	$0.90^{+0.14}_{-0.16}$	$^{+0.15}_{-0.14}$	$0.99^{+0.20}_{-0.20}$	$0.83^{+0.20}_{-0.21}$
κ_b	0.67		0.64	0.71
	$[-0.73, -0.47]\cup$	$[-1.24, -0.76]\cup$	$[-0.89, -0.33]\cup$	$[-0.91, -0.40]\cup$
	$[0.40, 0.89]$	$[0.74, 1.24]$	$[0.30, 0.94]$	$[0.35, 1.04]$
$|\kappa_\mu|$	$0.2^{+1.2}$	$^{+0.9}$	$0.0^{+1.4}$	$0.5^{+1.4}$

in which the total Higgs boson width is also allowed to vary. The main parameters of interest for these tests are $\lambda_{du} = \kappa_d/\kappa_u$ for the up- and down-type fermion symmetry, and $\lambda_{lq} = \kappa_l/\kappa_q$ for the lepton and quark symmetry, where both are allowed to be positive or negative. In this parameterisation, the loops are resolved in terms of their expected SM contributions.

6.3.1. Probing the up- and down-type fermion symmetry

The free parameters for this test are: $\lambda_{du} = \kappa_d/\kappa_u$, $\lambda_{Vu} = \kappa_V/\kappa_u$, and $\kappa_{uu} = \kappa_u \cdot \kappa_u/\kappa_H$, where this latter term is positive definite since κ_H is always assumed to be positive. The up-type fermion couplings are mainly probed by the ggF production process, the $H \to \gamma\gamma$ decay channel, and to a certain extent the ttH production process. The down-type fermion couplings are mainly probed by the $H \to bb$ and $H \to \tau\tau$ decays. A small sensitivity to the relative sign arises from the interference between top and bottom quarks in the gluon fusion loop.

The results of the fit are reported in Table 19 and Fig. 20. The p-value of the compatibility between the data and the SM predictions is 72%. The likelihood scan for the λ_{du} parameter is shown in Fig. 21 for the combination of ATLAS and CMS. Negative values for the parameter λ_{Vu} are excluded by more than 4σ.
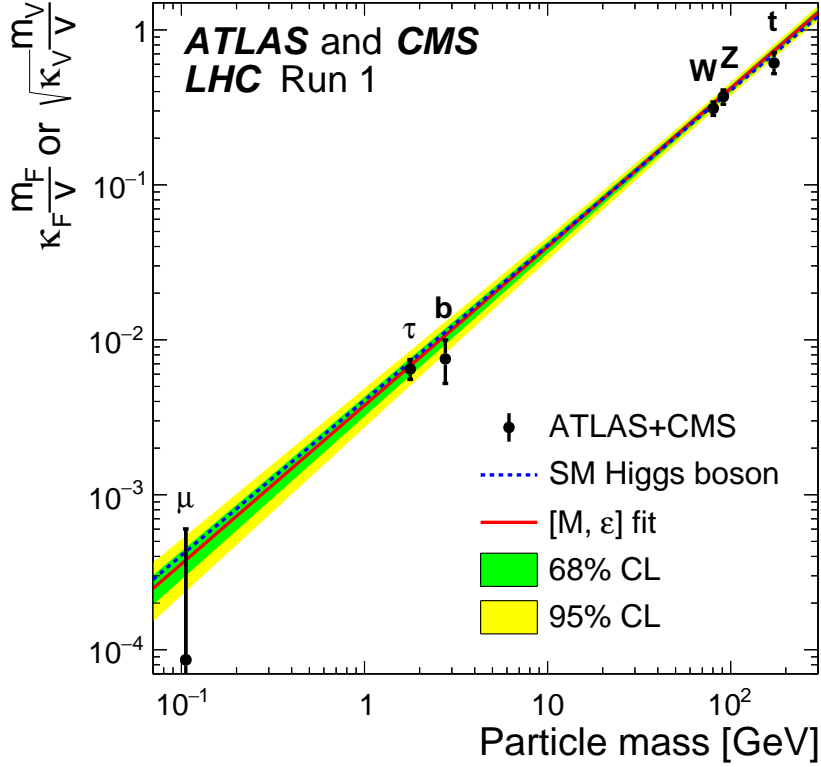
Figure 19: Best fit values as a function of particle mass for the combination of ATLAS and CMS data in the case of the parameterisation described in the text, with parameters defined as $\kappa_F \cdot m_F/v$ for the fermions, and as $\sqrt{\kappa_V} \cdot m_V/v$ for the weak vector bosons, where $v = 246$ GeV is the vacuum expectation value of the Higgs field. The dashed (blue) line indicates the predicted dependence on the particle mass in the case of the SM Higgs boson. The solid (red) line indicates the best fit result to the $[M, \epsilon]$ phenomenological model of Ref. [129] with the corresponding 68% and 95% CL bands.

6.3.2. Probing the lepton and quark symmetry

The parameterisation for this test is very similar to that of Section 6.3.1, which probes the up- and down-type fermion symmetry. In this case, the free parameters are $\lambda_{lq} = \kappa_l/\kappa_q$, $\lambda_{Vq} = \kappa_V/\kappa_q$, and $\kappa_{qq} = \kappa_q \cdot \kappa_q/\kappa_H$, where the latter term is positive definite, like κ_{uu}. The quark couplings are mainly probed by the ggF process, the $H \to \gamma\gamma$ and $H \to bb$ decays, and to a lesser extent by the ttH process. The lepton couplings are probed by the $H \to \tau\tau$ decays. The results are expected, however, to be insensitive to the relative sign of the couplings, because there is no sizeable lepton–quark interference in any of the relevant Higgs boson production processes and decay modes. Only the absolute value of the λ_{lq} parameter is therefore considered in the fit.

The results of the fit are reported in Table 19 and Fig. 22. The p-value of the compatibility between the data and the SM predictions is 79%. The likelihood scan for the λ_{lq} parameter is shown in Fig. 23 for the combination of ATLAS and CMS. Negative values for the parameter λ_{Vq} are excluded by more than 4σ.

Table 19: Summary of fit results for the two parameterisations probing the ratios of coupling modifiers for up-type versus down-type fermions and for leptons versus quarks. The results for the combination of ATLAS and CMS are reported together with their measured and expected uncertainties. Also shown are the results from each experiment. The parameters κ_{uu} and κ_{qq} are both positive definite since κ_H is always assumed to be positive. For the parameter λ_{du}, for which both signs are allowed, the 1σ CL intervals are shown on a second line. For the parameter λ_{lq}, for which there is no sensitivity to the sign, only the absolute values are shown. Negative values for the parameters λ_{Vu} and λ_{Vq} are excluded by more than 4σ.

| Parameter	ATLAS+CMS Measured	ATLAS+CMS Expected uncertainty	ATLAS Measured	CMS Measured
λ_{du}	0.92		0.86	1.01
	$[0.80, 1.04]$	$[-1.21, -0.92]\cup$	$[-1.03, -0.78]\cup$	$[-1.20, -0.94]\cup$
		$[0.87, 1.14]$	$[0.73, 1.01]$	$[0.83, 1.21]$
λ_{Vu}	$1.00^{+0.13}_{-0.12}$	$^{+0.20}_{-0.12}$	$0.88^{+0.18}_{-0.14}$	$1.16^{+0.23}_{-0.19}$
κ_{uu}	$1.07^{+0.22}_{-0.18}$	$^{+0.20}_{-0.27}$	$1.33^{+0.35}_{-0.34}$	$0.82^{+0.24}_{-0.21}$
$|\lambda_{lq}|$	$1.06^{+0.15}_{-0.14}$	$^{+0.16}_{-0.14}$	$1.10^{+0.20}_{-0.18}$	$1.05^{+0.24}_{-0.22}$
λ_{Vq}	$1.09^{+0.14}_{-0.13}$	$^{+0.13}_{-0.12}$	$1.01^{+0.17}_{-0.15}$	$1.18^{+0.22}_{-0.19}$
κ_{qq}	$0.93^{+0.17}_{-0.15}$	$^{+0.18}_{-0.16}$	$1.07^{+0.24}_{-0.21}$	$0.80^{+0.22}_{-0.18}$
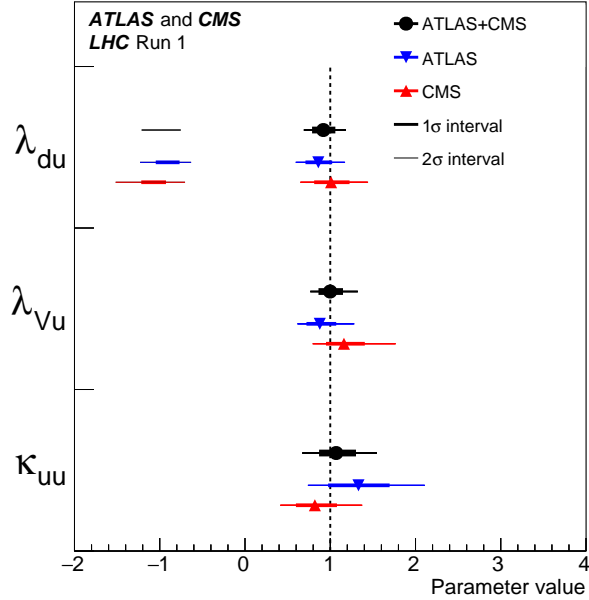
Figure 20: Best fit values of parameters for the combination of ATLAS and CMS data, and separately for each experiment, for the parameterisation testing the up- and down-type fermion coupling ratios. The error bars indicate the 1σ (thick lines) and 2σ (thin lines) intervals. The parameter κ_{uu} is positive definite since κ_H is always assumed to be positive. Negative values for the parameter λ_{Vu} are excluded by more than 4σ.
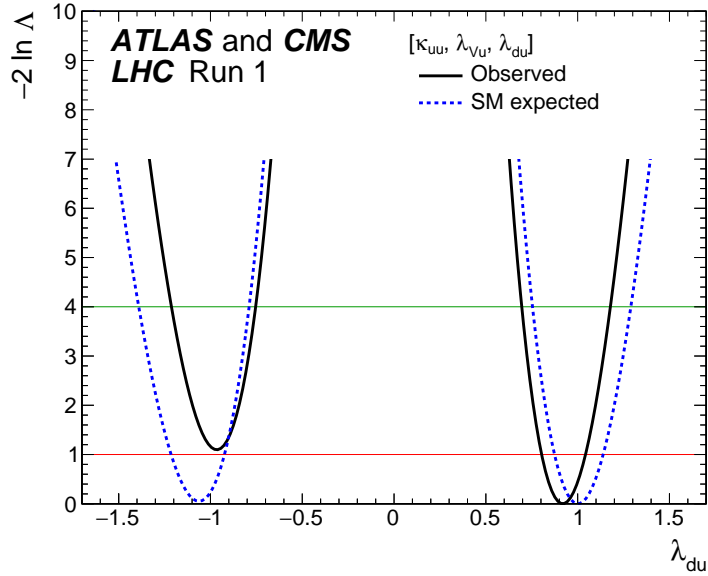
Figure 21: Observed (solid line) and expected (dashed line) negative log-likelihood scan of the λ_{du} parameter, probing the ratios of coupling modifiers for up-type versus down-type fermions for the combination of ATLAS and CMS. The other parameters of interest from the list in the legend are also varied in the minimisation procedure. The red (green) horizontal line at the $-2\Delta\ln\Lambda$ value of 1 (4) indicates the value of the profile likelihood ratio corresponding to a 1σ (2σ) CL interval for the parameter of interest, assuming the asymptotic χ^2 distribution of the test statistic.

6.4. Fermion and vector boson couplings

The last and most constrained parameterisation studied in this section is motivated by the intrinsic difference between the Higgs boson couplings to weak vector bosons, which originate from the breaking of the EW symmetry, and the Yukawa couplings to the fermions. Similarly to Section 6.2, it is assumed in this section that there are no new particles in the loops (ggF production process and $H \rightarrow \gamma\gamma$ decay mode) and that there are no BSM decays, i.e. $B_{BSM} = 0$. Vector and fermion coupling modifiers, κ_V and κ_F, are defined such that $\kappa_Z = \kappa_W = \kappa_V$ and $\kappa_t = \kappa_\tau = \kappa_b = \kappa_F$. These definitions can be applied either globally, yielding two parameters, or separately for each of the five decay channels, yielding ten parameters κ_V^f and κ_F^f (following the notation related to Higgs boson decays used for the signal strength parameterisation). Two fits are performed: a two-parameter fit as a function of κ_V and κ_F, and a ten-parameter fit as a function of κ_V^f and κ_F^f for each decay channel.

As explained in Section 2.4 and shown explicitly in Table 4, the Higgs boson production cross sections and partial decay widths are only sensitive to products of coupling modifiers and not to their absolute sign. Any sensitivity to the relative sign between κ_V and κ_F can only occur through interference terms, either in the $H \rightarrow \gamma\gamma$ decays, through the t–W interference in the $\gamma\gamma$ decay loop, or in $ggZH$ or tH production. Without any loss of generality, this parameterisation assumes that one of the two coupling modifiers, namely κ_V (or κ_V^f), is positive.

The combined ATLAS and CMS results are shown in Fig. 24 for the individual channels and their combination. The individual decay channels are seen to be compatible with each other only for positive values of κ_F^f. The incompatibility between the channels for negative values of κ_F^f arises mostly from the
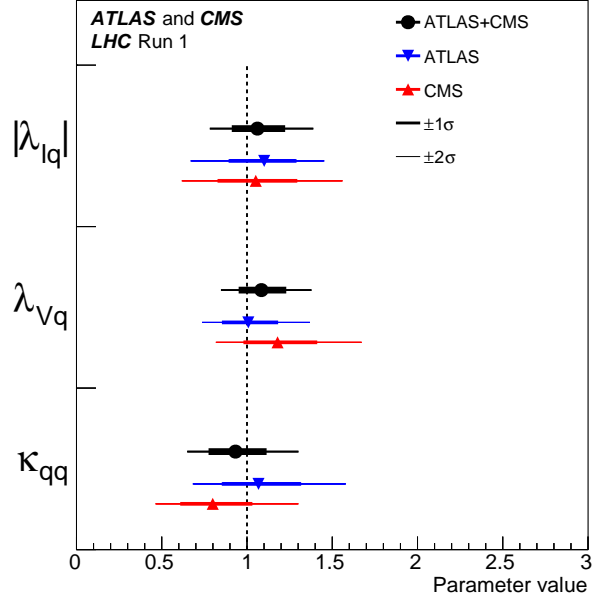
Figure 22: Best fit values of parameters for the combination of ATLAS and CMS data, and separately for each experiment, for the parameterisation testing the lepton and quark coupling ratios. The error bars indicate the 1σ (thick lines) and 2σ (thin lines) intervals. For the parameter λ_{lq}, for which there is no sensitivity to the sign, only the absolute values are shown. The parameter κ_{qq} is positive definite since κ_H is always assumed to be positive. Negative values for the parameter λ_{Vq} are excluded by more than 4σ.
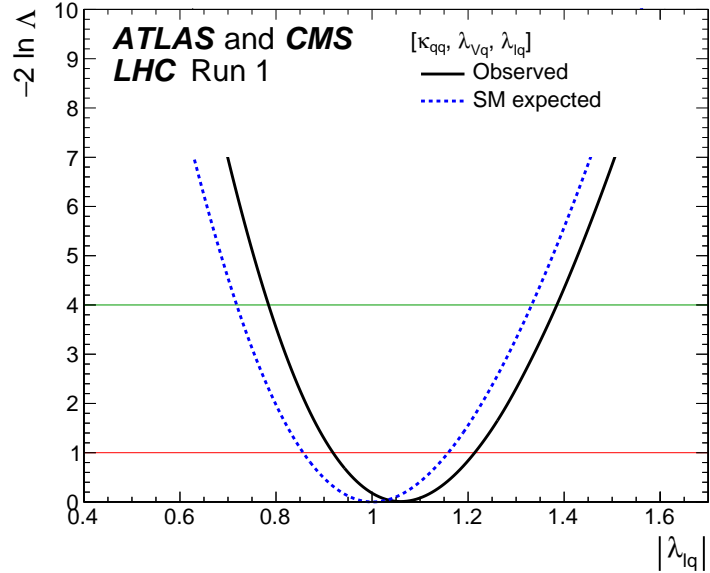
Figure 23: Observed (solid line) and expected (dashed line) negative log-likelihood scan of the λ_{lq} parameter, probing the ratios of coupling modifiers for leptons versus quarks for the combination of ATLAS and CMS. The other parameters of interest from the list in the legend are also varied in the minimisation procedure. The red (green) horizontal line at the $-2\Delta\ln\Lambda$ value of 1 (4) indicates the value of the profile likelihood ratio corresponding to a 1σ (2σ) CL interval for the parameter of interest, assuming the asymptotic χ^2 distribution of the test statistic.
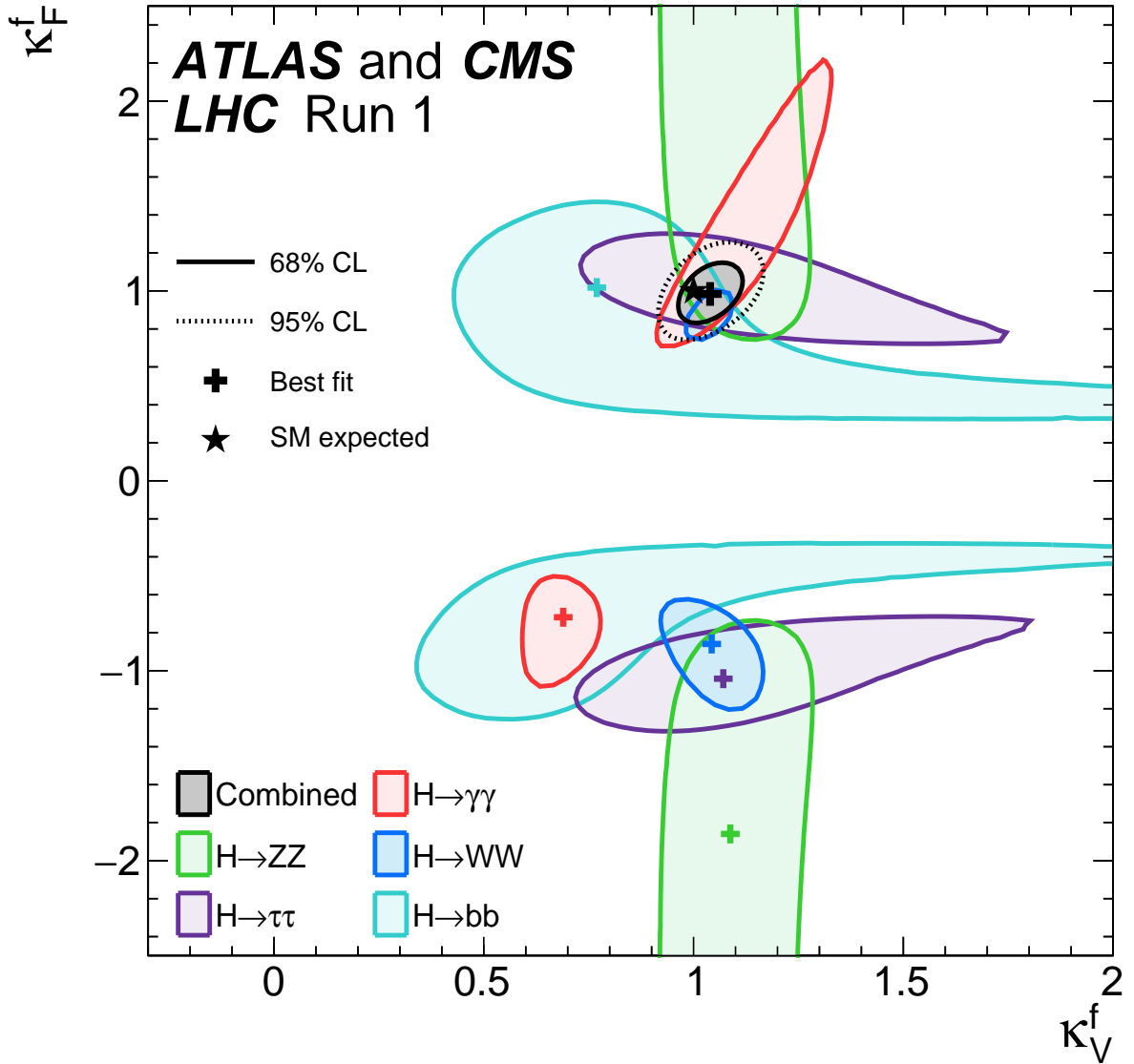
Figure 24: Negative log-likelihood contours at 68% and 95% CL in the (κ_F^f, κ_V^f) plane for the combination of ATLAS and CMS and for the individual decay channels, as well as for their combination (κ_F versus κ_V shown in black), without any assumption about the sign of the coupling modifiers. The other two quadrants (not shown) are symmetric with respect to the point (0,0).

$H \to \gamma\gamma$, $H \to WW$, and $H \to ZZ$ channels. Nonetheless, the best fit values for most of the individual channels correspond to negative values of κ_F^f. However, the best fit value from the global fit yields $\kappa_F \geq 0$, a result that is driven by the large asymmetry between the positive and negative coupling ratios in the case of $H \to \gamma\gamma$ decays.

The fact that, for four of the five individual channels, the best fit values correspond to $\kappa_F^f \leq 0$ is not significant, as shown by the likelihood curves in Figs. 25 (a-e). The $H \to bb$ decay channel displays the

largest expected sensitivity, mostly arising from the contribution of the $ggZH$ process, and the best fit value of κ_F^{bb} is positive. For all other decay modes, a small sensitivity arises because of the tH process. The excess observed in the combination of the two experiments for the ttH production process induces a preference for a relative negative sign between the two coupling modifiers, which increases significantly the tH cross section and thereby provides a better fit to the data. The only visible difference between the two minima at positive and negative values of κ_F^f is observed for the $H \rightarrow WW$ channel.

As stated above, the channel most affected by the relative sign of the couplings is the $H \rightarrow \gamma\gamma$ decay channel: because of the negative t–W interference in the $\gamma\gamma$ loop, the $H \rightarrow \gamma\gamma$ partial width would be much larger if the sign of $\kappa_F^{\gamma\gamma}$ were opposite to that of $\kappa_V^{\gamma\gamma}$. When combining the $H \rightarrow \gamma\gamma$ decay channel with all the other channels, the opposite sign case is excluded by almost 5σ, as can be inferred from Fig. 25 (f).

Figure 26 (top) presents, on an enlarged scale, the results of the scan for the global coupling modifiers as well as those obtained separately for each experiment. For completeness, additional likelihood scans are performed for the two global coupling modifiers and for those of each decay channel, assuming in all cases that κ_F and κ_V are both positive. The results of these scans are shown in Fig. 26 (bottom). The most precise determination of κ_F^f and κ_V^f is obtained from the $H \rightarrow WW$ decay channel because it is the only one that provides significant constraints on both parameters, through the measurements of the ggF and VBF production processes. The difference in size between the $H \rightarrow WW$ confidence regions obtained for $\kappa_F^f \geq 0$ in Fig. 24 and Fig. 26 (bottom), where it is explicitly assumed that $\kappa_F^f \geq 0$, is due to the fact that the negative log-likelihood contours are evaluated using as a reference the minima obtained from different likelihood fits. The combination of all decay modes provides significant additional constraints. All results are in agreement with the SM prediction, $\kappa_F^f = 1$ and $\kappa_V^f = 1$, and the p-value of the compatibility between the data and the SM predictions is 59%.

7. Summary

An extensive set of combined ATLAS and CMS measurements of the Higgs boson production and decay rates is presented, and a number of constraints on its couplings to vector bosons and fermions are derived based on various sets of assumptions. The combination is based on the analysis of approximately 600 categories of selected events, concerning five production processes, ggF, VBF, WH, ZH, and ttH, where ggF and VBF refer, respectively, to production through the gluon fusion and vector boson fusion processes; and six decay channels, $H \rightarrow ZZ, WW, \gamma\gamma, \tau\tau, bb$, and $\mu\mu$. All results are reported assuming a value of 125.09 GeV for the Higgs boson mass, the result of the combined Higgs boson mass measurement by the two experiments [22]. The analysis uses the LHC proton-proton collision data sets recorded by the ATLAS and CMS detectors in 2011 and 2012, corresponding to integrated luminosities per experiment of approximately 5 fb^{-1} at $\sqrt{s}$ = 7 TeV and 20 fb^{-1} at $\sqrt{s}$ = 8 TeV. This paper presents the final Higgs boson coupling combined results from ATLAS and CMS based on the LHC Run 1 data.

The combined analysis is sensitive to the couplings of the Higgs boson to the weak vector bosons and to the heavier fermions (top quarks, b quarks, τ leptons, and – marginally – muons). The analysis is also sensitive to the effective couplings of the Higgs boson to the photon and the gluon. At the LHC, only products of cross sections and branching fractions are measured, so the width of the Higgs boson cannot be probed without assumptions beyond the main one used for all measurements presented here, namely that the Higgs boson production and decay kinematics are close to those predicted by the Standard Model (SM). In general, the combined analysis presented in this paper provides a significant improvement

with respect to the individual combinations published by each experiment separately. The precision of the results improves in most cases by a factor of approximately $1/\sqrt{2}$, as one would expect for the combination of two largely uncorrelated measurements based on similar-size data samples. A few illustrative results are summarised below.

For the first time, results are shown for the most generic parameterisation of the observed event yields in terms of products of Higgs boson production cross sections times branching fractions, separately for each of 20 measurable (σ_i, B^f) pairs of production processes and decay modes. These measurements do not rely on theoretical predictions for the inclusive cross sections and the uncertainties are mostly dominated by their statistical component. In the context of this parameterisation, one can test whether the observed yields arise from more than one Higgs boson, all with experimentally indistinguishable masses, but possibly with different coupling structures to the SM particles. The data are compatible with the hypothesis of a single Higgs boson, yielding a *p*-value of 29%.

Fits to the observed event yields are also performed without any assumption about the Higgs boson width in the context of two other generic parameterisations. The first parameterisation is in terms of ratios of production cross sections and branching fractions, together with the reference cross section of the process $gg \rightarrow H \rightarrow ZZ$. All results are compatible with the SM. The best relative precision, of about 30%, is achieved for the ratio of cross sections $\sigma_{\mathrm{VBF}}/\sigma_{ggF}$ and for the ratios of branching fractions B^{WW}/B^{ZZ} and $B^{\gamma\gamma}/B^{ZZ}$. A relative precision of around 40% is achieved for the ratio of branching fractions $B^{\tau\tau}/B^{ZZ}$. The second parameterisation is in terms of ratios of coupling modifiers, together with one parameter expressing the $gg \rightarrow H \rightarrow ZZ$ reference process in terms of these modifiers. The ratios of coupling modifiers are measured with precisions of approximately 10–20%, where the improvement in precision in this second parameterisation arises because the signal yields are expressed as squares or products of these coupling modifiers.

All measurements based on the generic parameterisations are compatible between the two experiments and with the predictions of the SM. The potential presence of physics beyond the SM (BSM) is also probed using specific parameterisations. With minimal additional assumptions, the overall branching fraction of the Higgs boson into BSM decays is determined to be less than 34% at 95% CL. This constraint applies to invisible decays into BSM particles, decays into BSM particles that are not detected as such, and modifications of the decays into SM particles that are not directly measured by the experiments.

The combined signal yield relative to the SM expectation is measured to be 1.09 ± 0.07 (stat) ± 0.08 (syst), where the systematic uncertainty is dominated by the theoretical uncertainty in the inclusive cross sections. The measured (expected) significance for the direct observation of the VBF production process is at the level of 5.4σ (4.6σ), while that for the $H \rightarrow \tau\tau$ decay channel is at the level of 5.5σ (5.0σ).
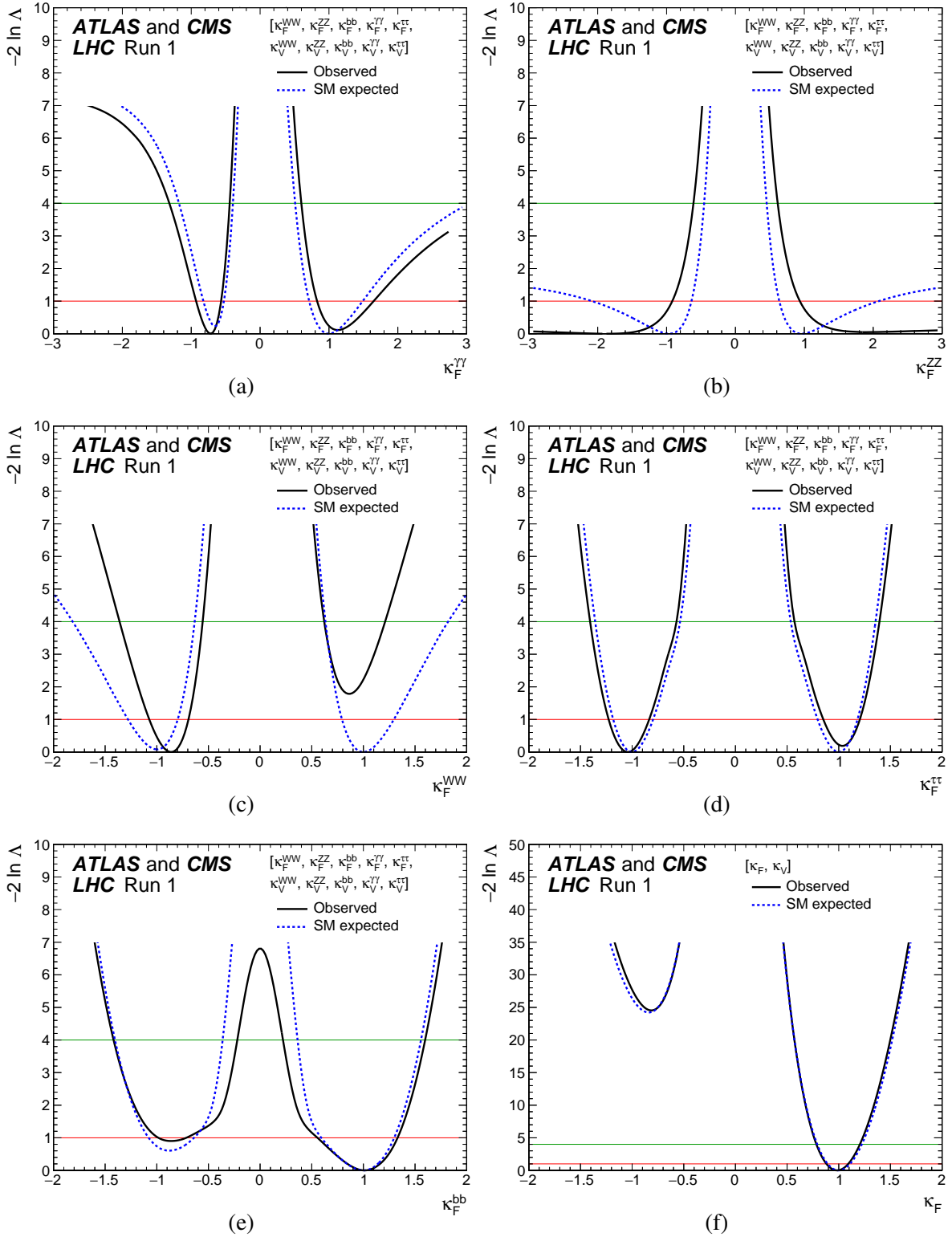
Figure 25: Observed (solid line) and expected (dashed line) negative log-likelihood scans for the five κ_F^f parameters, corresponding to each individual decay channel, and for the global κ_F parameter, corresponding to the combination of all decay channels: (a) $\kappa_F^{\gamma\gamma}$, (b) κ_F^{ZZ}, (c) κ_F^{WW}, (d) $\kappa_F^{\tau\tau}$, (e) κ_F^{bb}, and (f) κ_F. All the other parameters of interest from the list in the legends are also varied in the minimisation procedure. The red (green) horizontal lines at the $-2\Delta\ln\Lambda$ value of 1 (4) indicate the value of the profile likelihood ratio corresponding to a 1σ (2σ) CL interval for the parameter of interest, assuming the asymptotic χ^2 distribution of the test statistic.
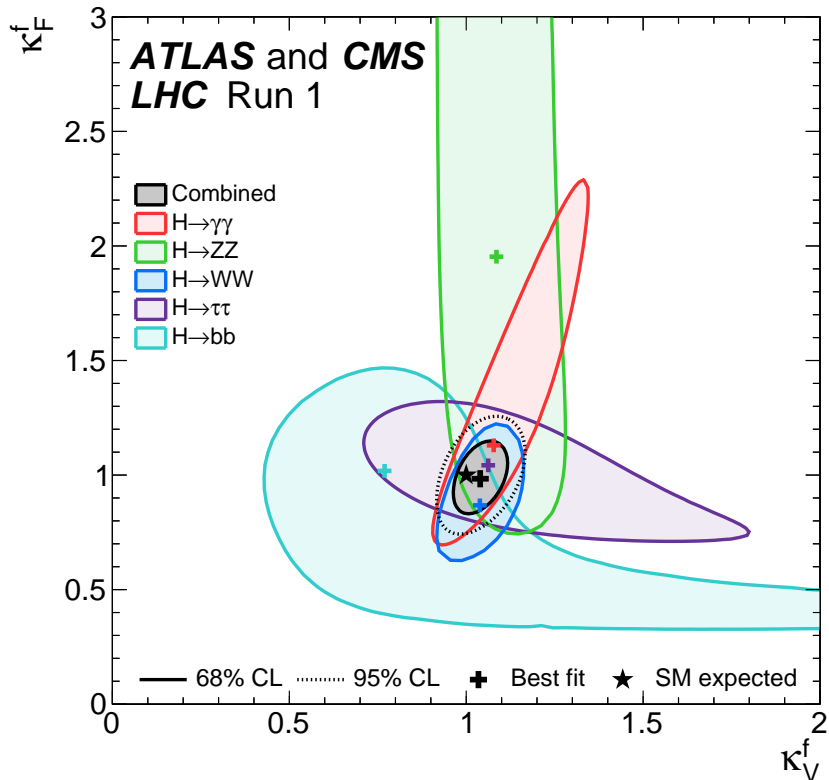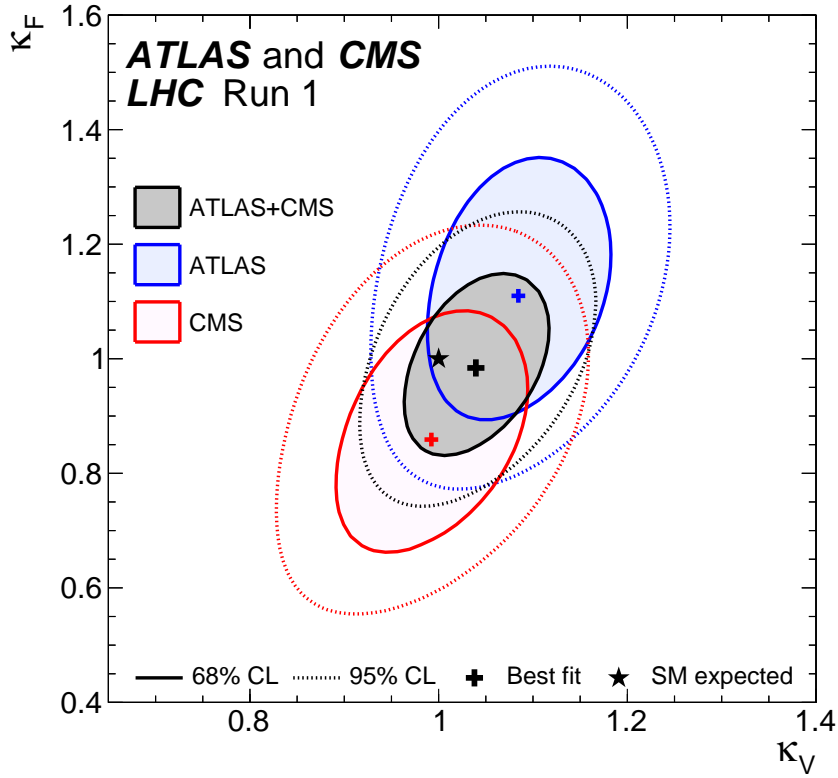
Figure 26: Top: negative log-likelihood contours at 68% and 95% CL in the (κ_F, κ_V) plane on an enlarged scale for the combination of ATLAS and CMS and for the global fit of all channels. Also shown are the contours obtained for each experiment separately. Bottom: negative log-likelihood contours at 68% CL in the (κ_F^f, κ_V^f) plane for the combination of ATLAS and CMS and for the individual decay channels as well as for their global combination (κ_F versus κ_V), assuming that all coupling modifiers are positive.

Acknowledgments

Appendix

A. Correlation matrices

Figures 27, 28 and 29 show the correlation matrices obtained from the fits to the generic parameterisations described respectively in Sections 4.1.1, 4.1.2, and 4.2. The correlation coefficients are evaluated around the best fit values, using the second derivatives of the negative log-likelihood ratio.

In the case of the parameterisation using 23 products of cross sections times branching fractions, most of the parameters are uncorrelated, as shown in Fig. 27. Some significant anticorrelations are present however, because of cross-contamination between different channels. These can be seen in the ggF versus VBF production processes for all decay modes, in the WH versus ZH production processes for the $H \to \gamma\gamma$ decay mode, and in the $H \to WW$ versus $H \to \tau\tau$ decay modes for the ttH production process.

In contrast, for the two parameterisations based on ratios shown in Figs. 28 and 29, correlations are present for all pairs of parameters. For example, in each of these parameterisations, the first parameter is anticorrelated to most of the others, which are all expressed as ratios of cross sections, branching fractions, or coupling modifiers, because it is directly correlated to the denominators of these ratios.

These correlation matrices are constructed as symmetric at the observed best fit values of the parameters of interest, and therefore are not fully representative of the asymmetric uncertainties observed in certain parameterisations, as shown for example in Fig. 9. The derivation of the results for a specific parameterisation, with additional assumptions compared to a more generic one, from the fit results and the covariance matrix of this more generic parameterisation, is therefore not straightforward. This is one of the reasons for quoting the best fit results in Sections 5 and 6 for a wide range of parameterisations, beyond the more generic ones discussed in Section 4.

B. Breakdown of systematic uncertainties

The results of the generic parameterisation of Section 4.1.2, in terms of ratios of cross sections and branching fractions, with $gg \to H \to ZZ$ as the reference channel, are shown with the full breakdown of the uncertainties in Table 20. The corresponding results for a similar parameterisation, with $gg \to H \to WW$ as reference, are shown in Table 21 and illustrated in Fig. 30. The parameters corresponding to ratios of cross sections are identical in each of these parameterisations, and they are included in both tables for convenience, as are the two ratios, B^{WW}/B^{ZZ} and B^{ZZ}/B^{WW}. Finally, the results of the generic parameterisation of Section 4.2, in terms of ratios of coupling modifiers, are shown with the full breakdown of the uncertainties in Table 22.

Figure 27: Correlation matrix obtained from the fit combining the ATLAS and CMS data using the generic parameterisation with 23 parameters described in Section 4.1.1. Only 20 parameters are shown because the other three, corresponding to the $H \rightarrow ZZ$ decay channel for the WH, ZH, and ttH production processes, are not measured with a meaningful precision.

Figure 28: Correlation matrix obtained from the fit combining the ATLAS and CMS data using the generic parameterisation with nine parameters described in Section 4.1.2.
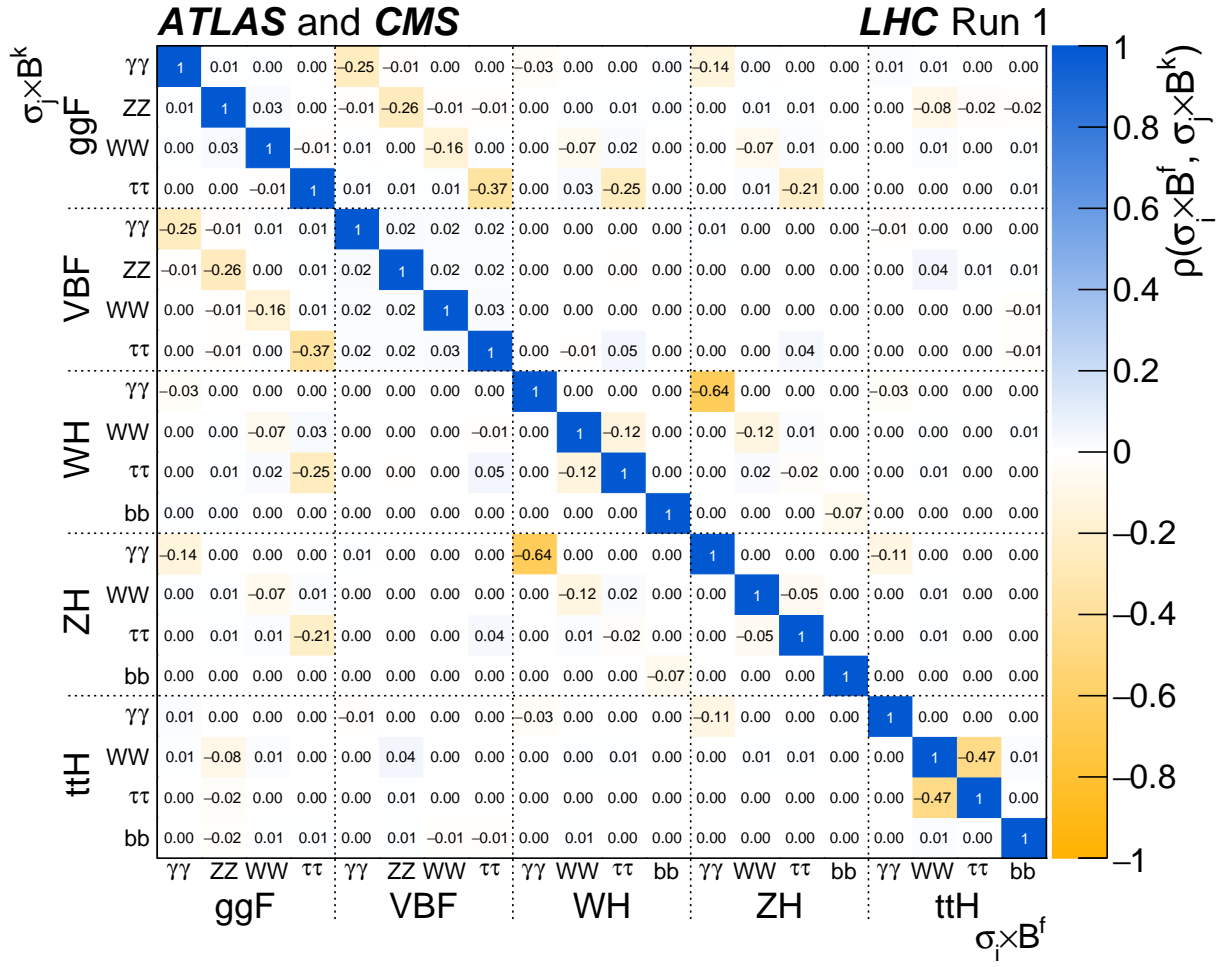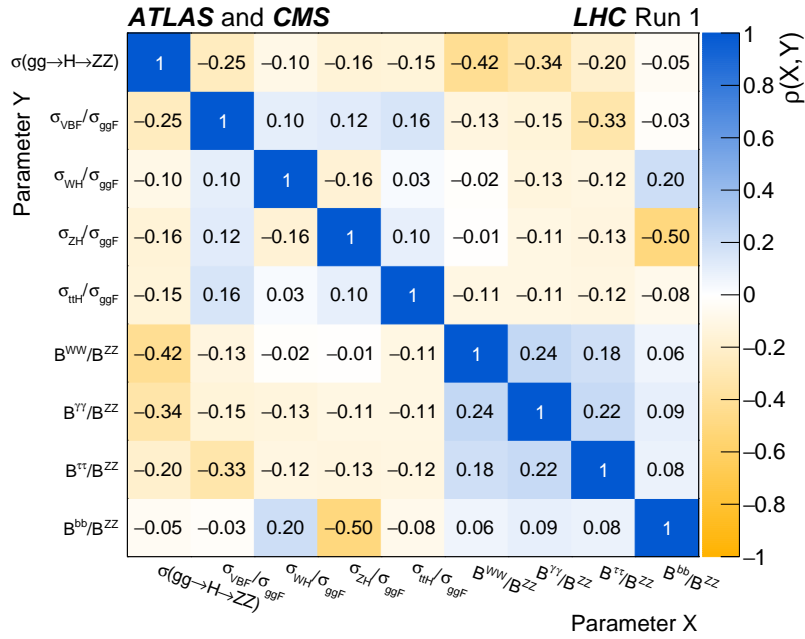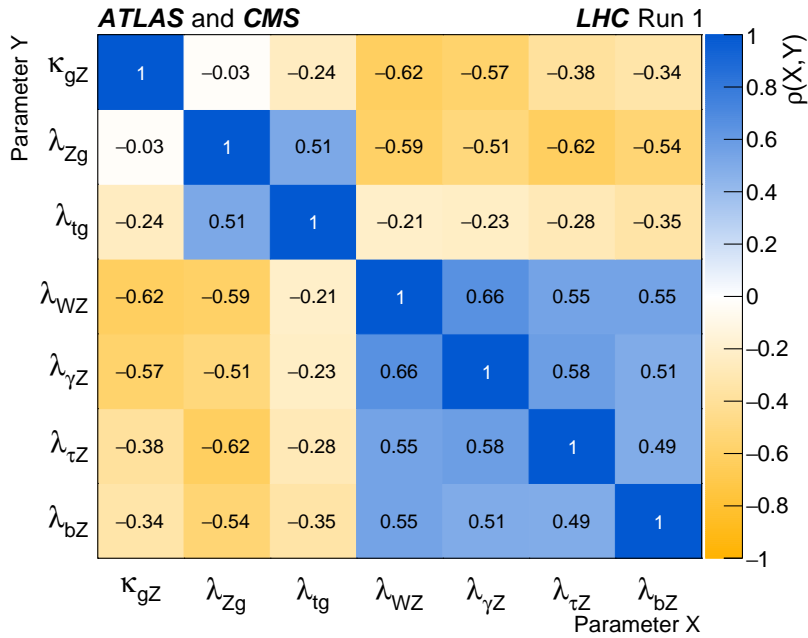

Figure 29: Correlation matrix obtained from the fit combining the ATLAS and CMS data using the generic parameterisation with seven parameters described in Section 4.2.

Table 20: Best fit values of $\sigma(gg \to H \to ZZ)$, σ_i/σ_{ggF}, and B^f/B^{ZZ} from the combined analysis of the $\sqrt{s} = 7$ and 8 TeV data. The values involving cross sections are given for $\sqrt{s} = 8$ TeV, assuming the SM values for $\sigma_i(7\ \text{TeV})/\sigma_i(8\ \text{TeV})$. The results are shown for the combination of ATLAS and CMS, and also separately for each experiment, together with their total uncertainties and their breakdown into the four components described in the text. The expected total uncertainties in the measurements are also shown in parentheses. The SM predictions [32] are also shown with their total uncertainties.

Parameter	SM prediction	ATLAS+CMS — Best fit value	Stat	Expt	Thbgd	Thsig	ATLAS — Best fit value	Stat	Expt	Thbgd	Thsig	CMS — Best fit value	Stat	Expt	Thbgd	Thsig
$\sigma(gg \to H \to ZZ)$ [pb]	0.51 ± 0.06	$0.59\ ^{+0.11}_{-0.10}\ (^{+0.11}_{-0.10})$	$^{+0.11}_{-0.10}\ (^{+0.11}_{-0.09})$	$^{+0.02}_{-0.01}\ (^{+0.02}_{-0.02})$	$^{+0.01}_{-0.01}\ (^{+0.01}_{-0.01})$	$^{+0.01}_{-0.01}\ (^{+0.01}_{-0.01})$	$0.77\ ^{+0.19}_{-0.17}\ (^{+0.16}_{-0.14})$	$^{+0.19}_{-0.16}\ (^{+0.16}_{-0.13})$	$^{+0.04}_{-0.03}\ (^{+0.03}_{-0.02})$	$^{+0.02}_{-0.02}\ (^{+0.01}_{-0.01})$	$^{+0.01}_{-0.01}\ (^{+0.01}_{-0.01})$	$0.44\ ^{+0.14}_{-0.12}\ (^{+0.15}_{-0.13})$	$^{+0.13}_{-0.11}\ (^{+0.15}_{-0.13})$	$^{+0.04}_{-0.03}\ (^{+0.03}_{-0.02})$	$^{+0.01}_{-0.01}\ (^{+0.01}_{-0.01})$	$^{+0.02}_{-0.01}\ (^{+0.02}_{-0.01})$
$\sigma_{VBF}/\sigma_{ggF}$	0.082 ± 0.009	$0.109\ ^{+0.034}_{-0.027}\ (^{+0.029}_{-0.024})$	$^{+0.029}_{-0.024}\ (^{+0.024}_{-0.020})$	$^{+0.013}_{-0.009}\ (^{+0.012}_{-0.009})$	$^{+0.006}_{-0.004}\ (^{+0.005}_{-0.003})$	$^{+0.010}_{-0.008}\ (^{+0.009}_{-0.007})$	$0.079\ ^{+0.035}_{-0.026}\ (^{+0.042}_{-0.031})$	$^{+0.030}_{-0.023}\ (^{+0.036}_{-0.028})$	$^{+0.014}_{-0.009}\ (^{+0.016}_{-0.010})$	$^{+0.008}_{-0.005}\ (^{+0.010}_{-0.006})$	$^{+0.009}_{-0.006}\ (^{+0.011}_{-0.008})$	$0.138\ ^{+0.073}_{-0.051}\ (^{+0.043}_{-0.033})$	$^{+0.061}_{-0.046}\ (^{+0.037}_{-0.029})$	$^{+0.033}_{-0.019}\ (^{+0.020}_{-0.012})$	$^{+0.014}_{-0.006}\ (^{+0.006}_{-0.003})$	$^{+0.015}_{-0.010}\ (^{+0.010}_{-0.008})$
σ_{WH}/σ_{ggF}	0.037 ± 0.004	$0.031\ ^{+0.028}_{-0.026}\ (^{+0.021}_{-0.017})$	$^{+0.024}_{-0.022}\ (^{+0.019}_{-0.015})$	$^{+0.012}_{-0.012}\ (^{+0.008}_{-0.005})$	$^{+0.008}_{-0.008}\ (^{+0.007}_{-0.005})$	$^{+0.003}_{-0.002}\ (^{+0.002}_{-0.002})$	$0.054\ ^{+0.036}_{-0.026}\ (^{+0.033}_{-0.022})$	$^{+0.031}_{-0.023}\ (^{+0.029}_{-0.020})$	$^{+0.012}_{-0.008}\ (^{+0.010}_{-0.006})$	$^{+0.014}_{-0.009}\ (^{+0.011}_{-0.006})$	$^{+0.007}_{-0.004}\ (^{+0.005}_{-0.002})$	$0.005\ ^{+0.044}_{-0.037}\ (^{+0.032}_{-0.022})$	$^{+0.037}_{-0.028}\ (^{+0.027}_{-0.020})$	$^{+0.021}_{-0.023}\ (^{+0.014}_{-0.008})$	$^{+0.010}_{-0.008}\ (^{+0.009}_{-0.006})$	$^{+0.003}_{-0.001}\ (^{+0.003}_{-0.001})$
σ_{ZH}/σ_{ggF}	0.0216 ± 0.0024	$0.066\ ^{+0.039}_{-0.031}\ (^{+0.016}_{-0.011})$	$^{+0.032}_{-0.025}\ (^{+0.014}_{-0.010})$	$^{+0.018}_{-0.012}\ (^{+0.006}_{-0.003})$	$^{+0.014}_{-0.012}\ (^{+0.006}_{-0.003})$	$^{+0.005}_{-0.003}\ (^{+0.002}_{-0.001})$	$0.013\ ^{+0.028}_{-0.014}\ (^{+0.027}_{-0.014})$	$^{+0.021}_{-0.012}\ (^{+0.023}_{-0.013})$	$^{+0.013}_{-0.005}\ (^{+0.009}_{-0.003})$	$^{+0.013}_{-0.005}\ (^{+0.011}_{-0.004})$	$^{+0.003}_{-0.002}\ (^{+0.003}_{-0.001})$	$0.123\ ^{+0.076}_{-0.053}\ (^{+0.024}_{-0.013})$	$^{+0.063}_{-0.046}\ (^{+0.020}_{-0.012})$	$^{+0.038}_{-0.022}\ (^{+0.010}_{-0.004})$	$^{+0.019}_{-0.013}\ (^{+0.009}_{-0.004})$	$^{+0.009}_{-0.005}\ (^{+0.002}_{-0.001})$
$\sigma_{ttH}/\sigma_{ggF}$	0.0067 ± 0.0010	$0.0220\ ^{+0.0068}_{-0.0057}\ (^{+0.0042}_{-0.0035})$	$^{+0.0055}_{-0.0048}\ (^{+0.0033}_{-0.0027})$	$^{+0.0031}_{-0.0023}\ (^{+0.0018}_{-0.0013})$	$^{+0.0023}_{-0.0020}\ (^{+0.0020}_{-0.0019})$	$^{+0.0014}_{-0.0010}\ (^{+0.0005}_{-0.0003})$	$0.0126\ ^{+0.0066}_{-0.0053}\ (^{+0.0061}_{-0.0045})$	$^{+0.0052}_{-0.0042}\ (^{+0.0047}_{-0.0035})$	$^{+0.0031}_{-0.0023}\ (^{+0.0026}_{-0.0017})$	$^{+0.0024}_{-0.0020}\ (^{+0.0027}_{-0.0022})$	$^{+0.0013}_{-0.0007}\ (^{+0.0008}_{-0.0004})$	$0.0340\ ^{+0.0158}_{-0.0116}\ (^{+0.0066}_{-0.0054})$	$^{+0.0121}_{-0.0097}\ (^{+0.0051}_{-0.0038})$	$^{+0.0085}_{-0.0051}\ (^{+0.0027}_{-0.0016})$	$^{+0.0048}_{-0.0036}\ (^{+0.0032}_{-0.0034})$	$^{+0.0026}_{-0.0015}\ (^{+0.0006}_{-0.0002})$
B^{WW}/B^{ZZ}	$8.09 \pm <0.01$	$6.7\ ^{+1.6}_{-1.3}\ (^{+2.2}_{-1.7})$	$^{+1.5}_{-1.2}\ (^{+2.0}_{-1.6})$	$^{+0.4}_{-0.3}\ (^{+0.7}_{-0.5})$	$^{+0.4}_{-0.3}\ (^{+0.5}_{-0.4})$	$^{+0.3}_{-0.2}\ (^{+0.3}_{-0.2})$	$6.5\ ^{+2.1}_{-1.6}\ (^{+3.5}_{-2.4})$	$^{+2.0}_{-1.4}\ (^{+3.3}_{-2.2})$	$^{+0.6}_{-0.4}\ (^{+0.9}_{-0.6})$	$^{+0.5}_{-0.4}\ (^{+0.8}_{-0.6})$	$^{+0.3}_{-0.2}\ (^{+0.4}_{-0.3})$	$7.1\ ^{+2.9}_{-2.1}\ (^{+3.2}_{-2.2})$	$^{+2.6}_{-1.8}\ (^{+2.9}_{-2.0})$	$^{+1.0}_{-0.7}\ (^{+1.1}_{-0.8})$	$^{+0.7}_{-0.5}\ (^{+0.7}_{-0.5})$	$^{+0.4}_{-0.3}\ (^{+0.5}_{-0.4})$
$B^{\gamma\gamma}/B^{ZZ}$	0.0854 ± 0.0010	$0.069\ ^{+0.018}_{-0.014}\ (^{+0.025}_{-0.019})$	$^{+0.018}_{-0.014}\ (^{+0.024}_{-0.019})$	$^{+0.003}_{-0.002}\ (^{+0.005}_{-0.003})$	$^{+0.002}_{-0.001}\ (^{+0.002}_{-0.001})$	$^{+0.002}_{-0.002}\ (^{+0.003}_{-0.002})$	$0.062\ ^{+0.024}_{-0.018}\ (^{+0.040}_{-0.027})$	$^{+0.023}_{-0.017}\ (^{+0.039}_{-0.027})$	$^{+0.007}_{-0.004}\ (^{+0.008}_{-0.005})$	$^{+0.002}_{-0.001}\ (^{+0.003}_{-0.002})$	$^{+0.003}_{-0.002}\ (^{+0.004}_{-0.003})$	$0.079\ ^{+0.034}_{-0.023}\ (^{+0.035}_{-0.025})$	$^{+0.032}_{-0.023}\ (^{+0.034}_{-0.024})$	$^{+0.009}_{-0.005}\ (^{+0.007}_{-0.004})$	$^{+0.003}_{-0.002}\ (^{+0.002}_{-0.001})$	$^{+0.004}_{-0.003}\ (^{+0.004}_{-0.003})$
$B^{\tau\tau}/B^{ZZ}$	2.36 ± 0.05	$1.77\ ^{+0.59}_{-0.46}\ (^{+0.90}_{-0.68})$	$^{+0.52}_{-0.41}\ (^{+0.75}_{-0.58})$	$^{+0.27}_{-0.20}\ (^{+0.47}_{-0.33})$	$^{+0.05}_{-0.04}\ (^{+0.08}_{-0.06})$	$^{+0.06}_{-0.04}\ (^{+0.10}_{-0.06})$	$2.17\ ^{+1.07}_{-0.74}\ (^{+1.54}_{-0.98})$	$^{+0.89}_{-0.64}\ (^{+1.30}_{-0.86})$	$^{+0.53}_{-0.35}\ (^{+0.76}_{-0.44})$	$^{+0.16}_{-0.10}\ (^{+0.22}_{-0.12})$	$^{+0.17}_{-0.09}\ (^{+0.22}_{-0.10})$	$1.56\ ^{+0.90}_{-0.61}\ (^{+1.23}_{-0.86})$	$^{+0.78}_{-0.54}\ (^{+1.03}_{-0.73})$	$^{+0.45}_{-0.26}\ (^{+0.66}_{-0.44})$	$^{+0.07}_{-0.05}\ (^{+0.04}_{-0.03})$	$^{+0.07}_{-0.04}\ (^{+0.12}_{-0.07})$
B^{bb}/B^{ZZ}	21.5 ± 1.0	$4.2\ ^{+4.4}_{-2.6}\ (^{+16.8}_{-9.0})$	$^{+2.8}_{-2.0}\ (^{+13.9}_{-7.9})$	$^{+2.3}_{-1.1}\ (^{+6.3}_{-2.8})$	$^{+2.5}_{-1.2}\ (^{+6.7}_{-3.3})$	$^{+0.4}_{-0.2}\ (^{+2.1}_{-0.9})$	$9.6\ ^{+10.1}_{-5.7}\ (^{+29.3}_{-11.8})$	$^{+7.4}_{-4.4}\ (^{+24.2}_{-10.5})$	$^{+4.5}_{-2.4}\ (^{+10.9}_{-3.3})$	$^{+5.1}_{-2.7}\ (^{+11.8}_{-4.0})$	$^{+1.3}_{-0.5}\ (^{+4.0}_{-1.2})$	$3.7\ ^{+4.1}_{-2.4}\ (^{+29.4}_{-11.9})$	$^{+3.1}_{-2.0}\ (^{+23.4}_{-10.4})$	$^{+1.8}_{-0.9}\ (^{+12.7}_{-3.8})$	$^{+1.9}_{-1.1}\ (^{+12.2}_{-4.4})$	$^{+0.4}_{-0.2}\ (^{+2.5}_{-0.9})$

Table 21: Best fit values of $\sigma(gg \to H \to WW)$, σ_i/σ_{ggF}, and B^f/B^{WW} from the combined analysis of the $\sqrt{s} = 7$ and 8 TeV data. The values involving cross sections are given for $\sqrt{s} = 8$ TeV, assuming the SM values for $\sigma_i(7\ \text{TeV})/\sigma_i(8\ \text{TeV})$. The results are shown for the combination of ATLAS and CMS, and also separately for each experiment, together with their total uncertainties and their breakdown into the four components described in the text. The expected total uncertainties in the measurements are also shown in parentheses. The SM predictions [32] are shown with their total uncertainties.

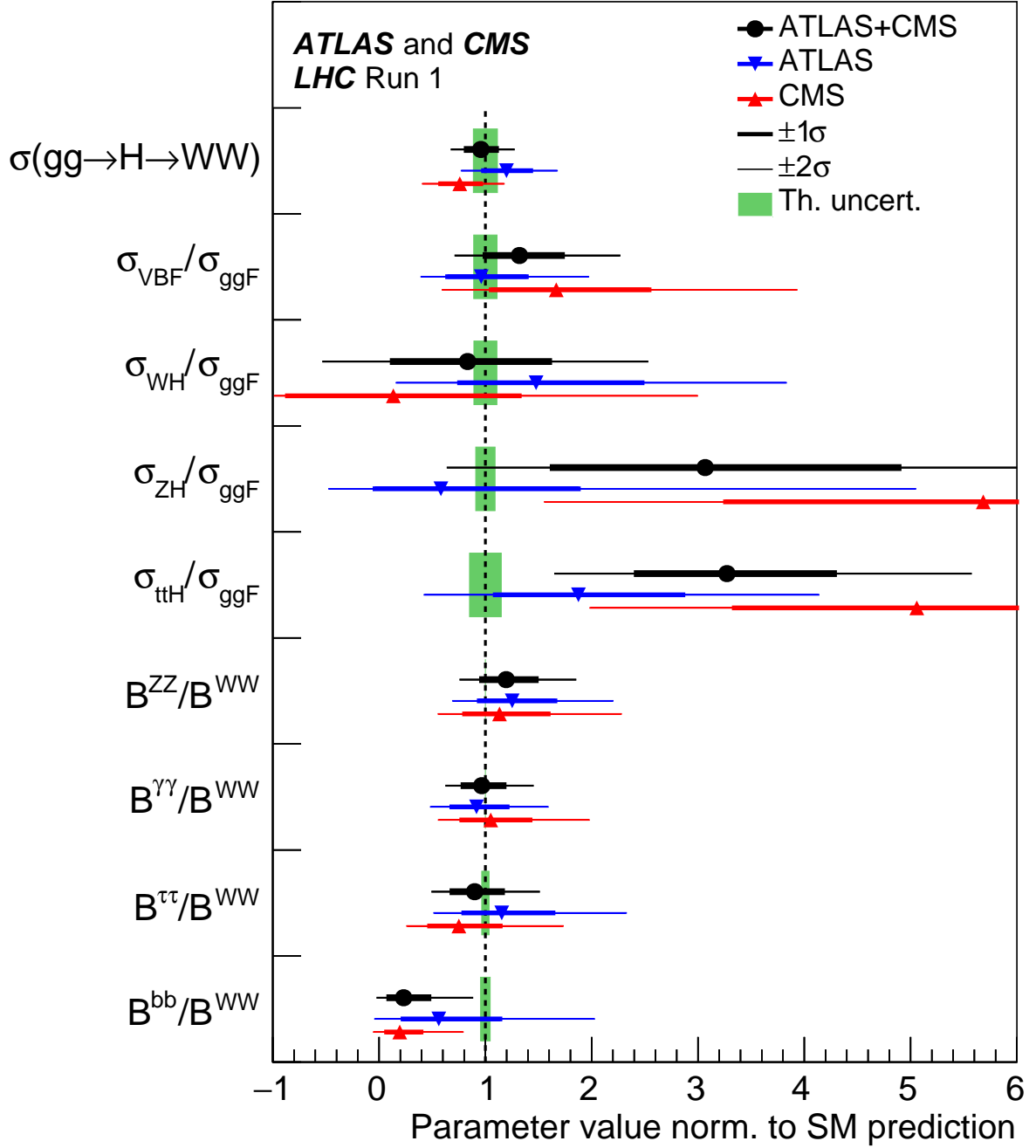| Parameter	SM prediction	ATLAS+CMS Best fit value	Stat	Expt	Thbgd	Thsig	ATLAS Best fit value	Stat	Expt	Thbgd	Thsig	CMS Best fit value	Stat	Expt	Thbgd	Thsig
$\sigma(gg \to H \to WW)$ [pb]	4.1 ±0.5	4.0 $^{+0.6}_{-0.6}$ ($^{+0.7}_{-0.6}$)	$^{+0.5}_{-0.5}$ ($^{+0.5}_{-0.5}$)	$^{+0.3}_{-0.3}$ ($^{+0.3}_{-0.3}$)	$^{+0.2}_{-0.2}$ ($^{+0.3}_{-0.3}$)	$^{+0.2}_{-0.1}$ ($^{+0.2}_{-0.1}$)	5.0 $^{+1.0}_{-0.9}$ ($^{+0.9}_{-0.9}$)	$^{+0.7}_{-0.7}$ ($^{+0.7}_{-0.7}$)	$^{+0.4}_{-0.4}$ ($^{+0.4}_{-0.4}$)	$^{+0.4}_{-0.4}$ ($^{+0.4}_{-0.4}$)	$^{+0.2}_{-0.2}$ ($^{+0.2}_{-0.1}$)	3.1 $^{+0.8}_{-0.8}$ ($^{+0.9}_{-0.9}$)	$^{+0.6}_{-0.6}$ ($^{+0.6}_{-0.6}$)	$^{+0.5}_{-0.4}$ ($^{+0.5}_{-0.5}$)	$^{+0.3}_{-0.3}$ ($^{+0.4}_{-0.3}$)	$^{+0.2}_{-0.1}$ ($^{+0.2}_{-0.2}$)
$\sigma_{VBF}/\sigma_{ggF}$	0.082 ±0.009	0.109 $^{+0.034}_{-0.027}$ ($^{+0.029}_{-0.024}$)	$^{+0.028}_{-0.024}$ ($^{+0.024}_{-0.020}$)	$^{+0.013}_{-0.009}$ ($^{+0.012}_{-0.009}$)	$^{+0.006}_{-0.004}$ ($^{+0.005}_{-0.003}$)	$^{+0.011}_{-0.008}$ ($^{+0.009}_{-0.007}$)	0.079 $^{+0.035}_{-0.026}$ ($^{+0.042}_{-0.031}$)	$^{+0.030}_{-0.023}$ ($^{+0.036}_{-0.028}$)	$^{+0.015}_{-0.009}$ ($^{+0.016}_{-0.010}$)	$^{+0.008}_{-0.005}$ ($^{+0.010}_{-0.006}$)	$^{+0.009}_{-0.006}$ ($^{+0.011}_{-0.008}$)	0.137 $^{+0.072}_{-0.051}$ ($^{+0.043}_{-0.033}$)	$^{+0.061}_{-0.046}$ ($^{+0.037}_{-0.029}$)	$^{+0.032}_{-0.018}$ ($^{+0.020}_{-0.012}$)	$^{+0.014}_{-0.006}$ ($^{+0.006}_{-0.003}$)	$^{+0.016}_{-0.010}$ ($^{+0.010}_{-0.008}$)
σ_{WH}/σ_{ggF}	0.037 ±0.004	0.030 $^{+0.028}_{-0.026}$ ($^{+0.021}_{-0.017}$)	$^{+0.024}_{-0.022}$ ($^{+0.019}_{-0.015}$)	$^{+0.012}_{-0.012}$ ($^{+0.008}_{-0.005}$)	$^{+0.008}_{-0.008}$ ($^{+0.007}_{-0.005}$)	$^{+0.003}_{-0.002}$ ($^{+0.003}_{-0.002}$)	0.054 $^{+0.037}_{-0.026}$ ($^{+0.032}_{-0.022}$)	$^{+0.031}_{-0.023}$ ($^{+0.029}_{-0.020}$)	$^{+0.012}_{-0.008}$ ($^{+0.010}_{-0.006}$)	$^{+0.014}_{-0.009}$ ($^{+0.011}_{-0.006}$)	$^{+0.007}_{-0.003}$ ($^{+0.004}_{-0.002}$)	0.005 $^{+0.043}_{-0.037}$ ($^{+0.032}_{-0.022}$)	$^{+0.037}_{-0.028}$ ($^{+0.027}_{-0.020}$)	$^{+0.021}_{-0.023}$ ($^{+0.014}_{-0.008}$)	$^{+0.010}_{-0.008}$ ($^{+0.009}_{-0.006}$)	$^{+0.003}_{-0.001}$ ($^{+0.003}_{-0.001}$)
σ_{ZH}/σ_{ggF}	0.0216 ±0.0024	0.066 $^{+0.039}_{-0.031}$ ($^{+0.016}_{-0.011}$)	$^{+0.032}_{-0.025}$ ($^{+0.014}_{-0.010}$)	$^{+0.018}_{-0.013}$ ($^{+0.006}_{-0.003}$)	$^{+0.014}_{-0.012}$ ($^{+0.006}_{-0.003}$)	$^{+0.005}_{-0.003}$ ($^{+0.002}_{-0.001}$)	0.013 $^{+0.028}_{-0.013}$ ($^{+0.027}_{-0.014}$)	$^{+0.021}_{-0.008}$ ($^{+0.023}_{-0.013}$)	$^{+0.013}_{-0.011}$ ($^{+0.009}_{-0.003}$)	$^{+0.013}_{-0.006}$ ($^{+0.011}_{-0.004}$)	$^{+0.003}_{-0.002}$ ($^{+0.003}_{-0.001}$)	0.123 $^{+0.075}_{-0.052}$ ($^{+0.024}_{-0.013}$)	$^{+0.062}_{-0.046}$ ($^{+0.020}_{-0.012}$)	$^{+0.037}_{-0.021}$ ($^{+0.010}_{-0.004}$)	$^{+0.018}_{-0.013}$ ($^{+0.009}_{-0.004}$)	$^{+0.009}_{-0.005}$ ($^{+0.002}_{-0.001}$)
$\sigma_{ttH}/\sigma_{ggF}$	0.0067 ±0.0010	0.0220 $^{+0.0068}_{-0.0057}$ ($^{+0.0042}_{-0.0035}$)	$^{+0.0055}_{-0.0048}$ ($^{+0.0033}_{-0.0027}$)	$^{+0.0031}_{-0.0023}$ ($^{+0.0018}_{-0.0013}$)	$^{+0.0023}_{-0.0020}$ ($^{+0.0020}_{-0.0019}$)	$^{+0.0014}_{-0.0010}$ ($^{+0.0005}_{-0.0003}$)	0.0126 $^{+0.0066}_{-0.0053}$ ($^{+0.0060}_{-0.0045}$)	$^{+0.0052}_{-0.0042}$ ($^{+0.0047}_{-0.0035}$)	$^{+0.0031}_{-0.0023}$ ($^{+0.0026}_{-0.0017}$)	$^{+0.0024}_{-0.0020}$ ($^{+0.0027}_{-0.0022}$)	$^{+0.0013}_{-0.0007}$ ($^{+0.0008}_{-0.0004}$)	0.0340 $^{+0.0157}_{-0.0116}$ ($^{+0.0067}_{-0.0054}$)	$^{+0.0121}_{-0.0096}$ ($^{+0.0051}_{-0.0038}$)	$^{+0.0085}_{-0.0050}$ ($^{+0.0027}_{-0.0016}$)	$^{+0.0048}_{-0.0036}$ ($^{+0.0032}_{-0.0034}$)	$^{+0.0026}_{-0.0015}$ ($^{+0.0006}_{-0.0002}$)
B^{ZZ}/B^{WW}	0.124 ± < 0.001	0.148 $^{+0.035}_{-0.029}$ ($^{+0.033}_{-0.027}$)	$^{+0.032}_{-0.027}$ ($^{+0.029}_{-0.025}$)	$^{+0.010}_{-0.007}$ ($^{+0.011}_{-0.007}$)	$^{+0.009}_{-0.006}$ ($^{+0.009}_{-0.006}$)	$^{+0.006}_{-0.004}$ ($^{+0.005}_{-0.003}$)	0.155 $^{+0.050}_{-0.039}$ ($^{+0.050}_{-0.037}$)	$^{+0.045}_{-0.036}$ ($^{+0.045}_{-0.035}$)	$^{+0.016}_{-0.009}$ ($^{+0.014}_{-0.008}$)	$^{+0.014}_{-0.008}$ ($^{+0.014}_{-0.007}$)	$^{+0.007}_{-0.005}$ ($^{+0.006}_{-0.004}$)	0.140 $^{+0.057}_{-0.041}$ ($^{+0.048}_{-0.035}$)	$^{+0.049}_{-0.038}$ ($^{+0.041}_{-0.033}$)	$^{+0.023}_{-0.012}$ ($^{+0.019}_{-0.010}$)	$^{+0.016}_{-0.008}$ ($^{+0.013}_{-0.007}$)	$^{+0.009}_{-0.005}$ ($^{+0.009}_{-0.005}$)
$B^{\gamma\gamma}/B^{WW}$	0.01056 ±0.00010	0.0102 $^{+0.0022}_{-0.0019}$ ($^{+0.0025}_{-0.0020}$)	$^{+0.0020}_{-0.0017}$ ($^{+0.0021}_{-0.0019}$)	$^{+0.0008}_{-0.0005}$ ($^{+0.0009}_{-0.0006}$)	$^{+0.0006}_{-0.0004}$ ($^{+0.0007}_{-0.0005}$)	$^{+0.0004}_{-0.0003}$ ($^{+0.0005}_{-0.0003}$)	0.0097 $^{+0.0031}_{-0.0025}$ ($^{+0.0037}_{-0.0029}$)	$^{+0.0026}_{-0.0023}$ ($^{+0.0032}_{-0.0027}$)	$^{+0.0013}_{-0.0008}$ ($^{+0.0014}_{-0.0008}$)	$^{+0.0008}_{-0.0005}$ ($^{+0.0011}_{-0.0006}$)	$^{+0.0006}_{-0.0004}$ ($^{+0.0007}_{-0.0005}$)	0.0111 $^{+0.0039}_{-0.0029}$ ($^{+0.0036}_{-0.0027}$)	$^{+0.0033}_{-0.0027}$ ($^{+0.0030}_{-0.0025}$)	$^{+0.0018}_{-0.0010}$ ($^{+0.0015}_{-0.0008}$)	$^{+0.0012}_{-0.0006}$ ($^{+0.0011}_{-0.0005}$)	$^{+0.0006}_{-0.0004}$ ($^{+0.0007}_{-0.0004}$)
$B^{\tau\tau}/B^{WW}$	0.292 ±0.006	0.26 $^{+0.08}_{-0.06}$ ($^{+0.09}_{-0.08}$)	$^{+0.06}_{-0.05}$ ($^{+0.07}_{-0.06}$)	$^{+0.04}_{-0.03}$ ($^{+0.06}_{-0.04}$)	$^{+0.02}_{-0.01}$ ($^{+0.02}_{-0.01}$)	$^{+0.01}_{-0.01}$ ($^{+0.01}_{-0.01}$)	0.34 $^{+0.14}_{-0.10}$ ($^{+0.15}_{-0.11}$)	$^{+0.11}_{-0.09}$ ($^{+0.12}_{-0.09}$)	$^{+0.08}_{-0.06}$ ($^{+0.09}_{-0.06}$)	$^{+0.03}_{-0.02}$ ($^{+0.03}_{-0.02}$)	$^{+0.03}_{-0.02}$ ($^{+0.03}_{-0.01}$)	0.22 $^{+0.11}_{-0.08}$ ($^{+0.13}_{-0.10}$)	$^{+0.09}_{-0.07}$ ($^{+0.10}_{-0.08}$)	$^{+0.06}_{-0.04}$ ($^{+0.08}_{-0.06}$)	$^{+0.02}_{-0.01}$ ($^{+0.03}_{-0.01}$)	$^{+0.01}_{-0.01}$ ($^{+0.02}_{-0.01}$)
B^{bb}/B^{WW}	2.66 ±0.12	0.61 $^{+0.64}_{-0.38}$ ($^{+2.01}_{-1.09}$)	$^{+0.39}_{-0.29}$ ($^{+1.63}_{-0.93}$)	$^{+0.34}_{-0.16}$ ($^{+0.78}_{-0.35}$)	$^{+0.37}_{-0.18}$ ($^{+0.84}_{-0.42}$)	$^{+0.05}_{-0.02}$ ($^{+0.23}_{-0.10}$)	1.50 $^{+1.54}_{-0.90}$ ($^{+3.49}_{-1.38}$)	$^{+1.06}_{-0.66}$ ($^{+2.83}_{-1.20}$)	$^{+0.73}_{-0.42}$ ($^{+1.37}_{-0.42}$)	$^{+0.82}_{-0.43}$ ($^{+1.45}_{-0.52}$)	$^{+0.20}_{-0.09}$ ($^{+0.45}_{-0.14}$)	0.52 $^{+0.54}_{-0.34}$ ($^{+3.57}_{-1.46}$)	$^{+0.39}_{-0.27}$ ($^{+2.78}_{-1.25}$)	$^{+0.25}_{-0.13}$ ($^{+1.58}_{-0.49}$)	$^{+0.28}_{-0.14}$ ($^{+1.56}_{-0.58}$)	$^{+0.05}_{-0.02}$ ($^{+0.26}_{-0.10}$)

Figure 30: Best fit values of the $gg \rightarrow H \rightarrow WW$ cross section and of ratios of cross sections and branching fractions, as obtained from the generic parameterisation described in Section 4.1.2 and as tabulated in Table 21 for the combination of the ATLAS and CMS measurements. Also shown are the results from each experiment. The values involving cross sections are given for $\sqrt{s} = 8$ TeV, assuming the SM values for $\sigma_i(7 \text{ TeV})/\sigma_i(8 \text{ TeV})$. The error bars indicate the 1σ (thick lines) and 2σ (thin lines) intervals. In this figure, the fit results are normalised to the SM predictions for the various parameters and the shaded bands indicate the theoretical uncertainties in these predictions.

Table 22: Best fit values of $\kappa_{gZ} = \kappa_g \cdot \kappa_Z/\kappa_H$ and of the ratios of coupling modifiers, as defined in the most generic parameterisation described in the context of the κ framework, from the combined analysis of the $\sqrt{s} = 7$ and 8 TeV data. The results are shown for the combination of ATLAS and CMS and also separately for each experiment, together with their total uncertainties and their breakdown into the four components described in the text. The uncertainties in λ_{tg} and λ_{WZ}, for which a negative solution is allowed, are calculated around the overall best fit value. The combined 1σ CL intervals are $\lambda_{tg} = [-2.00, -1.59] \cup [1.50, 2.07]$ and $\lambda_{WZ} = [-0.96, -0.82] \cup [0.80, 0.98]$. The expected total uncertainties in the measurements are also shown in parentheses. For those parameters with no sensitivity to the sign, only the absolute values are shown.

Parameter	ATLAS+CMS Best fit value	Stat	Expt	Thbgd	Thsig	ATLAS Best fit value	Stat	Expt	Thbgd	Thsig	CMS Best fit value	Stat	Expt	Thbgd	Thsig
κ_{gZ}	$1.09\ ^{+0.11}_{-0.11}\ (^{+0.11}_{-0.11})$	$^{+0.09}_{-0.09}\ (^{+0.09}_{-0.09})$	$^{+0.02}_{-0.02}\ (^{+0.02}_{-0.02})$	$^{+0.00}_{-0.01}\ (^{+0.01}_{-0.01})$	$^{+0.06}_{-0.05}\ (^{+0.06}_{-0.05})$	$1.20\ ^{+0.16}_{-0.15}\ (^{+0.15}_{-0.15})$	$^{+0.14}_{-0.14}\ (^{+0.14}_{-0.13})$	$^{+0.03}_{-0.03}\ (^{+0.03}_{-0.03})$	$^{+0.02}_{-0.02}\ (^{+0.01}_{-0.02})$	$^{+0.07}_{-0.06}\ (^{+0.06}_{-0.05})$	$0.99\ ^{+0.14}_{-0.13}\ (^{+0.14}_{-0.14})$	$^{+0.12}_{-0.12}\ (^{+0.13}_{-0.12})$	$^{+0.03}_{-0.04}\ (^{+0.03}_{-0.03})$	$^{+0.01}_{-0.01}\ (^{+0.01}_{-0.01})$	$^{+0.06}_{-0.04}\ (^{+0.06}_{-0.05})$
λ_{Zg}	$1.27\ ^{+0.23}_{-0.20}\ (^{+0.20}_{-0.17})$	$^{+0.18}_{-0.16}\ (^{+0.15}_{-0.14})$	$^{+0.10}_{-0.07}\ (^{+0.08}_{-0.06})$	$^{+0.06}_{-0.05}\ (^{+0.05}_{-0.04})$	$^{+0.10}_{-0.08}\ (^{+0.08}_{-0.07})$	$1.07\ ^{+0.26}_{-0.22}\ (^{+0.28}_{-0.23})$	$^{+0.21}_{-0.18}\ (^{+0.23}_{-0.20})$	$^{+0.10}_{-0.06}\ (^{+0.10}_{-0.07})$	$^{+0.07}_{-0.06}\ (^{+0.09}_{-0.05})$	$^{+0.09}_{-0.07}\ (^{+0.09}_{-0.07})$	$1.47\ ^{+0.45}_{-0.34}\ (^{+0.27}_{-0.23})$	$^{+0.35}_{-0.28}\ (^{+0.21}_{-0.19})$	$^{+0.22}_{-0.14}\ (^{+0.12}_{-0.09})$	$^{+0.11}_{-0.10}\ (^{+0.07}_{-0.05})$	$^{+0.13}_{-0.09}\ (^{+0.09}_{-0.07})$
λ_{tg}	$1.78\ ^{+0.30}_{-0.27}\ (^{+0.28}_{-0.38})$	$^{+0.21}_{-0.20}\ (^{+0.20}_{-0.30})$	$^{+0.13}_{-0.11}\ (^{+0.11}_{-0.13})$	$^{+0.09}_{-0.09}\ (^{+0.14}_{-0.20})$	$^{+0.14}_{-0.11}\ (^{+0.09}_{-0.05})$	$1.40\ ^{+0.34}_{-0.33}\ (^{+0.38}_{-0.54})$	$^{+0.25}_{-0.24}\ (^{+0.28}_{-0.39})$	$^{+0.14}_{-0.15}\ (^{+0.14}_{-0.22})$	$^{+0.12}_{-0.14}\ (^{+0.18}_{-0.29})$	$^{+0.14}_{-0.09}\ (^{+0.11}_{-0.06})$	$-2.26\ ^{+0.50}_{-0.53}\ (^{+0.42}_{-0.64})$	$^{+0.43}_{-0.39}\ (^{+0.31}_{-0.42})$	$^{+0.22}_{-0.23}\ (^{+0.16}_{-0.22})$	$^{+0.04}_{-0.18}\ (^{+0.21}_{-0.43})$	$^{+0.14}_{-0.21}\ (^{+0.11}_{-0.06})$
λ_{WZ}	$0.88\ ^{+0.10}_{-0.09}\ (^{+0.12}_{-0.10})$	$^{+0.09}_{-0.08}\ (^{+0.11}_{-0.09})$	$^{+0.03}_{-0.03}\ (^{+0.04}_{-0.03})$	$^{+0.03}_{-0.02}\ (^{+0.03}_{-0.03})$	$^{+0.02}_{-0.01}\ (^{+0.02}_{-0.01})$	$0.92\ ^{+0.14}_{-0.12}\ (^{+0.18}_{-0.15})$	$^{+0.13}_{-0.11}\ (^{+0.17}_{-0.13})$	$^{+0.04}_{-0.03}\ (^{+0.04}_{-0.04})$	$^{+0.03}_{-0.03}\ (^{+0.04}_{-0.04})$	$^{+0.02}_{-0.02}\ (^{+0.02}_{-0.02})$	$-0.85\ ^{+0.13}_{-0.15}\ (^{+0.17}_{-0.14})$	$^{+0.11}_{-0.13}\ (^{+0.15}_{-0.13})$	$^{+0.05}_{-0.06}\ (^{+0.06}_{-0.05})$	$^{+0.04}_{-0.04}\ (^{+0.03}_{-0.03})$	$^{+0.01}_{-0.03}\ (^{+0.03}_{-0.02})$
$\lvert\lambda_{\gamma Z}\rvert$	$0.89\ ^{+0.11}_{-0.10}\ (^{+0.13}_{-0.12})$	$^{+0.10}_{-0.09}\ (^{+0.13}_{-0.11})$	$^{+0.03}_{-0.02}\ (^{+0.03}_{-0.02})$	$^{+0.01}_{-0.02}\ (^{+0.01}_{-0.01})$	$^{+0.02}_{-0.01}\ (^{+0.02}_{-0.01})$	$0.87\ ^{+0.15}_{-0.13}\ (^{+0.20}_{-0.17})$	$^{+0.15}_{-0.13}\ (^{+0.20}_{-0.17})$	$^{+0.04}_{-0.04}\ (^{+0.05}_{-0.03})$	$^{+0.02}_{-0.01}\ (^{+0.03}_{-0.01})$	$^{+0.02}_{-0.02}\ (^{+0.02}_{-0.02})$	$0.91\ ^{+0.17}_{-0.14}\ (^{+0.18}_{-0.16})$	$^{+0.16}_{-0.14}\ (^{+0.18}_{-0.15})$	$^{+0.04}_{-0.03}\ (^{+0.04}_{-0.03})$	$^{+0.02}_{-0.02}\ (^{+0.01}_{-0.01})$	$^{+0.02}_{-0.02}\ (^{+0.02}_{-0.02})$
$\lvert\lambda_{\tau Z}\rvert$	$0.85\ ^{+0.13}_{-0.12}\ (^{+0.17}_{-0.15})$	$^{+0.12}_{-0.10}\ (^{+0.14}_{-0.13})$	$^{+0.07}_{-0.06}\ (^{+0.09}_{-0.08})$	$^{+0.01}_{-0.02}\ (^{+0.02}_{-0.02})$	$^{+0.02}_{-0.01}\ (^{+0.02}_{-0.02})$	$0.96\ ^{+0.21}_{-0.18}\ (^{+0.27}_{-0.23})$	$^{+0.18}_{-0.15}\ (^{+0.23}_{-0.19})$	$^{+0.10}_{-0.09}\ (^{+0.13}_{-0.11})$	$^{+0.04}_{-0.03}\ (^{+0.04}_{-0.03})$	$^{+0.03}_{-0.02}\ (^{+0.04}_{-0.02})$	$0.78\ ^{+0.20}_{-0.17}\ (^{+0.23}_{-0.20})$	$^{+0.17}_{-0.15}\ (^{+0.19}_{-0.17})$	$^{+0.10}_{-0.08}\ (^{+0.12}_{-0.11})$	$^{+0.01}_{-0.02}\ (^{+0.02}_{-0.01})$	$^{+0.02}_{-0.01}\ (^{+0.02}_{-0.02})$
$\lvert\lambda_{bZ}\rvert$	$0.58\ ^{+0.16}_{-0.20}\ (^{+0.25}_{-0.22})$	$^{+0.12}_{-0.17}\ (^{+0.21}_{-0.20})$	$^{+0.07}_{-0.06}\ (^{+0.09}_{-0.07})$	$^{+0.07}_{-0.07}\ (^{+0.08}_{-0.05})$	$^{+0.03}_{-0.04}\ (^{+0.06}_{-0.05})$	$0.61\ ^{+0.24}_{-0.24}\ (^{+0.36}_{-0.29})$	$^{+0.20}_{-0.19}\ (^{+0.31}_{-0.26})$	$^{+0.09}_{-0.12}\ (^{+0.12}_{-0.09})$	$^{+0.10}_{-0.10}\ (^{+0.11}_{-0.08})$	$^{+0.04}_{-0.03}\ (^{+0.08}_{-0.05})$	$0.47\ ^{+0.26}_{-0.17}\ (^{+0.38}_{-0.37})$	$^{+0.23}_{-0.13}\ (^{+0.32}_{-0.34})$	$^{+0.06}_{-0.07}\ (^{+0.15}_{-0.11})$	$^{+0.11}_{-0.08}\ (^{+0.11}_{-0.09})$	$^{+0.00}_{-0.04}\ (^{+0.07}_{-0.07})$

C. Likelihood scans for coupling modifier parameterisations

For the results based on certain coupling modifier parameterisations described in Sections 4.2 and 6, it is necessary to account for the relative signs between parameters that modify the rates of certain signal production processes and decay modes through interference effects. For example, in the generic parameterisation in terms of ratios of coupling modifiers, the signs of λ_{Zg}, λ_{WZ}, and λ_{tg} affect the rates of tH production through t–W interference, and of $ggZH$ production through t–Z interference. The parameters λ_{Zg} and, as a consequence, κ_{gZ} are assumed to be positive without loss of generality. From this follows that there are four relevant sign combinations of λ_{WZ} and λ_{tg}, which must be evaluated when performing all likelihood scans. An example is given in Fig. 31 for $|\lambda_{bZ}|$, with a separate curve shown for each sign combination. Each sign hypothesis gives rise to a distinct local minimum. As the negative log-likelihood for each case is determined relative to a common reference point, it is possible to identify the global minimum. For this parameterisation, the SM sign hypothesis ($\lambda_{WZ} > 0, \lambda_{tg} > 0$) corresponds to this global minimum. A new negative log-likelihood curve is defined as the envelope of the ones obtained for the different sign hypotheses, by taking the smallest value of $-2\ln\Lambda$ from the different sign hypotheses as a function of the parameter being considered in the scan. This curve, indicated by the solid line in Fig. 31, is used to determine the uncertainties and the confidence intervals. In the case of the example chosen here, but also more generally, this procedure results in larger confidence intervals than would be found from the ($\lambda_{WZ} > 0, \lambda_{tg} > 0$) hypothesis alone.

Another example of the effect of the different sign combinations is given in Fig. 32, which shows the observed and expected negative log-likelihood scans for B_{BSM} using the parameterisation described in Section 6.1. Given that in this parameterisation, opposite signs of κ_W and κ_Z are not considered, only two sign combination hypotheses, $\kappa_W > 0, \kappa_Z > 0$ and $\kappa_W < 0, \kappa_Z < 0$, are evaluated. In the expected negative log-likelihood curve, a transition between the two hypotheses occurs at $B_{BSM} \approx 0.175$. This has the effect of increasing the expected 95% CL upper limit on B_{BSM} from 0.35, when considering only the $\kappa_W > 0, \kappa_Z > 0$ case, to 0.39, once both sign combinations are considered.
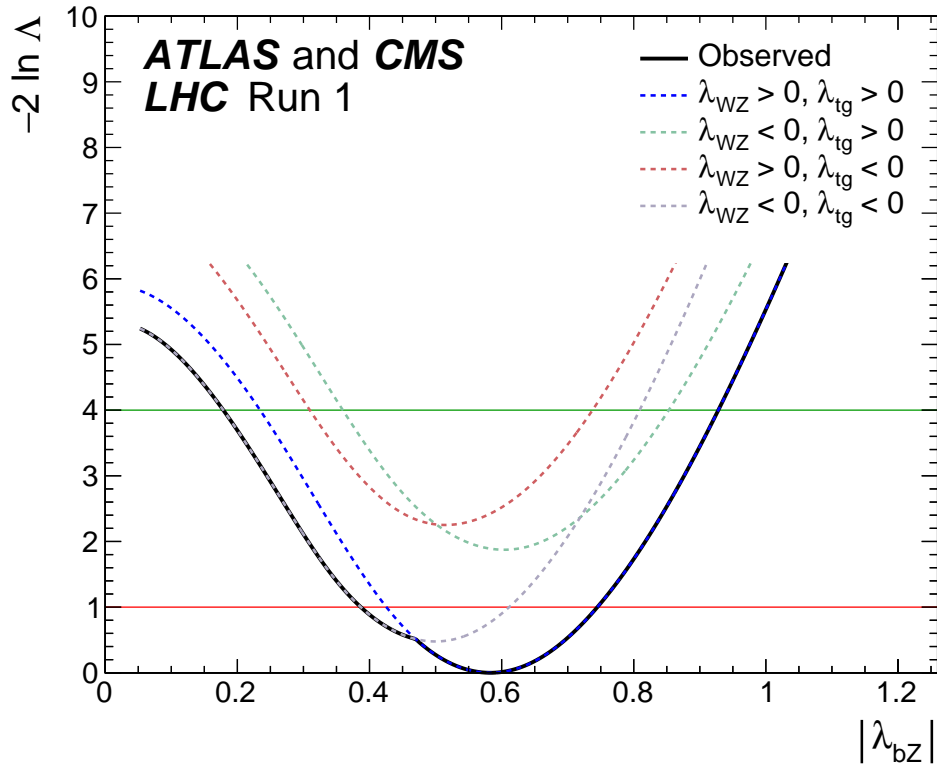
Figure 31: Negative log-likelihood scan for λ_{bZ} showing the minima obtained when considering all sign combinations (solid line) and each specific one separately (dashed lines).
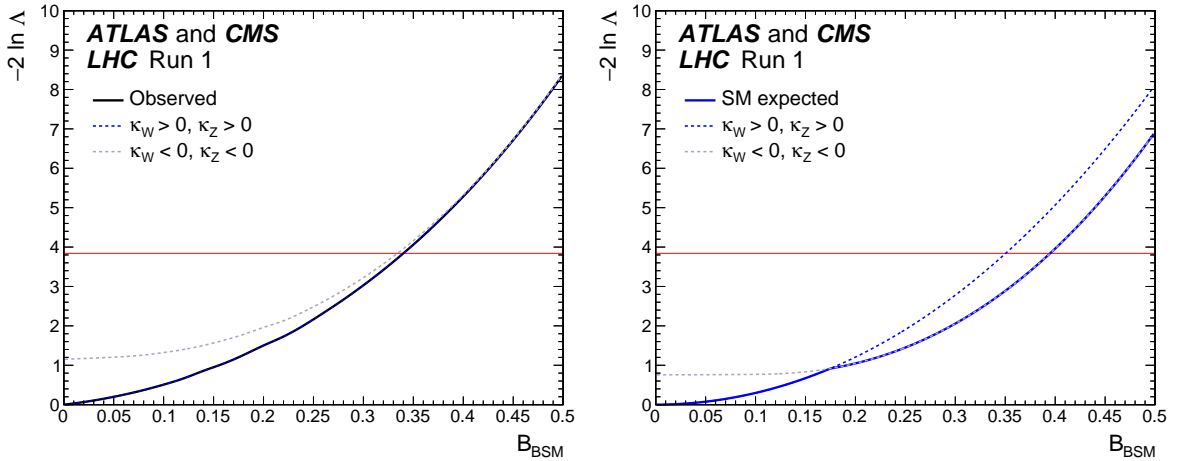

Figure 32: Observed (left) and expected (right) negative log-likelihood scan for B_{BSM}, the minima obtained when considering both sign combinations (solid line) and each specific one separately (dashed lines).

References

[1] ATLAS Collaboration, *The ATLAS Experiment at the CERN Large Hadron Collider*, JINST **3** (2008) S08003.

[2] CMS Collaboration, *The CMS experiment at the CERN LHC*, JINST **3** (2008) S08004.

[3] S. L. Glashow, *Partial-symmetries of weak interactions*, Nucl. Phys. **22** (1961) 579.

[4] S. Weinberg, *A model of leptons*, Phys. Rev. Lett. **19** (1967) 1264.

[5] A. Salam, *Weak and electromagnetic interactions*, in *Elementary particle physics: relativistic groups and analyticity*, N. Svartholm, ed. p.367 Almqvist & Wiskell, 1968. http://inspirehep.net/record/53083. Proceedings of the 8th Nobel symposium.

[6] G. 't Hooft and M. Veltman, *Regularization and Renormalization of Gauge Fields*, Nucl. Phys. B **44** (1972) 189.

[7] F. Englert and R. Brout, *Broken Symmetry and the Mass of Gauge Vector Mesons*, Phys. Rev. Lett. **13** (1964) 321.

[8] P. W. Higgs, *Broken symmetries, massless particles and gauge fields*, Phys. Lett. **12** (1964) 132.

[9] P. W. Higgs, *Broken Symmetries and the Masses of Gauge Bosons*, Phys. Rev. Lett. **13** (1964) 508.

[10] G. S. Guralnik, C. R. Hagen, and T. W. B. Kibble, *Global conservation laws and massless particles*, Phys. Rev. Lett. **13** (1964) 585.

[11] P. W. Higgs, *Spontaneous symmetry breakdown without massless bosons*, Phys. Rev. **145** (1966) 1156.

[12] T. W. B. Kibble, *Symmetry breaking in non-Abelian gauge theories*, Phys. Rev. **155** (1967) 1554.

[13] Y. Nambu and G. Jona-Lasinio, *Dynamical Model of Elementary Particles Based on an Analogy with Superconductivity. I*, Phys. Rev. **122** (1961) 345.

[14] ATLAS Collaboration, *Observation of a new particle in the search for the Standard Model Higgs boson with the ATLAS detector at the LHC*, Phys. Lett. B **716** (2012) 1, arXiv:1207.7214 [hep-ex].

[15] CMS Collaboration, *Observation of a new boson at a mass of 125 GeV with the CMS experiment at the LHC*, Phys. Lett. B **716** (2012) 30, arXiv:1207.7235 [hep-ex].

[16] CMS Collaboration, *Observation of a new boson with mass near 125 GeV in pp collisions at $\sqrt{s}$ = 7 and 8 TeV*, JHEP **06** (2013) 081, arXiv:1303.4571 [hep-ex].

[17] ATLAS Collaboration, *Measurements of the Higgs boson production and decay rates and coupling strengths using pp collision data at $\sqrt{s}$ = 7 and 8 TeV in the ATLAS experiment*, Eur. Phys. J. C **76** (2016) 6, arXiv:1507.04548 [hep-ex].

[18] CMS Collaboration, *Precise determination of the mass of the Higgs boson and tests of compatibility of its couplings with the standard model predictions using proton collisions at 7 and 8 TeV*, Eur. Phys. J. C **75** (2015) 212, arXiv:1412.8662 [hep-ex].

[19] CMS Collaboration, *Study of the Mass and Spin-Parity of the Higgs Boson Candidate via Its Decays to Z Boson Pairs*, Phys. Rev. Lett. **110** (2013) 081803, `arXiv:1212.6639 [hep-ex]`.

[20] ATLAS Collaboration, *Evidence for the spin-0 nature of the Higgs boson using ATLAS data*, Phys. Lett. B **726** (2013) 120, `arXiv:1307.1432 [hep-ex]`.

[21] CMS Collaboration, *Constraints on the spin-parity and anomalous HVV couplings of the Higgs boson in proton collisions at 7 and 8 TeV*, Phys. Rev. D **92** (2015) 012004, `arXiv:1411.3441 [hep-ex]`.

[22] ATLAS and CMS Collaborations, *Combined Measurement of the Higgs Boson Mass in pp Collisions at $\sqrt{s}$ = 7 and 8 TeV with the ATLAS and CMS Experiments*, Phys. Rev. Lett. **114** (2015) 191803, `arXiv:1503.07589 [hep-ex]`.

[23] ATLAS Collaboration, *Constraints on the off-shell Higgs boson signal strength in the high-mass ZZ and WW final states with the ATLAS detector*, Eur. Phys. J. C **75** (2015) 335, `arXiv:1503.01060 [hep-ex]`.

[24] CMS Collaboration, *Constraints on the Higgs boson width from off-shell production and decay to Z-boson pairs,*, Phys. Lett. B **736** (2014) 64, `arXiv:1405.3455 [hep-ex]`.

[25] CMS Collaboration, *Limits on the Higgs boson lifetime and width from its decay to four charged leptons*, Phys. Rev. D **92** (2015) 072010, `arXiv:1507.06656 [hep-ex]`.

[26] ATLAS Collaboration, *Measurements of fiducial and differential cross sections for Higgs boson production in the diphoton decay channel at $\sqrt{s}$ = 8 TeV with ATLAS*, JHEP **09** (2014) 112, `arXiv:1407.4222 [hep-ex]`.

[27] ATLAS Collaboration, *Fiducial and differential cross sections of Higgs boson production measured in the four-lepton decay channel in pp collisions at $\sqrt{s}$ = 8 TeV with the ATLAS detector*, Phys. Lett. B **738** (2014) 234, `arXiv:1408.3226 [hep-ex]`.

[28] CMS Collaboration, *Measurement of differential cross sections for Higgs boson production in the diphoton decay channel in pp collisions at $\sqrt{s}$ = 8 TeV*, Eur. Phys. J. C **76** (2016) 13, `arXiv:1508.07819 [hep-ex]`.

[29] CMS Collaboration, *Measurement of differential and integrated fiducial cross sections for Higgs boson production in the four-lepton decay channel in pp collisions at $\sqrt{s}$ = 7 and 8 TeV*, JHEP **04** (2016) 005, `arXiv:1512.08377 [hep-ex]`.

[30] S. Dittmaier et al., *Handbook of LHC Higgs Cross Sections: 1. Inclusive Observables*, CERN-2011-002, `arXiv:1101.0593 [hep-ph]`.

[31] S. Dittmaier et al., *Handbook of LHC Higgs Cross Sections: 2. Differential Distributions*, CERN-2012-002, `arXiv:1201.3084 [hep-ph]`.

[32] S. Heinemeyer et al., *Handbook of LHC Higgs Cross Sections: 3. Higgs Properties*, CERN-2013-004, FERMILAB-CONF-13-667-T, `arXiv:1307.1347 [hep-ph]`.

[33] H. M. Georgi, S. L. Glashow, M. E. Machacek, and D. V. Nanopoulos, *Higgs Bosons from Two Gluon Annihilation in Proton Proton Collisions*, Phys. Rev. Lett. **40** (1978) 692.

[34] A. Djouadi, M. Spira, and P. M. Zerwas, *Production of Higgs bosons in proton colliders: QCD corrections*, Phys. Lett. B **264** (1991) 440.

[35] S. Dawson, *Radiative corrections to Higgs boson production*, Nucl. Phys. B **359** (1991) 283.

[36] M. Spira, A. Djouadi, D. Graudenz, and P. M. Zerwas, *Higgs boson production at the LHC*, Nucl. Phys. B **453** (1995) 17, `arXiv:hep-ph/9504378`.

[37] R. V. Harlander and W. B. Kilgore, *Next-to-next-to-leading order Higgs production at hadron colliders*, Phys. Rev. Lett. **88** (2002) 201801, `arXiv:hep-ph/0201206`.

[38] C. Anastasiou and K. Melnikov, *Higgs boson production at hadron colliders in NNLO QCD*, Nucl. Phys. B **646** (2002) 220, `arXiv:hep-ph/0207004`.

[39] V. Ravindran, J. Smith, and W. L. van Neerven, *NNLO corrections to the total cross section for Higgs boson production in hadron hadron collisions*, Nucl. Phys. B **665** (2003) 325, `arXiv:hep-ph/0302135`.

[40] S. Catani, D. de Florian, M. Grazzini, and P. Nason, *Soft gluon resummation for Higgs boson production at hadron colliders*, JHEP **07** (2003) 028, `arXiv:hep-ph/0306211 [hep-ph]`.

[41] S. Actis, G. Passarino, C. Sturm, and S. Uccirati, *NLO Electroweak Corrections to Higgs Boson Production at Hadron Colliders*, Phys. Lett. B **670** (2008) 12, `arXiv:0809.1301 [hep-ph]`.

[42] C. Anastasiou, R. Boughezal, and F. Petriello, *Mixed QCD-electroweak corrections to Higgs boson production in gluon fusion*, JHEP **04** (2009) 003, `arXiv:0811.3458 [hep-ph]`.

[43] D. de Florian and M. Grazzini, *Higgs production through gluon fusion: updated cross sections at the Tevatron and the LHC*, Phys. Lett. B **674** (2009) 291, `arXiv:0901.2427 [hep-ph]`.

[44] D. de Florian and M. Grazzini, *Higgs production at the LHC: updated cross sections at $\sqrt{s} = 8$ TeV*, Phys. Lett. B **718** (2012) 117, `arXiv:1206.4133 [hep-ph]`.

[45] G. Bozzi, S. Catani, D. de Florian, and M. Grazzini, *Transverse-momentum resummation and the spectrum of the Higgs boson at the LHC*, Nucl. Phys. B **737** (2006) 73, `arXiv:hep-ph/0508068 [hep-ph]`.

[46] D. de Florian, G. Ferrera, M. Grazzini, and D. Tommasini, *Transverse-momentum resummation: Higgs boson production at the Tevatron and the LHC*, JHEP **11** (2011) 064, `arXiv:1109.2109 [hep-ph]`.

[47] M. Grazzini and H. Sargsyan, *Heavy-quark mass effects in Higgs boson production at the LHC*, JHEP **09** (2013) 129, `arXiv:1306.4581 [hep-ph]`.

[48] I. W. Stewart and F. J. Tackmann, *Theory Uncertainties for Higgs and Other Searches Using Jet Bins*, Phys. Rev. D **85** (2012) 034011, `arXiv:1107.2117 [hep-ph]`.

[49] A. Banfi, P. F. Monni, G. P. Salam, and G. Zanderighi, *Higgs and Z-boson production with a jet veto*, Phys. Rev. Lett. **109** (2012) 202001, `arXiv:1206.4998 [hep-ph]`.

[50] J. R. Ellis, M. K. Gaillard, and D. V. Nanopoulos, *A Phenomenological Profile of the Higgs Boson*, Nucl. Phys. B **106** (1976) 292.

[51] A. Djouadi, J. Kalinowski, and M. Spira, *HDECAY: A program for Higgs boson decays in the standard model and its supersymmetric extension*, Comput. Phys. Commun. **108** (1998) 56, `arXiv:hep-ph/9704448 [hep-ph]`.

[52] A. Bredenstein, A. Denner, S. Dittmaier, and M. M. Weber, *Precise predictions for the Higgs-boson decay H → WW/ZZ → 4 leptons*, Phys. Rev. D **74** (2006) 013004, `arXiv:hep-ph/0604011`.

[53] A. Bredenstein, A. Denner, S. Dittmaier, and M. M. Weber, *Radiative corrections to the semileptonic and hadronic Higgs-boson decays H → W W / Z Z → 4 fermions*, JHEP **02** (2007) 080, `arXiv:hep-ph/0611234 [hep-ph]`.

[54] A. Denner et al., *Standard Model Higgs-Boson Branching Ratios with Uncertainties*, Eur. Phys. J. C **71** (2011) 1753, `arXiv:1107.5909 [hep-ph]`.

[55] R. Cahn and S. Dawson, *Production of Very Massive Higgs Bosons*, Phys. Lett. B **136** (1984) 196.

[56] M. Ciccolini, A. Denner, and S. Dittmaier, *Strong and electroweak corrections to the production of Higgs + 2 jets via weak interactions at the LHC*, Phys. Rev. Lett. **99** (2007) 161803, `arXiv:0707.0381 [hep-ph]`.

[57] M. Ciccolini, A. Denner, and S. Dittmaier, *Electroweak and QCD corrections to Higgs production via vector-boson fusion at the LHC*, Phys. Rev. D **77** (2008) 013002, `arXiv:0710.4749 [hep-ph]`.

[58] P. Bolzoni, F. Maltoni, S.-O. Moch, and M. Zaro, *Higgs boson production via vector-boson fusion at NNLO in QCD*, Phys. Rev. Lett. **105** (2010) 011801, `arXiv:1003.4451 [hep-ph]`.

[59] M. Botje et al., *The PDF4LHC Working Group Interim Recommendations*, `arXiv:1101.0538 [hep-ph]`.

[60] H. Lai et al., *New parton distributions for collider physics*, Phys. Rev. D **82** (2010) 074024, `arXiv:1007.2241 [hep-ph]`.

[61] A. Martin, W. Stirling, R. Thorne, and G. Watt, *Parton distributions for the LHC*, Eur. Phys. J. C **63** (2009) 189, `arXiv:0901.0002 [hep-ph]`.

[62] R. D. Ball et al., *A first unbiased global NLO determination of parton distributions and their uncertainties*, Nucl. Phys. B **838** (2010) 136, `arXiv:1002.4407 [hep-ph]`.

[63] S. Glashow, D. V. Nanopoulos, and A. Yildiz, *Associated Production of Higgs Bosons and Z Particles*, Phys. Rev. D **18** (1978) 1724.

[64] O. Brein, A. Djouadi, and R. Harlander, *NNLO QCD corrections to the Higgs-strahlung processes at hadron colliders*, Phys. Lett. B **579** (2004) 149, `arXiv:hep-ph/0307206`.

[65] A. Denner, S. Dittmaier, S. Kallweit, and A. Mück, *Electroweak corrections to Higgs-strahlung off W/Z bosons at the Tevatron and the LHC with HAWK*, JHEP **03** (2012) 075, `arXiv:1112.5142 [hep-ph]`.

[66] C. Englert, M. McCullough, and M. Spannowsky, *Gluon-initiated associated production boosts Higgs physics*, Phys. Rev. D **89** (2014) 013013, `arXiv:1310.4828 [hep-ph]`.

[67] G. Ferrera, M. Grazzini, and F. Tramontano, *Associated ZH production at hadron colliders: the fully differential NNLO QCD calculation*, Phys. Lett. B **740** (2015) 51, `arXiv:1407.4747 [hep-ph]`.

[68] R. Raitio and W. W. Wada, *Higgs boson production at large transverse momentum in quantum chromodynamics*, Phys. Rev. D **19** (1979) 941.

[69] W. Beenakker et al., *NLO QCD corrections to $t\bar{t}H$ production in hadron collisions*, Nucl. Phys. B **653** (2003) 151, `arXiv:hep-ph/0211352`.

[70] S. Dawson et al., *Associated Higgs production with top quarks at the Large Hadron Collider: NLO QCD corrections*, Phys. Rev. D **68** (2003) 034022, `arXiv:hep-ph/0305087`.

[71] R. V. Harlander and W. B. Kilgore, *Higgs boson production in bottom quark fusion at next-to-next-to-leading order*, Phys. Rev. D **68** (2003) 013001, `arXiv:hep-ph/0304035`.

[72] S. Dittmaier, M. Krämer, and M. Spira, *Higgs radiation off bottom quarks at the Tevatron and the CERN LHC*, Phys. Rev. D **70** (2004) 074010, `arXiv:hep-ph/0309204 [hep-ph]`.

[73] S. Dawson, C. Jackson, L. Reina, and D. Wackeroth, *Exclusive Higgs boson production with bottom quarks at hadron colliders*, Phys. Rev. D **69** (2004) 074027, `arXiv:hep-ph/0311067 [hep-ph]`.

[74] R. Harlander, M. Krämer, and M. Schumacher, *Bottom-quark associated Higgs-boson production: Reconciling the four- and five-flavour scheme approach*, `arXiv:1112.3478 [hep-ph]`.

[75] M. Farina et al., *Lifting degeneracies in Higgs couplings using single top production in association with a Higgs boson*, JHEP **05** (2013) 022, `arXiv:1211.3736 [hep-ph]`.

[76] D. Zeppenfeld, R. Kinnunen, A. Nikitenko, and E. Richter-Was, *Measuring Higgs boson couplings at the CERN LHC*, Phys. Rev. D **62** (2000) 013009, `arXiv:hep-ph/0002036 [hep-ph]`.

[77] M. Dührssen et al., *Extracting Higgs boson couplings from CERN LHC data*, Phys. Rev. D **70** (2004) 113009, `arXiv:hep-ph/0406323 [hep-ph]`.

[78] ATLAS Collaboration, *Search for $H \rightarrow \gamma\gamma$ produced in association with top quarks and constraints on the Yukawa coupling between the top quark and the Higgs boson using data taken at 7 TeV and 8 TeV with the ATLAS detector*, Phys. Lett. B **740** (2015) 222, `arXiv:1409.3122 [hep-ex]`.

[79] J. Alwall et al., *The automated computation of tree-level and next-to-leading order differential cross sections, and their matching to parton shower simulations*, JHEP **07** (2014) 079, `arXiv:1405.0301 [hep-ph]`.

[80] P. Nason, *A New method for combining NLO QCD with shower Monte Carlo algorithms*, JHEP **11** (2004) 040, `arXiv:hep-ph/0409146 [hep-ph]`.

[81] S. Frixione, P. Nason, and C. Oleari, *Matching NLO QCD computations with Parton Shower simulations: the POWHEG method*, JHEP **11** (2007) 070, `arXiv:0709.2092 [hep-ph]`.

[82] S. Alioli, P. Nason, C. Oleari, and E. Re, *NLO Higgs boson production via gluon fusion matched with shower in POWHEG*, JHEP **04** (2009) 002, `arXiv:0812.0578 [hep-ph]`.

[83] S. Alioli, P. Nason, C. Oleari, and E. Re, *A general framework for implementing NLO calculations in shower Monte Carlo programs: the POWHEG BOX*, JHEP **06** (2010) 043, `arXiv:1002.2581 [hep-ph]`.

[84] E. Bagnaschi, G. Degrassi, P. Slavich, and A. Vicini, *Higgs production via gluon fusion in the POWHEG approach in the SM and in the MSSM*, JHEP **02** (2012) 088, `arXiv:1111.2854 [hep-ph]`.

[85] T. Sjöstrand, S. Mrenna, and P. Z. Skands, *A Brief Introduction to PYTHIA 8.1*, Comput. Phys. Commun. **178** (2008) 852, `arXiv:0710.3820 [hep-ph]`.

[86] T. Sjöstrand, S. Mrenna, and P. Z. Skands, *PYTHIA 6.4 Physics and Manual*, JHEP **05** (2006) 026, `arXiv:hep-ph/0603175 [hep-ph]`.

[87] M. Bahr et al., *Herwig++ Physics and Manual*, Eur. Phys. J. C **58** (2008) 639, `arXiv:0803.0883 [hep-ph]`.

[88] G. Bevilacqua et al., *HELAC-NLO*, Comput. Phys. Commun. **184** (2013) 986, `arXiv:1110.1499 [hep-ph]`.

[89] M. V. Garzelli, A. Kardos, C. G. Papadopoulos, and Z. Trocsanyi, *Standard Model Higgs boson production in association with a top anti-top pair at NLO with parton showering*, Europhys. Lett. **96** (2011) 11001, `arXiv:1108.0387 [hep-ph]`.

[90] F. Maltoni and T. Stelzer, *MadEvent: Automatic event generation with MadGraph*, JHEP **02** (2003) 027, `arXiv:hep-ph/0208156 [hep-ph]`.

[91] J. M. Campbell, R. K. Ellis, and G. Zanderighi, *Next-to-Leading order Higgs + 2 jet production via gluon fusion*, JHEP **10** (2006) 028, `arXiv:hep-ph/0608194 [hep-ph]`.

[92] ATLAS Collaboration, *Measurement of Higgs boson production in the diphoton decay channel in pp collisions at center-of-mass energies of 7 and 8 TeV with the ATLAS detector*, Phys. Rev. D **90** (2014) 112015, `arXiv:1408.7084 [hep-ex]`.

[93] CMS Collaboration, *Observation of the diphoton decay of the 125 GeV Higgs boson and measurement of its properties*, Eur. Phys. J. C **74** (2014) 3076, `arXiv:1407.0558 [hep-ex]`.

[94] ATLAS Collaboration, *Measurements of Higgs boson production and couplings in the four-lepton channel in pp collisions at center-of-mass energies of 7 and 8 TeV with the ATLAS detector*, Phys. Rev. D **91** (2015) 012006, `arXiv:1408.5191 [hep-ex]`.

[95] CMS Collaboration, *Measurement of the properties of a Higgs boson in the four-lepton final state*, Phys. Rev. D **89** (2014) 092007, `arXiv:1312.5353 [hep-ex]`.

[96] ATLAS Collaboration, *Observation and measurement of Higgs boson decays to WW^* with the ATLAS detector*, Phys. Rev. D **92** (2015) 012006, `arXiv:1412.2641 [hep-ex]`.

[97] ATLAS Collaboration, *Study of the (W/Z)H production and Higgs boson couplings using $H \to WW^*$ decays with the ATLAS detector*, JHEP **08** (2015) 137, `arXiv:1506.06641 [hep-ph]`.

[98] CMS Collaboration, *Measurement of Higgs boson production and properties in the WW decay channel with leptonic final states*, JHEP **01** (2014) 096, `arXiv:1312.1129 [hep-ex]`.

[99] ATLAS Collaboration, *Evidence for the Higgs-boson Yukawa coupling to tau leptons with the ATLAS detector*, JHEP **04** (2015) 117, `arXiv:1501.04943 [hep-ex]`.

[100] CMS Collaboration, *Evidence for the 125 GeV Higgs boson decaying to a pair of τ leptons*, JHEP **05** (2014) 104, `arXiv:1401.5041 [hep-ex]`.

[101] ATLAS Collaboration, *Search for the $b\bar{b}$ decay of the Standard Model Higgs boson in associated (W/Z)H production with the ATLAS detector*, JHEP **01** (2015) 069, `arXiv:1409.6212 [hep-ex]`.

[102] CMS Collaboration, *Search for the standard model Higgs boson produced in association with a W or a Z boson and decaying to bottom quarks*, Phys. Rev. D **89** (2014) 012003, `arXiv:1310.3687 [hep-ex]`.

[103] ATLAS Collaboration, *Search for the Standard Model Higgs boson decay to $\mu^+\mu^-$ with the ATLAS detector*, Phys. Lett. B **738** (2014) 68, `arXiv:1406.7663 [hep-ex]`.

[104] CMS Collaboration, *Search for a standard model-like Higgs boson in the $\mu^+\mu^-$ and e^+e^- decay channels at the LHC*, Phys. Lett. B **744** (2015) 184, `arXiv:1410.6679 [hep-ex]`.

[105] ATLAS Collaboration, *Search for the Standard Model Higgs boson produced in association with top quarks and decaying into $b\bar{b}$ in pp collisions at $\sqrt{s}$ = 8 TeV with the ATLAS detector*, Eur. Phys. J. C **75** (2015) 349, `arXiv:1503.05066 [hep-ex]`.

[106] ATLAS Collaboration, *Search for the associated production of the Higgs boson with a top quark pair in multi-lepton final states with the ATLAS detector*, Phys. Lett. B **749** (2015) 519, `arXiv:1506.05988 [hep-ex]`.

[107] CMS Collaboration, *Search for the standard model Higgs boson produced in association with a top-quark pair in pp collisions at the LHC*, JHEP **05** (2013) 145, `arXiv:1303.0763 [hep-ex]`.

[108] CMS Collaboration, *Search for the associated production of the Higgs boson with a top-quark pair*, JHEP **09** (2014) 087, `arXiv:1408.1682 [hep-ex]`.

[109] ATLAS Collaboration, *Search for Higgs boson decays to a photon and a Z boson in pp collisions at $\sqrt{s}$ = 7 and 8 TeV with the ATLAS detector*, Phys. Lett. B **732** (2014) 8, `arXiv:1402.3051 [hep-ex]`.

[110] CMS Collaboration, *Search for a Higgs boson decaying into a Z and a photon in pp collisions at $\sqrt{s}$ = 7 and 8 TeV*, Phys. Lett. B **726** (2013) 587, `arXiv:1307.5515 [hep-ex]`.

[111] CMS Collaboration, *Search for the standard model Higgs boson produced through vector boson fusion and decaying to $b\bar{b}$*, Phys. Rev. D **92** (2015) 032008, `arXiv:1506.01010 [hep-ex]`.

[112] ATLAS Collaboration, *Search for Invisible Decays of a Higgs Boson Produced in Association with a Z Boson in ATLAS*, Phys. Rev. Lett. **112** (2014) 201802, `arXiv:1402.3244 [hep-ex]`.

[113] ATLAS Collaboration, *Search for invisible decays of the Higgs boson produced in association with a hadronically decaying vector boson in pp collisions at $\sqrt{s}$ = 8 TeV with the ATLAS detector*, Eur. Phys. J. C **75** (2015) 337, `arXiv:1504.04324 [hep-ex]`.

[114] CMS Collaboration, *Search for invisible decays of Higgs bosons in the vector boson fusion and associated ZH production modes*, Eur. Phys. J. C **74** (2014) 2980, `arXiv:1404.1344 [hep-ex]`.

[115] ATLAS and CMS Collaborations, *Procedure for the LHC Higgs boson search combination in Summer 2011*, ATL-PHYS-PUB-2011-011, CERN-CMS-NOTE-2011-005 (2011), `http://cdsweb.cern.ch/record/1379837`.

[116] W. Verkerke and D. P. Kirkby, *The RooFit toolkit for data modeling*, eConf **C0303241** (2003) MOLT007, CHEP-2003-MOLT007, `arXiv:physics/0306116 [physics]`.

[117] L. Moneta et al., *The RooStats Project*, PoS **ACAT2010** (2010) 057, `arXiv:1009.1003 [physics.data-an]`.

[118] K. Cranmer et al., *HistFactory: A tool for creating statistical models for use with RooFit and RooStats*, CERN-OPEN-2012-016 (2012), `http://cds.cern.ch/record/1456844`.

[119] G. Cowan, K. Cranmer, E. Gross, and O. Vitells, *Asymptotic formulae for likelihood-based tests of new physics*, Eur. Phys. J. C **71** (2011) 1554, `arXiv:1007.1727 [physics.data-an]`.

[120] G. J. Feldman and R. D. Cousins, *Unified approach to the classical statistical analysis of small signals*, Phys. Rev. D **57** (1998) 3873, `arXiv:physics/9711021 [physics.data-an]`.

[121] J. Wenninger, *Energy Calibration of the LHC Beams at 4 TeV*, CERN-ATS-2013-40 (2013), `http://cds.cern.ch/record/1546734`.

[122] J. F. Gunion, Y. Jiang, and S. Kraml, *Could two NMSSM Higgs bosons be present near 125 GeV?*, Phys. Rev. D **86** (2012) 071702, `arXiv:1207.1545 [hep-ex]`.

[123] B. Grzadkowski, J. F. Gunion, and M. Toharia, *Higgs-Radion interpretation of the LHC data?*, Phys. Lett. B **712** (2012) 70, `arXiv:1202.5017 [hep-ex]`.

[124] A. Drozd, B. Grzadkowski, J. F. Gunion, and Y. Jiang, *Two-Higgs-doublet models and enhanced rates for a 125 GeV Higgs*, JHEP **05** (2013) 72, `arXiv:1211.3580 [hep-ex]`.

[125] P. M. Ferreira, R. Santos, H. E. Haber, and J. P. Silva, *Mass-degenerate Higgs bosons at 125 GeV in the two-Higgs-doublet model*, Phys. Rev. D **87** (2011) 055009, `arXiv:1211.3131 [hep-ex]`.

[126] J. F. Gunion, Y. Jiang, and S. Kraml, *Diagnosing Degenerate Higgs Bosons at 125 GeV*, Phys. Rev. Lett. **110** (2013) 051801, `arXiv:1208.1817 [hep-ex]`.

[127] Y. Grossman, Z. Surujon, and J. Zupan, *How to test for mass degenerate Higgs resonances*, JHEP **03** (2013) 176, `arXiv:1301.0328 [hep-ex]`.

[128] A. David, J. Heikkilä, and G. Petrucciani, *Searching for degenerate Higgs bosons*, Eur. Phys. J. C **75** (2015) 49, `arXiv:1409.6132 [hep-ph]`.

[129] J. Ellis and T. You, *Updated global analysis of Higgs couplings*, JHEP **06** (2013) 103, `arXiv:1303.3879 [hep-ph]`.

[130] T. D. Lee, *A Theory of Spontaneous T Violation*, Phys. Rev. D **8** (1973) 1226.

The ATLAS Collaboration

G. Aad[87], B. Abbott[114], J. Abdallah[65], O. Abdinov[12], B. Abeloos[118], R. Aben[108], O.S. AbouZeid[138], N.L. Abraham[150], H. Abramowicz[154], H. Abreu[153], R. Abreu[117], Y. Abulaiti[147a,147b], B.S. Acharya[164a,164b,a], L. Adamczyk[40a], D.L. Adams[27], J. Adelman[109], S. Adomeit[101], T. Adye[132], A.A. Affolder[76], T. Agatonovic-Jovin[14], J. Agricola[56], J.A. Aguilar-Saavedra[127a,127f], S.P. Ahlen[24], F. Ahmadov[67,b], G. Aielli[134a,134b], H. Akerstedt[147a,147b], T.P.A. Åkesson[83], A.V. Akimov[97], G.L. Alberghi[22a,22b], J. Albert[169], S. Albrand[57], M.J. Alconada Verzini[73], M. Aleksa[32], I.N. Aleksandrov[67], C. Alexa[28b], G. Alexander[154], T. Alexopoulos[10], M. Alhroob[114], M. Aliev[75a,75b], G. Alimonti[93a], J. Alison[33], S.P. Alkire[37], B.M.M. Allbrooke[150], B.W. Allen[117], P.P. Allport[19], A. Aloisio[105a,105b], A. Alonso[38], F. Alonso[73], C. Alpigiani[139], M. Alstaty[87], B. Alvarez Gonzalez[32], D. Álvarez Piqueras[167], M.G. Alviggi[105a,105b], B.T. Amadio[16], K. Amako[68], Y. Amaral Coutinho[26a], C. Amelung[25], D. Amidei[91], S.P. Amor Dos Santos[127a,127c], A. Amorim[127a,127b], S. Amoroso[32], G. Amundsen[25], C. Anastopoulos[140], L.S. Ancu[51], N. Andari[109], T. Andeen[11], C.F. Anders[60b], G. Anders[32], J.K. Anders[76], K.J. Anderson[33], A. Andreazza[93a,93b], V. Andrei[60a], S. Angelidakis[9], I. Angelozzi[108], P. Anger[46], A. Angerami[37], F. Anghinolfi[32], A.V. Anisenkov[110,c], N. Anjos[13], A. Annovi[125a,125b], M. Antonelli[49], A. Antonov[99], J. Antos[145b], F. Anulli[133a], M. Aoki[68], L. Aperio Bella[19], G. Arabidze[92], Y. Arai[68], J.P. Araque[127a], A.T.H. Arce[47], F.A. Arduh[73], J-F. Arguin[96], S. Argyropoulos[65], M. Arik[20a], A.J. Armbruster[144], L.J. Armitage[78], O. Arnaez[32], H. Arnold[50], M. Arratia[30], O. Arslan[23], A. Artamonov[98], G. Artoni[121], S. Artz[85], S. Asai[156], N. Asbah[44], A. Ashkenazi[154], B. Åsman[147a,147b], L. Asquith[150], K. Assamagan[27], R. Astalos[145a], M. Atkinson[166], N.B. Atlay[142], K. Augsten[129], G. Avolio[32], B. Axen[16], M.K. Ayoub[118], G. Azuelos[96,d], M.A. Baak[32], A.E. Baas[60a], M.J. Baca[19], H. Bachacou[137], K. Bachas[75a,75b], M. Backes[32], M. Backhaus[32], P. Bagiacchi[133a,133b], P. Bagnaia[133a,133b], Y. Bai[35a], J.T. Baines[132], O.K. Baker[176], E.M. Baldin[110,c], P. Balek[130], T. Balestri[149], F. Balli[137], W.K. Balunas[123], E. Banas[41], Sw. Banerjee[173,e], A.A.E. Bannoura[175], L. Barak[32], E.L. Barberio[90], D. Barberis[52a,52b], M. Barbero[87], T. Barillari[102], T. Barklow[144], N. Barlow[30], S.L. Barnes[86], B.M. Barnett[132], R.M. Barnett[16], Z. Barnovska[5], A. Baroncelli[135a], G. Barone[25], A.J. Barr[121], L. Barranco Navarro[167], F. Barreiro[84], J. Barreiro Guimarães da Costa[35a], R. Bartoldus[144], A.E. Barton[74], P. Bartos[145a], A. Basalaev[124], A. Bassalat[118], R.L. Bates[55], S.J. Batista[159], J.R. Batley[30], M. Battaglia[138], M. Bauce[133a,133b], F. Bauer[137], H.S. Bawa[144,f], J.B. Beacham[112], M.D. Beattie[74], T. Beau[82], P.H. Beauchemin[162], P. Bechtle[23], H.P. Beck[18,g], K. Becker[121], M. Becker[85], M. Beckingham[170], C. Becot[111], A.J. Beddall[20e], A. Beddall[20b], V.A. Bednyakov[67], M. Bedognetti[108], C.P. Bee[149], L.J. Beemster[108], T.A. Beermann[32], M. Begel[27], J.K. Behr[44], C. Belanger-Champagne[89], A.S. Bell[80], G. Bella[154], L. Bellagamba[22a], A. Bellerive[31], M. Bellomo[88], K. Belotskiy[99], O. Beltramello[32], N.L. Belyaev[99], O. Benary[154], D. Benchekroun[136a], M. Bender[101], K. Bendtz[147a,147b], N. Benekos[10], Y. Benhammou[154], E. Benhar Noccioli[176], J. Benitez[65], D.P. Benjamin[47], J.R. Bensinger[25], S. Bentvelsen[108], L. Beresford[121], M. Beretta[49], D. Berge[108], E. Bergeaas Kuutmann[165], N. Berger[5], J. Beringer[16], S. Berlendis[57], N.R. Bernard[88], C. Bernius[111], F.U. Bernlochner[23], T. Berry[79], P. Berta[130], C. Bertella[85], G. Bertoli[147a,147b], F. Bertolucci[125a,125b], I.A. Bertram[74], C. Bertsche[44], D. Bertsche[114], G.J. Besjes[38], O. Bessidskaia Bylund[147a,147b], M. Bessner[44], N. Besson[137], C. Betancourt[50], S. Bethke[102], A.J. Bevan[78], W. Bhimji[16], R.M. Bianchi[126], L. Bianchini[25], M. Bianco[32], O. Biebel[101], D. Biedermann[17], R. Bielski[86], N.V. Biesuz[125a,125b], M. Biglietti[135a], J. Bilbao De Mendizabal[51], H. Bilokon[49], M. Bindi[56], S. Binet[118], A. Bingul[20b], C. Bini[133a,133b], S. Biondi[22a,22b], D.M. Bjergaard[47], C.W. Black[151], J.E. Black[144], K.M. Black[24], D. Blackburn[139], R.E. Blair[6], J.-B. Blanchard[137], J.E. Blanco[79], T. Blazek[145a], I. Bloch[44], C. Blocker[25], W. Blum[85,*], U. Blumenschein[56], S. Blunier[34a],

G.J. Bobbink[108], V.S. Bobrovnikov[110,c], S.S. Bocchetta[83], A. Bocci[47], C. Bock[101], M. Boehler[50],
D. Boerner[175], J.A. Bogaerts[32], D. Bogavac[14], A.G. Bogdanchikov[110], C. Bohm[147a], V. Boisvert[79],
P. Bokan[14], T. Bold[40a], A.S. Boldyrev[164a,164c], M. Bomben[82], M. Bona[78], M. Boonekamp[137],
A. Borisov[131], G. Borissov[74], J. Bortfeldt[101], D. Bortoletto[121], V. Bortolotto[62a,62b,62c], K. Bos[108],
D. Boscherini[22a], M. Bosman[13], J.D. Bossio Sola[29], J. Boudreau[126], J. Bouffard[2],
E.V. Bouhova-Thacker[74], D. Boumediene[36], C. Bourdarios[118], S.K. Boutle[55], A. Boveia[32], J. Boyd[32],
I.R. Boyko[67], J. Bracinik[19], A. Brandt[8], G. Brandt[56], O. Brandt[60a], U. Bratzler[157], B. Brau[88],
J.E. Brau[117], H.M. Braun[175,*], W.D. Breaden Madden[55], K. Brendlinger[123], A.J. Brennan[90],
L. Brenner[108], R. Brenner[165], S. Bressler[172], T.M. Bristow[48], D. Britton[55], D. Britzger[44], F.M. Brochu[30],
I. Brock[23], R. Brock[92], G. Brooijmans[37], T. Brooks[79], W.K. Brooks[34b], J. Brosamer[16], E. Brost[117],
J.H Broughton[19], P.A. Bruckman de Renstrom[41], D. Bruncko[145b], R. Bruneliere[50], A. Bruni[22a],
G. Bruni[22a], BH Brunt[30], M. Bruschi[22a], N. Bruscino[23], P. Bryant[33], L. Bryngemark[83], T. Buanes[15],
Q. Buat[143], P. Buchholz[142], A.G. Buckley[55], I.A. Budagov[67], F. Buehrer[50], M.K. Bugge[120],
O. Bulekov[99], D. Bullock[8], H. Burckhart[32], S. Burdin[76], C.D. Burgard[50], B. Burghgrave[109], K. Burka[41],
S. Burke[132], I. Burmeister[45], E. Busato[36], D. Büscher[50], V. Büscher[85], P. Bussey[55], J.M. Butler[24],
C.M. Buttar[55], J.M. Butterworth[80], P. Butti[108], W. Buttinger[27], A. Buzatu[55], A.R. Buzykaev[110,c],
S. Cabrera Urbán[167], D. Caforio[129], V.M. Cairo[39a,39b], O. Cakir[4a], N. Calace[51], P. Calafiura[16],
A. Calandri[87], G. Calderini[82], P. Calfayan[101], L.P. Caloba[26a], D. Calvet[36], S. Calvet[36], T.P. Calvet[87],
R. Camacho Toro[33], S. Camarda[32], P. Camarri[134a,134b], D. Cameron[120], R. Caminal Armadans[166],
C. Camincher[57], S. Campana[32], M. Campanelli[80], A. Campani[93a,93b], A. Campoverde[149],
V. Canale[105a,105b], A. Canepa[160a], M. Cano Bret[35e], J. Cantero[115], R. Cantrill[127a], T. Cao[42],
M.D.M. Capeans Garrido[32], I. Caprini[28b], M. Caprini[28b], M. Capua[39a,39b], R. Caputo[85], R.M. Carbone[37],
R. Cardarelli[134a], F. Cardillo[50], I. Carli[130], T. Carli[32], G. Carlino[105a], L. Carminati[93a,93b], S. Caron[107],
E. Carquin[34b], G.D. Carrillo-Montoya[32], J.R. Carter[30], J. Carvalho[127a,127c], D. Casadei[19],
M.P. Casado[13,h], M. Casolino[13], D.W. Casper[163], E. Castaneda-Miranda[146a], R. Castelijn[108],
A. Castelli[108], V. Castillo Gimenez[167], N.F. Castro[127a,i], A. Catinaccio[32], J.R. Catmore[120], A. Cattai[32],
J. Caudron[85], V. Cavaliere[166], E. Cavallaro[13], D. Cavalli[93a], M. Cavalli-Sforza[13], V. Cavasinni[125a,125b],
F. Ceradini[135a,135b], L. Cerda Alberich[167], B.C. Cerio[47], A.S. Cerqueira[26b], A. Cerri[150], L. Cerrito[78],
F. Cerutti[16], M. Cerv[32], A. Cervelli[18], S.A. Cetin[20d], A. Chafaq[136a], D. Chakraborty[109], S.K. Chan[59],
Y.L. Chan[62a], P. Chang[166], J.D. Chapman[30], D.G. Charlton[19], A. Chatterjee[51], C.C. Chau[159],
C.A. Chavez Barajas[150], S. Che[112], S. Cheatham[74], A. Chegwidden[92], S. Chekanov[6],
S.V. Chekulaev[160a], G.A. Chelkov[67,j], M.A. Chelstowska[91], C. Chen[66], H. Chen[27], K. Chen[149],
S. Chen[35c], S. Chen[156], X. Chen[35f], Y. Chen[69], H.C. Cheng[91], H.J Cheng[35a], Y. Cheng[33],
A. Cheplakov[67], E. Cheremushkina[131], R. Cherkaoui El Moursli[136e], V. Chernyatin[27,*], E. Cheu[7],
L. Chevalier[137], V. Chiarella[49], G. Chiarelli[125a,125b], G. Chiodini[75a], A.S. Chisholm[19], A. Chitan[28b],
M.V. Chizhov[67], K. Choi[63], A.R. Chomont[36], S. Chouridou[9], B.K.B. Chow[101], V. Christodoulou[80],
D. Chromek-Burckhart[32], J. Chudoba[128], A.J. Chuinard[89], J.J. Chwastowski[41], L. Chytka[116],
G. Ciapetti[133a,133b], A.K. Ciftci[4a], D. Cinca[55], V. Cindro[77], I.A. Cioara[23], A. Ciocio[16], F. Cirotto[105a,105b],
Z.H. Citron[172], M. Citterio[93a], M. Ciubancan[28b], A. Clark[51], B.L. Clark[59], M.R. Clark[37], P.J. Clark[48],
R.N. Clarke[16], C. Clement[147a,147b], Y. Coadou[87], M. Cobal[164a,164c], A. Coccaro[51], J. Cochran[66],
L. Coffey[25], L. Colasurdo[107], B. Cole[37], A.P. Colijn[108], J. Collot[57], T. Colombo[32], G. Compostella[102],
P. Conde Muiño[127a,127b], E. Coniavitis[50], S.H. Connell[146b], I.A. Connelly[79], V. Consorti[50],
S. Constantinescu[28b], G. Conti[32], F. Conventi[105a,k], M. Cooke[16], B.D. Cooper[80], A.M. Cooper-Sarkar[121],
K.J.R. Cormier[159], T. Cornelissen[175], M. Corradi[133a,133b], F. Corriveau[89,l], A. Corso-Radu[163],
A. Cortes-Gonzalez[13], G. Cortiana[102], G. Costa[93a], M.J. Costa[167], D. Costanzo[140], G. Cottin[30],
G. Cowan[79], B.E. Cox[86], K. Cranmer[111], S.J. Crawley[55], G. Cree[31], S. Crépé-Renaudin[57], F. Crescioli[82],
W.A. Cribbs[147a,147b], M. Crispin Ortuzar[121], M. Cristinziani[23], V. Croft[107], G. Crosetti[39a,39b],

T. Cuhadar Donszelmann[140], J. Cummings[176], M. Curatolo[49], J. Cúth[85], C. Cuthbert[151], H. Czirr[142],
P. Czodrowski[3], G. D'amen[22a,22b], S. D'Auria[55], M. D'Onofrio[76],
M.J. Da Cunha Sargedas De Sousa[127a,127b], C. Da Via[86], W. Dabrowski[40a], T. Dado[145a], T. Dai[91],
O. Dale[15], F. Dallaire[96], C. Dallapiccola[88], M. Dam[38], J.R. Dandoy[33], N.P. Dang[50], A.C. Daniells[19],
N.S. Dann[86], M. Danninger[168], M. Dano Hoffmann[137], V. Dao[50], G. Darbo[52a], S. Darmora[8],
J. Dassoulas[3], A. Dattagupta[63], W. Davey[23], C. David[169], T. Davidek[130], M. Davies[154], P. Davison[80],
E. Dawe[90], I. Dawson[140], R.K. Daya-Ishmukhametova[88], K. De[8], R. de Asmundis[105a],
A. De Benedetti[114], S. De Castro[22a,22b], S. De Cecco[82], N. De Groot[107], P. de Jong[108], H. De la Torre[84],
F. De Lorenzi[66], A. De Maria[56], D. De Pedis[133a], A. De Salvo[133a], U. De Sanctis[150], A. De Santo[150],
J.B. De Vivie De Regie[118], W.J. Dearnaley[74], R. Debbe[27], C. Debenedetti[138], D.V. Dedovich[67],
N. Dehghanian[3], I. Deigaard[108], M. Del Gaudio[39a,39b], J. Del Peso[84], T. Del Prete[125a,125b],
D. Delgove[118], F. Deliot[137], C.M. Delitzsch[51], M. Deliyergiyev[77], A. Dell'Acqua[32], L. Dell'Asta[24],
M. Dell'Orso[125a,125b], M. Della Pietra[105a,k], D. della Volpe[51], M. Delmastro[5], P.A. Delsart[57],
C. Deluca[108], D.A. DeMarco[159], S. Demers[176], M. Demichev[67], A. Demilly[82], S.P. Denisov[131],
D. Denysiuk[137], D. Derendarz[41], J.E. Derkaoui[136d], F. Derue[82], P. Dervan[76], K. Desch[23], C. Deterre[44],
K. Dette[45], P.O. Deviveiros[32], A. Dewhurst[132], S. Dhaliwal[25], A. Di Ciaccio[134a,134b], L. Di Ciaccio[5],
W.K. Di Clemente[123], C. Di Donato[133a,133b], A. Di Girolamo[32], B. Di Girolamo[32], B. Di Micco[135a,135b],
R. Di Nardo[32], A. Di Simone[50], R. Di Sipio[159], D. Di Valentino[31], C. Diaconu[87], M. Diamond[159],
F.A. Dias[48], M.A. Diaz[34a], E.B. Diehl[91], J. Dietrich[17], S. Diglio[87], A. Dimitrievska[14], J. Dingfelder[23],
P. Dita[28b], S. Dita[28b], F. Dittus[32], F. Djama[87], T. Djobava[53b], J.I. Djuvsland[60a], M.A.B. do Vale[26c],
D. Dobos[32], M. Dobre[28b], C. Doglioni[83], T. Dohmae[156], J. Dolejsi[130], Z. Dolezal[130],
B.A. Dolgoshein[99,*], M. Donadelli[26d], S. Donati[125a,125b], P. Dondero[122a,122b], J. Donini[36], J. Dopke[132],
A. Doria[105a], M.T. Dova[73], A.T. Doyle[55], E. Drechsler[56], M. Dris[10], Y. Du[35d], J. Duarte-Campderros[154],
E. Duchovni[172], G. Duckeck[101], O.A. Ducu[96,m], D. Duda[108], A. Dudarev[32], L. Duflot[118], L. Duguid[79],
M. Dührssen[32], M. Dumancic[172], M. Dunford[60a], H. Duran Yildiz[4a], M. Düren[54], A. Durglishvili[53b],
D. Duschinger[46], B. Dutta[44], M. Dyndal[44], C. Eckardt[44], K.M. Ecker[102], R.C. Edgar[91], N.C. Edwards[48],
T. Eifert[32], G. Eigen[15], K. Einsweiler[16], T. Ekelof[165], M. El Kacimi[136c], V. Ellajosyula[87], M. Ellert[165],
S. Elles[5], F. Ellinghaus[175], A.A. Elliot[169], N. Ellis[32], J. Elmsheuser[27], M. Elsing[32], D. Emeliyanov[132],
Y. Enari[156], O.C. Endner[85], M. Endo[119], J.S. Ennis[170], J. Erdmann[45], A. Ereditato[18], G. Ernis[175],
J. Ernst[2], M. Ernst[27], S. Errede[166], E. Ertel[85], M. Escalier[118], H. Esch[45], C. Escobar[126], B. Esposito[49],
A.I. Etienvre[137], E. Etzion[154], H. Evans[63], A. Ezhilov[124], F. Fabbri[22a,22b], L. Fabbri[22a,22b], G. Facini[33],
R.M. Fakhrutdinov[131], S. Falciano[133a], R.J. Falla[80], J. Faltova[130], Y. Fang[35a], M. Fanti[93a,93b], A. Farbin[8],
A. Farilla[135a], C. Farina[126], T. Farooque[13], S. Farrell[16], S.M. Farrington[170], P. Farthouat[32], F. Fassi[136e],
P. Fassnacht[32], D. Fassouliotis[9], M. Faucci Giannelli[79], A. Favareto[52a,52b], W.J. Fawcett[121], L. Fayard[118],
O.L. Fedin[124,n], W. Fedorko[168], S. Feigl[120], L. Feligioni[87], C. Feng[35d], E.J. Feng[32], H. Feng[91],
A.B. Fenyuk[131], L. Feremenga[8], P. Fernandez Martinez[167], S. Fernandez Perez[13], J. Ferrando[55],
A. Ferrari[165], P. Ferrari[108], R. Ferrari[122a], D.E. Ferreira de Lima[60b], A. Ferrer[167], D. Ferrere[51],
C. Ferretti[91], A. Ferretto Parodi[52a,52b], F. Fiedler[85], A. Filipčič[77], M. Filipuzzi[44], F. Filthaut[107],
M. Fincke-Keeler[169], K.D. Finelli[151], M.C.N. Fiolhais[127a,127c], L. Fiorini[167], A. Firan[42], A. Fischer[2],
C. Fischer[13], J. Fischer[175], W.C. Fisher[92], N. Flaschel[44], I. Fleck[142], P. Fleischmann[91], G.T. Fletcher[140],
R.R.M. Fletcher[123], T. Flick[175], A. Floderus[83], L.R. Flores Castillo[62a], M.J. Flowerdew[102],
G.T. Forcolin[86], A. Formica[137], A. Forti[86], A.G. Foster[19], D. Fournier[118], H. Fox[74], S. Fracchia[13],
P. Francavilla[82], M. Franchini[22a,22b], D. Francis[32], L. Franconi[120], M. Franklin[59], M. Frate[163],
M. Fraternali[122a,122b], D. Freeborn[80], S.M. Fressard-Batraneanu[32], F. Friedrich[46], D. Froidevaux[32],
J.A. Frost[121], C. Fukunaga[157], E. Fullana Torregrosa[85], T. Fusayasu[103], J. Fuster[167], C. Gabaldon[57],
O. Gabizon[175], A. Gabrielli[22a,22b], A. Gabrielli[16], G.P. Gach[40a], S. Gadatsch[32], S. Gadomski[51],
G. Gagliardi[52a,52b], L.G. Gagnon[96], P. Gagnon[63], C. Galea[107], B. Galhardo[127a,127c], E.J. Gallas[121],

B.J. Gallop[132], P. Gallus[129], G. Galster[38], K.K. Gan[112], J. Gao[35b,87], Y. Gao[48], Y.S. Gao[144,f],
F.M. Garay Walls[48], C. García[167], J.E. García Navarro[167], M. Garcia-Sciveres[16], R.W. Gardner[33],
N. Garelli[144], V. Garonne[120], A. Gascon Bravo[44], C. Gatti[49], A. Gaudiello[52a,52b], G. Gaudio[122a],
B. Gaur[142], L. Gauthier[96], I.L. Gavrilenko[97], C. Gay[168], G. Gaycken[23], E.N. Gazis[10], Z. Gecse[168],
C.N.P. Gee[132], Ch. Geich-Gimbel[23], M.P. Geisler[60a], C. Gemme[52a], M.H. Genest[57], C. Geng[35b,o],
S. Gentile[133a,133b], S. George[79], D. Gerbaudo[13], A. Gershon[154], S. Ghasemi[142], H. Ghazlane[136b],
M. Ghneimat[23], B. Giacobbe[22a], S. Giagu[133a,133b], P. Giannetti[125a,125b], B. Gibbard[27], S.M. Gibson[79],
M. Gignac[168], M. Gilchriese[16], T.P.S. Gillam[30], D. Gillberg[31], G. Gilles[175], D.M. Gingrich[3,d],
N. Giokaris[9], M.P. Giordani[164a,164c], F.M. Giorgi[22a], F.M. Giorgi[17], P.F. Giraud[137], P. Giromini[59],
D. Giugni[93a], F. Giuli[121], C. Giuliani[102], M. Giulini[60b], B.K. Gjelsten[120], S. Gkaitatzis[155], I. Gkialas[155],
E.L. Gkougkousis[118], L.K. Gladilin[100], C. Glasman[84], J. Glatzer[32], P.C.F. Glaysher[48], A. Glazov[44],
M. Goblirsch-Kolb[102], J. Godlewski[41], S. Goldfarb[91], T. Golling[51], D. Golubkov[131],
A. Gomes[127a,127b,127d], R. Gonçalo[127a], J. Goncalves Pinto Firmino Da Costa[137], L. Gonella[19],
A. Gongadze[67], S. González de la Hoz[167], G. Gonzalez Parra[13], S. Gonzalez-Sevilla[51], L. Goossens[32],
P.A. Gorbounov[98], H.A. Gordon[27], I. Gorelov[106], B. Gorini[32], E. Gorini[75a,75b], A. Gorišek[77],
E. Gornicki[41], A.T. Goshaw[47], C. Gössling[45], M.I. Gostkin[67], C.R. Goudet[118], D. Goujdami[136c],
A.G. Goussiou[139], N. Govender[146b,p], E. Gozani[153], L. Graber[56], I. Grabowska-Bold[40a], P.O.J. Gradin[57],
P. Grafström[22a,22b], J. Gramling[51], E. Gramstad[120], S. Grancagnolo[17], V. Gratchev[124], H.M. Gray[32],
E. Graziani[135a], Z.D. Greenwood[81,q], C. Grefe[23], K. Gregersen[80], I.M. Gregor[44], P. Grenier[144],
K. Grevtsov[5], J. Griffiths[8], A.A. Grillo[138], K. Grimm[74], S. Grinstein[13,r], Ph. Gris[36], J.-F. Grivaz[118],
S. Groh[85], J.P. Grohs[46], E. Gross[172], J. Grosse-Knetter[56], G.C. Grossi[81], Z.J. Grout[150], L. Guan[91],
W. Guan[173], J. Guenther[129], F. Guescini[51], D. Guest[163], O. Gueta[154], E. Guido[52a,52b], T. Guillemin[5],
S. Guindon[2], U. Gul[55], C. Gumpert[32], J. Guo[35e], Y. Guo[35b,o], S. Gupta[121], G. Gustavino[133a,133b],
P. Gutierrez[114], N.G. Gutierrez Ortiz[80], C. Gutschow[46], C. Guyot[137], C. Gwenlan[121], C.B. Gwilliam[76],
A. Haas[111], C. Haber[16], H.K. Hadavand[8], N. Haddad[136e], A. Hadef[87], P. Haefner[23], S. Hageböck[23],
Z. Hajduk[41], H. Hakobyan[177,*], M. Haleem[44], J. Haley[115], G. Halladjian[92], G.D. Hallewell[87],
K. Hamacher[175], P. Hamal[116], K. Hamano[169], A. Hamilton[146a], G.N. Hamity[140], P.G. Hamnett[44],
L. Han[35b], K. Hanagaki[68,s], K. Hanawa[156], M. Hance[138], B. Haney[123], P. Hanke[60a], R. Hanna[137],
J.B. Hansen[38], J.D. Hansen[38], M.C. Hansen[23], P.H. Hansen[38], K. Hara[161], A.S. Hard[173], T. Harenberg[175],
F. Hariri[118], S. Harkusha[94], R.D. Harrington[48], P.F. Harrison[170], F. Hartjes[108], N.M. Hartmann[101],
M. Hasegawa[69], Y. Hasegawa[141], A. Hasib[114], S. Hassani[137], S. Haug[18], R. Hauser[92], L. Hauswald[46],
M. Havranek[128], C.M. Hawkes[19], R.J. Hawkings[32], D. Hayden[92], C.P. Hays[121], J.M. Hays[78],
H.S. Hayward[76], S.J. Haywood[132], S.J. Head[19], T. Heck[85], V. Hedberg[83], L. Heelan[8], S. Heim[123],
T. Heim[16], B. Heinemann[16], J.J. Heinrich[101], L. Heinrich[111], C. Heinz[54], J. Hejbal[128], L. Helary[24],
S. Hellman[147a,147b], C. Helsens[32], J. Henderson[121], R.C.W. Henderson[74], Y. Heng[173], S. Henkelmann[168],
A.M. Henriques Correia[32], S. Henrot-Versille[118], G.H. Herbert[17], Y. Hernández Jiménez[167], G. Herten[50],
R. Hertenberger[101], L. Hervas[32], G.G. Hesketh[80], N.P. Hessey[108], J.W. Hetherly[42], R. Hickling[78],
E. Higón-Rodriguez[167], E. Hill[169], J.C. Hill[30], K.H. Hiller[44], S.J. Hillier[19], I. Hinchliffe[16], E. Hines[123],
R.R. Hinman[16], M. Hirose[158], D. Hirschbuehl[175], J. Hobbs[149], N. Hod[160a], M.C. Hodgkinson[140],
P. Hodgson[140], A. Hoecker[32], M.R. Hoeferkamp[106], F. Hoenig[101], M. Hohlfeld[85], D. Hohn[23],
T.R. Holmes[16], M. Homann[45], T.M. Hong[126], B.H. Hooberman[166], W.H. Hopkins[117], Y. Horii[104],
A.J. Horton[143], J-Y. Hostachy[57], S. Hou[152], A. Hoummada[136a], J. Howarth[44], M. Hrabovsky[116],
I. Hristova[17], J. Hrivnac[118], T. Hryn'ova[5], A. Hrynevich[95], C. Hsu[146c], P.J. Hsu[152,t], S.-C. Hsu[139],
D. Hu[37], Q. Hu[35b], Y. Huang[44], Z. Hubacek[129], F. Hubaut[87], F. Huegging[23], T.B. Huffman[121],
E.W. Hughes[37], G. Hughes[74], M. Huhtinen[32], T.A. Hülsing[85], P. Huo[149], N. Huseynov[67,b], J. Huston[92],
J. Huth[59], G. Iacobucci[51], G. Iakovidis[27], I. Ibragimov[142], L. Iconomidou-Fayard[118], E. Ideal[176],
Z. Idrissi[136e], P. Iengo[32], O. Igonkina[108,u], T. Iizawa[171], Y. Ikegami[68], M. Ikeno[68], Y. Ilchenko[11,v],

D. Iliadis[155], N. Ilic[144], T. Ince[102], G. Introzzi[122a,122b], P. Ioannou[9,*], M. Iodice[135a], K. Iordanidou[37],
V. Ippolito[59], M. Ishino[70], M. Ishitsuka[158], R. Ishmukhametov[112], C. Issever[121], S. Istin[20a], F. Ito[161],
J.M. Iturbe Ponce[86], R. Iuppa[134a,134b], W. Iwanski[41], H. Iwasaki[68], J.M. Izen[43], V. Izzo[105a], S. Jabbar[3],
B. Jackson[123], M. Jackson[76], P. Jackson[1], V. Jain[2], K.B. Jakobi[85], K. Jakobs[50], S. Jakobsen[32],
T. Jakoubek[128], D.O. Jamin[115], D.K. Jana[81], E. Jansen[80], R. Jansky[64], J. Janssen[23], M. Janus[56],
G. Jarlskog[83], N. Javadov[67,b], T. Javůrek[50], F. Jeanneau[137], L. Jeanty[16], J. Jejelava[53a,w], G.-Y. Jeng[151],
D. Jennens[90], P. Jenni[50,x], J. Jentzsch[45], C. Jeske[170], S. Jézéquel[5], H. Ji[173], J. Jia[149], H. Jiang[66],
Y. Jiang[35b], S. Jiggins[80], J. Jimenez Pena[167], S. Jin[35a], A. Jinaru[28b], O. Jinnouchi[158], P. Johansson[140],
K.A. Johns[7], W.J. Johnson[139], K. Jon-And[147a,147b], G. Jones[170], R.W.L. Jones[74], S. Jones[7], T.J. Jones[76],
J. Jongmanns[60a], P.M. Jorge[127a,127b], J. Jovicevic[160a], X. Ju[173], A. Juste Rozas[13,r], M.K. Köhler[172],
A. Kaczmarska[41], M. Kado[118], H. Kagan[112], M. Kagan[144], S.J. Kahn[87], E. Kajomovitz[47],
C.W. Kalderon[121], A. Kaluza[85], S. Kama[42], A. Kamenshchikov[131], N. Kanaya[156], S. Kaneti[30],
L. Kanjir[77], V.A. Kantserov[99], J. Kanzaki[68], B. Kaplan[111], L.S. Kaplan[173], A. Kapliy[33], D. Kar[146c],
K. Karakostas[10], A. Karamaoun[3], N. Karastathis[10], M.J. Kareem[56], E. Karentzos[10], M. Karnevskiy[85],
S.N. Karpov[67], Z.M. Karpova[67], K. Karthik[111], V. Kartvelishvili[74], A.N. Karyukhin[131], K. Kasahara[161],
L. Kashif[173], R.D. Kass[112], A. Kastanas[15], Y. Kataoka[156], C. Kato[156], A. Katre[51], J. Katzy[44],
K. Kawagoe[72], T. Kawamoto[156], G. Kawamura[56], S. Kazama[156], V.F. Kazanin[110,c], R. Keeler[169],
R. Kehoe[42], J.S. Keller[44], J.J. Kempster[79], K Kentaro[104], H. Keoshkerian[159], O. Kepka[128],
B.P. Kerševan[77], S. Kersten[175], R.A. Keyes[89], F. Khalil-zada[12], A. Khanov[115], A.G. Kharlamov[110,c],
T.J. Khoo[51], V. Khovanskiy[98], E. Khramov[67], J. Khubua[53b,y], S. Kido[69], H.Y. Kim[8], S.H. Kim[161],
Y.K. Kim[33], N. Kimura[155], O.M. Kind[17], B.T. King[76], M. King[167], S.B. King[168], J. Kirk[132],
A.E. Kiryunin[102], T. Kishimoto[69], D. Kisielewska[40a], F. Kiss[50], K. Kiuchi[161], O. Kivernyk[137],
E. Kladiva[145b], M.H. Klein[37], M. Klein[76], U. Klein[76], K. Kleinknecht[85], P. Klimek[147a,147b],
A. Klimentov[27], R. Klingenberg[45], J.A. Klinger[140], T. Klioutchnikova[32], E.-E. Kluge[60a], P. Kluit[108],
S. Kluth[102], J. Knapik[41], E. Kneringer[64], E.B.F.G. Knoops[87], A. Knue[55], A. Kobayashi[156],
D. Kobayashi[158], T. Kobayashi[156], M. Kobel[46], M. Kocian[144], P. Kodys[130], T. Koffas[31], E. Koffeman[108],
T. Koi[144], H. Kolanoski[17], M. Kolb[60b], I. Koletsou[5], A.A. Komar[97,*], Y. Komori[156], T. Kondo[68],
N. Kondrashova[44], K. Köneke[50], A.C. König[107], T. Kono[68,z], R. Konoplich[111,aa], N. Konstantinidis[80],
R. Kopeliansky[63], S. Koperny[40a], L. Köpke[85], A.K. Kopp[50], K. Korcyl[41], K. Kordas[155], A. Korn[80],
A.A. Korol[110,c], I. Korolkov[13], E.V. Korolkova[140], O. Kortner[102], S. Kortner[102], T. Kosek[130],
V.V. Kostyukhin[23], A. Kotwal[47], A. Kourkoumeli-Charalampidi[155], C. Kourkoumelis[9], V. Kouskoura[27],
A.B. Kowalewska[41], R. Kowalewski[169], T.Z. Kowalski[40a], C. Kozakai[156], W. Kozanecki[137],
A.S. Kozhin[131], V.A. Kramarenko[100], G. Kramberger[77], D. Krasnopevtsev[99], A. Krasznahorkay[32],
J.K. Kraus[23], A. Kravchenko[27], M. Kretz[60c], J. Kretzschmar[76], K. Kreutzfeldt[54], P. Krieger[159],
K. Krizka[33], K. Kroeninger[45], H. Kroha[102], J. Kroll[123], J. Kroseberg[23], J. Krstic[14], U. Kruchonak[67],
H. Krüger[23], N. Krumnack[66], A. Kruse[173], M.C. Kruse[47], M. Kruskal[24], T. Kubota[90], H. Kucuk[80],
S. Kuday[4b], J.T. Kuechler[175], S. Kuehn[50], A. Kugel[60c], F. Kuger[174], A. Kuhl[138], T. Kuhl[44], V. Kukhtin[67],
R. Kukla[137], Y. Kulchitsky[94], S. Kuleshov[34b], M. Kuna[133a,133b], T. Kunigo[70], A. Kupco[128],
H. Kurashige[69], Y.A. Kurochkin[94], V. Kus[128], E.S. Kuwertz[169], M. Kuze[158], J. Kvita[116], T. Kwan[169],
D. Kyriazopoulos[140], A. La Rosa[102], J.L. La Rosa Navarro[26d], L. La Rotonda[39a,39b], C. Lacasta[167],
F. Lacava[133a,133b], J. Lacey[31], H. Lacker[17], D. Lacour[82], V.R. Lacuesta[167], E. Ladygin[67], R. Lafaye[5],
B. Laforge[82], T. Lagouri[176], S. Lai[56], S. Lammers[63], W. Lampl[7], E. Lançon[137], U. Landgraf[50],
M.P.J. Landon[78], V.S. Lang[60a], J.C. Lange[13], A.J. Lankford[163], F. Lanni[27], K. Lantzsch[23], A. Lanza[122a],
S. Laplace[82], C. Lapoire[32], J.F. Laporte[137], T. Lari[93a], F. Lasagni Manghi[22a,22b], M. Lassnig[32],
P. Laurelli[49], W. Lavrijsen[16], A.T. Law[138], P. Laycock[76], T. Lazovich[59], M. Lazzaroni[93a,93b], B. Le[90],
O. Le Dortz[82], E. Le Guirriec[87], E.P. Le Quilleuc[137], M. LeBlanc[169], T. LeCompte[6],
F. Ledroit-Guillon[57], C.A. Lee[27], S.C. Lee[152], L. Lee[1], G. Lefebvre[82], M. Lefebvre[169], F. Legger[101],

C. Leggett[16], A. Lehan[76], G. Lehmann Miotto[32], X. Lei[7], W.A. Leight[31], A. Leisos[155,ab],
A.G. Leister[176], M.A.L. Leite[26d], R. Leitner[130], D. Lellouch[172], B. Lemmer[56], K.J.C. Leney[80], T. Lenz[23],
B. Lenzi[32], R. Leone[7], S. Leone[125a,125b], C. Leonidopoulos[48], S. Leontsinis[10], G. Lerner[150], C. Leroy[96],
A.A.J. Lesage[137], C.G. Lester[30], M. Levchenko[124], J. Levêque[5], D. Levin[91], L.J. Levinson[172],
M. Levy[19], A.M. Leyko[23], M. Leyton[43], B. Li[35b,o], H. Li[149], H.L. Li[33], L. Li[47], L. Li[35e], Q. Li[35a],
S. Li[47], X. Li[86], Y. Li[142], Z. Liang[35a], B. Liberti[134a], A. Liblong[159], P. Lichard[32], K. Lie[166], J. Liebal[23],
W. Liebig[15], A. Limosani[151], S.C. Lin[152,ac], T.H. Lin[85], B.E. Lindquist[149], A.E. Lionti[51], E. Lipeles[123],
A. Lipniacka[15], M. Lisovyi[60b], T.M. Liss[166], A. Lister[168], A.M. Litke[138], B. Liu[152,ad], D. Liu[152],
H. Liu[91], H. Liu[27], J. Liu[87], J.B. Liu[35b], K. Liu[87], L. Liu[166], M. Liu[47], M. Liu[35b], Y.L. Liu[35b], Y. Liu[35b],
M. Livan[122a,122b], A. Lleres[57], J. Llorente Merino[35a], S.L. Lloyd[78], F. Lo Sterzo[152], E. Lobodzinska[44],
P. Loch[7], W.S. Lockman[138], F.K. Loebinger[86], A.E. Loevschall-Jensen[38], K.M. Loew[25], A. Loginov[176],
T. Lohse[17], K. Lohwasser[44], M. Lokajicek[128], B.A. Long[24], J.D. Long[166], R.E. Long[74], L. Longo[75a,75b],
K.A. Looper[112], L. Lopes[127a], D. Lopez Mateos[59], B. Lopez Paredes[140], I. Lopez Paz[13],
A. Lopez Solis[82], J. Lorenz[101], N. Lorenzo Martinez[63], M. Losada[21], P.J. Lösel[101], X. Lou[35a],
A. Lounis[118], J. Love[6], P.A. Love[74], H. Lu[62a], N. Lu[91], H.J. Lubatti[139], C. Luci[133a,133b], A. Lucotte[57],
C. Luedtke[50], F. Luehring[63], W. Lukas[64], L. Luminari[133a], O. Lundberg[147a,147b], B. Lund-Jensen[148],
D. Lynn[27], R. Lysak[128], E. Lytken[83], V. Lyubushkin[67], H. Ma[27], L.L. Ma[35d], Y. Ma[35d], G. Maccarrone[49],
A. Macchiolo[102], C.M. Macdonald[140], B. Maček[77], J. Machado Miguens[123,127b], D. Madaffari[87],
R. Madar[36], H.J. Maddocks[165], W.F. Mader[46], A. Madsen[44], J. Maeda[69], S. Maeland[15], T. Maeno[27],
A. Maevskiy[100], E. Magradze[56], J. Mahlstedt[108], C. Maiani[118], C. Maidantchik[26a], A.A. Maier[102],
T. Maier[101], A. Maio[127a,127b,127d], S. Majewski[117], Y. Makida[68], N. Makovec[118], B. Malaescu[82],
Pa. Malecki[41], V.P. Maleev[124], F. Malek[57], U. Mallik[65], D. Malon[6], C. Malone[144], S. Maltezos[10],
S. Malyukov[32], J. Mamuzic[167], G. Mancini[49], B. Mandelli[32], L. Mandelli[93a], I. Mandić[77],
J. Maneira[127a,127b], L. Manhaes de Andrade Filho[26b], J. Manjarres Ramos[160b], A. Mann[101],
B. Mansoulie[137], J.D. Mansour[35a], R. Mantifel[89], M. Mantoani[56], S. Manzoni[93a,93b], L. Mapelli[32],
G. Marceca[29], L. March[51], G. Marchiori[82], M. Marcisovsky[128], M. Marjanovic[14], D.E. Marley[91],
F. Marroquim[26a], S.P. Marsden[86], Z. Marshall[16], S. Marti-Garcia[167], B. Martin[92], T.A. Martin[170],
V.J. Martin[48], B. Martin dit Latour[15], M. Martinez[13,r], S. Martin-Haugh[132], V.S. Martoiu[28b],
A.C. Martyniuk[80], M. Marx[139], A. Marzin[32], L. Masetti[85], T. Mashimo[156], R. Mashinistov[97], J. Masik[86],
A.L. Maslennikov[110,c], I. Massa[22a,22b], L. Massa[22a,22b], P. Mastrandrea[5], A. Mastroberardino[39a,39b],
T. Masubuchi[156], P. Mättig[175], J. Mattmann[85], J. Maurer[28b], S.J. Maxfield[76], D.A. Maximov[110,c],
R. Mazini[152], S.M. Mazza[93a,93b], N.C. Mc Fadden[106], G. Mc Goldrick[159], S.P. Mc Kee[91], A. McCarn[91],
R.L. McCarthy[149], T.G. McCarthy[31], L.I. McClymont[80], E.F. McDonald[90], K.W. McFarlane[58,*],
J.A. Mcfayden[80], G. Mchedlidze[56], S.J. McMahon[132], R.A. McPherson[169,l], M. Medinnis[44],
S. Meehan[139], S. Mehlhase[101], A. Mehta[76], K. Meier[60a], C. Meineck[101], B. Meirose[43], D. Melini[167],
B.R. Mellado Garcia[146c], M. Melo[145a], F. Meloni[18], A. Mengarelli[22a,22b], S. Menke[102], E. Meoni[162],
S. Mergelmeyer[17], P. Mermod[51], L. Merola[105a,105b], C. Meroni[93a], F.S. Merritt[33], A. Messina[133a,133b],
J. Metcalfe[6], A.S. Mete[163], C. Meyer[85], C. Meyer[123], J-P. Meyer[137], J. Meyer[108],
H. Meyer Zu Theenhausen[60a], F. Miano[150], R.P. Middleton[132], S. Miglioranzi[52a,52b], L. Mijović[23],
G. Mikenberg[172], M. Mikestikova[128], M. Mikuž[77], M. Milesi[90], A. Milic[64], D.W. Miller[33], C. Mills[48],
A. Milov[172], D.A. Milstead[147a,147b], A.A. Minaenko[131], Y. Minami[156], I.A. Minashvili[67], A.I. Mincer[111],
B. Mindur[40a], M. Mineev[67], Y. Ming[173], L.M. Mir[13], K.P. Mistry[123], T. Mitani[171], J. Mitrevski[101],
V.A. Mitsou[167], A. Miucci[51], P.S. Miyagawa[140], J.U. Mjörnmark[83], T. Moa[147a,147b], K. Mochizuki[96],
S. Mohapatra[37], S. Molander[147a,147b], R. Moles-Valls[23], R. Monden[70], M.C. Mondragon[92], K. Mönig[44],
J. Monk[38], E. Monnier[87], A. Montalbano[149], J. Montejo Berlingen[32], F. Monticelli[73], S. Monzani[93a,93b],
R.W. Moore[3], N. Morange[118], D. Moreno[21], M. Moreno Llácer[56], P. Morettini[52a], D. Mori[143],
T. Mori[156], M. Morii[59], M. Morinaga[156], V. Morisbak[120], S. Moritz[85], A.K. Morley[151], G. Mornacchi[32],

J.D. Morris[78], S.S. Mortensen[38], L. Morvaj[149], M. Mosidze[53b], J. Moss[144], K. Motohashi[158],
R. Mount[144], E. Mountricha[27], S.V. Mouraviev[97,*], E.J.W. Moyse[88], S. Muanza[87], R.D. Mudd[19],
F. Mueller[102], J. Mueller[126], R.S.P. Mueller[101], T. Mueller[30], D. Muenstermann[74], P. Mullen[55],
G.A. Mullier[18], F.J. Munoz Sanchez[86], J.A. Murillo Quijada[19], W.J. Murray[170,132], H. Musheghyan[56],
M. Muškinja[77], A.G. Myagkov[131,ae], M. Myska[129], B.P. Nachman[144], O. Nackenhorst[51], K. Nagai[121],
R. Nagai[68,z], K. Nagano[68], Y. Nagasaka[61], K. Nagata[161], M. Nagel[50], E. Nagy[87], A.M. Nairz[32],
Y. Nakahama[32], K. Nakamura[68], T. Nakamura[156], I. Nakano[113], H. Namasivayam[43],
R.F. Naranjo Garcia[44], R. Narayan[11], D.I. Narrias Villar[60a], I. Naryshkin[124], T. Naumann[44],
G. Navarro[21], R. Nayyar[7], H.A. Neal[91], P.Yu. Nechaeva[97], T.J. Neep[86], P.D. Nef[144], A. Negri[122a,122b],
M. Negrini[22a], S. Nektarijevic[107], C. Nellist[118], A. Nelson[163], S. Nemecek[128], P. Nemethy[111],
A.A. Nepomuceno[26a], M. Nessi[32,af], M.S. Neubauer[166], M. Neumann[175], R.M. Neves[111], P. Nevski[27],
P.R. Newman[19], D.H. Nguyen[6], T. Nguyen Manh[96], R.B. Nickerson[121], R. Nicolaidou[137], J. Nielsen[138],
A. Nikiforov[17], V. Nikolaenko[131,ae], I. Nikolic-Audit[82], K. Nikolopoulos[19], J.K. Nilsen[120], P. Nilsson[27],
Y. Ninomiya[156], A. Nisati[133a], R. Nisius[102], T. Nobe[156], L. Nodulman[6], M. Nomachi[119], I. Nomidis[31],
T. Nooney[78], S. Norberg[114], M. Nordberg[32], N. Norjoharuddeen[121], O. Novgorodova[46], S. Nowak[102],
M. Nozaki[68], L. Nozka[116], K. Ntekas[10], E. Nurse[80], F. Nuti[90], F. O'grady[7], D.C. O'Neil[143],
A.A. O'Rourke[44], V. O'Shea[55], F.G. Oakham[31,d], H. Oberlack[102], T. Obermann[23], J. Ocariz[82],
A. Ochi[69], I. Ochoa[37], J.P. Ochoa-Ricoux[34a], S. Oda[72], S. Odaka[68], H. Ogren[63], A. Oh[86], S.H. Oh[47],
C.C. Ohm[16], H. Ohman[165], H. Oide[32], H. Okawa[161], Y. Okumura[33], T. Okuyama[68], A. Olariu[28b],
L.F. Oleiro Seabra[127a], S.A. Olivares Pino[48], D. Oliveira Damazio[27], A. Olszewski[41], J. Olszowska[41],
A. Onofre[127a,127e], K. Onogi[104], P.U.E. Onyisi[11,v], M.J. Oreglia[33], Y. Oren[154], D. Orestano[135a,135b],
N. Orlando[62b], R.S. Orr[159], B. Osculati[52a,52b], R. Ospanov[86], G. Otero y Garzon[29], H. Otono[72],
M. Ouchrif[136d], F. Ould-Saada[120], A. Ouraou[137], K.P. Oussoren[108], Q. Ouyang[35a], M. Owen[55],
R.E. Owen[19], V.E. Ozcan[20a], N. Ozturk[8], K. Pachal[143], A. Pacheco Pages[13], C. Padilla Aranda[13],
M. Pagáčová[50], S. Pagan Griso[16], F. Paige[27], P. Pais[88], K. Pajchel[120], G. Palacino[160b], S. Palestini[32],
M. Palka[40b], D. Pallin[36], A. Palma[127a,127b], E.St. Panagiotopoulou[10], C.E. Pandini[82],
J.G. Panduro Vazquez[79], P. Pani[147a,147b], S. Panitkin[27], D. Pantea[28b], L. Paolozzi[51],
Th.D. Papadopoulou[10], K. Papageorgiou[155], A. Paramonov[6], D. Paredes Hernandez[176], A.J. Parker[74],
M.A. Parker[30], K.A. Parker[140], F. Parodi[52a,52b], J.A. Parsons[37], U. Parzefall[50], V.R. Pascuzzi[159],
E. Pasqualucci[133a], S. Passaggio[52a], F. Pastore[135a,135b,*], Fr. Pastore[79], G. Pásztor[31,ag], S. Pataraia[175],
J.R. Pater[86], T. Pauly[32], J. Pearce[169], B. Pearson[114], L.E. Pedersen[38], M. Pedersen[120],
S. Pedraza Lopez[167], R. Pedro[127a,127b], S.V. Peleganchuk[110,c], D. Pelikan[165], O. Penc[128], C. Peng[35a],
H. Peng[35b], J. Penwell[63], B.S. Peralva[26b], M.M. Perego[137], D.V. Perepelitsa[27], E. Perez Codina[160a],
L. Perini[93a,93b], H. Pernegger[32], S. Perrella[105a,105b], R. Peschke[44], V.D. Peshekhonov[67], K. Peters[44],
R.F.Y. Peters[86], B.A. Petersen[32], T.C. Petersen[38], E. Petit[57], A. Petridis[1], C. Petridou[155], P. Petroff[118],
E. Petrolo[133a], M. Petrov[121], F. Petrucci[135a,135b], N.E. Pettersson[88], A. Peyaud[137], R. Pezoa[34b],
P.W. Phillips[132], G. Piacquadio[144], E. Pianori[170], A. Picazio[88], E. Piccaro[78], M. Piccinini[22a,22b],
M.A. Pickering[121], R. Piegaia[29], J.E. Pilcher[33], A.D. Pilkington[86], A.W.J. Pin[86],
M. Pinamonti[164a,164c,ah], J.L. Pinfold[3], A. Pingel[38], S. Pires[82], H. Pirumov[44], M. Pitt[172], L. Plazak[145a],
M.-A. Pleier[27], V. Pleskot[85], E. Plotnikova[67], P. Plucinski[92], D. Pluth[66], R. Poettgen[147a,147b],
L. Poggioli[118], D. Pohl[23], G. Polesello[122a], A. Poley[44], A. Policicchio[39a,39b], R. Polifka[159], A. Polini[22a],
C.S. Pollard[55], V. Polychronakos[27], K. Pommès[32], L. Pontecorvo[133a], B.G. Pope[92], G.A. Popeneciu[28c],
D.S. Popovic[14], A. Poppleton[32], S. Pospisil[129], K. Potamianos[16], I.N. Potrap[67], C.J. Potter[30],
C.T. Potter[117], G. Poulard[32], J. Poveda[32], V. Pozdnyakov[67], M.E. Pozo Astigarraga[32], P. Pralavorio[87],
A. Pranko[16], S. Prell[66], D. Price[86], L.E. Price[6], M. Primavera[75a], S. Prince[89], M. Proissl[48],
K. Prokofiev[62c], F. Prokoshin[34b], S. Protopopescu[27], J. Proudfoot[6], M. Przybycien[40a], D. Puddu[135a,135b],
D. Puldon[149], M. Purohit[27,ai], P. Puzo[118], J. Qian[91], G. Qin[55], Y. Qin[86], A. Quadt[56],

78

W.B. Quayle[164a,164b], M. Queitsch-Maitland[86], D. Quilty[55], S. Raddum[120], V. Radeka[27], V. Radescu[60b],
S.K. Radhakrishnan[149], P. Radloff[117], P. Rados[90], F. Ragusa[93a,93b], G. Rahal[178], J.A. Raine[86],
S. Rajagopalan[27], M. Rammensee[32], C. Rangel-Smith[165], M.G. Ratti[93a,93b], F. Rauscher[101], S. Rave[85],
T. Ravenscroft[55], I. Ravinovich[172], M. Raymond[32], A.L. Read[120], N.P. Readioff[76], M. Reale[75a,75b],
D.M. Rebuzzi[122a,122b], A. Redelbach[174], G. Redlinger[27], R. Reece[138], K. Reeves[43], L. Rehnisch[17],
J. Reichert[123], H. Reisin[29], C. Rembser[32], H. Ren[35a], M. Rescigno[133a], S. Resconi[93a],
O.L. Rezanova[110,c], P. Reznicek[130], R. Rezvani[96], R. Richter[102], S. Richter[80], E. Richter-Was[40b],
O. Ricken[23], M. Ridel[82], P. Rieck[17], C.J. Riegel[175], J. Rieger[56], O. Rifki[114], M. Rijssenbeek[149],
A. Rimoldi[122a,122b], M. Rimoldi[18], L. Rinaldi[22a], B. Ristić[51], E. Ritsch[32], I. Riu[13], F. Rizatdinova[115],
E. Rizvi[78], C. Rizzi[13], S.H. Robertson[89,l], A. Robichaud-Veronneau[89], D. Robinson[30],
J.E.M. Robinson[44], A. Robson[55], C. Roda[125a,125b], Y. Rodina[87], A. Rodriguez Perez[13],
D. Rodriguez Rodriguez[167], S. Roe[32], C.S. Rogan[59], O. Røhne[120], A. Romaniouk[99], M. Romano[22a,22b],
S.M. Romano Saez[36], E. Romero Adam[167], N. Rompotis[139], M. Ronzani[50], L. Roos[82], E. Ros[167],
S. Rosati[133a], K. Rosbach[50], P. Rose[138], O. Rosenthal[142], N.-A. Rosien[56], V. Rossetti[147a,147b],
E. Rossi[105a,105b], L.P. Rossi[52a], J.H.N. Rosten[30], R. Rosten[139], M. Rotaru[28a], I. Roth[172], J. Rothberg[139],
D. Rousseau[118], C.R. Royon[137], A. Rozanov[87], Y. Rozen[153], X. Ruan[146c], F. Rubbo[144],
M.S. Rudolph[159], F. Rühr[50], A. Ruiz-Martinez[31], Z. Rurikova[50], N.A. Rusakovich[67], A. Ruschke[101],
H.L. Russell[139], J.P. Rutherfoord[7], N. Ruthmann[32], Y.F. Ryabov[124], M. Rybar[166], G. Rybkin[118], S. Ryu[6],
A. Ryzhov[131], G.F. Rzehorz[56], A.F. Saavedra[151], G. Sabato[108], S. Sacerdoti[29], H.F-W. Sadrozinski[138],
R. Sadykov[67], F. Safai Tehrani[133a], P. Saha[109], M. Sahinsoy[60a], M. Saimpert[137], T. Saito[156],
H. Sakamoto[156], Y. Sakurai[171], G. Salamanna[135a,135b], A. Salamon[134a,134b], J.E. Salazar Loyola[34b],
D. Salek[108], P.H. Sales De Bruin[139], D. Salihagic[102], A. Salnikov[144], J. Salt[167], D. Salvatore[39a,39b],
F. Salvatore[150], A. Salvucci[62a], A. Salzburger[32], D. Sammel[50], D. Sampsonidis[155], A. Sanchez[105a,105b],
J. Sánchez[167], V. Sanchez Martinez[167], H. Sandaker[120], R.L. Sandbach[78], H.G. Sander[85],
M. Sandhoff[175], C. Sandoval[21], R. Sandstroem[102], D.P.C. Sankey[132], M. Sannino[52a,52b], A. Sansoni[49],
C. Santoni[36], R. Santonico[134a,134b], H. Santos[127a], I. Santoyo Castillo[150], K. Sapp[126], A. Sapronov[67],
J.G. Saraiva[127a,127d], B. Sarrazin[23], O. Sasaki[68], Y. Sasaki[156], K. Sato[161], G. Sauvage[5,*], E. Sauvan[5],
G. Savage[79], P. Savard[159,d], C. Sawyer[132], L. Sawyer[81,q], J. Saxon[33], C. Sbarra[22a], A. Sbrizzi[22a,22b],
T. Scanlon[80], D.A. Scannicchio[163], M. Scarcella[151], V. Scarfone[39a,39b], J. Schaarschmidt[172],
P. Schacht[102], B.M. Schachtner[101], D. Schaefer[32], R. Schaefer[44], J. Schaeffer[85], S. Schaepe[23],
S. Schaetzel[60b], U. Schäfer[85], A.C. Schaffer[118], D. Schaile[101], R.D. Schamberger[149], V. Scharf[60a],
V.A. Schegelsky[124], D. Scheirich[130], M. Schernau[163], C. Schiavi[52a,52b], S. Schier[138], C. Schillo[50],
M. Schioppa[39a,39b], S. Schlenker[32], K. Schmieden[32], C. Schmitt[85], S. Schmitt[44], S. Schmitz[85],
B. Schneider[160a], U. Schnoor[50], L. Schoeffel[137], A. Schoening[60b], B.D. Schoenrock[92], E. Schopf[23],
M. Schott[85], J. Schovancova[8], S. Schramm[51], M. Schreyer[174], N. Schuh[85], M.J. Schultens[23],
H.-C. Schultz-Coulon[60a], H. Schulz[17], M. Schumacher[50], B.A. Schumm[138], Ph. Schune[137],
A. Schwartzman[144], T.A. Schwarz[91], Ph. Schwegler[102], H. Schweiger[86], Ph. Schwemling[137],
R. Schwienhorst[92], J. Schwindling[137], T. Schwindt[23], G. Sciolla[25], F. Scuri[125a,125b], F. Scutti[90],
J. Searcy[91], P. Seema[23], S.C. Seidel[106], A. Seiden[138], F. Seifert[129], J.M. Seixas[26a], G. Sekhniaidze[105a],
K. Sekhon[91], S.J. Sekula[42], D.M. Seliverstov[124,*], N. Semprini-Cesari[22a,22b], C. Serfon[120], L. Serin[118],
L. Serkin[164a,164b], M. Sessa[135a,135b], R. Seuster[169], H. Severini[114], T. Sfiligoj[77], F. Sforza[32], A. Sfyrla[51],
E. Shabalina[56], N.W. Shaikh[147a,147b], L.Y. Shan[35a], R. Shang[166], J.T. Shank[24], M. Shapiro[16],
P.B. Shatalov[98], K. Shaw[164a,164b], S.M. Shaw[86], A. Shcherbakova[147a,147b], C.Y. Shehu[150], P. Sherwood[80],
L. Shi[152,aj], S. Shimizu[69], C.O. Shimmin[163], M. Shimojima[103], M. Shiyakova[67,ak], A. Shmeleva[97],
D. Shoaleh Saadi[96], M.J. Shochet[33], S. Shojaii[93a,93b], S. Shrestha[112], E. Shulga[99], M.A. Shupe[7],
P. Sicho[128], P.E. Sidebo[148], O. Sidiropoulou[174], D. Sidorov[115], A. Sidoti[22a,22b], F. Siegert[46], Dj. Sijacki[14],
J. Silva[127a,127d], S.B. Silverstein[147a], V. Simak[129], O. Simard[5], Lj. Simic[14], S. Simion[118], E. Simioni[85],

B. Simmons[80], D. Simon[36], M. Simon[85], P. Sinervo[159], N.B. Sinev[117], M. Sioli[22a,22b], G. Siragusa[174], S.Yu. Sivoklokov[100], J. Sjölin[147a,147b], T.B. Sjursen[15], M.B. Skinner[74], H.P. Skottowe[59], P. Skubic[114], M. Slater[19], T. Slavicek[129], M. Slawinska[108], K. Sliwa[162], R. Slovak[130], V. Smakhtin[172], B.H. Smart[5], L. Smestad[15], J. Smiesko[145a], S.Yu. Smirnov[99], Y. Smirnov[99], L.N. Smirnova[100,al], O. Smirnova[83], M.N.K. Smith[37], R.W. Smith[37], M. Smizanska[74], K. Smolek[129], A.A. Snesarev[97], S. Snyder[27], R. Sobie[169,l], F. Socher[46], A. Soffer[154], D.A. Soh[152], G. Sokhrannyi[77], C.A. Solans Sanchez[32], M. Solar[129], E.Yu. Soldatov[99], U. Soldevila[167], A.A. Solodkov[131], A. Soloshenko[67], O.V. Solovyanov[131], V. Solovyev[124], P. Sommer[50], H. Son[162], H.Y. Song[35b,am], A. Sood[16], A. Sopczak[129], V. Sopko[129], V. Sorin[13], D. Sosa[60b], C.L. Sotiropoulou[125a,125b], R. Soualah[164a,164c], A.M. Soukharev[110,c], D. South[44], B.C. Sowden[79], S. Spagnolo[75a,75b], M. Spalla[125a,125b], M. Spangenberg[170], F. Spanò[79], D. Sperlich[17], F. Spettel[102], R. Spighi[22a], G. Spigo[32], L.A. Spiller[90], M. Spousta[130], R.D. St. Denis[55,*], A. Stabile[93a], R. Stamen[60a], S. Stamm[17], E. Stanecka[41], R.W. Stanek[6], C. Stanescu[135a], M. Stanescu-Bellu[44], M.M. Stanitzki[44], S. Stapnes[120], E.A. Starchenko[131], G.H. Stark[33], J. Stark[57], P. Staroba[128], P. Starovoitov[60a], S. Stärz[32], R. Staszewski[41], P. Steinberg[27], B. Stelzer[143], H.J. Stelzer[32], O. Stelzer-Chilton[160a], H. Stenzel[54], G.A. Stewart[55], J.A. Stillings[23], M.C. Stockton[89], M. Stoebe[89], G. Stoicea[28b], P. Stolte[56], S. Stonjek[102], A.R. Stradling[8], A. Straessner[46], M.E. Stramaglia[18], J. Strandberg[148], S. Strandberg[147a,147b], A. Strandlie[120], M. Strauss[114], P. Strizenec[145b], R. Ströhmer[174], D.M. Strom[117], R. Stroynowski[42], A. Strubig[107], S.A. Stucci[18], B. Stugu[15], N.A. Styles[44], D. Su[144], J. Su[126], R. Subramaniam[81], S. Suchek[60a], Y. Sugaya[119], M. Suk[129], V.V. Sulin[97], S. Sultansoy[4c], T. Sumida[70], S. Sun[59], X. Sun[35a], J.E. Sundermann[50], K. Suruliz[150], G. Susinno[39a,39b], M.R. Sutton[150], S. Suzuki[68], M. Svatos[128], M. Swiatlowski[33], I. Sykora[145a], T. Sykora[130], D. Ta[50], C. Taccini[135a,135b], K. Tackmann[44], J. Taenzer[159], A. Taffard[163], R. Tafirout[160a], N. Taiblum[154], H. Takai[27], R. Takashima[71], T. Takeshita[141], Y. Takubo[68], M. Talby[87], A.A. Talyshev[110,c], K.G. Tan[90], J. Tanaka[156], R. Tanaka[118], S. Tanaka[68], B.B. Tannenwald[112], S. Tapia Araya[34b], S. Tapprogge[85], S. Tarem[153], G.F. Tartarelli[93a], P. Tas[130], M. Tasevsky[128], T. Tashiro[70], E. Tassi[39a,39b], A. Tavares Delgado[127a,127b], Y. Tayalati[136d], A.C. Taylor[106], G.N. Taylor[90], P.T.E. Taylor[90], W. Taylor[160b], F.A. Teischinger[32], P. Teixeira-Dias[79], K.K. Temming[50], D. Temple[143], H. Ten Kate[32], P.K. Teng[152], J.J. Teoh[119], F. Tepel[175], S. Terada[68], K. Terashi[156], J. Terron[84], S. Terzo[102], M. Testa[49], R.J. Teuscher[159,l], T. Theveneaux-Pelzer[87], J.P. Thomas[19], J. Thomas-Wilsker[79], E.N. Thompson[37], P.D. Thompson[19], A.S. Thompson[55], L.A. Thomsen[176], E. Thomson[123], M. Thomson[30], M.J. Tibbetts[16], R.E. Ticse Torres[87], V.O. Tikhomirov[97,an], Yu.A. Tikhonov[110,c], S. Timoshenko[99], P. Tipton[176], S. Tisserant[87], K. Todome[158], T. Todorov[5,*], S. Todorova-Nova[130], J. Tojo[72], S. Tokár[145a], K. Tokushuku[68], E. Tolley[59], L. Tomlinson[86], M. Tomoto[104], L. Tompkins[144,ao], K. Toms[106], B. Tong[59], E. Torrence[117], H. Torres[143], E. Torró Pastor[139], J. Toth[87,ap], F. Touchard[87], D.R. Tovey[140], T. Trefzger[174], A. Tricoli[27], I.M. Trigger[160a], S. Trincaz-Duvoid[82], M.F. Tripiana[13], W. Trischuk[159], B. Trocmé[57], A. Trofymov[44], C. Troncon[93a], M. Trottier-McDonald[16], M. Trovatelli[169], L. Truong[164a,164c], M. Trzebinski[41], A. Trzupek[41], J.C-L. Tseng[121], P.V. Tsiareshka[94], G. Tsipolitis[10], N. Tsirintanis[9], S. Tsiskaridze[13], V. Tsiskaridze[50], E.G. Tskhadadze[53a], K.M. Tsui[62a], I.I. Tsukerman[98], V. Tsulaia[16], S. Tsuno[68], D. Tsybychev[149], A. Tudorache[28b], V. Tudorache[28b], A.N. Tuna[59], S.A. Tupputi[22a,22b], S. Turchikhin[100,al], D. Turecek[129], D. Turgeman[172], R. Turra[93a,93b], A.J. Turvey[42], P.M. Tuts[37], M. Tyndel[132], G. Ucchielli[22a,22b], I. Ueda[156], R. Ueno[31], M. Ughetto[147a,147b], F. Ukegawa[161], G. Unal[32], A. Undrus[27], G. Unel[163], F.C. Ungaro[90], Y. Unno[68], C. Unverdorben[101], J. Urban[145b], P. Urquijo[90], P. Urrejola[85], G. Usai[8], A. Usanova[64], L. Vacavant[87], V. Vacek[129], B. Vachon[89], C. Valderanis[101], E. Valdes Santurio[147a,147b], N. Valencic[108], S. Valentinetti[22a,22b], A. Valero[167], L. Valery[13], S. Valkar[130], S. Vallecorsa[51], J.A. Valls Ferrer[167], W. Van Den Wollenberg[108], P.C. Van Der Deijl[108], R. van der Geer[108], H. van der Graaf[108], N. van Eldik[153], P. van Gemmeren[6], J. Van Nieuwkoop[143], I. van Vulpen[108], M.C. van Woerden[32], M. Vanadia[133a,133b], W. Vandelli[32],

R. Vanguri[123], A. Vaniachine[6], P. Vankov[108], G. Vardanyan[177], R. Vari[133a], E.W. Varnes[7], T. Varol[42], D. Varouchas[82], A. Vartapetian[8], K.E. Varvell[151], J.G. Vasquez[176], F. Vazeille[36], T. Vazquez Schroeder[89], J. Veatch[56], L.M. Veloce[159], F. Veloso[127a,127c], S. Veneziano[133a], A. Ventura[75a,75b], M. Venturi[169], N. Venturi[159], A. Venturini[25], V. Vercesi[122a], M. Verducci[133a,133b], W. Verkerke[108], J.C. Vermeulen[108], A. Vest[46,aq], M.C. Vetterli[143,d], O. Viazlo[83], I. Vichou[166], T. Vickey[140], O.E. Vickey Boeriu[140], G.H.A. Viehhauser[121], S. Viel[16], L. Vigani[121], R. Vigne[64], M. Villa[22a,22b], M. Villaplana Perez[93a,93b], E. Vilucchi[49], M.G. Vincter[31], V.B. Vinogradov[67], C. Vittori[22a,22b], I. Vivarelli[150], S. Vlachos[10], M. Vlasak[129], M. Vogel[175], P. Vokac[129], G. Volpi[125a,125b], M. Volpi[90], H. von der Schmitt[102], E. von Toerne[23], V. Vorobel[130], K. Vorobev[99], M. Vos[167], R. Voss[32], J.H. Vossebeld[76], N. Vranjes[14], M. Vranjes Milosavljevic[14], V. Vrba[128], M. Vreeswijk[108], R. Vuillermet[32], I. Vukotic[33], Z. Vykydal[129], P. Wagner[23], W. Wagner[175], H. Wahlberg[73], S. Wahrmund[46], J. Wakabayashi[104], J. Walder[74], R. Walker[101], W. Walkowiak[142], V. Wallangen[147a,147b], C. Wang[35c], C. Wang[35d,87], F. Wang[173], H. Wang[16], H. Wang[42], J. Wang[44], J. Wang[151], K. Wang[89], R. Wang[6], S.M. Wang[152], T. Wang[23], T. Wang[37], X. Wang[176], C. Wanotayaroj[117], A. Warburton[89], C.P. Ward[30], D.R. Wardrope[80], A. Washbrook[48], P.M. Watkins[19], A.T. Watson[19], M.F. Watson[19], G. Watts[139], S. Watts[86], B.M. Waugh[80], S. Webb[85], M.S. Weber[18], S.W. Weber[174], J.S. Webster[6], A.R. Weidberg[121], B. Weinert[63], J. Weingarten[56], C. Weiser[50], H. Weits[108], P.S. Wells[32], T. Wenaus[27], T. Wengler[32], S. Wenig[32], N. Wermes[23], M. Werner[50], P. Werner[32], M. Wessels[60a], J. Wetter[162], K. Whalen[117], N.L. Whallon[139], A.M. Wharton[74], A. White[8], M.J. White[1], R. White[34b], D. Whiteson[163], F.J. Wickens[132], W. Wiedenmann[173], M. Wielers[132], P. Wienemann[23], C. Wiglesworth[38], L.A.M. Wiik-Fuchs[23], A. Wildauer[102], F. Wilk[86], H.G. Wilkens[32], H.H. Williams[123], S. Williams[108], C. Willis[92], S. Willocq[88], J.A. Wilson[19], I. Wingerter-Seez[5], F. Winklmeier[117], O.J. Winston[150], B.T. Winter[23], M. Wittgen[144], J. Wittkowski[101], S.J. Wollstadt[85], M.W. Wolter[41], H. Wolters[127a,127c], B.K. Wosiek[41], J. Wotschack[32], M.J. Woudstra[86], K.W. Wozniak[41], M. Wu[57], M. Wu[33], S.L. Wu[173], X. Wu[51], Y. Wu[91], T.R. Wyatt[86], B.M. Wynne[48], S. Xella[38], D. Xu[35a], L. Xu[27], B. Yabsley[151], S. Yacoob[146a], R. Yakabe[69], D. Yamaguchi[158], Y. Yamaguchi[119], A. Yamamoto[68], S. Yamamoto[156], T. Yamanaka[156], K. Yamauchi[104], Y. Yamazaki[69], Z. Yan[24], H. Yang[35e], H. Yang[173], Y. Yang[152], Z. Yang[15], W-M. Yao[16], Y.C. Yap[82], Y. Yasu[68], E. Yatsenko[5], K.H. Yau Wong[23], J. Ye[42], S. Ye[27], I. Yeletskikh[67], A.L. Yen[59], E. Yildirim[85], K. Yorita[171], R. Yoshida[6], K. Yoshihara[123], C. Young[144], C.J.S. Young[32], S. Youssef[24], D.R. Yu[16], J. Yu[8], J.M. Yu[91], J. Yu[66], L. Yuan[69], S.P.Y. Yuen[23], I. Yusuff[30,ar], B. Zabinski[41], R. Zaidan[35d], A.M. Zaitsev[131,ae], N. Zakharchuk[44], J. Zalieckas[15], A. Zaman[149], S. Zambito[59], L. Zanello[133a,133b], D. Zanzi[90], C. Zeitnitz[175], M. Zeman[129], A. Zemla[40a], J.C. Zeng[166], Q. Zeng[144], K. Zengel[25], O. Zenin[131], T. Ženiš[145a], D. Zerwas[118], D. Zhang[91], F. Zhang[173], G. Zhang[35b,am], H. Zhang[35c], J. Zhang[6], L. Zhang[50], R. Zhang[23], R. Zhang[35b,as], X. Zhang[35d], Z. Zhang[118], X. Zhao[42], Y. Zhao[35d], Z. Zhao[35b], A. Zhemchugov[67], J. Zhong[121], B. Zhou[91], C. Zhou[47], L. Zhou[37], L. Zhou[42], M. Zhou[149], N. Zhou[35f], C.G. Zhu[35d], H. Zhu[35a], J. Zhu[91], Y. Zhu[35b], X. Zhuang[35a], K. Zhukov[97], A. Zibell[174], D. Zieminska[63], N.I. Zimine[67], C. Zimmermann[85], S. Zimmermann[50], Z. Zinonos[56], M. Zinser[85], M. Ziolkowski[142], L. Živković[14], G. Zobernig[173], A. Zoccoli[22a,22b], M. zur Nedden[17], G. Zurzolo[105a,105b], L. Zwalinski[32].

[1] Department of Physics, University of Adelaide, Adelaide, Australia

[2] Physics Department, SUNY Albany, Albany NY, United States of America

[3] Department of Physics, University of Alberta, Edmonton AB, Canada

[4] [a] Department of Physics, Ankara University, Ankara; [b] Istanbul Aydin University, Istanbul; [c] Division of Physics, TOBB University of Economics and Technology, Ankara, Turkey

[5] LAPP, CNRS/IN2P3 and Université Savoie Mont Blanc, Annecy-le-Vieux, France

[6] High Energy Physics Division, Argonne National Laboratory, Argonne IL, United States of America

[7] Department of Physics, University of Arizona, Tucson AZ, United States of America

[8] Department of Physics, The University of Texas at Arlington, Arlington TX, United States of America

[9] Physics Department, University of Athens, Athens, Greece

[10] Physics Department, National Technical University of Athens, Zografou, Greece

[11] Department of Physics, The University of Texas at Austin, Austin TX, United States of America

[12] Institute of Physics, Azerbaijan Academy of Sciences, Baku, Azerbaijan

[13] Institut de Física d'Altes Energies (IFAE), The Barcelona Institute of Science and Technology, Barcelona, Spain, Spain

[14] Institute of Physics, University of Belgrade, Belgrade, Serbia

[15] Department for Physics and Technology, University of Bergen, Bergen, Norway

[16] Physics Division, Lawrence Berkeley National Laboratory and University of California, Berkeley CA, United States of America

[17] Department of Physics, Humboldt University, Berlin, Germany

[18] Albert Einstein Center for Fundamental Physics and Laboratory for High Energy Physics, University of Bern, Bern, Switzerland

[19] School of Physics and Astronomy, University of Birmingham, Birmingham, United Kingdom

[20] [a] Department of Physics, Bogazici University, Istanbul; [b] Department of Physics Engineering, Gaziantep University, Gaziantep; [d] Istanbul Bilgi University, Faculty of Engineering and Natural Sciences, Istanbul,Turkey; [e] Bahcesehir University, Faculty of Engineering and Natural Sciences, Istanbul, Turkey, Turkey

[21] Centro de Investigaciones, Universidad Antonio Narino, Bogota, Colombia

[22] [a] INFN Sezione di Bologna; [b] Dipartimento di Fisica e Astronomia, Università di Bologna, Bologna, Italy

[23] Physikalisches Institut, University of Bonn, Bonn, Germany

[24] Department of Physics, Boston University, Boston MA, United States of America

[25] Department of Physics, Brandeis University, Waltham MA, United States of America

[26] [a] Universidade Federal do Rio De Janeiro COPPE/EE/IF, Rio de Janeiro; [b] Electrical Circuits Department, Federal University of Juiz de Fora (UFJF), Juiz de Fora; [c] Federal University of Sao Joao del Rei (UFSJ), Sao Joao del Rei; [d] Instituto de Fisica, Universidade de Sao Paulo, Sao Paulo, Brazil

[27] Physics Department, Brookhaven National Laboratory, Upton NY, United States of America

[28] [a] Transilvania University of Brasov, Brasov, Romania; [b] National Institute of Physics and Nuclear Engineering, Bucharest; [c] National Institute for Research and Development of Isotopic and Molecular Technologies, Physics Department, Cluj Napoca; [d] University Politehnica Bucharest, Bucharest; [e] West University in Timisoara, Timisoara, Romania

[29] Departamento de Física, Universidad de Buenos Aires, Buenos Aires, Argentina

[30] Cavendish Laboratory, University of Cambridge, Cambridge, United Kingdom

[31] Department of Physics, Carleton University, Ottawa ON, Canada

[32] CERN, Geneva, Switzerland

[33] Enrico Fermi Institute, University of Chicago, Chicago IL, United States of America

[34] [a] Departamento de Física, Pontificia Universidad Católica de Chile, Santiago; [b] Departamento de Física, Universidad Técnica Federico Santa María, Valparaíso, Chile

[35] [a] Institute of High Energy Physics, Chinese Academy of Sciences, Beijing; [b] Department of Modern Physics, University of Science and Technology of China, Anhui; [c] Department of Physics, Nanjing University, Jiangsu; [d] School of Physics, Shandong University, Shandong; [e] Department of Physics and Astronomy, Shanghai Key Laboratory for Particle Physics and Cosmology, Shanghai Jiao Tong University, Shanghai; (also affiliated with PKU-CHEP); [f] Physics Department, Tsinghua University, Beijing 100084, China

[36] Laboratoire de Physique Corpusculaire, Clermont Université and Université Blaise Pascal and CNRS/IN2P3, Clermont-Ferrand, France

[37] Nevis Laboratory, Columbia University, Irvington NY, United States of America

[38] Niels Bohr Institute, University of Copenhagen, Kobenhavn, Denmark

[39] [a] INFN Gruppo Collegato di Cosenza, Laboratori Nazionali di Frascati; [b] Dipartimento di Fisica, Università della Calabria, Rende, Italy

[40] [a] AGH University of Science and Technology, Faculty of Physics and Applied Computer Science, Krakow; [b] Marian Smoluchowski Institute of Physics, Jagiellonian University, Krakow, Poland

[41] Institute of Nuclear Physics Polish Academy of Sciences, Krakow, Poland

[42] Physics Department, Southern Methodist University, Dallas TX, United States of America

[43] Physics Department, University of Texas at Dallas, Richardson TX, United States of America

[44] DESY, Hamburg and Zeuthen, Germany

[45] Institut für Experimentelle Physik IV, Technische Universität Dortmund, Dortmund, Germany

[46] Institut für Kern- und Teilchenphysik, Technische Universität Dresden, Dresden, Germany

[47] Department of Physics, Duke University, Durham NC, United States of America

[48] SUPA - School of Physics and Astronomy, University of Edinburgh, Edinburgh, United Kingdom

[49] INFN Laboratori Nazionali di Frascati, Frascati, Italy

[50] Fakultät für Mathematik und Physik, Albert-Ludwigs-Universität, Freiburg, Germany

[51] Section de Physique, Université de Genève, Geneva, Switzerland

[52] [a] INFN Sezione di Genova; [b] Dipartimento di Fisica, Università di Genova, Genova, Italy

[53] [a] E. Andronikashvili Institute of Physics, Iv. Javakhishvili Tbilisi State University, Tbilisi; [b] High Energy Physics Institute, Tbilisi State University, Tbilisi, Georgia

[54] II Physikalisches Institut, Justus-Liebig-Universität Giessen, Giessen, Germany

[55] SUPA - School of Physics and Astronomy, University of Glasgow, Glasgow, United Kingdom

[56] II Physikalisches Institut, Georg-August-Universität, Göttingen, Germany

[57] Laboratoire de Physique Subatomique et de Cosmologie, Université Grenoble-Alpes, CNRS/IN2P3, Grenoble, France

[58] Department of Physics, Hampton University, Hampton VA, United States of America

[59] Laboratory for Particle Physics and Cosmology, Harvard University, Cambridge MA, United States of America

[60] [a] Kirchhoff-Institut für Physik, Ruprecht-Karls-Universität Heidelberg, Heidelberg; [b] Physikalisches Institut, Ruprecht-Karls-Universität Heidelberg, Heidelberg; [c] ZITI Institut für technische Informatik, Ruprecht-Karls-Universität Heidelberg, Mannheim, Germany

[61] Faculty of Applied Information Science, Hiroshima Institute of Technology, Hiroshima, Japan

[62] [a] Department of Physics, The Chinese University of Hong Kong, Shatin, N.T., Hong Kong; [b] Department of Physics, The University of Hong Kong, Hong Kong; [c] Department of Physics, The Hong Kong University of Science and Technology, Clear Water Bay, Kowloon, Hong Kong, China

[63] Department of Physics, Indiana University, Bloomington IN, United States of America

[64] Institut für Astro- und Teilchenphysik, Leopold-Franzens-Universität, Innsbruck, Austria

[65] University of Iowa, Iowa City IA, United States of America

[66] Department of Physics and Astronomy, Iowa State University, Ames IA, United States of America

[67] Joint Institute for Nuclear Research, JINR Dubna, Dubna, Russia

[68] KEK, High Energy Accelerator Research Organization, Tsukuba, Japan

[69] Graduate School of Science, Kobe University, Kobe, Japan

[70] Faculty of Science, Kyoto University, Kyoto, Japan

[71] Kyoto University of Education, Kyoto, Japan

[72] Department of Physics, Kyushu University, Fukuoka, Japan

[73] Instituto de Física La Plata, Universidad Nacional de La Plata and CONICET, La Plata, Argentina

[74] Physics Department, Lancaster University, Lancaster, United Kingdom

[75] (a) INFN Sezione di Lecce; (b) Dipartimento di Matematica e Fisica, Università del Salento, Lecce, Italy

[76] Oliver Lodge Laboratory, University of Liverpool, Liverpool, United Kingdom

[77] Department of Physics, Jožef Stefan Institute and University of Ljubljana, Ljubljana, Slovenia

[78] School of Physics and Astronomy, Queen Mary University of London, London, United Kingdom

[79] Department of Physics, Royal Holloway University of London, Surrey, United Kingdom

[80] Department of Physics and Astronomy, University College London, London, United Kingdom

[81] Louisiana Tech University, Ruston LA, United States of America

[82] Laboratoire de Physique Nucléaire et de Hautes Energies, UPMC and Université Paris-Diderot and CNRS/IN2P3, Paris, France

[83] Fysiska institutionen, Lunds universitet, Lund, Sweden

[84] Departamento de Fisica Teorica C-15, Universidad Autonoma de Madrid, Madrid, Spain

[85] Institut für Physik, Universität Mainz, Mainz, Germany

[86] School of Physics and Astronomy, University of Manchester, Manchester, United Kingdom

[87] CPPM, Aix-Marseille Université and CNRS/IN2P3, Marseille, France

[88] Department of Physics, University of Massachusetts, Amherst MA, United States of America

[89] Department of Physics, McGill University, Montreal QC, Canada

[90] School of Physics, University of Melbourne, Victoria, Australia

[91] Department of Physics, The University of Michigan, Ann Arbor MI, United States of America

[92] Department of Physics and Astronomy, Michigan State University, East Lansing MI, United States of America

[93] (a) INFN Sezione di Milano; (b) Dipartimento di Fisica, Università di Milano, Milano, Italy

[94] B.I. Stepanov Institute of Physics, National Academy of Sciences of Belarus, Minsk, Republic of Belarus

[95] National Scientific and Educational Centre for Particle and High Energy Physics, Minsk, Republic of Belarus

[96] Group of Particle Physics, University of Montreal, Montreal QC, Canada

[97] P.N. Lebedev Physical Institute of the Russian Academy of Sciences, Moscow, Russia

[98] Institute for Theoretical and Experimental Physics (ITEP), Moscow, Russia

[99] National Research Nuclear University MEPhI, Moscow, Russia

[100] D.V. Skobeltsyn Institute of Nuclear Physics, M.V. Lomonosov Moscow State University, Moscow, Russia

[101] Fakultät für Physik, Ludwig-Maximilians-Universität München, München, Germany

[102] Max-Planck-Institut für Physik (Werner-Heisenberg-Institut), München, Germany

[103] Nagasaki Institute of Applied Science, Nagasaki, Japan

[104] Graduate School of Science and Kobayashi-Maskawa Institute, Nagoya University, Nagoya, Japan

[105] (a) INFN Sezione di Napoli; (b) Dipartimento di Fisica, Università di Napoli, Napoli, Italy

[106] Department of Physics and Astronomy, University of New Mexico, Albuquerque NM, United States of America

[107] Institute for Mathematics, Astrophysics and Particle Physics, Radboud University Nijmegen/Nikhef, Nijmegen, Netherlands

[108] Nikhef National Institute for Subatomic Physics and University of Amsterdam, Amsterdam, Netherlands

[109] Department of Physics, Northern Illinois University, DeKalb IL, United States of America

[110] Budker Institute of Nuclear Physics, SB RAS, Novosibirsk, Russia

[111] Department of Physics, New York University, New York NY, United States of America

[112] Ohio State University, Columbus OH, United States of America

[113] Faculty of Science, Okayama University, Okayama, Japan

[114] Homer L. Dodge Department of Physics and Astronomy, University of Oklahoma, Norman OK, United States of America

[115] Department of Physics, Oklahoma State University, Stillwater OK, United States of America

[116] Palacký University, RCPTM, Olomouc, Czech Republic

[117] Center for High Energy Physics, University of Oregon, Eugene OR, United States of America

[118] LAL, Univ. Paris-Sud, CNRS/IN2P3, Université Paris-Saclay, Orsay, France

[119] Graduate School of Science, Osaka University, Osaka, Japan

[120] Department of Physics, University of Oslo, Oslo, Norway

[121] Department of Physics, Oxford University, Oxford, United Kingdom

[122] [a] INFN Sezione di Pavia; [b] Dipartimento di Fisica, Università di Pavia, Pavia, Italy

[123] Department of Physics, University of Pennsylvania, Philadelphia PA, United States of America

[124] National Research Centre "Kurchatov Institute" B.P.Konstantinov Petersburg Nuclear Physics Institute, St. Petersburg, Russia

[125] [a] INFN Sezione di Pisa; [b] Dipartimento di Fisica E. Fermi, Università di Pisa, Pisa, Italy

[126] Department of Physics and Astronomy, University of Pittsburgh, Pittsburgh PA, United States of America

[127] [a] Laboratório de Instrumentação e Física Experimental de Partículas - LIP, Lisboa; [b] Faculdade de Ciências, Universidade de Lisboa, Lisboa; [c] Department of Physics, University of Coimbra, Coimbra; [d] Centro de Física Nuclear da Universidade de Lisboa, Lisboa; [e] Departamento de Fisica, Universidade do Minho, Braga; [f] Departamento de Fisica Teorica y del Cosmos and CAFPE, Universidad de Granada, Granada (Spain); [g] Dep Fisica and CEFITEC of Faculdade de Ciencias e Tecnologia, Universidade Nova de Lisboa, Caparica, Portugal

[128] Institute of Physics, Academy of Sciences of the Czech Republic, Praha, Czech Republic

[129] Czech Technical University in Prague, Praha, Czech Republic

[130] Faculty of Mathematics and Physics, Charles University in Prague, Praha, Czech Republic

[131] State Research Center Institute for High Energy Physics (Protvino), NRC KI, Russia

[132] Particle Physics Department, Rutherford Appleton Laboratory, Didcot, United Kingdom

[133] [a] INFN Sezione di Roma; [b] Dipartimento di Fisica, Sapienza Università di Roma, Roma, Italy

[134] [a] INFN Sezione di Roma Tor Vergata; [b] Dipartimento di Fisica, Università di Roma Tor Vergata, Roma, Italy

[135] [a] INFN Sezione di Roma Tre; [b] Dipartimento di Matematica e Fisica, Università Roma Tre, Roma, Italy

[136] [a] Faculté des Sciences Ain Chock, Réseau Universitaire de Physique des Hautes Energies - Université Hassan II, Casablanca; [b] Centre National de l'Energie des Sciences Techniques Nucleaires, Rabat; [c] Faculté des Sciences Semlalia, Université Cadi Ayyad, LPHEA-Marrakech; [d] Faculté des Sciences, Université Mohamed Premier and LPTPM, Oujda; [e] Faculté des sciences, Université Mohammed V, Rabat, Morocco

[137] DSM/IRFU (Institut de Recherches sur les Lois Fondamentales de l'Univers), CEA Saclay (Commissariat à l'Energie Atomique et aux Energies Alternatives), Gif-sur-Yvette, France

[138] Santa Cruz Institute for Particle Physics, University of California Santa Cruz, Santa Cruz CA, United States of America

[139] Department of Physics, University of Washington, Seattle WA, United States of America

[140] Department of Physics and Astronomy, University of Sheffield, Sheffield, United Kingdom

[141] Department of Physics, Shinshu University, Nagano, Japan

[142] Fachbereich Physik, Universität Siegen, Siegen, Germany

[143] Department of Physics, Simon Fraser University, Burnaby BC, Canada

[144] SLAC National Accelerator Laboratory, Stanford CA, United States of America

[145] [a] Faculty of Mathematics, Physics & Informatics, Comenius University, Bratislava; [b] Department of Subnuclear Physics, Institute of Experimental Physics of the Slovak Academy of Sciences, Kosice, Slovak Republic

[146] [a] Department of Physics, University of Cape Town, Cape Town; [b] Department of Physics, University of Johannesburg, Johannesburg; [c] School of Physics, University of the Witwatersrand, Johannesburg, South Africa

[147] [a] Department of Physics, Stockholm University; [b] The Oskar Klein Centre, Stockholm, Sweden

[148] Physics Department, Royal Institute of Technology, Stockholm, Sweden

[149] Departments of Physics & Astronomy and Chemistry, Stony Brook University, Stony Brook NY, United States of America

[150] Department of Physics and Astronomy, University of Sussex, Brighton, United Kingdom

[151] School of Physics, University of Sydney, Sydney, Australia

[152] Institute of Physics, Academia Sinica, Taipei, Taiwan

[153] Department of Physics, Technion: Israel Institute of Technology, Haifa, Israel

[154] Raymond and Beverly Sackler School of Physics and Astronomy, Tel Aviv University, Tel Aviv, Israel

[155] Department of Physics, Aristotle University of Thessaloniki, Thessaloniki, Greece

[156] International Center for Elementary Particle Physics and Department of Physics, The University of Tokyo, Tokyo, Japan

[157] Graduate School of Science and Technology, Tokyo Metropolitan University, Tokyo, Japan

[158] Department of Physics, Tokyo Institute of Technology, Tokyo, Japan

[159] Department of Physics, University of Toronto, Toronto ON, Canada

[160] [a] TRIUMF, Vancouver BC; [b] Department of Physics and Astronomy, York University, Toronto ON, Canada

[161] Faculty of Pure and Applied Sciences, and Center for Integrated Research in Fundamental Science and Engineering, University of Tsukuba, Tsukuba, Japan

[162] Department of Physics and Astronomy, Tufts University, Medford MA, United States of America

[163] Department of Physics and Astronomy, University of California Irvine, Irvine CA, United States of America

[164] [a] INFN Gruppo Collegato di Udine, Sezione di Trieste, Udine; [b] ICTP, Trieste; [c] Dipartimento di Chimica, Fisica e Ambiente, Università di Udine, Udine, Italy

[165] Department of Physics and Astronomy, University of Uppsala, Uppsala, Sweden

[166] Department of Physics, University of Illinois, Urbana IL, United States of America

[167] Instituto de Fisica Corpuscular (IFIC) and Departamento de Fisica Atomica, Molecular y Nuclear and Departamento de Ingeniería Electrónica and Instituto de Microelectrónica de Barcelona (IMB-CNM), University of Valencia and CSIC, Valencia, Spain

[168] Department of Physics, University of British Columbia, Vancouver BC, Canada

[169] Department of Physics and Astronomy, University of Victoria, Victoria BC, Canada

[170] Department of Physics, University of Warwick, Coventry, United Kingdom

[171] Waseda University, Tokyo, Japan

[172] Department of Particle Physics, The Weizmann Institute of Science, Rehovot, Israel

[173] Department of Physics, University of Wisconsin, Madison WI, United States of America

[174] Fakultät für Physik und Astronomie, Julius-Maximilians-Universität, Würzburg, Germany

[175] Fakultät für Mathematik und Naturwissenschaften, Fachgruppe Physik, Bergische Universität

Wuppertal, Wuppertal, Germany
[176] Department of Physics, Yale University, New Haven CT, United States of America
[177] Yerevan Physics Institute, Yerevan, Armenia
[178] Centre de Calcul de l'Institut National de Physique Nucléaire et de Physique des Particules (IN2P3), Villeurbanne, France
[a] Also at Department of Physics, King's College London, London, United Kingdom
[b] Also at Institute of Physics, Azerbaijan Academy of Sciences, Baku, Azerbaijan
[c] Also at Novosibirsk State University, Novosibirsk, Russia
[d] Also at TRIUMF, Vancouver BC, Canada
[e] Also at Department of Physics & Astronomy, University of Louisville, Louisville, KY, United States of America
[f] Also at Department of Physics, California State University, Fresno CA, United States of America
[g] Also at Department of Physics, University of Fribourg, Fribourg, Switzerland
[h] Also at Departament de Fisica de la Universitat Autonoma de Barcelona, Barcelona, Spain
[i] Also at Departamento de Fisica e Astronomia, Faculdade de Ciencias, Universidade do Porto, Portugal
[j] Also at Tomsk State University, Tomsk, Russia
[k] Also at Universita di Napoli Parthenope, Napoli, Italy
[l] Also at Institute of Particle Physics (IPP), Canada
[m] Also at National Institute of Physics and Nuclear Engineering, Bucharest, Romania
[n] Also at Department of Physics, St. Petersburg State Polytechnical University, St. Petersburg, Russia
[o] Also at Department of Physics, The University of Michigan, Ann Arbor MI, United States of America
[p] Also at Centre for High Performance Computing, CSIR Campus, Rosebank, Cape Town, South Africa
[q] Also at Louisiana Tech University, Ruston LA, United States of America
[r] Also at Institucio Catalana de Recerca i Estudis Avancats, ICREA, Barcelona, Spain
[s] Also at Graduate School of Science, Osaka University, Osaka, Japan
[t] Also at Department of Physics, National Tsing Hua University, Taiwan
[u] Also at Institute for Mathematics, Astrophysics and Particle Physics, Radboud University Nijmegen/Nikhef, Nijmegen, Netherlands
[v] Also at Department of Physics, The University of Texas at Austin, Austin TX, United States of America
[w] Also at Institute of Theoretical Physics, Ilia State University, Tbilisi, Georgia
[x] Also at CERN, Geneva, Switzerland
[y] Also at Georgian Technical University (GTU),Tbilisi, Georgia
[z] Also at Ochadai Academic Production, Ochanomizu University, Tokyo, Japan
[aa] Also at Manhattan College, New York NY, United States of America
[ab] Also at Hellenic Open University, Patras, Greece
[ac] Also at Academia Sinica Grid Computing, Institute of Physics, Academia Sinica, Taipei, Taiwan
[ad] Also at School of Physics, Shandong University, Shandong, China
[ae] Also at Moscow Institute of Physics and Technology State University, Dolgoprudny, Russia
[af] Also at Section de Physique, Université de Genève, Geneva, Switzerland
[ag] Also at Eotvos Lorand University, Budapest, Hungary
[ah] Also at International School for Advanced Studies (SISSA), Trieste, Italy
[ai] Also at Department of Physics and Astronomy, University of South Carolina, Columbia SC, United States of America
[aj] Also at School of Physics and Engineering, Sun Yat-sen University, Guangzhou, China
[ak] Also at Institute for Nuclear Research and Nuclear Energy (INRNE) of the Bulgarian Academy of Sciences, Sofia, Bulgaria
[al] Also at Faculty of Physics, M.V.Lomonosov Moscow State University, Moscow, Russia

am Also at Institute of Physics, Academia Sinica, Taipei, Taiwan

an Also at National Research Nuclear University MEPhI, Moscow, Russia

ao Also at Department of Physics, Stanford University, Stanford CA, United States of America

ap Also at Institute for Particle and Nuclear Physics, Wigner Research Centre for Physics, Budapest, Hungary

aq Also at Flensburg University of Applied Sciences, Flensburg, Germany

ar Also at University of Malaya, Department of Physics, Kuala Lumpur, Malaysia

as Also at CPPM, Aix-Marseille Université and CNRS/IN2P3, Marseille, France

* Deceased

The CMS Collaboration

Yerevan Physics Institute, Yerevan, Armenia
V. Khachatryan, A.M. Sirunyan, A. Tumasyan

Institut für Hochenergiephysik der OeAW, Wien, Austria
W. Adam, E. Asilar, T. Bergauer, J. Brandstetter, E. Brondolin, M. Dragicevic, J. Erö, M. Flechl, M. Friedl, R. Frühwirth[1], V.M. Ghete, C. Hartl, N. Hörmann, J. Hrubec, M. Jeitler[1], A. König, I. Krätschmer, D. Liko, T. Matsushita, I. Mikulec, D. Rabady, N. Rad, B. Rahbaran, H. Rohringer, J. Schieck[1], J. Strauss, W. Treberer-Treberspurg, W. Waltenberger, C.-E. Wulz[1]

National Centre for Particle and High Energy Physics, Minsk, Belarus
V. Mossolov, N. Shumeiko, J. Suarez Gonzalez

Universiteit Antwerpen, Antwerpen, Belgium
S. Alderweireldt, E.A. De Wolf, X. Janssen, A. Knutsson, J. Lauwers, M. Van De Klundert, H. Van Haevermaet, P. Van Mechelen, N. Van Remortel, A. Van Spilbeeck

Vrije Universiteit Brussel, Brussel, Belgium
S. Abu Zeid, F. Blekman, J. D'Hondt, N. Daci, I. De Bruyn, K. Deroover, N. Heracleous, S. Lowette, S. Moortgat, L. Moreels, A. Olbrechts, Q. Python, S. Tavernier, W. Van Doninck, P. Van Mulders, I. Van Parijs

Université Libre de Bruxelles, Bruxelles, Belgium
H. Brun, C. Caillol, B. Clerbaux, G. De Lentdecker, H. Delannoy, G. Fasanella, L. Favart, R. Goldouzian, A. Grebenyuk, G. Karapostoli, T. Lenzi, A. Léonard, J. Luetic, T. Maerschalk, A. Marinov, A. Randle-conde, T. Seva, C. Vander Velde, P. Vanlaer, R. Yonamine, F. Zenoni, F. Zhang[2]

Ghent University, Ghent, Belgium
A. Cimmino, T. Cornelis, D. Dobur, A. Fagot, G. Garcia, M. Gul, J. Mccartin, D. Poyraz, S. Salva, R. Schöfbeck, M. Tytgat, W. Van Driessche, E. Yazgan, N. Zaganidis

Université Catholique de Louvain, Louvain-la-Neuve, Belgium
C. Beluffi[3], O. Bondu, S. Brochet, G. Bruno, A. Caudron, L. Ceard, S. De Visscher, C. Delaere, M. Delcourt, L. Forthomme, B. Francois, A. Giammanco, A. Jafari, P. Jez, M. Komm, V. Lemaitre, A. Magitteri, A. Mertens, M. Musich, C. Nuttens, K. Piotrzkowski, L. Quertenmont, M. Selvaggi, M. Vidal Marono, S. Wertz

Université de Mons, Mons, Belgium
N. Beliy

Centro Brasileiro de Pesquisas Fisicas, Rio de Janeiro, Brazil
W.L. Aldá Júnior, F.L. Alves, G.A. Alves, L. Brito, M. Correa Martins Junior, C. Hensel, A. Moraes, M.E. Pol, P. Rebello Teles

Universidade do Estado do Rio de Janeiro, Rio de Janeiro, Brazil

E. Belchior Batista Das Chagas, W. Carvalho, J. Chinellato[4], A. Custódio, E.M. Da Costa, G.G. Da Silveira, D. De Jesus Damiao, C. De Oliveira Martins, S. Fonseca De Souza, L.M. Huertas Guativa, H. Malbouisson, D. Matos Figueiredo, C. Mora Herrera, L. Mundim, H. Nogima, W.L. Prado Da Silva, A. Santoro, A. Sznajder, E.J. Tonelli Manganote[4], A. Vilela Pereira

Universidade Estadual Paulista [a], Universidade Federal do ABC [b], São Paulo, Brazil

S. Ahuja[a], C.A. Bernardes[b], S. Dogra[a], T.R. Fernandez Perez Tomei[a], E.M. Gregores[b], P.G. Mercadante[b], C.S. Moon[a,5], S.F. Novaes[a], Sandra S. Padula[a], D. Romero Abad[b], gas

Institute for Nuclear Research and Nuclear Energy, Sofia, Bulgaria

A. Aleksandrov, R. Hadjiiska, P. Iaydjiev, M. Rodozov, S. Stoykova, G. Sultanov, M. Vutova

University of Sofia, Sofia, Bulgaria

A. Dimitrov, I. Glushkov, L. Litov, B. Pavlov, P. Petkov

Beihang University, Beijing, China

W. Fang[6]

Institute of High Energy Physics, Beijing, China

M. Ahmad, J.G. Bian, G.M. Chen, H.S. Chen, M. Chen, Y. Chen[7], T. Cheng, R. Du, C.H. Jiang, D. Leggat, Z. Liu, F. Romeo, S.M. Shaheen, A. Spiezia, J. Tao, C. Wang, Z. Wang, H. Zhang, J. Zhao

State Key Laboratory of Nuclear Physics and Technology, Peking University, Beijing, China

C. Asawatangtrakuldee, Y. Ban, Q. Li, S. Liu, Y. Mao, S.J. Qian, D. Wang, Z. Xu

Universidad de Los Andes, Bogota, Colombia

C. Avila, A. Cabrera, L.F. Chaparro Sierra, C. Florez, J.P. Gomez, C.F. González Hernández, J.D. Ruiz Alvarez, J.C. Sanabria

University of Split, Faculty of Electrical Engineering, Mechanical Engineering and Naval Architecture, Split, Croatia

N. Godinovic, D. Lelas, I. Puljak, P.M. Ribeiro Cipriano

University of Split, Faculty of Science, Split, Croatia

Z. Antunovic, M. Kovac

Institute Rudjer Boskovic, Zagreb, Croatia

V. Brigljevic, D. Ferencek, K. Kadija, S. Micanovic, L. Sudic

University of Cyprus, Nicosia, Cyprus

A. Attikis, G. Mavromanolakis, J. Mousa, C. Nicolaou, F. Ptochos, P.A. Razis, H. Rykaczewski

Charles University, Prague, Czech Republic

M. Finger[8], M. Finger Jr.[8]

Universidad San Francisco de Quito, Quito, Ecuador

E. Carrera Jarrin

Academy of Scientific Research and Technology of the Arab Republic of Egypt, Egyptian Network of High Energy Physics, Cairo, Egypt

A.A. Abdelalim[9,10], E. El-khateeb[11], M.A. Mahmoud[12,13], A. Radi[13,11]

National Institute of Chemical Physics and Biophysics, Tallinn, Estonia
B. Calpas, M. Kadastik, M. Murumaa, L. Perrini, M. Raidal, A. Tiko, C. Veelken

Department of Physics, University of Helsinki, Helsinki, Finland
P. Eerola, J. Pekkanen, M. Voutilainen

Helsinki Institute of Physics, Helsinki, Finland
J. Härkönen, J.K. Heikkilä, V. Karimäki, R. Kinnunen, T. Lampén, K. Lassila-
Perini, S. Lehti, T. Lindén, P. Luukka, T. Peltola, J. Tuominiemi, E. Tuovinen, L. Wendland

Lappeenranta University of Technology, Lappeenranta, Finland
J. Talvitie, T. Tuuva

DSM/IRFU, CEA/Saclay, Gif-sur-Yvette, France
M. Besancon, F. Couderc, M. Dejardin, D. Denegri, B. Fabbro, J.L. Faure, C. Favaro, F. Ferri, S. Gan-
jour, S. Ghosh, A. Givernaud, P. Gras, G. Hamel de Monchenault, P. Jarry, I. Kucher, E. Locci, M. Machet, J. Mal-
cles, J. Rander, A. Rosowsky, M. Titov, A. Zghiche

Laboratoire Leprince-Ringuet, Ecole Polytechnique, IN2P3-CNRS, Palaiseau, France
A. Abdulsalam, I. Antropov, S. Baffioni, F. Beaudette, P. Busson, L. Cadamuro, E. Chapon, C. Char-
lot, O. Davignon, R. Granier de Cassagnac, M. Jo, S. Lis-
niak, P. Miné, I.N. Naranjo, M. Nguyen, C. Ochando, G. Ortona, P. Pa-
ganini, P. Pigard, S. Regnard, R. Salerno, Y. Sirois, T. Strebler, Y. Yilmaz, A. Zabi

**Institut Pluridisciplinaire Hubert Curien, Université de Strasbourg, Uni-
versité de Haute Alsace Mulhouse, CNRS/IN2P3, Strasbourg, France**
J.-L. Agram[14], J. Andrea, A. Aubin, D. Bloch, J.-
M. Brom, M. Buttignol, E.C. Chabert, N. Chanon, C. Collard, E. Conte[14], X. Coubez, J.-
C. Fontaine[14], D. Gelé, U. Goerlach, A.-C. Le Bihan, J.A. Merlin[15], K. Skovpen, P. Van Hove

**Centre de Calcul de l'Institut National de Physique Nucleaire et de Physique des Partic-
ules, CNRS/IN2P3, Villeurbanne, France**
S. Gadrat

**Université de Lyon, Université Claude Bernard Lyon 1, CNRS-
IN2P3, Institut de Physique Nucléaire de Lyon, Villeurbanne, France**
S. Beauceron, C. Bernet, G. Boudoul, E. Bouvier, C.A. Carrillo Montoya, R. Chierici, D. Con-
tardo, B. Courbon, P. Depasse, H. El Mamouni, J. Fan, J. Fay, S. Gascon, M. Gouzevitch, G. Gren-
ier, B. Ille, F. Lagarde, I.B. Laktineh, M. Lethuillier, L. Mirabito, A.L. Pequegnot, S. Per-
ries, A. Popov[16], D. Sabes, V. Sordini, M. Vander Donckt, P. Verdier, S. Viret

Georgian Technical University, Tbilisi, Georgia
T. Toriashvili[17]

Tbilisi State University, Tbilisi, Georgia
Z. Tsamalaidze[8]

RWTH Aachen University, I. Physikalisches Institut, Aachen, Germany
C. Autermann, S. Beranek, L. Feld, A. Heister, M.K. Kiesel, K. Klein, M. Lipinski, A. Os-
tapchuk, M. Preuten, F. Raupach, S. Schael, C. Schomakers, J.F. Schulte, J. Schulz, T. Ver-
lage, H. Weber, V. Zhukov[16]

RWTH Aachen University, III. Physikalisches Institut A, Aachen, Germany

M. Brodski, E. Dietz-Laursonn, D. Duchardt, M. Endres, M. Erdmann, S. Erdweg, T. Esch, R. Fischer, A. Güth, T. Hebbeker, C. Heidemann, K. Hoepfner, S. Knutzen, M. Merschmeyer, A. Meyer, P. Millet, S. Mukherjee, M. Olschewski, K. Padeken, P. Papacz, T. Pook, M. Radziej, H. Reithler, M. Rieger, F. Scheuch, L. Sonnenschein, D. Teyssier, S. Thüer

RWTH Aachen University, III. Physikalisches Institut B, Aachen, Germany

V. Cherepanov, Y. Erdogan, G. Flügge, F. Hoehle, B. Kargoll, T. Kress, A. Künsken, J. Lingemann, A. Nehrkorn, A. Nowack, I.M. Nugent, C. Pistone, O. Pooth, A. Stahl[15]

Deutsches Elektronen-Synchrotron, Hamburg, Germany

M. Aldaya Martin, I. Asin, K. Beernaert, O. Behnke, U. Behrens, A.A. Bin Anuar, K. Borras[18], A. Campbell, P. Connor, C. Contreras-Campana, F. Costanza, C. Diez Pardos, G. Dolinska, G. Eckerlin, D. Eckstein, T. Eichhorn, E. Gallo[19], J. Garay Garcia, A. Geiser, A. Gizhko, J.M. Grados Luyando, P. Gunnellini, A. Harb, J. Hauk, M. Hempel[20], H. Jung, A. Kalogeropoulos, O. Karacheban[20], M. Kasemann, J. Keaveney, J. Kieseler, C. Kleinwort, I. Korol, W. Lange, A. Lelek, J. Leonard, K. Lipka, A. Lobanov, W. Lohmann[20], R. Mankel, I.-A. Melzer-Pellmann, A.B. Meyer, G. Mittag, J. Mnich, A. Mussgiller, E. Ntomari, D. Pitzl, R. Placakyte, A. Raspereza, B. Roland, M.Ö. Sahin, P. Saxena, T. Schoerner-Sadenius, C. Seitz, S. Spannagel, N. Stefaniuk, K.D. Trippkewitz, G.P. Van Onsem, R. Walsh, C. Wissing

University of Hamburg, Hamburg, Germany

V. Blobel, M. Centis Vignali, A.R. Draeger, T. Dreyer, J. Erfle, E. Garutti, K. Goebel, D. Gonzalez, M. Görner, J. Haller, M. Hoffmann, R.S. Höing, A. Junkes, R. Klanner, R. Kogler, N. Kovalchuk, T. Lapsien, T. Lenz, I. Marchesini, D. Marconi, M. Meyer, M. Niedziela, D. Nowatschin, J. Ott, F. Pantaleo[15], T. Peiffer, A. Perieanu, N. Pietsch, J. Poehlsen, C. Sander, C. Scharf, P. Schleper, E. Schlieckau, A. Schmidt, S. Schumann, J. Schwandt, H. Stadie, G. Steinbrück, F.M. Stober, M. Stöver, H. Tholen, D. Troendle, E. Usai, L. Vanelderen, A. Vanhoefer, B. Vormwald

Institut für Experimentelle Kernphysik, Karlsruhe, Germany

C. Barth, C. Baus, J. Berger, E. Butz, T. Chwalek, F. Colombo, W. De Boer, A. Dierlamm, S. Fink, R. Friese, M. Giffels, A. Gilbert, D. Haitz, F. Hartmann[15], S.M. Heindl, U. Husemann, I. Katkov[16], A. Kornmayer[15], P. Lobelle Pardo, B. Maier, H. Mildner, M.U. Mozer, T. Müller, Th. Müller, M. Plagge, G. Quast, K. Rabbertz, S. Röcker, F. Roscher, M. Schröder, G. Sieber, H.J. Simonis, R. Ulrich, J. Wagner-Kuhr, S. Wayand, M. Weber, T. Weiler, S. Williamson, C. Wöhrmann, R. Wolf

Institute of Nuclear and Particle Physics (INPP), NCSR Demokritos, Aghia Paraskevi, Greece

G. Anagnostou, G. Daskalakis, T. Geralis, V.A. Giakoumopoulou, A. Kyriakis, D. Loukas, I. Topsis-Giotis

National and Kapodistrian University of Athens, Athens, Greece

A. Agapitos, S. Kesisoglou, A. Panagiotou, N. Saoulidou, E. Tziaferi

University of Ioánnina, Ioánnina, Greece

I. Evangelou, G. Flouris, C. Foudas, P. Kokkas, N. Loukas, N. Manthos, I. Papadopoulos, E. Paradas

MTA-ELTE Lendület CMS Particle and Nuclear Physics Group, Eötvös Loránd University

N. Filipovic

Wigner Research Centre for Physics, Budapest, Hungary
G. Bencze, C. Hajdu, P. Hidas, D. Horvath[21], F. Sikler, V. Veszpremi, G. Vesztergombi[22], A.J. Zsigmond

Institute of Nuclear Research ATOMKI, Debrecen, Hungary
N. Beni, S. Czellar, J. Karancsi[23], J. Molnar, Z. Szillasi

University of Debrecen, Debrecen, Hungary
M. Bartók[22], A. Makovec, P. Raics, Z.L. Trocsanyi, B. Ujvari

National Institute of Science Education and Research, Bhubaneswar, India
S. Bahinipati, S. Choudhury[24], P. Mal, K. Mandal, A. Nayak[25], D.K. Sahoo, N. Sahoo, S.K. Swain

Panjab University, Chandigarh, India
S. Bansal, S.B. Beri, V. Bhatnagar, R. Chawla, R. Gupta, U.Bhawandeep, A.K. Kalsi, A. Kaur, M. Kaur, R. Kumar, A. Mehta, M. Mittal, J.B. Singh, G. Walia

University of Delhi, Delhi, India
Ashok Kumar, A. Bhardwaj, B.C. Choudhary, R.B. Garg, S. Keshri, A. Kumar, S. Malhotra, M. Naimuddin, N. Nishu, K. Ranjan, R. Sharma, V. Sharma

Saha Institute of Nuclear Physics, Kolkata, India
R. Bhattacharya, S. Bhattacharya, K. Chatterjee, S. Dey, S. Dutt, S. Dutta, S. Ghosh, N. Majumdar, A. Modak, K. Mondal, S. Mukhopadhyay, S. Nandan, A. Purohit, A. Roy, D. Roy, S. Roy Chowdhury, S. Sarkar, M. Sharan, S. Thakur

Indian Institute of Technology Madras, Madras, India
P.K. Behera

Bhabha Atomic Research Centre, Mumbai, India
R. Chudasama, D. Dutta, V. Jha, V. Kumar, A.K. Mohanty[15], P.K. Netrakanti, L.M. Pant, P. Shukla, A. Topkar

Tata Institute of Fundamental Research-A, Mumbai, India
T. Aziz, S. Dugad, G. Kole, B. Mahakud, S. Mitra, G.B. Mohanty, N. Sur, B. Sutar

Tata Institute of Fundamental Research-B, Mumbai, India
S. Banerjee, S. Bhowmik[26], R.K. Dewanjee, S. Ganguly, M. Guchait, Sa. Jain, S. Kumar, M. Maity[26], G. Majumder, K. Mazumdar, B. Parida, T. Sarkar[26], N. Wickramage[27]

Indian Institute of Science Education and Research (IISER), Pune, India
S. Chauhan, S. Dube, A. Kapoor, K. Kothekar, A. Rane, S. Sharma

Institute for Research in Fundamental Sciences (IPM), Tehran, Iran
H. Bakhshiansohi, H. Behnamian, S. Chenarani[28], E. Eskandari Tadavani, S.M. Etesami[28], A. Fahim[29], M. Khakzad, M. Mohammadi Najafabadi, M. Naseri, S. Paktinat Mehdiabadi, F. Rezaei Hosseinabadi, B. Safarzadeh[30], M. Zeinali

University College Dublin, Dublin, Ireland
M. Felcini, M. Grunewald

INFN Sezione di Bari ^{a}, Università di Bari ^{b}, Politecnico di Bari ^{c}, Bari, Italy
M. Abbrescia^{a,b}, C. Calabria^{a,b}, C. Caputo^{a,b}, A. Colaleo^a, D. Creanza^{a,c}, L. Cristella^{a,b}, N. De Filippis^{a,c}, M. De Palma$^{}$

INFN Sezione di Bologna [a], Università di Bologna [b], Bologna, Italy

G. Abbiendi[a], C. Battilana, D. Bonacorsi[a,b], S. Braibant-Giacomelli[a,b], L. Brigliadori[a,b], R. Campanini[a,b], P. Capiluppi[a,b], A. Castro[a,b], F.R. Cavallo[a], S.S. Chhibra[a,b], G. Codisp

INFN Sezione di Catania [a], Università di Catania [b], Catania, Italy

S. Albergo[a,b], M. Chiorboli[a,b], S. Costa[a,b], A. Di Mattia[a], F. Giordano[a,b], R. Potenza[a,b], A. Tricomi[a,b], C. Tuve[a,b]

INFN Sezione di Firenze [a], Università di Firenze [b], Firenze, Italy

G. Barbagli[a], V. Ciulli[a,b], C. Civinini[a], R. D'Alessandro[a,b], E. Focardi[a,b], V. Gori[a,b], P. Lenzi[a,b], M. Meschini[a], S. Paolet

INFN Laboratori Nazionali di Frascati, Frascati, Italy

L. Benussi, S. Bianco, F. Fabbri, D. Piccolo, F. Primavera[15]

INFN Sezione di Genova [a], Università di Genova [b], Genova, Italy

V. Calvelli[a,b], F. Ferro[a], M. Lo Vetere[a,b], M.R. Monge[a,b], E. Robutti[a], S. Tosi[a,b]

INFN Sezione di Milano-Bicocca [a], Università di Milano-Bicocca [b], Milano, Italy

L. Brianza, M.E. Dinardo[a,b], S. Fiorendi[a,b], S. Gennai[a], A. Ghezzi[a,b], P. Govoni[a,b], S. Malvezzi[a], R.A. Manzoni[a,b,15], B. Marzarelli de Fatis[a,b]

INFN Sezione di Napoli [a], Università di Napoli 'Federico II' [b], Napoli, Italy, Università della Basilicata [c], Potenza, Italy, Università G. Marconi [d], Roma, Italy

S. Buontempo[a], N. Cavallo[a,c], G. De Nardo, S. Di Guida[a,d,15], M. Esposito[a,b], F. Fabozzi[a,c], A.O.M. Iorio[a,b], G. Lanza[a],

INFN Sezione di Padova [a], Università di Padova [b], Padova, Italy, Università di Trento [c], Trento, Italy

P. Azzi[a,15], N. Bacchetta[a], L. Benato[a,b], D. Bisello[a,b], A. Boletti[a,b], R. Carlin[a,b], A. Carvalho Antunes De Oliveira[a,b], P. Checchia[a], M. Dall'Osso[a,b], P. De Castro Manzano[a], T. Dorigo[a], U. Dosselli[a], F. Gasparini[a,b], U.

INFN Sezione di Pavia [a], Università di Pavia [b], Pavia, Italy

A. Braghieri[a], A. Magnani[a,b], P. Montagna[a,b], S.P. Ratti[a,b], V. Re[a], C. Riccardi[a,b], P. Salvini[a], I. Vai[a,b], P. Vitulo[a,b]

INFN Sezione di Perugia [a], Università di Perugia [b], Perugia, Italy

L. Alunni Solestizi[a,b], G.M. Bilei[a], D. Ciangottini[a,b], L. Fanò[a,b], P. Lariccia[a,b], R. Leonardi[a,b], G. Mantovani[a,b], M. Men

INFN Sezione di Pisa [a], Università di Pisa [b], Scuola Normale Superiore di Pisa [c], Pisa, Italy

K. Androsov[a,31], P. Azzurri[a,15], G. Bagliesi[a], J. Bernardini[a], T. Boccali[a], R. Castaldi[a], M.A. Ciocci[a,31], R. Dell'Orso[a], S. Navarro[a,32], P. Spagnolo[a], R. Tenchini[a], G. Tonelli[a,b], A. Venturi[a], P.G. Verdini[a]

INFN Sezione di Roma [a], Università di Roma [b], Roma, Italy

L. Barone[a,b], F. Cavallari[a], M. Cipriani[a,b], G. D'imperio[a,b,15], D. Del Re[a,b,15], M. Diemoz[a], S. Gelli[a,b], C. Jorda[a], E. Lon

INFN Sezione di Torino [a], Università di Torino [b], Torino, Italy, Università del Piemonte Orientale [c], Novara, Italy

N. Amapane[a,b], R. Arcidiacono[a,c,15], S. Argiro[a,b], M. Arneodo[a,c], N. Bartosik[a], R. Bellan[a,b], C. Biino[a], N. Cartiglia[a], M.

INFN Sezione di Trieste [a], Università di Trieste [b], Trieste, Italy

S. Belforte[a], V. Candelise[a,b], M. Casarsa[a], F. Cossutti[a], G. Della Ricca[a,b], C. La Licata[a,b], A. Schizzi[a,b], A. Zanetti[a]

Kyungpook National University, Daegu, Korea

D.H. Kim, G.N. Kim, M.S. Kim, S. Lee, S.W. Lee, Y.D. Oh, S. Sekmen, D.C. Son, Y.C. Yang

Chonbuk National University, Jeonju, Korea
H. Kim, A. Lee

Hanyang University, Seoul, Korea
J.A. Brochero Cifuentes, T.J. Kim

Korea University, Seoul, Korea
S. Cho, S. Choi, Y. Go, D. Gyun, S. Ha, B. Hong, Y. Jo, Y. Kim, B. Lee, K. Lee, K.S. Lee, S. Lee, J. Lim, S.K. Park, Y. Roh

Seoul National University, Seoul, Korea
J. Almond, J. Kim, S.B. Oh, S.h. Seo, U.K. Yang, H.D. Yoo, G.B. Yu

University of Seoul, Seoul, Korea
M. Choi, H. Kim, H. Kim, J.H. Kim, J.S.H. Lee, I.C. Park, G. Ryu, M.S. Ryu

Sungkyunkwan University, Suwon, Korea
Y. Choi, J. Goh, D. Kim, E. Kwon, J. Lee, I. Yu

Vilnius University, Vilnius, Lithuania
V. Dudenas, A. Juodagalvis, J. Vaitkus

National Centre for Particle Physics, Universiti Malaya, Kuala Lumpur, Malaysia
I. Ahmed, Z.A. Ibrahim, J.R. Komaragiri, M.A.B. Md Ali[33], F. Mohamad Idris[34], W.A.T. Wan Abdullah, M.N. Yusli, Z. Zolkapli

Centro de Investigacion y de Estudios Avanzados del IPN, Mexico City, Mexico
E. Casimiro Linares, H. Castilla-Valdez, E. De La Cruz-Burelo, I. Heredia-De La Cruz[35], A. Hernandez-Almada, R. Lopez-Fernandez, J. Mejia Guisao, A. Sanchez-Hernandez

Universidad Iberoamericana, Mexico City, Mexico
S. Carrillo Moreno, F. Vazquez Valencia

Benemerita Universidad Autonoma de Puebla, Puebla, Mexico
I. Pedraza, H.A. Salazar Ibarguen, C. Uribe Estrada

Universidad Autónoma de San Luis Potosí, San Luis Potosí, Mexico
A. Morelos Pineda

University of Auckland, Auckland, New Zealand
D. Krofcheck

University of Canterbury, Christchurch, New Zealand
P.H. Butler

National Centre for Physics, Quaid-I-Azam University, Islamabad, Pakistan
A. Ahmad, M. Ahmad, Q. Hassan, H.R. Hoorani, W.A. Khan, T. Khurshid, S. Qazi, M. Waqas

National Centre for Nuclear Research, Swierk, Poland
H. Bialkowska, M. Bluj, B. Boimska, T. Frueboes, M. Górski, M. Kazana, K. Nawrocki, K. Romanowska-Rybinska, M. Szleper, P. Zalewski

Institute of Experimental Physics, Faculty of Physics, University of Warsaw, Warsaw, Poland
K. Bunkowski, A. Byszuk[36], K. Doroba, A. Kalinowski, M. Konecki, J. Krolikowski, M. Misiura, M. Olszewski, M. Walczak

Laboratório de Instrumentação e Física Experimental de Partículas, Lisboa, Portugal
P. Bargassa, C. Beirão Da Cruz E Silva, A. Di Francesco, P. Faccioli, P.G. Ferreira Parracho, M. Gallinaro, J. Hollar, N. Leonardo, L. Lloret Iglesias, M.V. Nemallapudi, J. Rodrigues Antunes, J. Seixas, O. Toldaiev, D. Vadruccio, J. Varela, P. Vischia

Joint Institute for Nuclear Research, Dubna, Russia
S. Afanasiev, M. Gavrilenko, I. Golutvin, I. Gorbunov, V. Karjavin, G. Kozlov, A. Lanev, A. Malakhov, V. Matveev[37,38], P. Moisenz, V. Palichik, V. Perelygin, M. Savina, S. Shmatov, S. Shulha, N. Skatchkov, V. Smirnov, N. Voytishin, A. Zarubin

Petersburg Nuclear Physics Institute, Gatchina (St. Petersburg), Russia
L. Chtchipounov, V. Golovtsov, Y. Ivanov, V. Kim[39], E. Kuznetsova[40], V. Murzin, V. Oreshkin, V. Sulimov, A. Vorobyev

Institute for Nuclear Research, Moscow, Russia
Yu. Andreev, A. Dermenev, S. Gninenko, N. Golubev, A. Karneyeu, M. Kirsanov, N. Krasnikov, A. Pashenkov, D. Tlisov, A. Toropin

Institute for Theoretical and Experimental Physics, Moscow, Russia
V. Epshteyn, V. Gavrilov, N. Lychkovskaya, V. Popov, I. Pozdnyakov, G. Safronov, A. Spiridonov, M. Toms, E. Vlasov, A. Zhokin

National Research Nuclear University 'Moscow Engineering Physics Institute' (MEPhI), Moscow, Russia
R. Chistov, O. Markin, V. Rusinov

P.N. Lebedev Physical Institute, Moscow, Russia
V. Andreev, M. Azarkin[38], I. Dremin[38], M. Kirakosyan, A. Leonidov[38], S.V. Rusakov, A. Terkulov

Skobeltsyn Institute of Nuclear Physics, Lomonosov Moscow State University, Moscow, Russia
A. Baskakov, A. Belyaev, E. Boos, V. Bunichev, M. Dubinin[41], L. Dudko, A. Ershov, A. Gribushin, V. Klyukhin, O. Kodolova, I. Lokhtin, I. Miagkov, S. Obraztsov, S. Petrushanko, V. Savrin

State Research Center of Russian Federation, Institute for High Energy Physics, Protvino, Russia
I. Azhgirey, I. Bayshev, S. Bitioukov, D. Elumakhov, V. Kachanov, A. Kalinin, D. Konstantinov, V. Krychkine, V. Petrov, R. Ryutin, A. Sobol, S. Troshin, N. Tyurin, A. Uzunian, A. Volkov

University of Belgrade, Faculty of Physics and Vinca Institute of Nuclear Sciences, Belgrade, Serbia
P. Adzic[42], P. Cirkovic, D. Devetak, J. Milosevic, V. Rekovic

Centro de Investigaciones Energéticas Medioambientales y Tecnológicas (CIEMAT), Madrid, Spain
J. Alcaraz Maestre, E. Calvo, M. Cerrada, M. Chamizo Llatas, N. Colino, B. De La Cruz, A. Delgado Peris, A. Escalante Del Valle, C. Fernandez Bedoya, J.P. Fernández Ramos, J. Flix, M.C. Fouz, P. Garcia-Abia, O. Gonzalez Lopez, S. Goy Lopez, J.M. Hernandez, M.I. Josa, E. Navarro De Martino, A. Pérez-Calero Yzquierdo, J. Puerta Pelayo, A. Quintario Olmeda, I. Redondo, L. Romero, M.S. Soares

Universidad Autónoma de Madrid, Madrid, Spain
J.F. de Trocóniz, M. Missiroli, D. Moran

Universidad de Oviedo, Oviedo, Spain
J. Cuevas, J. Fernandez Menendez, I. Gonzalez Caballero, E. Palencia Cortezon, S. Sanchez Cruz, J.M. Vizan Garcia

Instituto de Física de Cantabria (IFCA), CSIC-Universidad de Cantabria, Santander, Spain
I.J. Cabrillo, A. Calderon, J.R. Castiñeiras De Saa, E. Curras, M. Fernandez, J. Garcia-Ferrero, G. Gomez, A. Lopez Virto, J. Marco, C. Martinez Rivero, F. Matorras, J. Piedra Gomez, T. Rodrigo, A. Ruiz-Jimeno, L. Scodellaro, N. Trevisani, I. Vila, R. Vilar Cortabitarte

CERN, European Organization for Nuclear Research, Geneva, Switzerland
D. Abbaneo, E. Auffray, G. Auzinger, M. Bachtis, P. Baillon, A.H. Ball, D. Barney, P. Bloch, A. Bocci, A. Bonato, C. Botta, T. Camporesi, R. Castello, M. Cepeda, G. Cerminara, M. D'Alfonso, D. d'Enterria, A. Dabrowski, V. Daponte, A. David, M. De Gruttola, F. De Guio, A. De Roeck, E. Di Marco[43], M. Dobson, M. Dordevic, B. Dorney, T. du Pree, D. Duggan, M. Dünser, N. Dupont, A. Elliott-Peisert, S. Fartoukh, G. Franzoni, J. Fulcher, W. Funk, D. Gigi, K. Gill, M. Girone, F. Glege, S. Gundacker, M. Guthoff, J. Hammer, P. Harris, J. Hegeman, V. Innocente, P. Janot, H. Kirschenmann, V. Knünz, M.J. Kortelainen, K. Kousouris, M. Krammer[1], P. Lecoq, C. Lourenço, M.T. Lucchini, N. Magini, L. Malgeri, M. Mannelli, A. Martelli, F. Meijers, S. Mersi, E. Meschi, F. Moortgat, S. Morovic, M. Mulders, H. Neugebauer, S. Orfanelli[44], L. Orsini, L. Pape, E. Perez, M. Peruzzi, A. Petrilli, G. Petrucciani, A. Pfeiffer, M. Pierini, A. Racz, T. Reis, G. Rolandi[45], M. Rovere, M. Ruan, H. Sakulin, J.B. Sauvan, C. Schäfer, C. Schwick, M. Seidel, A. Sharma, P. Silva, M. Simon, P. Sphicas[46], J. Steggemann, M. Stoye, Y. Takahashi, D. Treille, A. Triossi, A. Tsirou, V. Veckalns[47], G.I. Veres[22], N. Wardle, A. Zagozdzinska[36], W.D. Zeuner

Paul Scherrer Institut, Villigen, Switzerland
W. Bertl, K. Deiters, W. Erdmann, R. Horisberger, Q. Ingram, H.C. Kaestli, D. Kotlinski, U. Langenegger, T. Rohe

Institute for Particle Physics, ETH Zurich, Zurich, Switzerland
F. Bachmair, L. Bäni, L. Bianchini, B. Casal, G. Dissertori, M. Dittmar, M. Donegà, P. Eller, C. Grab, C. Heidegger, D. Hits, J. Hoss, G. Kasieczka, P. Lecomte[†], W. Lustermann, B. Mangano, M. Marionneau, P. Martinez Ruiz del Arbol, M. Masciovecchio, M.T. Meinhard, D. Meister, F. Micheli, P. Musella, F. Nessi-Tedaldi, F. Pandolfi, J. Pata, F. Pauss, G. Perrin, L. Perrozzi, M. Quittnat, M. Rossini, M. Schönenberger, A. Starodumov[48], M. Takahashi, V.R. Tavolaro, K. Theofilatos, R. Wallny

Universität Zürich, Zurich, Switzerland
T.K. Aarrestad, C. Amsler[49], L. Caminada, M.F. Canelli, V. Chiochia, A. De Cosa, C. Galloni, A. Hinzmann, T. Hreus, B. Kilminster, C. Lange, J. Ngadiuba, D. Pinna, G. Rauco, P. Robmann, D. Salerno, Y. Yang

National Central University, Chung-Li, Taiwan
T.H. Doan, Sh. Jain, R. Khurana, M. Konyushikhin, C.M. Kuo, W. Lin, Y.J. Lu, A. Pozdnyakov, S.S. Yu

National Taiwan University (NTU), Taipei, Taiwan
Arun Kumar, P. Chang, Y.H. Chang, Y.W. Chang, Y. Chao, K.F. Chen, P.H. Chen, C. Dietz, F. Fiori, Y. Hsiung, Y.F. Liu, R.-S. Lu, M. Miñano Moya, E. Paganis, A. Psallidas, J.f. Tsai, Y.M. Tzeng

Chulalongkorn University, Faculty of Science, Department of Physics, Bangkok, Thailand
B. Asavapibhop, G. Singh, N. Srimanobhas, N. Suwonjandee

Cukurova University, Adana, Turkey

A. Adiguzel, M.N. Bakirci[50], S. Damarseckin, Z.S. Demiroglu, C. Dozen, I. Dumanoglu, S. Girgis, G. Gokbulut, Y. Guler, E. Gurpinar, I. Hos, E.E. Kangal[51], A. Kayis Topaksu, G. Onengut[52], K. Ozdemir[53], D. Sunar Cerci[54], B. Tali[54], C. Zorbilmez

Middle East Technical University, Physics Department, Ankara, Turkey

B. Bilin, S. Bilmis, B. Isildak[55], G. Karapinar[56], M. Yalvac, M. Zeyrek

Bogazici University, Istanbul, Turkey

E. Gülmez, M. Kaya[57], O. Kaya[58], E.A. Yetkin[59], T. Yetkin[60]

Istanbul Technical University, Istanbul, Turkey

A. Cakir, K. Cankocak, S. Sen[61], F.I. Vardarlı

Institute for Scintillation Materials of National Academy of Science of Ukraine, Kharkov, Ukraine

B. Grynyov

National Scientific Center, Kharkov Institute of Physics and Technology, Kharkov, Ukraine

L. Levchuk, P. Sorokin

University of Bristol, Bristol, United Kingdom

R. Aggleton, F. Ball, L. Beck, J.J. Brooke, D. Burns, E. Clement, D. Cussans, H. Flacher, J. Goldstein, M. Grimes, G.P. Heath, H.F. Heath, J. Jacob, L. Kreczko, C. Lucas, Z. Meng, D.M. Newbold[62], S. Paramesvaran, A. Poll, T. Sakuma, S. Seif El Nasr-storey, S. Senkin, D. Smith, V.J. Smith

Rutherford Appleton Laboratory, Didcot, United Kingdom

K.W. Bell, A. Belyaev[63], C. Brew, R.M. Brown, L. Calligaris, D. Cieri, D.J.A. Cockerill, J.A. Coughlan, K. Harder, S. Harper, E. Olaiya, D. Petyt, C.H. Shepherd-Themistocleous, A. Thea, I.R. Tomalin, T. Williams

Imperial College, London, United Kingdom

M. Baber, R. Bainbridge, O. Buchmuller, A. Bundock, D. Burton, S. Casasso, M. Citron, D. Colling, L. Corpe, P. Dauncey, G. Davies, A. De Wit, M. Della Negra, P. Dunne, A. Elwood, D. Futyan, Y. Haddad, G. Hall, G. Iles, R. Lane, C. Laner, R. Lucas[62], L. Lyons, A.-M. Magnan, S. Malik, L. Mastrolorenzo, J. Nash, A. Nikitenko[48], J. Pela, B. Penning, M. Pesaresi, D.M. Raymond, A. Richards, A. Rose, C. Seez, A. Tapper, K. Uchida, M. Vazquez Acosta[64], T. Virdee[15], S.C. Zenz

Brunel University, Uxbridge, United Kingdom

J.E. Cole, P.R. Hobson, A. Khan, P. Kyberd, D. Leslie, I.D. Reid, P. Symonds, L. Teodorescu, M. Turner

Baylor University, Waco, USA

A. Borzou, K. Call, J. Dittmann, K. Hatakeyama, H. Liu, N. Pastika

The University of Alabama, Tuscaloosa, USA

O. Charaf, S.I. Cooper, C. Henderson, P. Rumerio

Boston University, Boston, USA

D. Arcaro, A. Avetisyan, T. Bose, D. Gastler, D. Rankin, C. Richardson, J. Rohlf, L. Sulak, D. Zou

Brown University, Providence, USA

G. Benelli, E. Berry, D. Cutts, A. Ferapontov, A. Garabedian, J. Hakala, U. Heintz, O. Jesus, E. Laird, G. Landsberg, Z. Mao, M. Narain, S. Piperov, S. Sagir, E. Spencer, R. Syarif

University of California, Davis, Davis, USA
R. Breedon, G. Breto, D. Burns, M. Calderon De La Barca Sanchez, S. Chauhan, M. Chertok, J. Conway, R. Conway, P.T. Cox, R. Erbacher, C. Flores, G. Funk, M. Gardner, W. Ko, R. Lander, C. Mclean, M. Mulhearn, D. Pellett, J. Pilot, F. Ricci-Tam, S. Shalhout, J. Smith, M. Squires, D. Stolp, M. Tripathi, S. Wilbur, R. Yohay

University of California, Los Angeles, USA
R. Cousins, P. Everaerts, A. Florent, J. Hauser, M. Ignatenko, D. Saltzberg, E. Takasugi, V. Valuev, M. Weber

University of California, Riverside, Riverside, USA
K. Burt, R. Clare, J. Ellison, J.W. Gary, G. Hanson, J. Heilman, P. Jandir, E. Kennedy, F. Lacroix, O.R. Long, M. Malberti, M. Olmedo Negrete, M.I. Paneva, A. Shrinivas, H. Wei, S. Wimpenny, B. R. Yates

University of California, San Diego, La Jolla, USA
J.G. Branson, G.B. Cerati, S. Cittolin, R.T. D'Agnolo, M. Derdzinski, R. Gerosa, A. Holzner, R. Kelley, D. Klein, J. Letts, I. Macneill, D. Olivito, S. Padhi, M. Pieri, M. Sani, V. Sharma, S. Simon, M. Tadel, A. Vartak, S. Wasserbaech[65], C. Welke, J. Wood, F. Würthwein, A. Yagil, G. Zevi Della Porta

University of California, Santa Barbara, Santa Barbara, USA
R. Bhandari, J. Bradmiller-Feld, C. Campagnari, A. Dishaw, V. Dutta, K. Flowers, M. Franco Sevilla, P. Geffert, C. George, F. Golf, L. Gouskos, J. Gran, R. Heller, J. Incandela, N. Mccoll, S.D. Mullin, A. Ovcharova, J. Richman, D. Stuart, I. Suarez, C. West, J. Yoo

California Institute of Technology, Pasadena, USA
D. Anderson, A. Apresyan, J. Bendavid, A. Bornheim, J. Bunn, Y. Chen, J. Duarte, A. Mott, H.B. Newman, C. Pena, M. Spiropulu, J.R. Vlimant, S. Xie, R.Y. Zhu

Carnegie Mellon University, Pittsburgh, USA
M.B. Andrews, V. Azzolini, A. Calamba, B. Carlson, T. Ferguson, M. Paulini, J. Russ, M. Sun, H. Vogel, I. Vorobiev

University of Colorado Boulder, Boulder, USA
J.P. Cumalat, W.T. Ford, F. Jensen, A. Johnson, M. Krohn, T. Mulholland, K. Stenson, S.R. Wagner

Cornell University, Ithaca, USA
J. Alexander, J. Chaves, J. Chu, S. Dittmer, N. Mirman, G. Nicolas Kaufman, J.R. Patterson, A. Rinkevicius, A. Ryd, L. Skinnari, W. Sun, S.M. Tan, Z. Tao, J. Thom, J. Tucker, P. Wittich

Fairfield University, Fairfield, USA
D. Winn

Fermi National Accelerator Laboratory, Batavia, USA
S. Abdullin, M. Albrow, G. Apollinari, S. Banerjee, L.A.T. Bauerdick, A. Beretvas, J. Berryhill, P.C. Bhat, G. Bolla, K. Burkett, J.N. Butler, H.W.K. Cheung, F. Chlebana, S. Cihangir, M. Cremonesi, V.D. Elvira, I. Fisk, J. Freeman, E. Gottschalk, L. Gray, D. Green, S. Grünendahl, O. Gutsche, D. Hare, R.M. Harris, S. Hasegawa, J. Hirschauer, Z. Hu, B. Jayatilaka, S. Jindariani, M. Johnson, U. Joshi, B. Klima, B. Kreis, S. Lammel, J. Linacre, D. Lincoln, R. Lipton, T. Liu, R. Lopes De Sá, J. Lykken, K. Maeshima, J.M. Mar-

raffino, S. Maruyama, D. Mason, P. McBride, P. Merkel, S. Mrenna, S. Nahn, C. Newman-Holmes[†], V. O'Dell, K. Pedro, O. Prokofyev, G. Rakness, L. Ristori, E. Sexton-Kennedy, A. Soha, W.J. Spald-ing, L. Spiegel, S. Stoynev, N. Strobbe, L. Taylor, S. Tkaczyk, N.V. Tran, L. Uplegger, E.W. Vaander-ing, C. Vernieri, M. Verzocchi, R. Vidal, M. Wang, H.A. Weber, A. Whitbeck

University of Florida, Gainesville, USA
D. Acosta, P. Avery, P. Bortignon, D. Bourilkov, A. Brinker-hoff, A. Carnes, M. Carver, D. Curry, S. Das, R.D. Field, I.K. Furic, J. Konigs-berg, A. Korytov, P. Ma, K. Matchev, H. Mei, P. Milenovic[66], G. Mitselmakher, D. Rank, L. Shchut-ska, D. Sperka, L. Thomas, J. Wang, S. Wang, J. Yelton

Florida International University, Miami, USA
S. Linn, P. Markowitz, G. Martinez, J.L. Rodriguez

Florida State University, Tallahassee, USA
A. Ackert, J.R. Adams, T. Adams, A. Askew, S. Bein, B. Dia-mond, S. Hagopian, V. Hagopian, K.F. Johnson, A. Khatiwada, H. Prosper, A. Santra, M. Weinberg

Florida Institute of Technology, Melbourne, USA
M.M. Baarmand, V. Bhopatkar, S. Colafranceschi[67], M. Hohl-mann, H. Kalakhety, D. Noonan, T. Roy, F. Yumiceva

University of Illinois at Chicago (UIC), Chicago, USA
M.R. Adams, L. Apanasevich, D. Berry, R.R. Betts, I. Bucinskaite, R. Cavanaugh, O. Ev-dokimov, L. Gauthier, C.E. Gerber, D.J. Hofman, P. Kurt, C. O'Brien, I.D. Sandoval Gonza-lez, P. Turner, N. Varelas, Z. Wu, M. Zakaria, J. Zhang

The University of Iowa, Iowa City, USA
B. Bilki[68], W. Clarida, K. Dilsiz, S. Durgut, R.P. Gandrajula, M. Haytmyradov, V. Khristenko, J.-P. Merlo, H. Mermerkaya[69], A. Mestvirishvili, A. Moeller, J. Nacht-man, H. Ogul, Y. Onel, F. Ozok[70], A. Penzo, C. Snyder, E. Tiras, J. Wetzel, K. Yi

Johns Hopkins University, Baltimore, USA
I. Anderson, B. Blumenfeld, A. Cocoros, N. Eminizer, D. Fehling, L. Feng, A.V. Gritsan, P. Mak-simovic, M. Osherson, J. Roskes, U. Sarica, M. Swartz, M. Xiao, Y. Xin, C. You

The University of Kansas, Lawrence, USA
A. Al-bataineh, P. Baringer, A. Bean, J. Bowen, C. Bruner, J. Castle, R.P. Kenny III, A. Kropivnit-skaya, D. Majumder, W. Mcbrayer, M. Murray, S. Sanders, R. Stringer, J.D. Tapia Takaki, Q. Wang

Kansas State University, Manhattan, USA
A. Ivanov, K. Kaadze, S. Khalil, M. Makouski, Y. Maravin, A. Moham-madi, L.K. Saini, N. Skhirtladze, S. Toda

Lawrence Livermore National Laboratory, Livermore, USA
D. Lange, F. Rebassoo, D. Wright

University of Maryland, College Park, USA
C. Anelli, A. Baden, O. Baron, A. Belloni, B. Calvert, S.C. Eno, C. Ferraioli, J.A. Gomez, N.J. Had-ley, S. Jabeen, R.G. Kellogg, T. Kolberg, J. Kunkle, Y. Lu, A.C. Mign-erey, Y.H. Shin, A. Skuja, M.B. Tonjes, S.C. Tonwar

Massachusetts Institute of Technology, Cambridge, USA

A. Apyan, R. Barbieri, A. Baty, R. Bi, K. Bierwagen, S. Brandt, W. Busza, I.A. Cali, Z. Demiragli, L. Di Matteo, G. Gomez Ceballos, M. Goncharov, D. Gulhan, D. Hsu, Y. Iiyama, G.M. Innocenti, M. Klute, D. Kovalskyi, K. Krajczar, Y.S. Lai, Y.-J. Lee, A. Levin, P.D. Luckey, A.C. Marini, C. Mcginn, C. Mironov, S. Narayanan, X. Niu, C. Paus, C. Roland, G. Roland, J. Salfeld-Nebgen, G.S.F. Stephans, K. Sumorok, K. Tatar, M. Varma, D. Velicanu, J. Veverka, J. Wang, T.W. Wang, B. Wyslouch, M. Yang, V. Zhukova

University of Minnesota, Minneapolis, USA

A.C. Benvenuti, R.M. Chatterjee, B. Dahmes, A. Evans, A. Finkel, A. Gude, P. Hansen, S. Kalafut, S.C. Kao, K. Klapoetke, Y. Kubota, Z. Lesko, J. Mans, S. Nourbakhsh, N. Ruckstuhl, R. Rusack, N. Tambe, J. Turkewitz

University of Mississippi, Oxford, USA

J.G. Acosta, S. Oliveros

University of Nebraska-Lincoln, Lincoln, USA

E. Avdeeva, R. Bartek, K. Bloom, S. Bose, D.R. Claes, A. Dominguez, C. Fangmeier, R. Gonzalez Suarez, R. Kamalieddin, D. Knowlton, I. Kravchenko, F. Meier, J. Monroy, J.E. Siado, G.R. Snow, B. Stieger

State University of New York at Buffalo, Buffalo, USA

M. Alyari, J. Dolen, J. George, A. Godshalk, C. Harrington, I. Iashvili, J. Kaisen, A. Kharchilava, A. Kumar, A. Parker, S. Rappoccio, B. Roozbahani

Northeastern University, Boston, USA

G. Alverson, E. Barberis, D. Baumgartel, M. Chasco, A. Hortiangtham, A. Massironi, D.M. Morse, D. Nash, T. Orimoto, R. Teixeira De Lima, D. Trocino, R.-J. Wang, D. Wood

Northwestern University, Evanston, USA

S. Bhattacharya, K.A. Hahn, A. Kubik, J.F. Low, N. Mucia, N. Odell, B. Pollack, M.H. Schmitt, K. Sung, M. Trovato, M. Velasco

University of Notre Dame, Notre Dame, USA

N. Dev, M. Hildreth, K. Hurtado Anampa, C. Jessop, D.J. Karmgard, N. Kellams, K. Lannon, N. Marinelli, F. Meng, C. Mueller, Y. Musienko[37], M. Planer, A. Reinsvold, R. Ruchti, N. Rupprecht, G. Smith, S. Taroni, N. Valls, M. Wayne, M. Wolf, A. Woodard

The Ohio State University, Columbus, USA

J. Alimena, L. Antonelli, J. Brinson, B. Bylsma, L.S. Durkin, S. Flowers, B. Francis, A. Hart, C. Hill, R. Hughes, W. Ji, B. Liu, W. Luo, D. Puigh, M. Rodenburg, B.L. Winer, H.W. Wulsin

Princeton University, Princeton, USA

S. Cooperstein, O. Driga, P. Elmer, J. Hardenbrook, P. Hebda, J. Luo, D. Marlow, T. Medvedeva, M. Mooney, J. Olsen, C. Palmer, P. Piroué, D. Stickland, C. Tully, A. Zuranski

University of Puerto Rico, Mayaguez, USA

S. Malik

Purdue University, West Lafayette, USA

A. Barker, V.E. Barnes, D. Benedetti, S. Folgueras, L. Gutay, M.K. Jha, M. Jones, A.W. Jung, K. Jung, D.H. Miller, N. Neumeister, B.C. Radburn-Smith, X. Shi, J. Sun, A. Svyatkovskiy, F. Wang, W. Xie, L. Xu

Purdue University Calumet, Hammond, USA

N. Parashar, J. Stupak

Rice University, Houston, USA

A. Adair, B. Akgun, Z. Chen, K.M. Ecklund, F.J.M. Geurts, M. Guilbaud, W. Li, B. Michlin, M. Northup, B.P. Padley, R. Redjimi, J. Roberts, J. Rorie, Z. Tu, J. Zabel

University of Rochester, Rochester, USA

B. Betchart, A. Bodek, P. de Barbaro, R. Demina, Y.t. Duh, T. Ferbel, M. Galanti, A. Garcia-Bellido, J. Han, O. Hindrichs, A. Khukhunaishvili, K.H. Lo, P. Tan, M. Verzetti

Rutgers, The State University of New Jersey, Piscataway, USA

J.P. Chou, E. Contreras-Campana, Y. Gershtein, T.A. Gómez Espinosa, E. Halkiadakis, M. Heindl, D. Hidas, E. Hughes, S. Kaplan, R. Kunnawalkam Elayavalli, S. Kyriacou, A. Lath, K. Nash, H. Saka, S. Salur, S. Schnetzer, D. Sheffield, S. Somalwar, R. Stone, S. Thomas, P. Thomassen, M. Walker

University of Tennessee, Knoxville, USA

M. Foerster, J. Heideman, G. Riley, K. Rose, S. Spanier, K. Thapa

Texas A&M University, College Station, USA

O. Bouhali[71], A. Castaneda Hernandez[71], A. Celik, M. Dalchenko, M. De Mattia, A. Delgado, S. Dildick, R. Eusebi, J. Gilmore, T. Huang, E. Juska, T. Kamon[72], V. Krutelyov, R. Mueller, Y. Pakhotin, R. Patel, A. Perloff, L. Perniè, D. Rathjens, A. Rose, A. Safonov, A. Tatarinov, K.A. Ulmer

Texas Tech University, Lubbock, USA

N. Akchurin, C. Cowden, J. Damgov, C. Dragoiu, P.R. Dudero, J. Faulkner, S. Kunori, K. Lamichhane, S.W. Lee, T. Libeiro, S. Undleeb, I. Volobouev, Z. Wang

Vanderbilt University, Nashville, USA

A.G. Delannoy, S. Greene, A. Gurrola, R. Janjam, W. Johns, C. Maguire, A. Melo, H. Ni, P. Sheldon, S. Tuo, J. Velkovska, Q. Xu

University of Virginia, Charlottesville, USA

M.W. Arenton, P. Barria, B. Cox, J. Goodell, R. Hirosky, A. Ledovskoy, H. Li, C. Neu, T. Sinthuprasith, X. Sun, Y. Wang, E. Wolfe, F. Xia

Wayne State University, Detroit, USA

C. Clarke, R. Harr, P.E. Karchin, P. Lamichhane, J. Sturdy

University of Wisconsin - Madison, Madison, WI, USA

D.A. Belknap, S. Dasu, L. Dodd, S. Duric, B. Gomber, M. Grothe, M. Herndon, A. Hervé, P. Klabbers, A. Lanaro, A. Levine, K. Long, R. Loveless, I. Ojalvo, T. Perry, G.A. Pierro, G. Polese, T. Ruggles, A. Savin, A. Sharma, N. Smith, W.H. Smith, D. Taylor, P. Verwilligen, N. Woods

†: Deceased
1: Also at Vienna University of Technology, Vienna, Austria
2: Also at State Key Laboratory of Nuclear Physics and Technology, Peking University, Beijing, China

3: Also at Institut Pluridisciplinaire Hubert Curien, Université de Strasbourg, Université de Haute Alsace Mulhouse, CNRS/IN2P3, Strasbourg, France

4: Also at Universidade Estadual de Campinas, Campinas, Brazil

5: Also at Centre National de la Recherche Scientifique (CNRS) - IN2P3, Paris, France

6: Also at Université Libre de Bruxelles, Bruxelles, Belgium

7: Also at Deutsches Elektronen-Synchrotron, Hamburg, Germany

8: Also at Joint Institute for Nuclear Research, Dubna, Russia

9: Also at Helwan University, Cairo, Egypt

10: Now at Zewail City of Science and Technology, Zewail, Egypt

11: Also at Ain Shams University, Cairo, Egypt

12: Also at Fayoum University, El-Fayoum, Egypt

13: Now at British University in Egypt, Cairo, Egypt

14: Also at Université de Haute Alsace, Mulhouse, France

15: Also at CERN, European Organization for Nuclear Research, Geneva, Switzerland

16: Also at Skobeltsyn Institute of Nuclear Physics, Lomonosov Moscow State University, Moscow, Russia

17: Also at Tbilisi State University, Tbilisi, Georgia

18: Also at RWTH Aachen University, III. Physikalisches Institut A, Aachen, Germany

19: Also at University of Hamburg, Hamburg, Germany

20: Also at Brandenburg University of Technology, Cottbus, Germany

21: Also at Institute of Nuclear Research ATOMKI, Debrecen, Hungary

22: Also at MTA-ELTE Lendület CMS Particle and Nuclear Physics Group, Eötvös Loránd University, Budapest, Hungary

23: Also at University of Debrecen, Debrecen, Hungary

24: Also at Indian Institute of Science Education and Research, Bhopal, India

25: Also at Institute of Physics, Bhubaneswar, India

26: Also at University of Visva-Bharati, Santiniketan, India

27: Also at University of Ruhuna, Matara, Sri Lanka

28: Also at Isfahan University of Technology, Isfahan, Iran

29: Also at University of Tehran, Department of Engineering Science, Tehran, Iran

30: Also at Plasma Physics Research Center, Science and Research Branch, Islamic Azad University, Tehran, Iran

31: Also at Università degli Studi di Siena, Siena, Italy

32: Also at Purdue University, West Lafayette, USA

33: Also at International Islamic University of Malaysia, Kuala Lumpur, Malaysia

34: Also at Malaysian Nuclear Agency, MOSTI, Kajang, Malaysia

35: Also at Consejo Nacional de Ciencia y Tecnología, Mexico city, Mexico

36: Also at Warsaw University of Technology, Institute of Electronic Systems, Warsaw, Poland

37: Also at Institute for Nuclear Research, Moscow, Russia

38: Now at National Research Nuclear University 'Moscow Engineering Physics Institute' (MEPhI), Moscow, Russia

39: Also at St. Petersburg State Polytechnical University, St. Petersburg, Russia

40: Also at University of Florida, Gainesville, USA

41: Also at California Institute of Technology, Pasadena, USA

42: Also at Faculty of Physics, University of Belgrade, Belgrade, Serbia

43: Also at INFN Sezione di Roma; Università di Roma, Roma, Italy

44: Also at National Technical University of Athens, Athens, Greece

45: Also at Scuola Normale e Sezione dell'INFN, Pisa, Italy
46: Also at National and Kapodistrian University of Athens, Athens, Greece
47: Also at Riga Technical University, Riga, Latvia
48: Also at Institute for Theoretical and Experimental Physics, Moscow, Russia
49: Also at Albert Einstein Center for Fundamental Physics, Bern, Switzerland
50: Also at Gaziosmanpasa University, Tokat, Turkey
51: Also at Mersin University, Mersin, Turkey
52: Also at Cag University, Mersin, Turkey
53: Also at Piri Reis University, Istanbul, Turkey
54: Also at Adiyaman University, Adiyaman, Turkey
55: Also at Ozyegin University, Istanbul, Turkey
56: Also at Izmir Institute of Technology, Izmir, Turkey
57: Also at Marmara University, Istanbul, Turkey
58: Also at Kafkas University, Kars, Turkey
59: Also at Istanbul Bilgi University, Istanbul, Turkey
60: Also at Yildiz Technical University, Istanbul, Turkey
61: Also at Hacettepe University, Ankara, Turkey
62: Also at Rutherford Appleton Laboratory, Didcot, United Kingdom
63: Also
at School of Physics and Astronomy, University of Southampton, Southampton, United Kingdom
64: Also at Instituto de Astrofísica de Canarias, La Laguna, Spain
65: Also at Utah Valley University, Orem, USA
66: Also
at University of Belgrade, Faculty of Physics and Vinca Institute of Nuclear Sciences, Belgrade, Serbia
67: Also at Facoltà Ingegneria, Università di Roma, Roma, Italy
68: Also at Argonne National Laboratory, Argonne, USA
69: Also at Erzincan University, Erzincan, Turkey
70: Also at Mimar Sinan University, Istanbul, Istanbul, Turkey
71: Also at Texas A&M University at Qatar, Doha, Qatar
72: Also at Kyungpook National University, Daegu, Korea